Impaired epithelium in asthma: mechanisms driving ciliary dysfunction

Thesis submitted for the degree of

Doctor of Philosophy

At the University of Leicester

by

Wing Yan Heidi Wan BSc (Hons)

Department of Infection, Immunity and Inflammation

University of Leicester, U.K.

[2012]

Supervisor: Professor Christopher E. Brightling

Impaired epithelium in asthma: mechanisms driving ciliary dysfunction

Wing Yan Heidi Wan

Abstract

Rationale Epithelial ciliary dysfunction is a feature of asthma that is believed to contribute to persistent symptoms and recurrent exacerbations. However, the mechanism underlying this dysfunction is unknown.

Hypotheses The ciliary dysfunction of asthmatic airway epithelial cells is due to an intrinsic abnormality that leads to a high susceptibility of these cells to an environmental challenge, which results in a chronic inflammation and thus a predisposition of asthma exacerbations.

Methods Primary airway epithelial cells from basal cells and ciliated cultures, and fresh ciliated strips, were used. Baseline protein and gene expression were assessed by protein quantification and microarrays. Ciliary function was studied using video-microscopy. Asthmatic sputa were used as the environmental stimuli; microbiology was assessed. Oxidative stress and the role of NADPH oxidase (NOX) 4 were assessed using immunohistology, reactive oxygen species (ROS) quantification, quantitative gene expression, and the NOX1/4 inhibitor GKT137831.

Results In *ex vivo* ciliated cultures, ciliary dysfunction did not persist but was evident in cells from asthmatics following asthmatic sputum inoculation. Bacterial 16S load increased equally in asthmatic and control samples. Oxidative burden in asthmatic bronchial epithelium was increased and was related to the percentage of sputum neutrophils. NOX4 expression and hydrogen peroxide-induced intracellular ROS generation were significantly elevated in epithelial cells from neutrophilic subjects, with the latter being attenuated by NOX4 inhibition. In asthmatic ciliated cells obtained directly from bronchoscopy, inhibiting NOX4 markedly improved ciliary function and was related to the intensity of neutrophilic inflammation.

Summary The up-regulation of NOX4 expression that is evident in asthmatic ALI cultures might promote the susceptibility of the bronchial epithelium to the development of ciliary dysfunction in the presence of an abnormal microenvironment, implicating NOX4 as a potential therapeutic target for neutrophilic asthma. An increase in the sample size is required to increase the strength of this conclusion.

Acknowledgement

Firstly, I would like to give a huge amount of gratitude to my supervisor, Prof Chris Brightling, for his support not just from the scientific prospective, but also from the very beginning before I joined his group. Without him, I would not be able to do a postgraduate degree in this country. I have certainly got the best supervisor.

I would like to thank Prof Chris O'Callaghan for being my scientific mentors, and for sharing his knowledge and equipment so generously. Special thanks to my previously colleagues, now friends, for their all-round support and help during the highs and lows, both in the lab and outside work. They include everyone in Chris' harem: Lucy, Amanda, Ruth, Fay and Davinder, as well as Rob, Edith, Cat and Koirobi. Mr Martin Coffey has been my "life mentor" during these 4 years and without him, I would have lost all my hair by now.

These are the bodies to be credited: Wellcome Trust Senior Clinical Fellowship (CEB), GlaxoSmithKline, Leicester Air and European Regional Fund for funding my project; Genkyotex, Switzerland for compound donation.

I would like to dedicate this thesis especially to my parents Becky and Simon, for their sacrifice and unconditional love throughout the past 10 years – it is not easy to let their only child go to chase her dream; to my boyfriend Mike, for him being so understanding, and driving me forward in these past years.

Content List

Content

List of Abbreviations

ABPA	allergic bronchopulmonary aspergillosis
ACF	apical chamber fluid (of Transwell insert)
AJs	adherens junctions
ALI	air-liquid-interface
ALI S/N	basolateral supernatant of ALI cultures
ASF	apical surface fluid
ASM	airway smooth muscle
αSMA	α-smooth muscle actin
ATP	adenosine triphosphate
aRNA	amplified RNA
AUC	area under curve
BAL	bronchoalveolar lavage
bdp	beclometasone
BEGM	Bronchial Epithelial Growth Medium
$[Ca^{2+}]_i$	intracellular calcium ion
BSA	bovine serum albumin
CBF	ciliary beat frequency
cAMP	cyclic adenosine monophosphate
CCL	chemokine ligand
cDNA	complementary DNA
CFSE	5-(and 6)-carboxyfluorescein diacetate succinimidyl ester
cfu	colony forming unit
cGMA	cyclic guanosine monophosphate
CI	confidence interval
COPD	chronic obstructive pulmonary disease
Co Q	coenzyme Q
CT	computed Tomography
C(t)	threshold cycle
CXCL	CXC chemokine
Cyt *c*	cytochrome *c*
DAMPs	damage-associated molecular patterns
DAPI	4', 6'–diamidino-2-phenylinodole dihydrochloride
DC	dendritic cells
DCF-DA	5-(and-6)-carboxy-2', 7'-duchlorofluorescein diacetate
dH_2O	distilled water
DMEM	Dulbecco's Modified Eagle's Medium
dsDNA	double-stranded deoxyribonucleic acid
DTT	dithiothreitol
DUOX	dual oxidase
ECM	extracellular matrix
EDTA	ethylenediaminetetraacetic acid
EGF	epidermal growth factor
eGPx	extracellular glutathione peroxidase
ELISA	enzyme-linked immunosorbant assay
EMT	Epithelial-mesenchymal transition
EMTU	epithelial-mesenchymal trophic unit
eSOD	extracellular superoxide dismutase
ER	endoplasmic reticulum
EU	endotoxin unit
FAD	flavin adenine dinucleotide
FBS	fetal bovine serum
FEV_1	forced expiratory volume in 1 second
FVC	forced vital capacity
fps	frames per second
GM-CSF	Granulocyte Macrophage Colony Stimulating Factor
GINA	Global Initiative for Asthma
GMA	glycol methacrylate

GPx	glutathione peroxidase
GSH	reduced glutathione
GSR	glutathione reductase
GSSG	oxidised glutathione
h	hour
HAEBC	human airway epithelial basal cells
HASMC	human airway smooth muscle cells
hBD	human β-defensins
HBSS	Hank's balanced saline solution
HCl	hydrochloride acid
hc-myosin	myosin heavy chain
HEPES	N-2-Hydroxyethylpiperazine-N'-2-Ethanesulfonic acid
HMGB1	high mobility group box 1
H&E	hematoxylin & eosin
$HO_2^{\bullet}$	hydroperoxyl
HSP	heat shock protein
H_2O_2	superoxide
ICS	inhaled corticosteroid
i/eNOS	inducible/endothelial nitric oxide synthase
IFN	interferon
IgE	immunoglobulin E
IL	interleukin
IMS	industrial methylated spirit
IPF	idiopathic pulmonary fibrosis
iROS	intracellular reactive oxygen species
ITS	insulin, human transferrin, and sodium selenite supplement
LABA	long-acting β_2-adrenoceptor agonist
LAL	Limulus Amebocyte Lysate
LPP	lipoprotein
LPS	lipopolysaccharide
MAPK	mitogen-activated protein kinase
mcg	microgram
MEM	minimum essential medium
min	minute
MMPs	matrix metalloproteinases
MRI	Magnetic Resonance Imaging
MSD	Meso-Scale Discovery
NAC	N-acetylcysteine
NADPH	Nicotinamide adenine dinucleotide phosphate
NBS	neutral buffered saline
NF-κB	nuclear factor-kappa B
$NO^{\bullet}$	nitric oxide
NOS	nitric oxide synthase
NOX	NADPH oxidase
NOX4i	NOX4 inhibitor GKT137831
OCS	oral corticosteroid
OD	optical density (fluorescence)
$ONOO^{-}$	peroxynitrite
$O_2^{\bullet -}$	superoxide
PAMPs	pathogen-associated molecular patterns
PBS	phosphate-buffered saline
PC_{20}	Provocative concentration of methacholine that leads to a 20% drop in FEV_1
PCD	primary ciliary dyskinesia
PDA	potato dextrose agar
PDGF	platelet-derived growth factor
phox	phagocytic oxidase
PKG	protein kinase G
PM	plasma membrane
PMSF	phenylmethylsulfonyl fluoride

PRRs	pathogen recognition receptors
RA	retinoic acid
rFC	recombinant Factor C
RFU	relative fluorescence unit
RIN	RNA Integrity Number
RNS	reactive nitrogen species
ROS	reactive oxygen species
RPE	R-Phycoerythrin
RQ	relative quantity
RT-qPCR	Reverse-Transcription quantitative Polymerase Chain Reaction
SABA	short-acting β_2-adrenoceptor agonist
SD	standard deviation
sec	second
SEM	standard error of mean
siRNA	small interfering RNA
SOD	superoxide dismutase
SQS	semi-quantified with scores
ssRNA	single-stranded ribonucleic acid
TBS(-T)	Tris buffered saline (-Tween 20)
TEER	trans-epithelial electric resistance
TGF-β	transforming growth factor β
TIMPs	tissue inhibitor of metalloproteinases
TJs	tight junctions
TLR	Toll-like receptor
TNF-α	tumour necrosis factor-α
TSLP	Thymic Stromal-Derived Lymphopoietin
ZO	zonula occludins
8-oxo-dG	8-oxo-7,8-dihydro 2'-deoxyguanosine
%	percentage

List of Tables

List of Figures

Publications Arising From This Thesis

Papers

Wan, WYH; Woodman, L; Hirst,R; Pashley, C; Haldar, K;Gomez, E; Sutcliffe, A; Desai, D; Wardlaw, A; Barer,M; O'Callaghan, C; Brightling, C. NADPH oxidase 4 over-expression mediates epithelial ciliary dysfunction in neutrophilic asthma (in preparation)

Woodman, LB; **Wan, WYH**; Milone, R; Grace, K; Sousa, A; Williamson, R; Brightling, CE. Synthetic Response of Stimulated Respiratory Epithelium: Modulation by Prednisolone and iKK2 Inhibition. Chest 2012 Dec 13. doi: 10.1378/chest.12-1187

Martin, N; Ruddick, A; Arthur, GK; **Wan, H**; Woodman, L; Brightling, CE; Jones, DJ; Pavord, ID; Bradding, P. Primary human airway epithelial cell-dependent inhibition of human lung mast cell degranulation. PLoS One 2012; 7 (8):e43545

Kaur, D; Doe, C; Woodman, L; **Wan, H**; Sutcliffe, A; Hollins, F; Brightling, C. Mast cell-airway smooth muscle crosstalk: the role of thymic stromal lymphopoietin. Chest 2012;142(1):76-85. doi:10.1378/chest.11-1782

Published Abstracts

Wan, WYH; Woodman, L; Hirst, R; Haldar, K; Gomez, E; Sutcliffe, A; Desai, A; Barer, M; O'Callaghan, C; Brightling, C. NADPH oxidase 4 over-expression mediates epithelial ciliary dysfunction in neutrophilic asthma. December 2012

2012 British Thoracic Society Winter Meeting

Wan, WYH; Woodman, L; Hirst, R; Wardlaw, A; O'Callaghan, C; Brightling, C. Intrinsic and environmental factors contribute to ciliary dysfunction of human airway epithelial cells in asthma. September 2012; P3731

2012 European Respiratory Society Summer Meeting

Wan, WYH; Woodman, L; Hirst, R; Wardlaw, A; O'Callaghan, C; Brightling, C. Both intrinsic and environmental factors contribute to ciliary dysfunction of human airway epithelial cells in asthma. April 2011; Poster 16

2010 Injury and Repair Mechanisms in Chronic Airway Disease Conference, Abcam, London

1. Introduction

1.1 Asthma – A Chronic Inflammatory Airway Disease

1.1.1 Definition of Asthma

Asthma affects 300 million people worldwide and causes 250,000 deaths annually (1), which will reach 400 million by 2025 if the current trend continues (2). It is estimated that 5.4 million people in the UK are currently affected by asthma, causing the NHS to spend around £1 billion per year on asthma care and treatment (3). This financial burden is mainly contributed from the hospitalisation of patients with asthma attacks due to the inefficient treatments in controlling asthma symptoms (3, 4).

Asthma is defined by the presence of 1) asthma symptoms, 2) an abnormal lung physiology, and 3) abnormal lung pathological features. Clinical symptoms of asthma include wheeze, cough, breathlessness and chest tightness, all of which indicate a reduction in lung function. An asthmatic lung physiology includes the presence of airway hyperresponsiveness, an airflow limitation and an airflow obstruction that is reversible. Airway hyperresponsiveness is defined by a PC_{20} <8 mg/ml; PC_{20} is the concentration of methacholine causing a 20% reduction in forced expiratory volume in 1 second (FEV_1). An airflow limitation is defined by <80% FEV_1 predicted normal, or <70% FEV_1/FVC (forced vital capacity) predicted normal (5). A reversibility of 12% after bronchodilation, using a bronchodilator, such as salbutamol indicates a reversible lung function. Abnormal lung pathological features in asthma include airway remodelling and signs of persistent inflammation. Evidence of airway remodelling includes thickening in airway wall and reduction in lumen size, an increase in airway smooth muscle mass, increase in extracellular matrix mass, and a disrupted epithelium. Mast cell infiltration in smooth muscle bundle, high eosinophil and neutrophil counts, and high-exhaled nitric oxide levels indicate the presence of a persistent inflammation.

1.1.2 Severity

Classifying asthma into severity bands has been used as a guide for diagnosis and treatment in the past 20 years (6), but has proved inadequate due to the inconsistent treatment outcomes caused by the heterogeneity of the disease (5). The current guidelines for asthma management are based on the control of the disease – a treatment set, including the use of corticosteroids and/or β_2-adrenoceptor agonists, that can concurrently achieve the ideal control of asthma (asymptomatic, normal daily activity, minimal-to-none use of β_2-adrenoceptor agonists and normal lung function) and reduce future risks (exacerbation, symptom worsening, treatment side-effects) (5). When asthma becomes less/more controlled, a step-up/step-down in treatment will be considered. **Table 1.1** summarises the stepwise treatment approach used by the Global Initiative for Asthma (GINA) guidelines. These treatment steps are partly comparable to the mild-to-severe asthma classification used previously. Asthma treatment is further discussed in Section1.2.

Uncontrolled asthma leads to an increased risk in asthma exacerbation. An exacerbation (asthma attack) is defined by an episode of worsening in symptoms and lung function that requires an immediate addition or change of treatment, which can take from minutes to weeks to resolve. It usually involves the application of systemic corticosteroids (oral or by injection) for at least 1 day and/or an extensive use of a bronchodilator (7). Asthma exacerbation might be classified into severe and moderate despite the lack of literature consistency. Mild exacerbation is hard to define due to a lack of reference control.

←reduce		Treatment Steps		increase→
Step 1	Step 2	Step 3	Step 4	Step 5
Asthma education				
Environmental control				
SABA when required				
Controller options	Select one	Select one	Add one or more	Add one or both
	low-dose ICS	low-dose ICS + LABA	medium- or high-dose ICS + LABA	OCS (lowest dose as possible)
	leukotriene modifier	medium- or high-dose ICS	leukotriene modifier	anti-IgE treatment
		low-dose ICS + leukotriene modifier	sustained-release theophylline	
		low-dose ICS + sustained-release theophylline		

SABA, short-acting β_2-agonist; LABA, long-acting β_2-agonist; ICS, inhaled corticosteroid; OCS, oral corticosteroid; ICS low-dose: ≤800 mcg bdp; medium-dose: 800-1600 mcg bdp; high-dose: ≥1600 mcg bdp; mcg bdp, beclometasone equivalent dose in 24 h = budesonide x2 = fluticasone x1.25; leukotriene modifier, receptor antagonist or synthesis inhibitors

Table 1.1 **Global Initiative for Asthma (GINA) treatment steps.** This table shows the common treatment across all steps, and identifies the controller options including a preferred option (grey) and other alternatives (5).

1.1.3 Heterogeneity of Asthma

Asthma is a complex disease with its heterogeneity spanning across scales from a molecular level to the functional organ level in the human body (**Figure 1.1**).

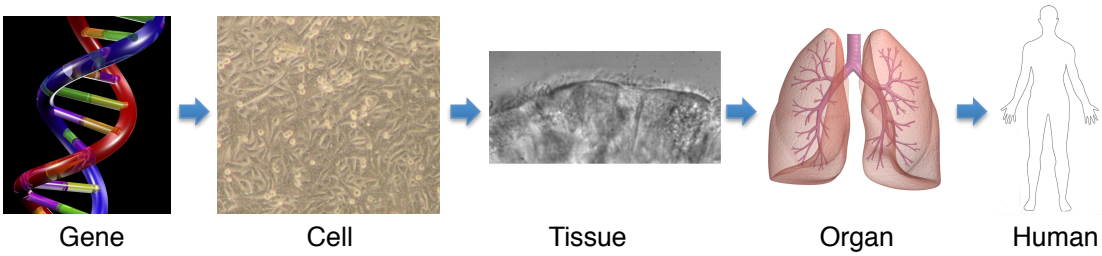

Figure 1.1 **The heterogeneity of asthma span across different scales in humans.** The underlying gene polymorphisms and abnormalities at a molecular level have been reported in literature. These result in altered cell behaviour and cell-to-cell interaction. The exposure to environmental factors adds another level of complexity due to a variety of gene-environment interaction. Together it causes altered tissue behaviours, leading to the development of different features of airway damage and remodelling as observed clinically.

Recent genetic variant and genome-wide association studies allowed researchers to study asthma at a genetic level, and identified genes that are associated with the risk of asthma and pathogenesis (8-15). Single nucleotide polymorphisms (SNPs) have been identified to be associated with asthma in terms of the impaired lung function and airflow obstruction (15-17), and the modulation of immunity in response to a spectrum of stimuli, including infection and oxidative stress (12, 15, 16). Furthermore, SNPs that are specific to severe asthma have been identified (13, 15), suggesting the implication of genetic diversity in asthma heterogeneity. Following the study of genomics and transcriptomics, proteomics allows researchers to understand the protein structure, its regulation and function to the cell. Proteome-based studies using human bronchoalveolar (BAL) fluid identified potential asthma biomarkers (18). Together they reflect on the heterogeneity of asthma at a gene-to-cell scale. The asthma heterogeneity at the cell-to-tissue scale is more complex, with the involvement of cell-to-cell interaction, cell-to-matrix interactions, the cross-interaction between them and the interaction with the environment (19). Inhaled particulate species are diverse and environment-dependent, ranging from allergens to pathogens to pollutants. Different particulates (e.g. allergen/bacteria) trigger different responses of different airway cells (e.g. epithelial and leukocyte Toll-like receptors (TLRs)). Interaction between various structural and inflammatory cells facilitates a continuous secretion of (pro-) inflammatory mediators (e.g. T_H2/T_H1 cytokines, growth factors, chemokines) and matrix components (e.g. collagen IV, fibronectin). Persistent inflammation leads to airway remodelling. The associated changes in tissue structures that can be observed are therefore related to the presence of abnormal inflammatory responses. As shown by quantitative computed tomography (CT) analysis (20), airway structure is diverse within an individual and between individuals. This collective evidence shows the heterogeneity

at a tissue-to-organ scale that reflects on the differences in asthma phenotypes as seen in the clinics.

My project focused on the cell-to-tissue scales. To expand further, asthma can be divided into 4 subgroups based on the heterogeneity in inflammatory cell profiles obtained from induced sputum assessment (21, 22). Typical allergic asthma has an eosinophilic inflammatory profile (≥3% total sputum cell count). Non-allergic, non-eosinophilic asthma generally has a neutrophilic profile (≥61% total sputum cell count). In between there is paucigranulocytic (non-eosinophilic/non-neutrophilic) and mixed granulocytic (eosinophilic and neutrophilic) asthma. **Table 1.2** summarises different inflammatory cell profiles in asthma. This heterogeneity in inflammatory profiles can also be associated with the asthmatic remodelling of extracellular matrix at the tissue level as illustrated on **Figure 1.1**, and can be associated with the steroid sensitivity and clinical outcomes at the organ-to-human scale (23).

1.1.4 Neutrophilic asthma

Compared to typical eosinophilic asthma, neutrophilia can be found across asthma severity but is most common in severe asthma (24-26). In fact, neutrophilia occurs in ~50% of the asthma population (25, 27). It is characterised by the high neutrophil count in sputum and its correlation with airflow obstruction (28), and is associated with exacerbation (29, 30) that is independent from smoking (31). The reduction in neutrophil count and CXCL8 concentration post clarithromycin supports a relationship between infection, T_H1 inflammation and neutrophil chemotaxis (32).

Intermittent eosinophilic asthma also tended to become neutrophilic or mixed granulocytic overtime (26). The change, however, is not likely to be a time-dependent progression because basement membrane thickening is observed in eosinophilic, but not in neutrophilic asthmatic airways (23). Neutrophilic asthmatics are mostly corticosteroid-insensitive (25, 29), suggesting the presence of neutrophilia-specific pathways that lead to the different clinical outcomes. Whether the sensitivity of corticosteroids in eosinophilic asthmatics has driven the inflammatory profile towards neutrophilia has yet to be confirmed, despite evidence suggesting that corticosteroids promote neutrophil survival (33). In addition, the underlying mechanisms driving the development of this subgroup have yet to be identified. This increases the difficulty in developing therapies, and thus results in uncontrolled symptoms leading to a high risk of exacerbation, which is common in this asthma subgroup.

The inflammatory profiles of neutrophilic asthma and bronchiectasis share common features (32), with frequent microbial colonisation/infection, such as *Pseudomonas aeruginosa* (34), leading to persistent activation of Toll-like receptors 2 and 4, and thus resulting a similar neutrophil infiltration into the airway. High-resolution CT revealed 40% of asthmatic airways contain bronchiectasis (35). It is plausible that neutrophilic asthmatic airways share common, specific features with bronchiectasis that differentiate itself from eosinophilic asthma.

% Differential Sputum Count	**Non-neutrophilic Asthma**	**Neutrophilic Asthma**
	≤61% neutrophils	>61% neutrophils
≤3% eosinophils	**Paucigranulocytic** Well controlled Corticosteroid sensitive	**Neutrophilic** Refractory asthma Acute and chronic infection Pollutants (reactive species) T_H1 inflammatory profile Corticosteroid insensitive
>3% eosinophils	**Eosinophilic** Typical asthma Allergen-initiated T_H2 inflammatory profile Corticosteroid sensitive (mostly)	**Mixed Granulocytic** Exacerbation Severe asthma T_H1/T_H2 inflammatory profile Corticosteroid (in-)sensitive

Table 1.2 Heterogeneity of asthma and the associated characteristics. Asthma can be divided into 4 different subtypes based on the inflammatory profiles in the sputum differential cell count: Paucigranulocytic (low eosinophils; low neutrophils), eosinophilic (high eosinophils; low neutrophils), neutrophilic (low eosinophils; high neutrophils) and mixed granulocytic (high eosinophils; high neutrophils). Each subtype of asthma is usually associated with specific characteristics (26, 32, 36, 37).

1.2 Treatments For Asthma

Early development of asthma treatment focused on suppressing the allergen-associated eosinophilic inflammation. Steroids are generally used for their anti-inflammatory properties in many diseases (38, 39), including asthma. Corticosteroids target cytosolic glucocorticoid receptors translocating them to the nucleus and activating NFκB-dependent inflammatory pathways (38, 39). Inhaled and oral corticosteroids arise local and systemic effect respectively. β_2-adrenoceptor agonists can be prescribed alongside with corticosteroids to asthmatic subjects. There are two types of β_2-agonists – short-acting β_2-agonists (SABA) with an onset of action within 15 min of administration, and long-acting (LABA) with an onset of action >15 min of administration. β_2-agonists suppress bronchoconstriction by acting on adrenergic receptors in airway smooth muscle cells (40). They also have an effect on ciliary beat frequency (CBF), which will be discussed later (41-43). However, corticosteroid insensitivity has been observed in

subgroups of asthma (25, 29), with different corticosteroid-resistant mechanisms being proposed (44). In addition, evidence of β_2-agonist tolerance has also been reported (45).

In light of this, the focus has switched recently to developing other small molecules that inhibit other inflammatory components. Elevated IgE is associated with mast cell activation in allergic asthma; anti-IgE reduced asthma symptoms and exacerbation (46), eosinophil infiltration and remodelling (47), and showed corticosteroid sparing effects (48). IL-5 is required for eosinophil maturation and survival; anti-IL-5 reduced sputum eosinophil level and the associated symptoms (49, 50). IL-13 is a powerful epithelium activator; anti-IL-13 improved epithelium hyperactivity (51), asthma symptoms (52, 53), and airway inflammation (54). These add-on therapies were effective in combination with the treatment from stage 4 (**Table 1.2**). However, they have proved to be inefficient in controlling other non-T_H2-driven subtypes of asthma.

TNF-α has been suggested to be specific to neutrophilic asthma (55-57). Anti-TNFα treatment however showed no promising effect in the majority of the asthma population (58). Neutrophilic inflammation may be attenuated using macrolides clarithromycin (32, 59) and azithromycin (60), which acts as immuno-modulators with a corticosteroid sparing effect in severe asthma (61). Details on anti-microbial and antioxidant therapies will be discussed in Section 1.4 and 1.5.

The heterogeneity of asthma highlights the importance of patient-specific treatment regimens to maximise effectiveness.

1.3 Human Airway Epithelium

1.3.1 Overview

Human airways can be divided into bronchi (trachea plus all branches with cartilages), bronchioli (all "cartilage-less" distal airways with epithelium), and terminal bronchioli before reaching the alveoli where the gas exchange takes place (62). Using a symmetrical dichotomous branching system in the Weibel's lung model (63), the generations of the branches are numbered in an ascending order with the trachea as Generation 0. Generations 0 to 7/8 represents large airways, 12-23 represents small airways. The lumen diameter of the airways ranges from 18 mm to <0.4 mm (63).

Generally the human airway structure consists of a surface epithelium exposed to air, a basement membrane separating the epithelium and the sub-mucosal region below and the sub-mucosal matrix region directly underneath the basement membrane, where the mesenchymal cells and infiltrated inflammatory cells are located. This has been described as the epithelial-mesenchymal trophic unit (EMTU) (64). As the airways become more peripheral and smaller, the structure becomes simpler and more cuboidal, with the epithelium gradually becomes thinner and with shorter cilia. My PhD project focused on large airways (Generations <7/8) where a fully differentiated epithelial structure can be found.

1.3.2 Biology of the airway epithelium

1.3.2.1 Structure

The airway epithelium is composed of three major components: the actual epithelial cell layers, the basement membrane underneath it, and the apical surface fluid (ASF) above it (**Figure 1.2**A). Together they form the first barrier lining the airway lumen, defending

against inhaled harmful particulates. Each component has its own role in this defence system and is crucial to the general protective function of the epithelium.

The multi-layered epithelium consists of epithelial cell subtypes that are at different stages of differentiation (62). Each subtype has its own purpose. Non-ciliated pseudo-stratified columnar cells form the mid-layer of the epithelium, acting as a supportive scaffold for the epithelial structure. The polarity of these cells also helps with material transportation between cell layers (65). The top layer of the epithelium contains ciliated epithelial cells with cilia protruding from the cell surface. These cilia are responsible for clearing foreign particulates trapped above the epithelium by a coordinated beating mechanism. This process is known as the mucociliary clearance. The ciliated cells are interspersed with secretory epithelial cells, which are responsible for the composition of the ASF atop the epithelium that traps particulates. Epithelial basal cells reside at the most basolateral (bottom) layer of the epithelium (66) and the subpopulation of epithelial progenitor/stem cells (67), are believed to have the ability to trans-differentiate into different epithelial subtypes above. Proliferation rate is <1% per 24 h at resting state and is increased to 17% after injury (68, 69). These epithelial cell subtypes are packed tightly together by adherent junctions (AJs) and (hemi)desmosomes using catenin's/cadherin complexes and intermediate filaments forming transmembrane adhesion protein complexes (70). Different epithelial cell subtypes express different cell markers as summarised in (71).

Epithelial basal cells also act as anchors of the epithelial layers to the basement membrane via α3β1 and α6β4 integrin interaction (72). The general term "basement membrane" can be divided into layers (**Figure 1.2**B) (73, 74). The top basal lamina can

be subdivided into lamina lucida/rara and lamina densa, of which the latter one is a collagen IV/laminin V-rich matrix layer. The bottom, lamina reticularis is rich in collagen III/V and fibronectin, in directly contact with the mesenchymal region. These two layers are separated by a baseline membrane, which contains different matrix proteins.

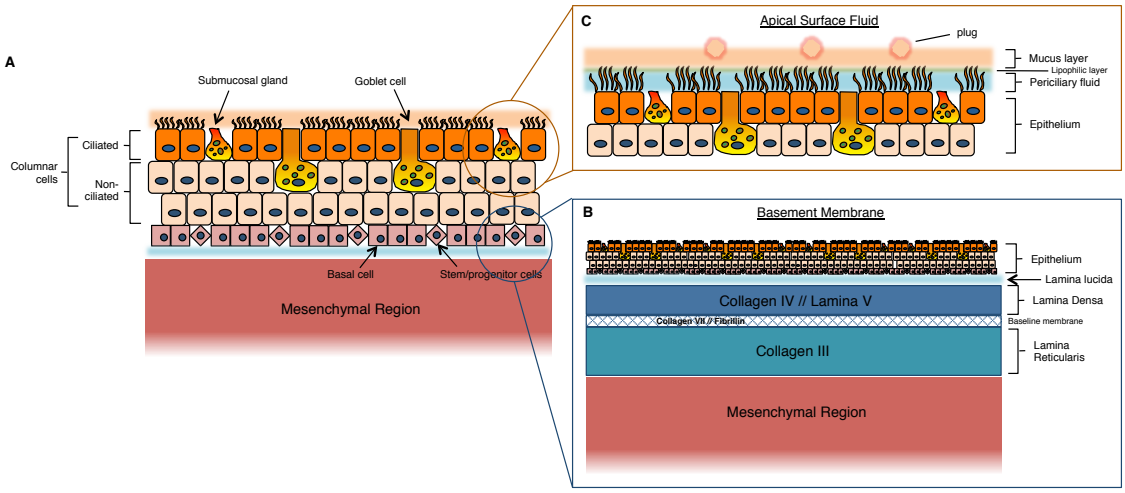

Figure 1.2 **Schematic structure of the human airway epithelium.** A shows the structure of the airway epithelium. B shows the structure of the basement membrane. C shows the composition of the ASF (73-75).

1.3.2.2 Secretory epithelial cells and the ASF

A complete and healthy epithelium contains 6,000 goblet cells/mm^2 (75); in a 1:5 ratio with ciliated cells (68). There are three subtypes of secretory epithelial cells in human airways: goblet cells (mainly in large airways), Clara cells (mainly in small airways), and submucosal glands (associated with cartilage) (76, 77). They are responsible for the composition of the ASF lining on the surface of the entire epithelium. ASF is the true first barrier that is in the first contact with any inhaled particulates in the airways. It is believed that it contains three layers: top mucus layer, middle lipophilic layer, and bottom periciliary layer (78) (**Figure 1.2**C).

The mucus layer is the most viscous layer of the three, despite being composed of 95% water (78). It is a mixture of materials secreted by the epithelium including mucin (2-3%), proteoglycans, ions, proteases and antimicrobial proteins (78, 79). Normally it is 5-50μm thick (80-82). Mucins are large glycosylated proteins that are described as the "gel-forming" unit of the airway mucus. Different *O*-glycosylation in serine/threonine-rich regions form different types of mucins (83). To date, 15 mucins, either membrane-associated or secretory, have been identified. The secretory MUC2, MUC5B and MUC5AC are predominantly expressed on the airway epithelial surface (76, 84). The regulation in mucin induction and secretion has been extensively reviewed (76). Briefly, mucin induction and secretion should be treated as independent events that each can be regulated by a wide range of signalling pathways, such as growth factor (e.g. EGF and TGF-β), and inflammatory signalling (e.g. TLR cascades, T_H1/T_H2 cytokines) mediators. The mucins and glycoproteins trap the particulates on the airway surface, where the action of other mucus components such as proteases (e.g. lysozymes) and antimicrobial proteins (e.g. human β-defensins and LL-37) takes place.

The lipophilic layer lies between the mucus layer and the periciliary layer (68, 85). Its function has yet to be confirmed. Compared to the mucus layer, the periciliary layer is a more fluid phase on the bottom of the ASF, only 5-10 μm in depth (68). This layer is directly in contact with the epithelial cilia. Its fluidity allows the ciliary to beat continuously to propel the top mucus layer up and out of the airways. Therefore, any change in the content of this layer would expect to directly affect the ciliary function.

1.3.2.3 Ciliated epithelial cells

Ciliated epithelial cells (**Figure 1.3**) can be found from the trachea to bronchiole (75, 86). This top layer of the epithelium contains ciliated cells that are believed to be the terminally differentiated epithelial cells and is the most abundant cell subtype within the epithelium (68). Ciliated cells are packed tightly together via the apical tight junctions (TJs) with protein complexes including zonula occludens (ZO) 1-3, claudins 1-5, occludins and E-cadherin (64, 70). The integrity of these TJs is very important in maintaining the polarity of the cells, while the cellular polarity directs ciliary growth and function (87-89). The integrity of TJs, i.e. the permeability of the epithelium, can be reflected by the trans-epithelial electric resistance (TEER), which is generated by the ion exchange across the selectively permeable epithelium. TEER increases as basal cells differentiate (90). A TEER value ranged 700-1000 Ω/cm^2 has been reported in healthy, intact and ciliated epithelium, but is also likely to be cell- and culture method-dependent (90-92).

A ciliated cell is characterised by the presence of 100-300 cilia projections/cell on the apical surface (86). The cilia are packed into a hexagon-shaped array, with the density reducing gradually from the centre to the edge of the apical surface. A high number of mitochondria can be found in the apical side of the cells, that is most likely to supply energy for the ciliary motion. Located towards the basolateral side is the nucleus and Golgi apparatus as the "control centre" and the sites of synthesis respectively (93, 94).

A mature cilium is ~0.3 μm in width, and 7 μm in maximum length, which is depending on the ciliary development and the airway generations (86, 95). Each cilium is surrounded by 6 microvilli (96). Each microvillus is 1-3 μm in length and 0.1-0.3 μm in

width and with no definite function (**Figure 1.3**) (97). The ciliary membranes are the continuation of the cell surface (68, 86). Claw-like projections can be found at the tips (98). Motile cilium development is in waves and has been described in detail (87, 99), as illustrated in **Figure 1.4**. Briefly, it requires the formation of primary cilia on the basal/progenitor cell to direct centriole replicates, precentrioles to mature and dock on to the apical surface. Mature precentrioles, called basal bodies, then become the sites of cilium budding and as an anchor of a mature cilium.

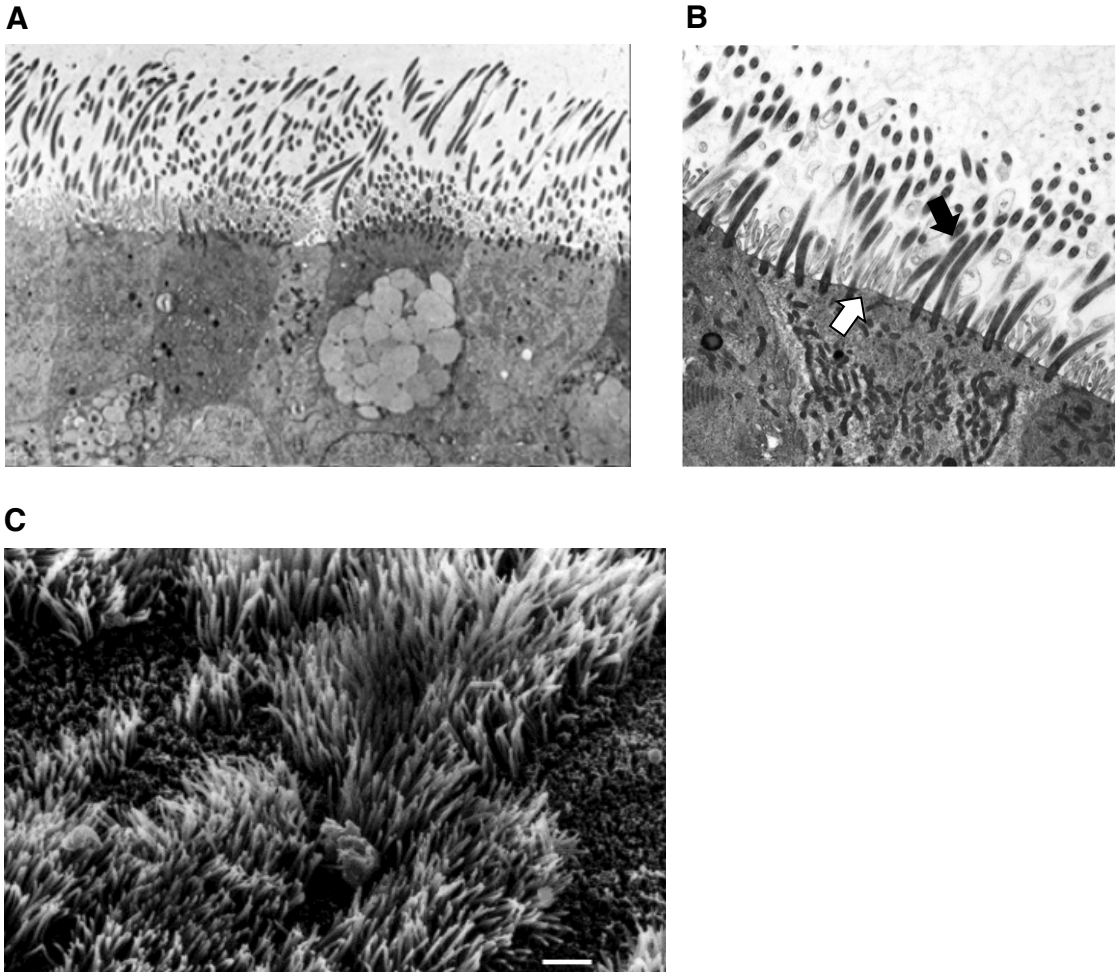

Figure 1.3 Transmission electron microscopic images of ciliated human airway epithelium from a healthy subject. A shows a ciliated epithelial surface. B shows the presence of cilia (black arrow) and microvilli (open arrow). C shows a scanning electron microscopy (SEM) image of ciliated respiratory epithelium of human nasal mucosa. Scale bar = 7 μm (from Dr. Thomas' thesis, with permission) (100).

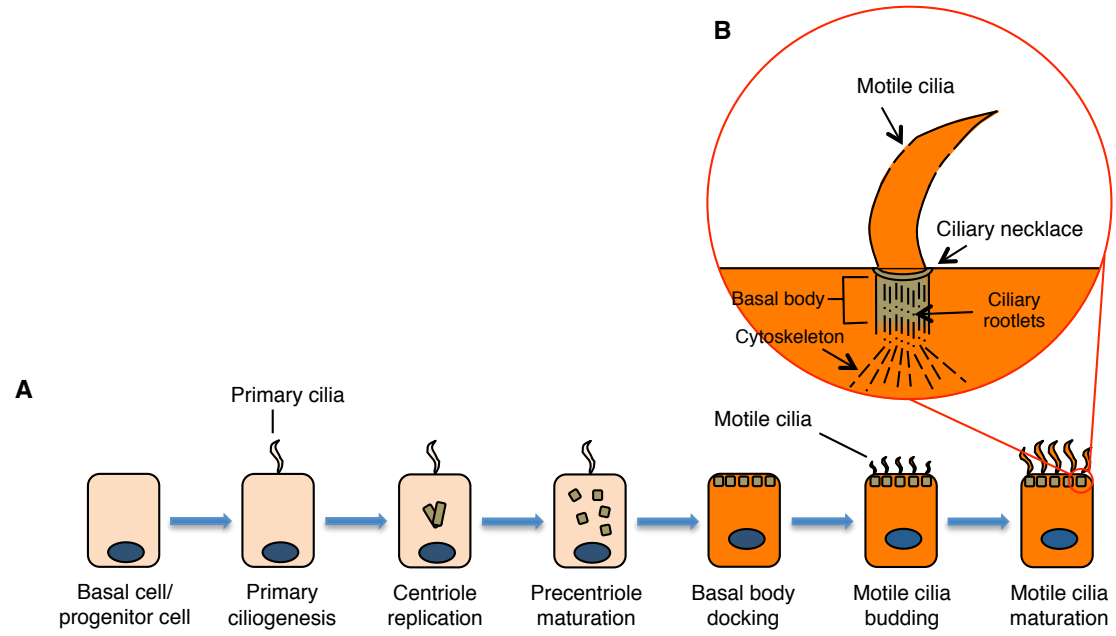

Marker Expression	Basal cell/ progenitor cell	Primary ciliogenesis	Centriole replication	Precentriole maturation	Basal body docking	Motile cilia budding	Motile cilia maturation
PC-1/2	+	+	+	-	+	+	
Acetylated α-tubulin	+	+	+	-	-	-	
Foxj1	-	-	+	+	+	+	
γ-tubulin	-	-	+	+	+	+	
Arl13b	-	-	+	+	+	+	

Figure 1.4 **Development of motile cilia on airway epithelial cells.** A shows the development of motile cilia from basal/progenitor cells. Briefly, the presence of primary cilia is essential to for basal body docking followed by motile cilia budding and growth. The table shows the markers that were identified to be specific to different stages of motile cilia development. B shows the structure of the root of a motile cilium. The microtubules extending from the tip to the bottom of a cilium are anchored to the epithelial cell surface via the ciliary rootlets in the basal body (87, 93, 99).

A mature cilium adopts the "9+2" microtubule structure: a central microtubular pair connecting to the 9 peripheral microtubule doublets via radial spokes. Each microtubule doublet is projecting 2 dynein arms (outer and inner) and a nexin link that connects to the adjacent doublet (**Figure 1.5**A) (101). A microtubule is a polymer of α- and β-tubulins arranged with a helical pitch, forming a protofilament with a 96 nm longitudinal repeat unit. The central pair consists two subfibres, each composted of 13 protofilaments, which defines the ciliary axis (101). In comparison, each peripheral microtubule doublet consists of a 13-protofilament subfibre A and a 10-protofilament

subfibre B. Inner and outer dynein arms are attached to subfibre A with a 24 nm periodicity (102). They facilitate ciliary beating by interacting with microtubules. Each dynein arm contains an adenosine 5'-triphosphate (ATP) binding unit with an ATPase. During each beating cycle, the dynein arms undergo conformational changes between subfibres A and B by hydrolysing the ATP (102). These movements cause the subfibres to slide along each other, leading to cilium bending. The opposite movement of the two dynein arms leads to the movements of forward power strokes and backward recovery strokes. The basal foot of the basal bodies (**Figure 1.4**B) in each cell and among the adjacent cells, are arranged in a similar direction. This direction represents the direction of the effective ciliary stroke.

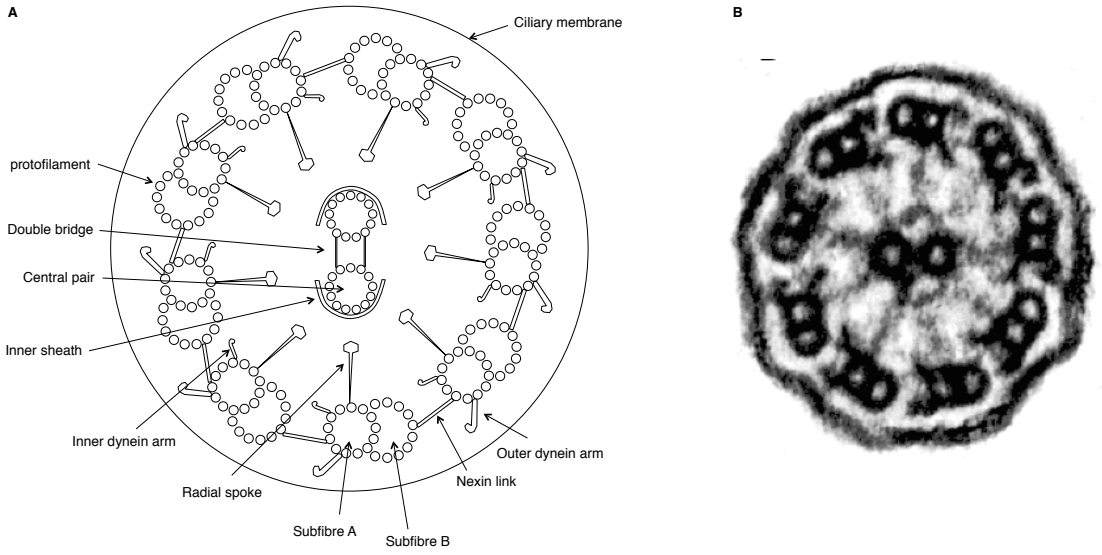

Figure 1.5 **A normal ultrastructure of a human airway cilium.** A shows the schematic of the "9+2" structure of a motile cilium. B shows a cross sectional transmission electron microscopy image of a human respiratory cilium (from Dr Thomas' thesis, with permission) (100).

1.3.3 Mucociliary clearance

1.3.3.1 Function

Mucociliary clearance is an essential factor in pulmonary defence against invasion and injury by inhaled particulates. The viscous mucus layer of the ASF traps particulates, while the periciliary layer allows an undisturbed ciliary beating to propel the mucus up the airways. It is believed that the claw-like projections on the ciliary tips reach the mucus layer to aid the propulsion (68). The mucus propulsion, i.e. the clearance of any trapped particulates, is facilitated by the constantly beating epithelial cilia.

1.3.3.2 Regulation of ciliary beat frequency (CBF)

CBF is important in mucociliary clearance and is directly correlated to the transport efficiency (103, 104). The cilia beat in a coordinate, metachronal wave fashion, with a CBF of 11-14 Hz in normal human airways (68, 86, 105). It can be affected by various factors in the surrounding environment, such as temperature (106, 107), pH (108, 109), humidity (110, 111) and ionic charge (112, 113). The physiological regulation of CBF is highly Ca^{2+}-dependent (114) (**Figure 1.6**). CBF increases in response to an increase in the concentration of intracellular Ca^{2+} ($[Ca^{2+}]_i$) in epithelial cells. This could be facilitated via the cyclic nucleotide-dependent pathways (115, 116), and/or the ATP/phospholipase-dependent pathways (117-120). Nitric oxide ($NO^{\bullet}$) synthesized by nitric oxide synthase (NOS) in the epithelium also regulates CBF via the cGMP-dependent PKG pathway (121, 122), which suggests a role of oxidative handling in ciliary function regulation. Other pathogenic causes of changes in CBF are discussed in later sections.

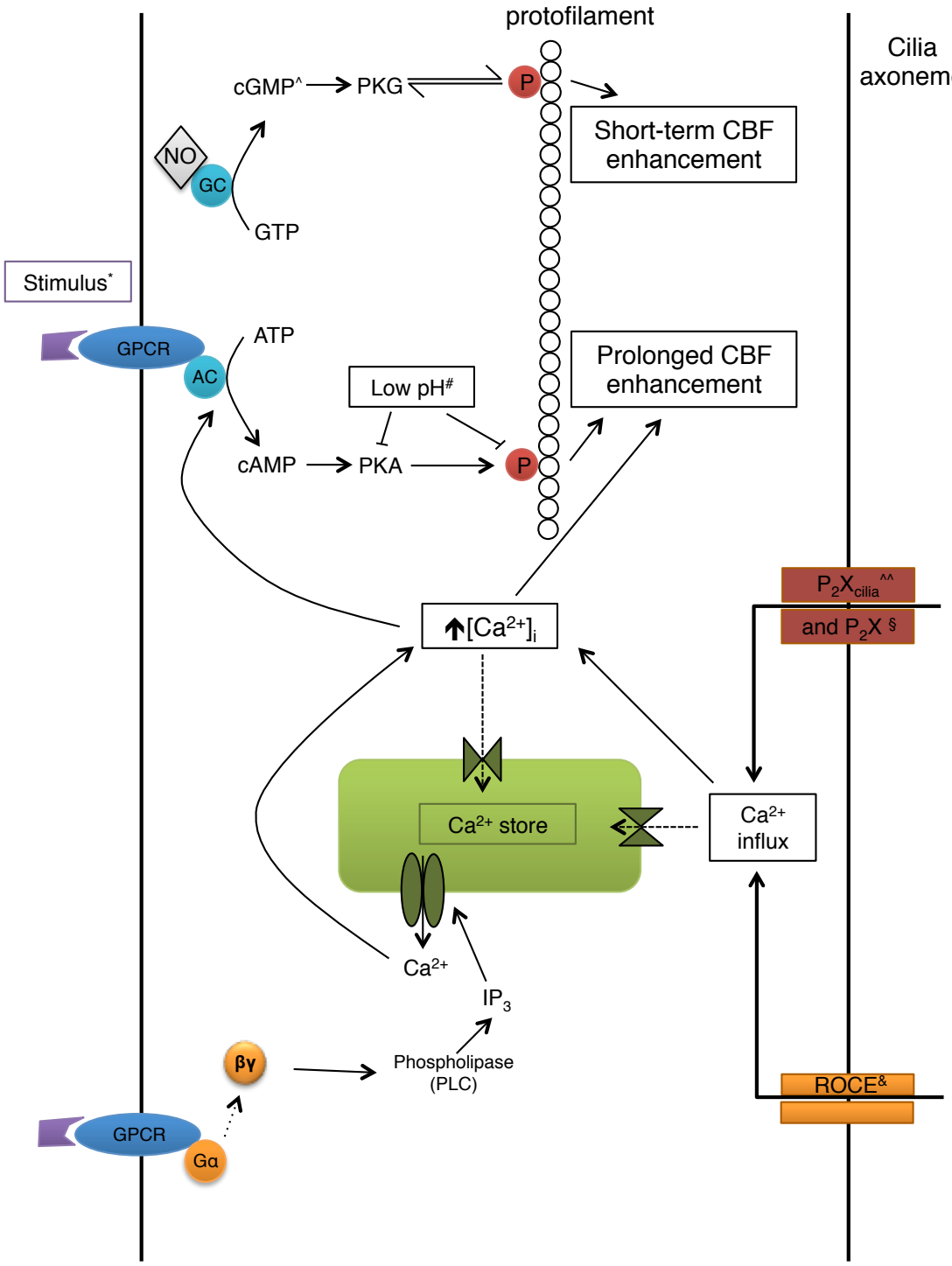

Figure 1.6 **Physiological regulation of ciliary beat frequency (CBF).** CBF is regulated by the intracellular concentration of calcium ions ($[Ca^{2+}]_i$). The Ca^{2+} can be regulated by active ion transport via cell surface channels such as P_2X receptors and receptor-operated calcium entry (ROCE). $[Ca^{2+}]_i$ can also be regulated internally by intracellular Ca^{2+} stores, such as mitochondria and endoplasmic reticulum. The interaction of a substrate with a G protein-coupled receptor (GPCR) leads to the conformational change of the G protein. The Gβγ subunit is released to interact with phospholipase C (PLC) which activates the IP_3 receptor on the Ca^{2+} stores to release Ca^{2+}.Ca^{2+} activates adenylyl cyclase (AC) and aid the generation of second messenger cAMP. cAMP activates PKA that leads to a prolonged CBF enhancement. On the other hand the presence of nitric oxide (NO) facilitates cGMP generation. cGMP activates PKG that leads to a short-term CBF enhancement. * (116); ^ (122, 123); # (109, 124); § (118); ^^ (120); & (119)

1.3.3.3 Regulation of ciliary beat patterns

Other than CBF, ciliary beat patterns may also be important in normal mucociliary clearance (125, 126). Using high-speed videomicroscopy, it was revealed that human airway cilia beat with forward and backward movements (105). The forward power stroke is a rapid motion, with the tip of the cilium bending towards to epithelial surface. It then stops briefly, followed by the slower backward recovery stroke with a sideward movement of <4°. This pattern is likely to be controlled by the interaction between dynein arms and the microtubules. Primary ciliary dyskinesia (PCD) is a genetic defect in cilia axoneme structure (127, 128). The abnormal beat patterns are caused by the loss of one or both dynein arm pair, or the central pair, or the transposition of the peripheral microtubule doublets. It has yet to be confirmed whether PCD is associated with asthma. The presence of abnormal beat patterns in asthmatic airway epithelium, however, has been suggested to be a secondary effect upon the exposure to injury and/or infection (129-131). Dyskinetic cilia in PCD may possess normal CBF (128) and beat patterns should therefore be treated as separate event, as both contribute to ciliary function in general.

Apart from CBF and beat patterns, other parameters have been suggested to contribute to the general ciliary function. Beat amplitude is the distance the tip of a cilium travels in one beating cycle. It has been shown that the exposure to highly viscous material atop the cilia reduces the beat amplitude (132), with an acute increase in CBF followed by persistent CBF reduction (119, 132). Using atomic force microscopy (103, 104), it has been revealed that the reduction in amplitude is due to regulated changes during the recovery stroke, i.e. the cilium does not bend as backward as usual to achieve the faster CBF.

In spite of the presence of an efficient mucociliary clearance, antigenic materials such as bacterial and fungal protease could still go through the surface fluid layer and reach the surface of the epithelial cells. This rapidly activates the innate immune response of the epithelium, followed by the more specific adaptive immune response, to act against this invasion.

1.3.4 Epithelial innate immunity

Innate immunity is a rapid response upon the exposure of the airway surface to stimuli such as allergens and pathogens. These stimuli express conservative structures on their surfaces or as secretion, known as pathogen-associated molecular patterns (PAMPs). Typical examples of PAMPs that trigger airway innate immune response are allergens such as dust mite, pollen and mould, pathogens, and airborne pollutants, such as ozone, nitric oxide and other reactive species. Damage-associated molecular patterns (DAMPs) are danger signalling molecules endogenously produced by infected cells. These PAMPs and DAMPs can be recognised by pathogen recognition receptors (PRRs) expressed on airway cell surfaces, which activate the downstream inflammatory responses.

PRRs	TLR1	TLR2	TLR3	TLR4	TLR5	TLR6	TLR7
Dimerisation	TLR2	TLR1/6	(TLR3)	(TLR4)	(TLR5)	TLR2	-
Location	PM	PM	ER	PM	PM	PM	ER
PAMPs	LPP	LPP, LPS	Double-stranded (ds)RNA	LPS	Flagellin	LPP	Single-stranded (ss)RNA
PAMP source	Gram+ve bacteria, fungi	Gram+ve bacteria, fungi	Viruses	Gram-ve bacteria	Bacterial flagellum	Gram+ve bacteria, fungi	Viruses
DAMPs	-	-	-	HMGB1 HSP	-	-	-
PRRs	**TLR8**	**TLR9**	**TLR10**	**TLR11**	**RAGE**	**CD14**	**P2X**
Dimerisation	-	(TLR9)	TLR1/2	?	-	-	-
Location	ER	ER	PM	PM	PM	PM + ER	PM
PAMPs	ssRNA/ dsDNA	Unmethy-lated DNA, CpG DNA	?	Profiling-like molecules	-	LPS	-
PAMP source	Bacteria, Viruses	Bacteria	?	*Toxo-plasma*	-	Gram-ve bacteria	-
DAMPs	-	-	?	?	HMGB1	HMGB1 HSP	ATP

TLR, Toll-like receptor; PM, plasma membrane; ER, endoplasmic reticulum; LPP, lipoprotein; LPS, lipopolysaccharide; HMGBs, high mobility group box 1; RAGE, receptor for advanced glycation end products; HSP, heat shock protein; ATP, adenosine triphosphate.

Table 1.3 Pathogen recognition receptors (PRRs) and their pathogen-/danger-associated molecular patterns (PAMPs/DAMPs) recognition. PPRs may express on cell surface or intracellular. They recognise specific PAMPs, mostly inhaled microbial components, and DAMPs such as HMGB1, HSP and ATP produced by molecular signalling pathways. TLR-10 and TLR-11 were recently identified with PAMPs/DAMPs yet to confirm (78, 133-136).

1.3.4.1 Initiation

As the first barrier of defence, the airway epithelium expresses a range of PRRs, including cell surface Toll-like receptors (TLRs), secretory surfactant proteins and cytosolic CD14 that recognise PAMPs/DAMPs (**Table 1.3**). Toll-like receptors (TLRs) are a class of pattern-recognising molecules expressed on the epithelial cell surface (137, 138). To date there are 11 TLRs (78), each specifically recognising different PAMPs (78, 135, 136). Interactions between TLRs and PAMPs/DAMPs activate downstream inflammatory pathways leading to the secretion of a vast variety of (pro) inflammatory mediators from the epithelial cells.

1.3.4.2 Facilitation

Innate immunity is facilitated and maintained by concurrent cell filtration and activation by epithelium-derived (pro-)inflammatory mediators: CCL2, CCL20 (139) and IL-12p40 (140) are macrophage chemokines; CXCL8 (141, 142) induces neutrophil chemotaxis and activation; CCL11 (143) and IL-5 (144) are involved in the eosinophils infiltration. These inflammatory cells (32, 135), as well as other structural cells such as smooth muscle cells (145), also express surface TLRs that recognise PAMPs/DAMPs. Activated macrophages and neutrophils actively phagocytose and eliminate pathogenic molecules by oxidative burst (146, 147). Resident IgE promotes recruitment and activation of mast cells. Mast cells and eosinophils eliminate allergenic reagents by degranulation.

Apart from inflammatory cell recruitment, the epithelium is also responsible for cell activation by secreting cytokines. When there is a PAMP/DAMP-PRR interaction induced by allergens, epithelial cells secrete T_H2 cytokines, such as IL-4, IL-5 and IL-13. On the other hand, if the immune response is initiated by infection, T_H1 cytokines, such as IL-6; CXCL8 (IL-8) and IFNs are released. The airway epithelium also potently secretes TNF-α and TGF-β (148). These cytokines help to recruit and activate downstream airway structural and inflammatory cells in/to the mesenchymal region to facilitate innate response. Other activated airway cells also secrete different cytokines and chemokines to cross interaction with one another. TNF-α and IL-1 cytokine family from activated epithelium and macrophages maintain epithelial activation (142, 149). CXCL8 from activated macrophages and neutrophils enhance neutrophil recruitment and activation (142). T_H2 cytokines IL-4 and IL-13, TSLP, IL-1 cytokines and IFNs from the activated epithelium drive further epithelial activation (142, 150). Reactive

species from activated epithelium (151), neutrophils and macrophages may also promote signalling cascades that require them as the second messengers (152-154). These complex cell-mediator interactions across cell types generate a positive feedback loop that persist inflammation.

1.3.4.3 Bridging adaptive immunity

More specific adaptive immunity is initiated after the activation of innate immunity (150). TLR-mediated activation of the epithelium secretes chemokines CCL2 and CCL20 to recruit dendritic cells (DCs) (139). It secretes IL-6, IL-17-like innate cytokines TSLP, IL-33 and GM-CSF to active DCs (150, 155, 156). DCs also express surface TLRs. On activation these cells can actively recognise DAMPs and present them to naïve T cells, and initiate and determine T cell and B cell differentiation. Meanwhile, the activated epithelium also secretes T_H2 cytokines, such as IL-4 and IL-13 on allergic response, and T_H1 cytokines IL-10 and interferons (IFNs) on pathogenic colonisation and infection. These cytokines determine the fate of T cell differentiation and thus the adaptive immune response by facilitating either T_H2 or T_H1-dependent inflammatory pathways. Polarised DCs and T cells further secrete corresponding cytokines that feedback to the upstream epithelial cells to enhance the corresponding differentiated immune response.

1.3.4.4 Ubiquitous antimicrobial peptides

Airway epithelium-derived antimicrobial peptides, particularly human β-defensins (hBDs), play a major role in the defence function of the ASF. hBDs are characterised by the presence of a 6-cysteine motif, a β-hairpin structure, and high arginine/lysine contents (157). To date there are 10 hBDs found in human (158), with hBD-1-4 being

found in human airway epithelium (159-162). hBD-1 is constitutively expressed in airway epithelial cells (159); hBD-2 and hBD-3 can be rapidly induced upon microbial exposure via LPS-TLR cascade and IFN signalling pathways, and inflammation via the TNFα pathway (161, 163, 164). Both hBD-1 and hBD-2 have a wide range of antimicrobial activity targeting bacteria (165), fungi (166, 167) and viruses (165, 168). hBD monomers polymerise and penetrate into the microbial membranes with their cationic nature (169). Increased membrane permeability leads to microbial cell lysis and death. The maintenance of the ASF ionic charge (95) is crucial to hBD function (170, 171).

Recently evidence also suggested a role of hBDs other than its anti-microbial property. All hBDs has been shown to induce macrophage and mast cell migration via a MAP-kinase signalling pathway (172). hBD-2 may recruit immature DCs and naïve T cells (173). Moreover, hBD-3 has been shown to activate macrophages and DCs via a TLR-dependent cascade (174), which in turn induces TLR expression (174, 175). All these evidence suggest that hBDs may bridge innate and adaptive immunity by modulating TLR signalling pathways on airway cells.

1.3.5 Epithelial abnormality in asthma

1.3.5.1 Structural abnormality

The airway epithelium in asthma is structurally abnormal. Reductions in ZO-1 (64) and E-cadherin (176), and an increase in soluble E-cadherin (177) imply the presence of damage to TJs and AJs and a consequent in the barrier function of the epithelium. The loss of TJs comes with the disruption in the epithelial layers. Cell shredding and gaps have been observed (178). The loss of integrity was found to correlate to disease

severity (179). Some have showed a defective apoptosis of epithelial cells causing regional epithelial cell metaplasia (178), which may be caused by abnormal gene expression (178, 180) and/or viral infection (181, 182). This is in agreement with the hypothesis that an impaired repair system is present in asthmatic airways. Sub-epithelial fibrosis has been observed with an increase in collagen IV derived from the epithelial cells. The thickening of the lamina reticularis, on the other hand, was found predominantly in asthmatic airways with eosinophilia (23), suggesting the presence of a specific remodelling pathway in response to the epithelium-eosinophil interaction leads to this structural abnormality.

These features persisted in culture when the asthmatic epithelial cells were differentiated into the ciliated air-liquid-interface (ALI) – cell cultures with multiple cell layers that resemble the *in vivo* epithelial structure. A significantly higher level of cytokeratin-5-positive cells has been found in asthmatic ALI cultures compared to healthy controls (176), which suggests that asthmatic cells may have an intrinsic deficiency in differentiation. Structurally, TJ proteins, such as ZO-1 and occludin were irregularly expressed on cell borders (183). Asthmatic ALI cultures possessed a significant reduction in E-cadherin (176), ZO-1 and TEER (183) as shown *in vivo*. The thickness of basement membrane and epithelial thickness and mucin production were found significantly higher in asthmatic ALI cultures (184). The contribution of epithelial cells to wound healing has also been found altered in asthmatic cultures. Fibronectin mRNA and protein expression has been found reduced in ALI cultures, which directly impacted the rate of wound closure (185).

Epithelial-mesenchymal transition (EMT) is another phenomenon found in asthma, meaning the epithelial cells undergo dysregulated differentiation due to the loss of TJs followed by the loss of cell polarity, or a de-differentiation into potentially other mesenchymal cell types, such as fibroblasts (186, 187). This transition is likely to be induced by the constantly elevated TGF-β and TNF-α levels observed during persistent asthmatic inflammation (186, 188, 189).

1.3.5.2 Abnormal mucociliary clearance

The presence of occluded airways is one of the features found in subjects who died as a consequence of asthma (190), suggesting that mucociliary clearance in these airways is prone to be inefficient in disease. In fact, the abnormal mucociliary clearance is likely to arise as a result of a mucus dysfunction, as well as a defective ciliary function in asthma.

Goblet cell hyperplasia is a common feature in both childhood and adult asthma (191, 192), leading to mucus hypersecretion. Mucins MUC5AC and MUC5B have been found to be up-regulated in asthma and to correlate with disease symptoms (193). In fact, the compositions and the characteristics of mucus in asthmatic airways have been found to be abnormal. Asthmatic mucus contains an elevated amount of MUC5AC, proteins, lipids, cell-specific mediators and ions (176, 194-196). These features persist in differentiated cultures derived from asthmatic subjects. Epithelium-derived EGF has been identified as the key growth factor, which promotes goblet cell hyperplasia by down-regulating the expression of the FOXa2 transcription factor that suppress epithelial cell trans-differentiation (197). Elevated IL-1β secretion in asthmatic airways (198) has also been shown to activate mucous cell metaplasia (transformation of the cells from a normal state to an abnormal state) and MUC5AC production (199, 200), via

the cAMP-dependent, p38 MAP kinase pathway (201). This collective evidence suggests that the persistent inflammation in asthmatic airways is highly associated with ASF dysregulation. Interestingly, there is emerging evidence suggesting that ASF dysregulation is specific to the eosinophilic asthma subgroup (202, 203). For instance, Gob-5, a calcium-activated chloride channel on airway epithelium, has been found to be responsible for goblet cell hyperplasia, but only in allergen-induced, but not bacterial-induced inflammation (204). T_H2 cytokine IL-13 has also been shown to elevate mucin production (197, 205). This evidence further indicates that heterogeneity of asthma indeed spans across different scales, at both a cellular level and a tissue level.

In addition to the presence of excess mucus in the airways, the ciliary function of the asthmatic epithelium has been found to be abnormal (68). By monitoring radiolabeled aerosols, it has been revealed that asthmatic airways have higher depositions (206, 207) and lower rates of clearance (208, 209). A recent study using advanced high-speed video-microscopy provided further indications that asthmatic ciliary dysfunction is caused by a reduction in CBF and an elevation in ciliary dyskinesia and immotility (210). Using electron microscopy, it was revealed that cell shedding and the loss of cilia were evident in asthmatic bronchial biopsies (100, 194), and was not correlated to the asthmatic age groups (176). These abnormalities are also correlated to asthma severity. It has been suggested that >50% damage of the bronchial ciliary apparatus is required to cause significant reduction in mucociliary clearance (194). However, interaction between other elements, such as inflammatory mediators and different cell types, should also be taken into account. Hydrostatic pressure could affect the polarity across the epithelium (90) and ion channel expression (211); whether the water content of the ASF also contributes to the ASF abnormality has yet to be confirmed. Indeed, asthmatic

mucus has been found to be more viscous and elastic due to the high mucin and plasma protein levels (195, 196) that cannot be digested (212). Plug formation could therefore increase the burden on the cilia and hence further obstruct the ciliary function (132). The spontaneous sputum production in asthmatic subjects implies the accumulation of inhaled particulates, microbes in particular, that can only be cleared away by coughs (95). This reflects the inefficient mucociliary clearance. It is noteworthy that none of these reports has proposed any plausible mechanisms that may explain the presence of ciliary dysfunction in asthma.

The inefficient mucociliary clearance increases the exposure of the epithelium to the trapped PAMPs and DAMPs. Without a normal innate and adaptive immune response, these particulates are able to worsen epithelial degradation and activation leading to a recurring colonisation/infection. A persistent immune response therefore gradually develops.

1.3.5.3 Abnormal persistent immune response

Asthma is a chronic inflammatory disease with persistent inflammation (148, 150). Gene polymorphisms were found in crucial innate immunity proteins, such as TSLP (213) and TLRs (214), and hence their altered expression pattern may lead to hypersensitivity of the cells to stimulation (150). It has been shown that the asthmatic epithelium hyper-secretes chemokines, such as GM-CSF (215) and cytokines, such as IL-33 (216), IL-1β (198) and TGF-β (186, 188), which enhance both structural and inflammatory cell activation. IL-13 is another up-regulated cytokine in asthmatic airways, and has been demonstrated to affect the wound healing process by altering epithelial cell differentiation and thus the epithelial regeneration (217). Deficiency in

epithelial IFN types I and III (181, 182) suggested an increased susceptibility to prolonged infection, particularly by viruses, in the airways. Persistent activation of the airway epithelium also implies a continuous generation of reactive species (218, 219), putting the airways under an oxidative burden that could prolong downstream pathway activation (153, 154, 220) and may cause intracellular damage (221, 222). Indeed, this prolonged inflammation persists in asthmatic cultures. Similar to the structural outcomes, asthmatic ALI cultures possess the abnormal pro-inflammatory secretory profile observed *in vivo*. The baseline secretions of IL-8 (184, 223), TGF-β2 (224), ICAM-1 and GM-CSF (223) were found to be significantly higher from asthmatic cultures compared to those from healthy controls. This suggests that asthmatic epithelial cells may be intrinsically active. Furthermore, asthmatic cultures produced a significantly higher induced level of IL-8 and GM-CSF compared to healthy controls (184, 223). CCL5 (RANTES), a chemokine for eosinophils, T cells and basophils, was suggested to be expressed specifically in asthmatic ALI cultures (223). In addition, lipoxin LXA_4, which is a metabolite formed by lipoxygenase isoenzzymes, was found to be down-regulated in asthmatic ALI cultures (184). This implies that a dysregulated inflammatory response is present in asthmatic cells that could result in persistent chronic inflammation.

The presence of heterogeneity in the inflammatory cell profiles of asthma suggests differential immune responses to stimuli, but little is known about their underlying mechanisms. It is generally believed that eosinophilic and neutrophilic asthma are initiated by different sensitivities to allergens and non-allergenic stimuli, which respectively leads to the development of T_H2 and T_H1-driven inflammation. Indeed, the elevated level of CXCL8 has only been found in association with infection (142). On

the other hand, the elevation in T_H2 cytokines, such as IL-4 (52) and IL-13 (225, 226) were mostly found in atopic/eosinophilic asthmatics. However, viral infection (227) and the epithelial tolerance to low levels of infections (228) that induces a T_H2 response suggest that crosstalk is present between the two inflammatory profiles.

A prolonged inflammatory response leads to a dysregulated repair mechanism due to the persistent cell activation that can eventually result in airway remodelling. The effect of an abnormal extracellular matrix environment on cell behaviour is discussed in later sections. On the whole, the dysregulated intrinsic cellular regulation, together with the presence of an abnormal micro-environment, form a positive feedback loop across different scales leading to a persistent immune response in the asthmatic airways.

1.3.6 Existing treatments that improve asthmatic airway epithelial function

There is currently no specific treatment that targets the abnormal epithelial features or functions in asthma. However, other asthma treatments have been shown to improve asthmatic epithelial functions. Inhaled corticosteroids have been shown to reduce basement membrane thickening (229, 230). EGF treatment may promote TJ formation (183) and thus improve barrier function. Both SABA and LABA β2-agonists have been shown to stimulate CBF. Salbutamol is a SABA, which was shown to have a transient stimulatory effect on CBF *in vitro* (43) and in a murine model *in vivo* (231). It may also improve the composition of the periciliary fluid to facilitate more efficient mucus propulsion (231). In comparison, salmeterol, as commonly used LABA, was shown to improve CBF and mucus transport efficiency (41) and to do this with a more prolonged effect (43). Both types of β_2-agonist are likely to act via a cAMP/$[Ca^{2+}]_i$ pathway (43, 232). Leukotrienes receptor antagonists are another type of anti-inflammatory treatment

for asthma. Leukotrienes (Cys-LT) are potent inflammatory mediators that have been found to be elevated in asthmatic BAL (233). Previous evidence showed contradictory results in their stimulatory effect of LTD_4 and ciliary function (234, 235). On the other hand, leukotriene receptor antagonists such as Zafirlukast (233) and Montelukast (235) have been shown to improve CBF and potentially prevent Cys-LT-induced ciliary dis-orientation. It has also been shown that female patients might be more susceptible to damages due to interactions between the sex hormone progesterone and its receptor (PR), and a selective PR modulator may improve ciliary function of these female individuals (236).

1.4 Microbiology in Asthma

1.4.1 Overview

A microbiota exists from, or even before birth in body lumens, such as the intestines and airways (237). This microbial community contains a huge diversity of microbes, including bacteria and fungi, with most species present yet to be identified due to the limitations in current technology (238). A normal microbiota with high microbial diversity is important in the host-defence system (237). The beneficial effect could be due to the counterbalance between constitutive T_H2 responses triggered by the allergen and the T_H1 responses triggered by low profile microbial colonisation (239). It could also be simply down to the local commensals acting as a physical barrier against colonisation by allergens and other pathogens. The lack of commensals causes a deficiency in allergen-induced inflammation (240). On the other hand, over-flourishing microbiota leads to infection.

As the first line of defence, the airway epithelium is able to recognise the colonisation/infection of microbes overloaded above the mucus lining the surface and those penetrated the peripheral fluid to the epithelium. TLRs on the airway cell surfaces sense PAMPs and DAMPs. Bacterial LPS (endotoxin) and flagellin, microbial toxins such as fungal gliotoxin, viral surface glycoproteins HA and NA, and microbial single-/double-stranded DNA/RNA are all PAMPs, recognised by different TLR isotypes (135). High microbial interaction with TLRs rapidly activates the innate immune response that drives a T_H1-dependent inflammatory process. Other PAMP-recognition receptors on the epithelium include CD14 and surfactant proteins (136). Persistent and abnormal colonisation/infection therefore prolongs the inflammatory process leading to chronic inflammation as found in asthma.

1.4.2 Asthma-related microbes

It has been generally accepted that pathogens play a major role in asthma exacerbation. Viral infection has been a popular field of study due to its role in both childhood and adult asthma in terms of symptoms and disease progression (241, 242). For instance, Chilvers *et al.* showed that coronavirus reduced epithelial function by disrupting the epithelial integrity, reducing the CBF, and increasing ciliary dyskinesia and immotility (69). On the other hand, the roles of other airway microbes, such as bacteria and fungi have recently emerged. The microbial community in asthma has been found abnormal, with less microbial diversity, but higher bacterial contents (243, 244).

1.4.2.1 Bacteria

It is generally accepted that bacteria play a major role in asthma exacerbation. For instance, infection by *Chlamydia pneumoniae* and *Mycoplasma pneumoniae* (245) has been shown to correlate to acute exacerbation in severe asthma (246). Recent evidence further suggests the roles of bacteria in asthma development and progression. The association between the presence of bacteria in asymptomatic infants and the onset of asthmatic symptoms (247) suggests that an early bacterial exposure could be a predisposing factor for asthma. Positive serology for intracellular pathogens is associated with airflow obstruction (248). Their presence in stable asthma from recent reports further suggests their role in disease progression (249, 250). A low profile asymptomatic colonisation may promote and maintain allergic inflammation (251) in the early stages of disease development. A recent study by Hilty *et al.* (243) reported an altered microbial community in the airways of mil-to-moderate asthmatic subjects across all ages. Species that are present in normal microbiota, such as the phylum

Bacteroidetes, were found significantly less frequently in the disease samples. In comparison, pathogenic bacteria including members of the phylum *Proteobacteria* (e.g. *Haemophilus*), *Staphyloccocus* and *Streptoccocus* were found significantly more frequent in disease samples. This altered microbiota persists in stable asthmatics (244). Huang *et al.* reported a significantly higher bacterial 16S load in the fresh bronchial brushings from stable adult asthmatics compared to healthy controls, and this was inversely correlated to airway hyperresponsiveness (AHR). Their results also suggested that specific phylotypes, such as *Nitrosomonadaceae*, *Comamonadaceae* and *Oxalobacteraceae* were likely to be responsible for the AHR. These results demonstrated that bacterial colonisation/infection is highly correlated to the chronic inflammation and the progression of asthma.

Microbial products from bacteria, such as *Streptococcus pneumoniae* (252), *Pseudomonas aeruginosa* (34, 253, 254) and *Haemophilus influenzae* (255), have been shown to directly reduce CBF. LPS (endotoxin) are glycoproteins found in the cell wall of Gram-negative bacteria, including *P. aeruginosa*, *H influenza*, and *Clamydiapneumoniae* that are commonly found in asthmatic airways (243, 256). They contain a common, conserved structure with different acylated Lipid A chains that contribute diversity to TLR recognition (257). It is Lipid A that is recognised by surface-expressed TLR2 (133) and surface-expressed or intracellular TLR4 (258) of epithelial cells. Effects of bacteria and their products on ciliary function could be attenuated or reversed by specific macrolides (254), suggesting their direct role in inhibition on ciliary function.

1.4.2.2 Fungi

Fungi are ubiquitous airborne microbes (259), and have been shown to be associated with asthma-related complications, such as allergic bronchopulmonary aspergillosis (ABPA). *Aspergillus* is one of the common fungal species associated with pulmonary diseases, and plays a major role in ABPA, with *A. fumigatus* colonisation was reported in up to 8% asthmatic patients (260), while at least 16% of asthmatics have a positive reaction to a skin prick test to *Aspergillus* (261). Association of ABPA with eosinophils (262) and neutrophils (263, 264) have been reported. *A. fumigatus* colonisation is also correlated to airflow obstruction (264).

1.4.2.3 Treating infection in asthma

Macrolides are a group of semi-synthetic antibiotics possessing a large macrocyclic lactone ring as a common structure (265), and acting as antibacterial protein synthesis inhibitors, or as immunomodulators (266). They have been shown to be effective in treating infections associated with asthma. The use of telithromycin improved recovery rate after exacerbation (267). Antibiotics have been shown to improve pathogen-induced ciliary dysfunction (254) and epithelium quality (268). In particular, clarithromycin can also lessen hyperresponsiveness (269) and reduce airway inflammation (270) by modulating neutrophil chemotaxis in neutrophilic asthmatics (32, 271, 272). Some have shown no corticosteroid sparing effect in asthmatic children (273), while the others have suggested an interaction with oral corticosteroid to cause an adverse effect (274). On the other hand, anti-fungal treatments may (275) or may not (276) be used in association with corticosteroid. Anti-fungal treatments have been shown to be beneficial, but only in certain groups of asthmatics (263), suggesting different microbial colonisation profiles may exist in different subgroups of asthma.

Side-effects when prescribed in association with corticosteroid (275) may reflect their usage in corticosteroid-insensitive asthmatic patients who were mostly neutrophilic (25).

1.5 Oxidative Stress in Asthma

1.5.1 Overview

A balance between oxidant and antioxidant activities is important in maintaining a normal cellular physiological status. They control the intracellular levels of free radicals and reactive species, including reactive oxygen species (ROS) and reactive nitrogen species (RNS), which are important in cell function and survival. Oxidative stress is caused by an imbalance between the production and removal of reactive species, leading to an oxidative burden. This results in oxidative damage that may exacerbate the degree of imbalance. This defect in oxidative handling is common in a wide range of diseases, including asthma.

1.5.2 Oxidative pathways to maintain oxidant/antioxidant balance

Oxidants are oxidising agents that are chemically active and oxidise another reactant through the removal of an electron (218, 277). Common intracellular free radicals include ROS superoxide ($O_2^{\bullet -}$) and hydroperoxyl ($HO_2^{\bullet}$), and RNS nitric oxide ($NO^{\bullet}$) and peroxynitrite ($ONOO^-$). They are all chemically very active in oxidising other molecules. Therefore, it is essential to remove any excess to prevent disturbances in normal cellular homeostasis. Hydrogen peroxide (H_2O_2) is not a free radical due to the lack of an unpaired electron, but is a ROS that is active enough to cause oxidative damage. On the other hand, antioxidants are reducing agents that normally replace a missing electron of another reactant, usually a reactive species in the oxidative pathway. They are either enzymes or non-enzymatic scavengers that convert reactive species to chemically stable molecules that can be removed, or used in other pathways during normal physiological conditions. The common intracellular sources of reactive species are mitochondria and peroxisomes. In airways structural and inflammatory cells,

including epithelium and leukocytes (such as neutrophils and eosinophils), act as the extracellular sources for the surrounding environment (219). **Figure 1.7** summarizes the major oxidative pathways that are known to be important in maintaining an oxidative balance.

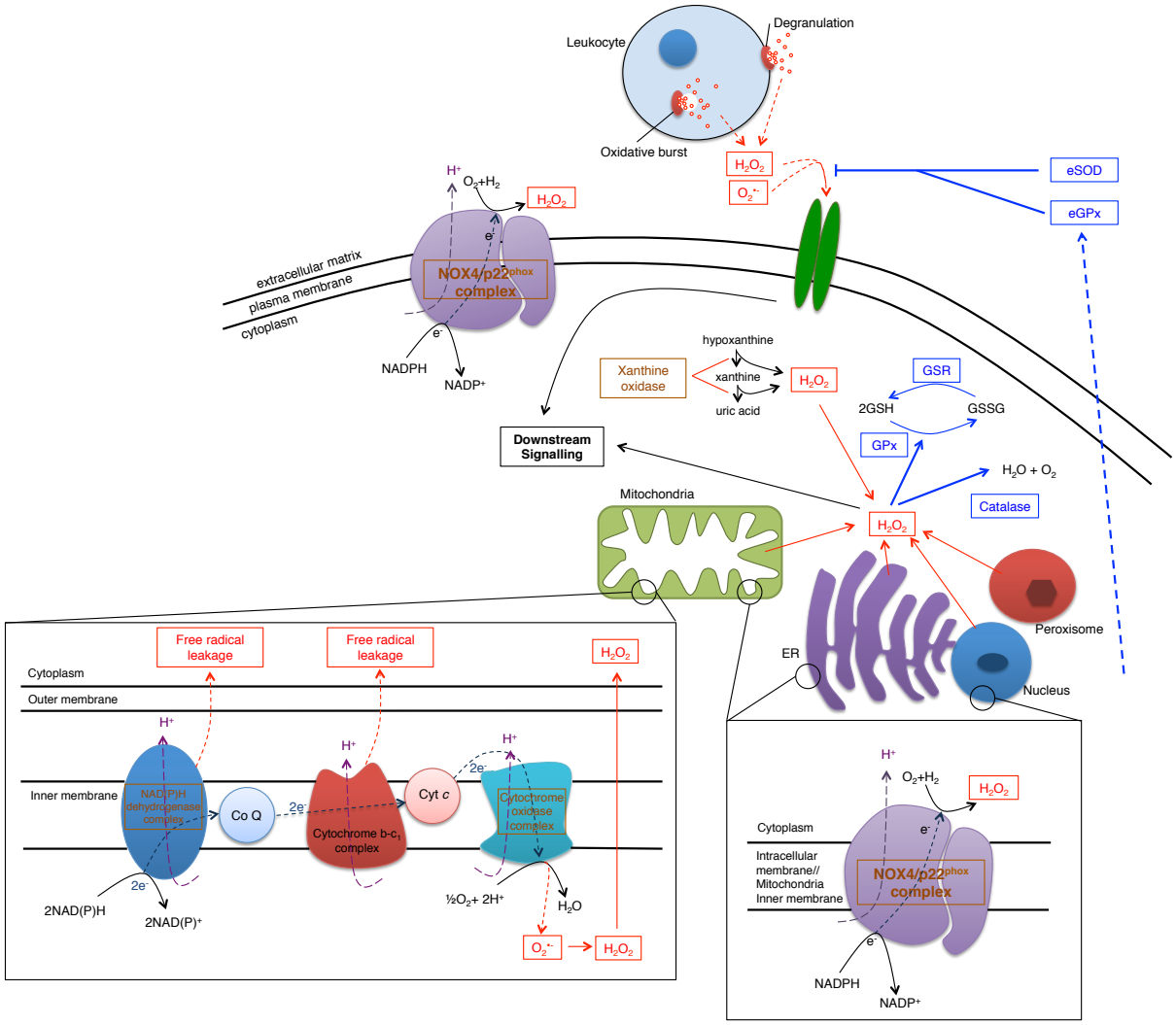

H_2O_2, hydrogen peroxide; $O_2^{\bullet-}$, superoxide; eSOD, extracellular superoxide dismutase; eGPx, extracellular glutathione peroxidase; NOX4, nicotinamide adenine dinucleotide phosphate (NADPH) oxidase; GSR, glutathione reductase; ER, endoplasmic reticulum; Co Q, coenzyme Q; Cyt c, cytochrome *c*.

Figure 1.7 **Oxidative pathways to maintain oxidative balance.** The mitochondria are known as the major source of intracellular reactive species due to free radical leakage from the electron transport chain. Extracellular sources of reactive species include inhaled particulates and the surrounding activated cells such as leukocytes. In particular, NADPH oxidases has recently be recognised as a major source of reactive species due to the localisation in multiple organelles. To main oxidative balance, enzymes generate antioxidants to uptake the unstable electron from the oxidants. Keys: reactive species (in red); oxidants-generating enzymes (in orange), antioxidants-generating enzymes (in blue) (218, 219, 277, 278).

A regulated level of reactive species is essential in maintaining normal cellular function and immunity (279-281). ROS can also act as second messengers downstream of G-protein coupling receptors, and have been shown to be important in cell proliferation (153, 154) and regulated apoptosis (282, 283). During a normal immune response, ROS are generated in leukocytes to facilitate their antimicrobial function (146, 218). As for RNS, $NO^{\bullet}$ at the low concentrations generated by constitutive nitric oxide synthase (eNOS), regulates cellular physiology, such as ion channel expression on airway epithelium (220) and function, such as smooth muscle cell relaxation (284). $NO^{\bullet}$ generation by inducible NOS (iNOS) in leukocytes (285) also facilitates oxidative burst activity. As a result, it is important to maintain the oxidant/antioxidant balance in order to regulate the normal physiological redox environment.

1.5.3 SOD

Superoxide dismutase (SOD) is an antioxidant that converts the reactive free radical superoxide ($O_2^{\bullet -}$) to the less reactive hydrogen peroxide (H_2O_2) and water (**Figure 1.7**). There are three types of SOD in human cells, each is a tetramer requiring ions as co-factors to function - SOD1 and SOD3, or Cu-Zn-SODs, binds copper and zinc ions; SOD2, or Mn-SOD, binds manganese ions; SOD3 also binds nickel ions. SOD1 can be found in the cytosol of cells, SOD2 is localised to the mitochondria and SOD3 is found in the extracellular matrix (286, 287).

1.5.4 Catalase

H_2O_2 resulting from SOD activity is quickly reduced by catalase. Catalase is an antioxidant that is commonly found in human cells both intracellularly and extracellularly. It is also a tetramer with four heme groups that form the active site for

the binding of H_2O_2 followed by its reduction to water and oxygen (**Figure 1.7**) (219, 288).

1.5.5 Glutathione peroxidases and the glutathione redox cycle

The glutathione redox cycle is another anti-oxidative mechanism that is in place to destroy H_2O_2 (**Figure 1.7**). Glutathione peroxidase (GPx) reduces H_2O_2 by using glutathione (GSH) as the electron donor to reduce H_2O_2 to water and oxygen and form glutathione disulphide (GSSH), an oxidised form of GSH, in order to compensate the loss of the electron. There are four GPx homologues, with GPx-1 (ubiquitous cellular GPx) and GPx-3 (extracellular) being predominantly expressed in human lungs. With the aid of glutathione reductase (GSR), GSSH can be reduced back to two GSH molecules to resupply co-substrate for the redox cycle (219, 289).

1.5.6 NOX

Nicotinamide adenine dinucleotide phosphate (NADPH) oxidase (NOX) is an oxidant because its catalytic reaction generates ROS. It was first identified as a cytochrome b_{558} subunit $gp91^{phox}$ on the plasma membrane of leukocytes, including macrophages and neutrophils, which carries out an antimicrobial function and was known as the phagocytic oxidase (phox) (278). Cytochrome b_{558} is composed of a heme-binding subunit $gp91^{phox}$ and a membrane-binding subunit $p22^{phox}$. To date there are 7 homologues of NOX identified: NOX1-5 and DUOX1 and DUOX2 (278), while NOX2 is equivalent to $gp91^{phox}$. They are a family of membrane-integrated enzymes consisting a common core of 6 transmembrane spanning units with 2 heme-binding domains, and a C-terminal dehydrogenase domain for both flavin adenine dinucleotide (FAD) and NADPH binding. The common core resembles the cytochrome b_{558} $gp91^{phox}$ /NOX2

component, with the $p22^{phox}$ component retained for recruitment and membrane binding function (290). NOX5 and DUOX1 and DUOX2 contain an extended N-terminus with EF-hands for Ca^{2+} regulation (278) (**Figure 1.8**).

Apart from NOX4, functional NOX proteins are plasma membrane-associated enzymes (278, 291-293). Cytosolic NOX proteins are recruited to the plasma membrane by associating with the component $p22^{phox}$ (290, 294). Once integrated to the plasma membrane, the cytosolic component $p47^{phox}$ is recruited. Acting as an adaptor protein, $p47^{phox}$ then recruit component $p67^{phox}$ and the small GTPase, Rac, which together act as a catalytic regulator. The C-terminus of NOX protein complex then allows the intracellular binding and oxidation of NADPH to $NADP^+$ (295), with the electrons trafficking via FAD in the dehydrogenase domain, through the two heme groups in the NOX protein domain, then to the extracellular side for ROS generation (296). NOX1 to NOX3 homologues generate $O_2^{\bullet-}$ from O_2, while NOX4, DUOX1 and DUOX2 produce H_2O_2. NOX5 may produce both ROS (293, 295).

All NOX expression, apart from NOX3, has been consistently reported in airway epithelium with differences in a constitutive and an induced expression levels (296-298). Among these, DUOX1, DUOX 2 and NOX4 are receiving increasing attention due to their association with diseases, including asthma.

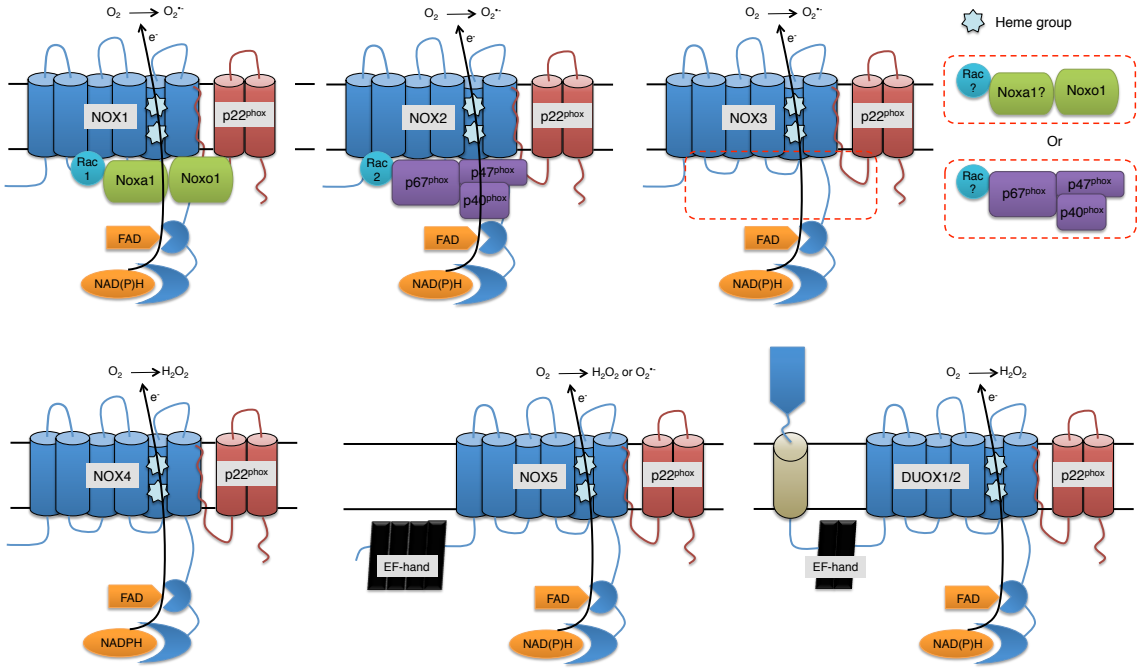

Figure 1.8 NADPH oxidase (NOX) homologues. NOX are superoxide/hydrogen peroxide producing enzymes. To date there are 7 NOX homologues consisting different subunits. All NOX require the interaction with $p22^{phox}$ the membrane-association component. NOX1-3 requires to recruitment of cytosolic subunits. NOX4 does not require any cytosolic subunits to function. NOX5 and DUOX1/2 contain EF-hand suggesting calcium sensitivity (278).

1.5.7 DUOX1 and DUOX2

Dual oxidase 1 and 2 (DUOX1 and DUOX2) were first described in mammalian thyroid gland (299). They contain a $gp91^{phox}$ domain, two EF-hand motifs and an N-terminal extracellular peroxidase-like domain (**Figure 1.8**) (278). The EF-hand subunit contains Ca^{2+} binding site, which suggests that DUOX1/2 activities are modulated by $[Ca^{2+}]_i$. Both DUOX1 and DUOX2 have been found abundantly expressed in human airway epithelium (296, 300). DUOX1 expression in airway epithelium could be induced by T_H2 cytokines (299). DUOX1-derived ROS has been shown to cause mucus hypersecretion (301). DUOX2 has been shown to be responsible for the ROS generation in human airway epithelial cells upon microbial and/or T_H1 cytokine simulation (299, 302). DUOX enzymes are also believed to contribute to the host defence system by

producing H_2O_2, which supports the anti-microbial activity of lactoperoxidase that is present in the ASF of human airways (303).

1.5.8 NOX4

NOX4 was first described in renal epithelial cells, sharing 35% sequence homology to $gp91^{phox}$/NOX2 (304). The regulation of NOX4 gene expression is still unclear, and might be via nuclear factor (erythroid-derived 2)-like 2 (Nrf2) (305). It has been suggested that once recruited to the membrane, NOX4 protein is able to generate ROS without further stimulation (290, 304). Therefore, it is plausible that NOX4 activity can be determined by its expression level alone other than its localisation. In fact, it has been shown that NOX4 and its membrane recruitment component $p22^{phox}$ are able to regulate each other (290).

1.5.8.1 Unique NOX4 structural function and intracellular localisation

Using mutational and functional analysis, it has been revealed that NOX4 has a unique functional characteristic. Similar to other NOX homologues, a cytosol to membranes translocation of NOX4 with the $p22^{phox}$ component is essential (290, 292, 294). However, only an intact N-terminus of the $p22^{phox}$ molecule, which faciliateds NOX4 integration, is required for NOX4 function (292). Unlike other NOX isoenzymes, the recruitment and interaction with other cytosolic components $p40^{phox}$, $p47^{phox}$, $p65^{phox}$ and Rac are not necessary (290, 295). Unlike NOX2 (290, 292), but similar to NOX1 (290), the localisation of the NOX4/$p22^{phox}$ complex has been found in the nucleus, plasma membrane and internal membranes (290, 292), mitochondria (306, 307) and ER (308). This suggests NOX4 may regulate ROS level both intracellularly and extracellularly.

To date there are four NOX4 isoforms (309), with the fourth one predicted to give rise to a nonsense-mediated decay of the protein. The localisation of each isoform has not yet been elucidated, although attempts have been made to dissect differential subunits and their function (310).

1.5.8.2 NOX4 expression in the lung

In human airways, NOX4 is expressed in pulmonary vascular endothelium (305), vascular smooth muscle cells (311), (myo-)fibroblasts (312, 313), airway epithelium (297, 298), and HASMC (314-316). Its baseline expression level in the airway epithelium and ASM is very low. ROS generation from NOX4 and NOX2 may have a compensatory mechanism in vascular cells (305). However, it is believed that in the airway epithelium DUOX1/2 are the major ROS regulators for epithelial antimicrobial function (278, 296, 317). On the other hand, NOX4 expression has been shown to be substantially inducible on PDGF, H_2O_2 or TGF-β stimulation (297, 313), with or without DUOX2 (302), suggesting NOX4 may in fact play an important role in oxidative handling in airway epithelial cells.

1.5.8.3 NOX4 cellular function

It has been shown that NOX4 produces predominantly H_2O_2 (292, 295), with a very low profile of $O_2^{\bullet-}$ production (295). $O_2^{\bullet-}$ is normally rapidly dismutated to H_2O_2 by superoxide dismutase 1 (SOD1) in the cytoplasm, and SOD2 in the mitochondria. Unlike NOX1 and NOX2 (278, 318), the function of NOX4 or NOX4-derived H_2O_2 in airway epithelial cells and the relevant mechanisms at normal physiological conditions, are not completely understood. In vascular cells, it has been shown that NOX4 regulates

ROS level via the MAPK/ERK pathway to regulate endothelial cell proliferation and survival (319). In renal cells NOX4 activity may be regulated by SOD1 and NOX1 (320). During inflammation, NOX4 may aid the antimicrobial action of inflammatory cells (321). It has also been shown to mediate LPS-induced immunity by a direct interaction with TLR-4 (279, 322). In HASM cells NOX4 modulates cell proliferation and apoptosis (314). How comparable this collective evidence is to airway epithelial NOX4 is yet established. In fact, in the literature the majority of studies on NOX4 have reported its role in disease pathogenesis.

1.5.9 Oxidative imbalance and asthma

Oxidative imbalance is a common feature of a variety of diseases including asthma (323). Evidence has shown its association with asthma in airway hyperresponsiveness (324), increased oxidative, but reduced anti-oxidative capacities (325-328) and inflammatory response (329, 330). An elevated ROS level was found in asthmatic BAL fluid and cells (327, 331). Increased exhaled $NO^{\bullet}$ level has also been found (332), and have been used as a biomarker in clinical diagnosis (131, 333, 334). Therefore, oxidative stress in asthma is orchestrated by the interaction of a range of reactive molecule species with the surrounding environment.

The oxidative imbalance in asthma is present both intracellularly and extracellularly. The leakage of ROS during oxidative respiration (335, 336) (**Figure 1.7**) makes the mitochondria one of the major intracellular sources of ROS and is believed to be the major source of oxidative stress in asthma (323). In parallel to the elevated level of reactive species, defective antioxidant pathways have been found to be associated with enzymatic SOD, catalase and GPx (277, 323), and non-enzymatic vitamins C and E

(337). Gene polymorphisms have been identified in sub-populations (16, 338, 339). This imbalance in redox environment puts the airway cells at a status of high oxidative burden. This burden causes intracellular damage in airway cells.

Damage caused by oxidative stress has been observed. Intracellular reactive species are able to react with metabolites (329, 340-342), signalling molecules (343) and genetic material (222). Exogenous reactive species could act as an "agonist" at surface receptors (344, 345). They act by altering the oxidative status and/or conformational structures of the receptors, followed by the disruption on the relevant downstream signalling pathways that lead to abnormal cell phenotypes. Furthermore, the continuous generation of mediators during asthma inflammation, such as cytokines TGF-β, IL-1 cytokine family and IFNs, and growth factors EGF and PDGF are all able to induce ROS generation in the airway epithelium (218). During inflammation, cells around the epithelium may also act as an extracellular source of reactive species. The leukocytes that are commonly found in asthmatic airways, for example, eosinophils and neutrophils, express and release reactive species that further increase the oxidative burden on the epithelium (219, 327, 346). A positive feedback loop develops, orchestrating the crosstalk between oxidant/antioxidant pathways and inflammatory pathways, and enhancing the impaired repair system in the asthmatic airways.

1.5.10 Oxidative stress and airway epithelium

Airway epithelial cells are able to produce a range of reactive species upon stimulation (347). Over-production of reactive species could cause damage to the epithelium as observed in pulmonary diseases such as asthma. Structurally, reactive species are able to disrupt the permeability of airway epithelium by targeting TJs (348). This has been

shown to be exaggerated in asthmatic airways (349). Oxidants/antioxidant expression has been found to be dysregulated in asthmatic airway epithelial cells (289, 337, 350). Furthermore, elevation in extracellular GPx (289) and SOD (351) levels has been found in the asthmatic epithelial ECM. As a result, the asthmatic airway epithelium is under oxidative stress both intra- and extracellularly. This oxidative damage of the epithelium has been shown to be correlated to airway hyperresponsiveness (352), suggesting a downstream effect of oxidative stress on the epithelium. NOX4-derived ROS was suggested to be the cause of epithelial cell death (313), leading to mesenchymal fibroblast activation, differentiation and consequently fibrogenesis (312). On the other hand, the higher expression of heat shock protein-27 in asthmatic epithelial cells upon oxidative challenge (353) may explain the epithelial metaplasia in some cases (178).

Functionally, reactive species has been shown directly affecting mucociliary clearance in the airways. Oxidative stress causes mucin hypersecretion (297, 300), leading to changes in ASF composition that may lead to ciliary dysfunction (132, 195, 196, 212). H_2O_2 stimulation on ciliary epithelial cells caused CBF reduction in a concentration-dependent manner, of which the DNA damage could be the basis of the effect (222, 354, 355). The addition of antioxidants such as catalase may reverse the H_2O_2-induced ciliary dysfunction (356). Interestingly, controlled endogenous $NO^{\bullet}$ has been shown to acutely stimulate CBF upon inflammatory stimulation (357), suggesting different reactive species may have different effects on ciliary function. Nevertheless, these pathways eventually merge at the $[Ca^{2+}]_i$ level in order to regulate epithelial ciliary function. Apart from being a source of reactive species, mitochondria also act as intracellular Ca^{2+} stores, which can be activated upon oxidative stress and other

inflammatory signalling pathways (323, 358). As a result, it is reasonable to presume a linkage between oxidative stress, mitochondria and ciliary function regulation in asthma.

1.5.11 NOX4 and asthma

NOX4 plays a role in the pathogenesis of chronic diseases, including cardiovascular disease (359), diabetic nephropathy (360) and cancer (361). To date, NOX4 has been shown to play a role in pulmonary disease, including idiopathic pulmonary fibrosis (IPF) (362), acute lung injury (363) and asthma (316).

NOX4 has been shown to cause pulmonary fibrogenesis (312, 320, 321), which was found to be mediated by activated (myo-)fibroblasts (312). In HASMC, NOX4 has been shown to mediate TGF-β induced hypertrophy (314) and hypercontractility, and is correlated to asthma (316). In the airway epithelium, NOX4 is believed to be the source of oxidative stress-induced mucin hypersecretion (297). NOX4-derived H_2O_2 in the epithelium was shown to be the cause to the epithelium-induced fibrogenesis in lung fibrosis (313). In another case, the over-expression of NOX4 was shown to cause persistent epithelial cell survival (306). In addition, NADPH has been shown to be important in antioxidant function. For example, it is required as a co-factor by GSH reductase to reduce GSSG back to its reduced GSH form for continuous ROS scavenging (364). The elevation in NOX expression and activity, together with the reduced GPx in the airway epithelium (277), therefore reflects the reduced anti-oxidation capacity of the cells.

1.5.12 Treating oxidative stress in asthma

Among the routine asthma therapies, corticosteroid treatment in steroid-naïve asthmatic subjects has been shown effective in reducing exhaled $NO^{\bullet}$ and H_2O_2 levels, and the associated hyperresponsiveness (333). More specifically, dietary antioxidant therapies have been developed to target oxidative stress in asthma. The beneficial effect of dietary vitamin C and E is controversial, with some studies reporting improvement in symptoms, inflammation, and a reduction in mitochondrial dysfunction and airway hyperresponsiveness (323). N-acetylcysteine (NAC) has been shown effective in treating patients with acute lung injury (365, 366) and lung fibrosis (362), which may act by attenuating neutrophil influx and epithelial disruption (367). Dietary coenzyme Q_{10} may produce a corticosteroid-sparing effect (368).

Small molecule inhibitors have recently been synthesized with a view to treating oxidative stress in disease. Specifically, NOX enzymes have been popular therapeutic targets for oxidative stress-related diseases, due to the beneficial effects of non-specific NOX inhibitors such as DPI and apocynin *in vitro* (295). NOX4 has been a popular target; siRNA silencing (316, 369) or genetic knockout (313, 360) of NOX4 prevented the corresponding disease pathological outcomes. Pyrazolo-pyrido-diazepine dione derivatives are a class of small NOX inhibitors that show desirable specificity and pharmacokinetics (320, 370). GKT137831 is a small molecule specific for NOX4 and NOX1, with a slightly higher potency (1.5-fold) and affinity (1.7-fold) towards NOX4 (320). In a mouse model, this inhibitor was shown to be effective in attenuating hepatocyte apoptosis and liver fibrosis (360), and is currently in a Phase 1 clinical trial (371). In cardiovascular disease, GKT137831 was shown to reduce hypoxia-induced metaplasia in vascular cells (372). In the case of lung diseases, the lack of a valid lung

fibrosis animal model, controls and standardised outcomes restricts its assessment in treating IPF.

1.6 Hypotheses

Evidence to date has been reported indicating the dysfunction of airway epithelium, and its role in asthma development and progression. For instance, the mucociliary clearance in asthmatic airways has been found to be abnormal, which is partially due to the altered ciliary function of the asthmatic epithelial cells. However, the cause and the underlying mechanism of this asthmatic ciliary dysfunction have not been well elucidated. This may explain the lack of specific therapies that target the restoration of function in asthmatic epithelium, despite some current therapies showing positive effects on epithelial function. As a result, there is a need to identify the mechanisms behind ciliary dysfunction in asthma.

I hypothesized that "*the ciliary abnormalities of the epithelial cells in asthmatic airways are due to intrinsic abnormalities that increase the susceptibility of these cells to challenge, and leads to a chronic inflammation and predisposition of exacerbation*". I tested this hypothesis by addressing the following aims:

1. To study if the cause of ciliary dysfunction in asthma is primary or secondary.

   With the limited supply of human bronchial brushes, this question was addressed by testing the following sub-hypotheses using different types of epithelial cell cultures:

   (i) The ciliary dysfunction in asthmatic epithelial cell is not due to a differential synthetic capability (in terms of cytokines and chemokines) of the epithelial cells at baseline compared to healthy controls

   (ii) The ciliary dysfunction in asthmatic epithelial cells is not due to a differential gene expression of the epithelial cells at baseline

(iii) The ciliary dysfunction as observed *in vivo* persists in differentiated epithelial cultures derived from asthmatic subjects.

2. To study the underlying mechanism(s) of ciliary dysfunction in asthma.

   Based on the evidence in current literature, various components have been reported to show alteration effect on airway epithelial ciliary function. To evaluate which component(s) is/are responsible for the asthmatic ciliary dysfunction, the following sub-hypotheses were tested:

   (i) Bacterial colonisation/infection is the cause of the asthmatic ciliary dysfunction, that antimicrobial treatments would improve ciliary function

   (ii) Fungal colonisation/infection is the cause of the asthmatic ciliary dysfunction, that antimicrobial treatments would improve ciliary function

   (iii) Bacterial cytotoxicity is the cause of the asthmatic ciliary dysfunction, that antimicrobial treatments would improve ciliary function

   (iv) Asthmatic epithelium facilitates microbial growth that leads to ciliary dysfunction.

   (v) Oxidative mishandling is not the cause of the asthmatic ciliary dysfunction, that an anti-oxidative treatment would not improve ciliary function

3. To study if this/these underlying mechanism(s) is/are consistent across different asthma subtypes.

   Evidence in literature has shown that asthma can be divided into subtypes based on the inflammatory cell profiles. The involvement of different triggers and the differential responses to treatments suggest that they may have different

pathways of disease progression. To assess if the same case apply to the underlying mechanism of ciliary dysfunction in asthma, the following sub-hypotheses were tested:

(i) The antimicrobial treatment has the same effect on improving ciliary function across different asthma subtypes

(ii) The anti-oxidative treatment has the same effect on improving ciliary function across different asthma subtypes

2. Materials and Methods

2.1 Chapter Overview

This chapter details the general materials and methods that were used throughout the experiments in this thesis. Any specific materials, samples and conditions that were linked to specific chapters are described in the corresponding "Methodology" section in each chapter.

2.2 Clinical Characterisation and Measurement

The studies in this thesis were approved by the Leicestershire Ethics Committee:
1) REC number: 08/H0406/189; R&D number: UHL 10613; 2) REC number: 4977; R&D number: UHL 06347; 3) REC number: 11/EM/0402; R&D number: CLRN 92275. All subjects gave written informed consents.

A total of 90 asthmatic subjects and 44 healthy controls were staff and patients attending Glenfield Hospital, Leicester, U.K., or recruited from local advertising. Asthma was defined according to the Global Initiative for Asthma (GINA) guideline (5, 373). Disease severity was also categorized based on this guideline. Clinical characteristics detailed the subjects' demographics, smoking status, treatment, atopic status, spirometry and methacholine challenge, blood total IgE and eosinophil levels, and sputum differential cell counts. Atopy was defined as one or more positive skin prick tests (wheal >2mm above negative control) to common aeroallergens (cat, dog, grass, trees, *Dermatophagoides pteronyssinus* and *Aspergillus*). Healthy controls had normal lung function with no history of asthma. Details are recorded in accordance with the studies in the corresponding chapters.

2.3 Human Primary Airway Epithelial Cells

The human airway epithelial cells used throughout this thesis were primary cells directly obtained from subjects who were attending Glenfield Hospital or recruited locally. Cells were extracted from human airways using bronchoscopy, and were used or cultured within 1.5 h after the procedure without any additional processing or freezing steps. No cell lines or commercial primary cells were used in this thesis.

2.3.1 Human airway epithelial basal cells (HAEBC) Culture

Human airway epithelial cells were isolated from human airways (generations 3 to 5) using bronchoscopy as previously described (374). Bronchial brushings were obtained using a 3 mm sterile (protected) bronchial brush (Olympus, Hamburg, Germany) as stated in the BTS guidelines (374). The brush head was kept in bronchial epithelial growth medium (BEGM) (**Table 2.1**) immediately after the procedure. The cells were then plated out on to a surface coated with 1% PureCol (Advanced BioMatrix, Nutacon BV, Leimuiden, The Netherlands). To do that, 1% PureCol made in PBS was left on the culture surface at room temperature for 1 h, followed by washing twice with warm HBSS (Gibco). The HBSS was completely removed before plating the cells on to the coated culture surface. A 12-well plate was usually used for the first round of epithelial cell culture. One brush worth of ciliated cell strips was usually divided into 2 wells to ensure a desirable initial cell expansion. To plate out the cells captured on the bronchial brush, ciliated epithelial cell strips on the brush were shaken off in the BEMG where the brush was kept initially. The BEGM with the cell strips were then centrifuged at 1,300 rpm at 20°C for 8 min. The cell pellet was re-suspended in 1 ml of fresh BEGM. 500 µl of cell suspension was added into each 1% PureCol-coated well. The human airway epithelial basal cells (HAEBC) among the ciliated cell strips would then start to expand.

When the HAEBC became confluent in the wells, 0.1% trypsin-EDTA (Sigma, Dorset, U.K.) was used for detaching the confluent cells. After a maximum of 5 min at 37ºC, the trypsin was neutralised with 1 volume of BEGM. Cell pellet was then collected by centrifugation at 1,300 rpm at 20°C for 8 min. One well worth of cell pellet was expanded further in one T75 flask – cells at this stage were at passage 1. HAEBC that became confluent in T75 flasks were then used for experiments. Cells were fed 3 times a week. HAEBC from passages 1-3 were used for experiments.

For primary cells, the centrifugation setting was always at 1,300 rpm at 20°C for 8 min unless stated.

2.3.2 HAEBC Characterisation

Cytokeratins 5 and 14 are markers specific to epithelial basal cells (375). The purpose of the characterisation was to make sure the cells obtained from the bronchoscopy were in fact airway epithelial basal cells.

To do this, the culture surface of an 8-wells permanox chamber slides (Lab-Tek, Nalge Nunc, Roskilde, Denmark) was first coated with 1% PureCol. HAEBC was then seeded into the wells at a density 15,000 cells/well. When a 100% confluence was reached, HAEBC were first fixed in ice-cold methanol (200 µl/well) for 20 min on ice, followed by air-drying at room temperature for 10 min. Cell cytoplasm was stained with anti-cytokeratins-5/14 duo-antibody (Abcam, Cambridge, U.K.) (0.8 µg/ml or 1.6 µg/ml, 200 µl/well), or with the appropriate isotype control (Dako) (3.2 µg/ml, 200 µl/well), for 90 min. PBS was used as the antibody diluent. HAEBC were washed 3 times with 0.05%

Tween-20 (Sigma)-PBS, and then probed in the dark with FITC anti-mouse antibody [dil. factor 1:100] (Dako, Ely, U.K.) for 90 min on ice. HAEBC were washed again 3 times in 0.05% Tween-20-PBS and then 3 times in PBS. Nuclei were stained with DAPI (4', 6'–diamidino-2-phenylinodole dihydrochloride) [dil. factor 1:1000] (Sigma) for less than 50 sec before rinsing off the stain with PBS, followed by 6 additional washes with PBS. The chamber wall was then removed. The slide was mounted with 3 drops of fluorescence mounting medium (Dako), cover-slipped, and rinsed 6 times with PBS. The slide was then dried and left at 4°C in the dark for storage. Images were captured by immunofluorescence microscopy at x10 magnification using the OpenLab software (PerkinElmer, Massachusetts).

2.3.3 Air-Liquid-Interface (ALI) Culture

HAEBC from passages 1 and 2 were used for air-liquid-interface (ALI) culture. Fully differentiated ALI cultures contain ciliated cells for mechanical function analysis, which could not be done using HAEBC monocultures.

To differentiate HAEBC, Transwell inserts (0.4 μm polyester membrane, 12 mm diameter) (Corning, Amsterdam, The Netherlands) were first coated with 1% PureCol (200 μl in the apical chamber; 1 ml in the basolateral chamber) and washed with warm HBSS twice before use. Cells were seeded into the apical chambers at a density 50,000 cells/well. Cells were submerged in BEGM (200 μl in the apical chamber; 800 μl in the basolateral chamber) until >99% confluent. The apical surface was then exposed to air, whilst the medium in the basolateral chamber was replaced by 700 μl ALI medium (**Table 2.1**). Cells were fed 3 times a week. To prevent suffocation, excess mucus in the apical chamber was removed, or gently washed off with 200 μl PBS. The neat excess

mucus and PBS wash were collected and stored as apical chamber fluid (ACF) samples. Heavily ciliated cultures were used for experiments.

2.4 Ciliary Function

The ciliary function of ciliated airway epithelial cells was assessed using two methods as described below: the overhead method or the scraping method, followed by videomicroscopy (376, 377). **Figure 2.1** shows the schematics of video-microscopy and ciliary function analysis.

2.4.1 Overhead method

Videos of epithelial cilia were recorded without disturbing the integrity of the cell layers as previously described (376). A light microscope at x40 magnification was set up in an airtight environment at 37ºC. A Transwell plate with ciliated epithelial cells was place on the resting stage. Areas of the epithelium with the least vacuoles and the most cilia were chosen. The visible field was adjusted to focus on the tips of the cilia. By using a high-speed digital camera and the software MotionStudio (Redlake Imaging, Cheshire CT, USA), videos were taken at a speed of 250 frames per second (fps) for ~2 sec. 3-5 videos were taken per sample.

2.4.2 Scraping method

Cells were videoed in suspension as previously described (377). Ciliated cell layers on the insert membrane was scored into sections and scraped off using a sterile spatula (**Figure 2.1**). Strips of ciliated cells were re-suspended in 1 ml M199 medium (**Table 2.1**). Without vortex, cells were shaken to detach any mucus on the ciliary surface that would affect ciliary beatings. Samples were left on the bench for 1 min for the cells to

settle/stabilise. Homemade chamber slides were prepared at least 1 day before use. They were prepared by creating a central chamber using two adjacent square cover glass (25x25 mm, VWR) affixed on opposite ends of a microscope slide (76x26 mm, VWR). 100 µl cell strip suspension was added to the chamber, and the slide was cover-slipped and securely taped down. The slide was placed on a heated platform of a microscope fixed at 37ºC and mounted with a high-speed camera that was linked to the software MotionStudio (DEL Imaging Systems). Videos of side profiles of the ciliated epithelial surfaces were recorded using x100 oil immersion microscopy. Videos were recorded at 500 fps for 2 sec. 6 to 10 side profiles were recorded per sample.

2.4.3 Ciliary function analysis

Videos were played back frame-by-frame using the software MotionStudio. Each video image was divided into 10 equal fields for multiple measurements per sample. When using the overhead method (376), a cilium with a clear, visible tip within each field was chosen for enumerating CBF. The beating amplitude of the cilium was measured using a transparent grid on the computer screen; a percentage (%) of amplitude was calculated. As for the scraping method, a cilium that represents the majority of the cilia in the field was chosen. As previously described (378), the number of frames the cilium took to beat 5 times was counted, and the CBF was calculated in Hz [CBF=500/(number frames for 5 beats/5)]. Beat pattern of the cilium was categorised as normal (smooth beating with bendable tips), dyskinetic (stiff, disturbed beating with tip fails to bend along the ciliary shaft) and static. The level of ciliogenesis was represented as a % of the total surface assessed. The epithelial surface morphology was scored with index 1 (smooth surface with no cell protrusion), 2 (part of uneven surface with little cell protrusion), 3 (irregular cell surface with cell protrusion) and 4 (single cells –for fresh cells only).

2.5 Sputum For Inflammatory Cell profiling

2.5.1 Collection and processing

Fresh sputa were collected as previously described (22). Subjects were first encouraged to produce sputum 'voluntarily' by coughing. If it was not successful, or if the subject was not able to produce a sufficient amount, sputum induction was performed.

Briefly, a subject inhaled a fixed concentration of hypertonic vaporized saline for 5 min (started from 3% and up to 5%) to encourage mucus production on the airways. The subject was then encouraged to cough out the induced sputum. The induction process was stopped when i) the expectoration of sputum was adequate, ii) the percentage drop in FEV_1 reached >20%, or iii) there was a significant increase in patient reported symptoms. The sputum collected was kept on ice and was used within 2 h. Only the sputum plugs were used in experiments.

The procedures of sputum processing were carried out as previously described (379). The selected sputum plug was first weighed. 8x volume of PBS was added to each plug, vortexed for 15 sec, and then rocked on ice for 15 min. Cells were centrifuged at 790 g for 10 min. 4 volumes of PBS supernatant were collected and stored at -80ºC for later use. The remaining PBS supernatant and cell pellet were incubated with 4 volumes of 0.2% DL-dithiothreitol (DTT) at 37ºC for 30 min. The sample was then filtered using a 48 μm nylon gauze (Fisher Scientific, Loughborough, U.K.) pre-wet with PBS. The sputum filtrate was used for differential cell count and for routine bacterial culture.

2.5.2 Differential Cell Count

Sputum filtrates were used for total and viable cell count using trypan blue staining. The filtrate that passed through the gauze was spun down at 790 g for 10 min. The cell pellet was re-suspended at a density 10^6 cells/ml in PBS. Cytocentrifuge was performed by passing 75 µl cell suspension through a Shandon cytospin funnel (with filter card) (Thermo Scientific, Basingstoke, U.K.) at 450 rpm for 6 min. The cytospin slide was air-dried before Romanowsky staining as previously described (379). A total of 400 cells were counted for the % of eosinophils, neutrophils, macrophages, epithelial cells and lymphocytes.

2.6 Bacteriology

To assess the bacterial quantity in human airways, sputa were collected for bacterial culture for colony-forming-unit (cfu) count. Bacterial 16S copy was also quantified in certain type of samples using real-time PCR.

2.6.1 Bacterial Culture

Sputum filtrates collected from the 48 µm gauze were diluted in a factor of 2 to 5 in sterile water. 3 fields (droplets) of 20 µl filtrates at each dilution were dropped onto a Columbia blood agar. The agar plates were incubated at 37°C for 24 h. Fields with up to 300 colonies/droplet were counted. The colony forming unit (cfu)/ml was calculated [average count*dilution factor/volume]. $\geq 10^7$ cfu/ml was used as a cut-off to represent a clinical significance as previously suggested (380).

2.6.2 Bacterial 16S quantification using real time polymerase chain reaction (PCR)

PCR is a biochemical technique that allows the quantification of a particular sequence of DNA material that has a very low quantity in samples. During the reaction the target DNA sequence is amplified. A fluorescence signal was released based on the amount of double-stranded DNA present after each reaction. The target is 'present' when the fluorescence intensity has reached the chosen threshold after a certain number of amplification cycles (i.e. real time). As a result the detection is based on the initial quantity present in the sample (**Figure 2.2**).

2.6.2.1 Microbial DNA Extraction

The total genomic DNA, instead of specific bacterial DNA, was extracted using QIAamp DNA Mini Kit (Qiagen), following the manufacturer's "Tissue" protocol. Briefly, all equipment and nuclease-free water were subjected to a 30 min low-level UV laminar flow before use. Samples of diluted and homogenised sputum plugs and ACF (20 µl) were first lysed using lysozyme (37°C, 30 min), and then using Proteinase K (55ºC, 30 min then 95°C, 15 min) (all from Qiagen, Crawley). The lysate obtained was buffered with ethanol, added to the QIAamp spin column, and then centrifuged at 6,000 g for 1 min for an optimal adsorption of DNA to the column's silica gel membrane. Samples were then washed with AW1 Buffer (500 µl), AW2 Buffer (500 µl) and then Buffer AE (500 µl). At last, DNA was eluted in 200 µl nucleases/pyrogen-free water and stored at -20°C. The DNA concentration was measured at the wavelength 260 nm using a Nanodrop spectrophotometer (Thermo Scientific, Wilmington, DE).

2.6.2.2 Bacterial 16S real time PCR

Total bacterial 16S was assessed by SYBR Green Real time-PCR assay (PE Applied Biosystems, Warrington, UK) using universal 16S rDNA primers (6.25 μM), 338F (5'-ACT-CCT-ACG-GGN-GGC-NGC-A-3') and 515R (5'-GTA-TTA-CCG-CNN-CTG-CTG-GCA-C-3') (integrated DNA technologies), following the manufacturer's protocol. Reaction and cycling conditions were used as previously described (380).

Briefly, all the apparatus and materials were UV-irradiated at 12,000 μJ in a UV crosslinker to denature foreign DNAs. A 25 μl reaction mix contained 12.5 μl 2x SYBR Green qPCR MasterMix (PE Applied Biosystems), 6.25 μM forward primer, 6.25 μM reverse primer, 9.5 μl dH_2O and 1 μl DNA sample. The supplied Escherichia coli K12 DNA was used as the standard. Sterile distilled nucleases/pyrogen-free water was used as a negative control. Samples were run in duplicates. Immunofluorescence was detected using a green channel (excitation 470 nm, detection 510 nm). Data was analysed using the software Corbett Rotor-gene 6000 (Qiagen). Threshold was set at the exponential phase of the amplification cycle and above any non-specific reaction. Based on the negative controls from each run, the maximum DNA contamination overall was 2.8%. The lowest detection limit was therefore set at 3%.

2.7 Fungology

To assess the fungal quantity in human airways, sputa were collected for fungal culture. Since *Aspergillus fumigatus* was of particular interest, the total genomic DNA extracted from the bacteria quantification process was also used for *A. fumigatus* qPCR (**Figure 2.2**).

2.7.1 Fungal Culture

Undiluted sputum plugs (approximately 150±80 mg) were inoculated on potato dextrose agars (PDA) containing 16 μg/ml chloramphenicol, 4 μg/ml gentamicin and 5 μg/ml fluconazole. The agar plates were sealed after the addition of sputum plugs, and were incubated at 37°C with regular inspection for up to 7 days. Fungal colonies were identified based on published morphology criteria (381).

2.7.2 Aspergillus fumigatus quantification

Aspergillus fumigatus was quantified by targeting the mitochondrial gene (AfMITO) L37095 using the 7500 Fast Real-Time PCR system (Applied Biosystems) (382), following the manufacturer's protocol. The amplification primers were forward 5'-GAA-AGG-TCA-GGT-GTT-CGA-GTCA-3' and reverse 5'-CAT-CAT-GAG-TGG-TCC-GCT-TTAC-3' (Invitrogen). The fluorogenic probe sequence was 5'FAM-ATC-CCT-AAA-CCC-GCA-ACC-AAA-GGC-3' TAMRA (Sigma). A 25 μl reaction mixture contained 1x PCR TaqMan buffer, 0.2 mM each nucleotide (dATP, dUTP, dCTP and dGTP), 20 pmol each of *Aspergillus* primers, 0.5 units of uracyl-N-glycosylase, 1.25 units of AmpliTaq Gold TM (Applied Biosystems), and 2 μl of sample DNA. A calibration curve of *A. fumigatus* DNA was included in each run using concentrations 1 pg to 1 ng with a 10-fold step dilution. Sterile water was used as the negative control. Samples were run in duplicate. Data was analysed using the Sequence Detection System version 1.4 (Applied Biosystems). The threshold of detection was set at 0.01, baseline from cycles 2 to 17.

2.8 Inoculation Study Using Ciliated Epithelial Cells For Ciliary Function Assessment

Heavily ciliated epithelial ALI cultures or fresh bronchial brushings were used for different inoculation studies. Ciliary function of ALI cultures or fresh bronchial brushings was assessed using the scraping method followed by videomicroscopy. Side profiles of ciliated epithelial surfaces were recorded for both types of cell samples. All inoculation was performed at 37°C in airtight, sterile eppendorf tubes. Sample conditions were staggered to ensure incubation timings were correct. To test the influence of an asthma-specific environmental on ciliary function, a sputum inoculation study using ALI cultures was performed, which is described in Chapter 3. To test the potential role of NOX4 on ciliary dysfunction in asthma, a NOX4 inhibition study using fresh brushings was performed, which is described in Chapter 5.

2.9 Bacterial LPS (endotoxin) Quantification

Bacterial LPS was quantified using the Endotoxin Recombinant Factor C (rFC) detection system (Lonza), following the manufacturer's protocol. The rFC assay utilises the Limulus blood coagulation cascade without reaching the pathway downstream of Factor C to minimise fault positive (**Figure 2.3**) (383, 384). Upon the interaction with endotoxins, rFC releases a detectable fluorescence of which the intensity corresponds to the quantity of LPS.

Briefly, cell-free samples were used in duplicate as the input material. 100 µl of standard or samples was added to a black 96-well plate (Corning) and was incubated at 37ºC for 10 min. 100 µl of enzyme-substrate cocktail was then added into each well. Fluorescence was measured at 0 h and 1 h at excitation 380 nm; emission 510 nm using

NOVOStar microplate reader (BMG Labtech, Aylesbury, U.K.). *E. coli* endotoxin (O55:B5) was used to generate the standard curve (ranging from 10 EU/ml to 0.01 EU/ml with a 10x step-down dilution). LAL water was used as the diluent. LAL water and PBS were used as the negative controls. 1 EU/ml endotoxin standard was used for spiking to check for positive product control.

2.10 Protein Analysis

2.10.1 Sandwich Enzyme-linked immunosorbant assay (ELISA)

A sandwich ELISA is a protein quantification assay that measures changes in luminescence given by the utilisation of antibodies. It quantifies 1 protein at a time (385). ELISAs were performed following the corresponding manufacturer's protocol. Depending on the manufacturer, the ELISA kit either came with an ELISA plate pre-coated with a capture antibody, or came with a vial of capture antibody that required a coating step using MaxiSorp microplates (NUNC). A specific primary antibody followed by a non-specific secondary antibody was added in order to bind to the protein of interest that was captured by the capture antibody. This created a sandwich of molecules. Horseradish peroxidase (HRP) was then added if the secondary antibody was not conjugated with a reporter enzyme. At last, a substrate was added to react with the reporter enzyme. This reaction generates a luminescence signal that is in proportion to the quantity of the protein of interest captured. 0.05-0.1% Tween-PBS was used as the wash buffer. Corresponding culture media were used as the sample diluent and the negative controls. ELISAs were performed in Chapter 3 for CCL5 and IFN-β, and in Chapter 4 for human β-defensins.

2.10.2 Meso-Scale Discovery (MSD) Multiplex Assays

An MSD assay is quantitative assay that measures multiple target proteins simultaneously. It uses a similar mechanism as an ELISA. Antibodies pre-coated on an assay plate first capture the proteins of interest in the sample. SULFO-TAG labels were then added to bind to the proteins of interest. Upon the electrochemical stimulation, light is emitted and detected that is in proportion to the amount of target proteins captured at the first place (386).

The secretion of different pro-inflammatory mediators from primary epithelial cells using MSD multiplex assays (Maryland, USA), following the manufacturer's instructions. Mediators IL-1β, TNF-α, CCL2, CXCL8, CXCL10, CCL11, CCL13, CCL17, CCL22 and CCL26 were measured. Limits of detection were below 2.4 pg/ml and above 10,000 pg/ml. 100 µl of undiluted conditioned culture medium was used in duplicate. Corresponding culture media were used as the negative controls.

2.10.3 Coomassie Bradford Assay

Coomassie Bradford protein assay (Thermo Scientific) was performed for protein quantification in a 96-well plate. The assay reagent provides an acidic environment for the coomassie dye to change from brown to blue upon protein binding, of which the intensity is in proportion to the protein quantity in the sample (387).

Briefly, after removing the reagents, the adherent HAEBC was lysed with 20 µl of Cell Lysis Buffer (Sigma) on a shaker at room temperature for 15 min, then stored at -20ºC if required. Detection reagent was left to warm up at room temperature before use. Bovine serum albumin (BSA) was used to generate a standard curve. Cell Lysis Buffer

was used as the diluent and the negative control. 5 µl lysed sample or BSA standard was added into the 96-well plate and mixed with 250 µl detection reagent. The plate was left at room temperature for 10 min before measuring the absorbance of the detection reagent at a wavelength 600 nm.

2.10.4 Whole Cell Lysate and Western Blot

Western Blot is a protein analytical assay that separates and quantifies specific proteins present in cell lysates. Denatured proteins of different molecular weights were first separated using acrylamide gel electrophoresis. Proteins were then transferred onto a membrane where the protein of interest is probed with specific antibodies by the mean of immunofluorescence (388). The probed target proteins are quantified using densitometry (389).

2.10.4.1 Whole cell lysate preparation

All reagent recipes can be found in **Table 2.1**. Confluent HAEBC lysed in 1x sample buffer, aid by scraping using a cell lifter (Corning). For ciliated ALI cultures, half or a whole membrane was cut from the Transwell insert before the lysis step. Lysates were stored at -80ºC before use.

2.10.4.2 Western Blot

All reagent recipes can be found in **Table 2.1**. 10% or 12% acrylamide running gels were used as appropriate. Running gels were polymerised at room temperature in a sandwich cassette using 0.75 cm glass plates (BioRad, Hempstead, U.K.). A 5% stacking gel was then added atop the polymerised running gel; stacking gel was allowed to polymerise with a 10-well comb at room temperature. The comb was removed after

gel was completed polymerised. The whole sandwich cassette was assembled in a gasket in the running tank, with the loading wells and the middle compartment of the gasket filled with 1x TGS running buffer. Cell lysate samples were defrosted and sonicated for 10-12 sec prior to any dilution in dH_2O. Samples were denatured at 100°C for 3-5 min before loading a maximum of 30 µl into each loading well. Gel electrophoresis was run at 180V (0.06A) for 45-60 min. The proteins separated in each acrylamide gel were then transferred on to a 0.45 µm PVDF transfer membrane (Immobilon-P, Millipore, Watford, U.K.) using the semi-dry transfer protocol. To do that, the membranes were first soaked in methanol for 1 min, followed by a further 5 min in the Transfer Buffer. Each membrane was sandwiched with 1 protein-loaded acrylamide gel and Transfer Buffer-soaked 3 mm chromatography papers (Whatman, GE Healthcare, Chalfont St Giles, U.K.) as shown below:

(Top, +ve electrode)	Filter paper x 3	(soaked in Transfer Buffer (TB))
	The gel	(in TB)
	Membrane x 1	(soaked in Methanol then TB)
(Bottom, -ve electrode)	Filter paper x 3	(soaked in Transfer buffer (TB)

Protein transfer was performed at 15V (0.4A) for 37 min. The membrane blots were then removed from the sandwich, blocked with 5% milk–TBS-T (**Table 2.1**) at room temperature for 1 h, followed by washing in 1x TBS-T 3 times for a total of 15 min. The blots were probed with primary antibody in 5% milk-TBS-T at 4°C overnight. The housekeeping protein, β-actin, was used as the reference. The blots were washed 3 times in PBS for a total of 15 min, followed by probing with the appropriate HRP-conjugated secondary antibody at room temperature for 1 h. The blots were washed again 3 times in

PBS for a total of 30 min. ECL (Amersham, Little Chalfont) was used as the HRP substrate for visualising the bands. The blots were kept in Saran film to prevent them from drying up. Kodak medical X-ray films (MXB blue, Wolflabs, Pocklington, U.K.) were used for film development. Images of the developed films were captured using an office scanner. Analysis was performed using the software ImageJ (densitometry) without any (rolling-ball) background correction.

To reuse the blots for another protein of interest, the blots were incubated in stripping buffer at 50°C for 30 min followed by washing in 1x TBS-T 3 times for a total of 30 min. The blots were then blocked with 5% milk-TBS-T for at least 15 min before probing with a new primary antibody.

2.11 5-(and-6)-carboxy-2', 7'-dichlorofluorescein diacetate (DCF-DA) Assay

The DCF-DA assay was used to quantify the generation of intracellular reactive oxygen species (iROS) in cell monolayer. DCF-DA is a non-fluorescent dye that can penetrate the cell membrane to the cytoplasm. DCF-DA in the cytoplasm reacts with intracellular esterases and is hydrolysed to an impermeable non-fluorescent molecule, DCFH. DCFH can then be oxidised by intracellular H_2O_2 to become a highly fluorescent molecule, dichlorofluorescein (DCF) (**Figure 2.4**) (390). The emitted fluorescence is directly proportional to the concentration of the intracellular H_2O_2.

To perform this assay, HAEBC were seeded in to black 96-well plates (Corning) at a density 15,000 cells/ml. When the confluence has reached 100%, HAEBC were first washed gently in PBS to remove the phenol red present in the BEGM. PBS was used as the wash buffer and the reagent diluent in this assay. HAEBC were then incubated with 10 μM DCF-DA (Sigma), or the equivalent concentration of DMSO (Sigma) as the

labelling control, at 37°C for 30 min in the dark. The plates were washed once, followed by the addition of 100 µl stimulus and/or compound. PBS was used as the negative control. Conditions were done in triplicate. Fluorescence (OD) was measured at 0 h and every 30 min afterwards for up to 2 h. OD was measured at excitation 485 nm; emission 520 nm using the NOVOStar microplate reader (BMG Labtech).

2.12 Gene Expression Analysis

Gene expression in human primary airway epithelial cells was measured using the extracted total RNA as the input material. RNA is an anti-sense genomic material. It is required to be converted to "sense" material, such as complementary DNA (cDNA), before being used in PCR (**Figure 2.2**). The expression of 50,000 genes was simultaneously measured using microarrays (316, 391). Specific gene expression was measured using reverse transcriptase real-time (quantitative) PCR (RT-qPCR) (316, 392).

2.12.1 Total RNA Extraction

Total RNA from epithelial cells was extracted using RNeasy mini kit plus DNaseI digestion (Qiagen) following the manufacturer's protocol. Confluent HAEBC from two wells of a 6-well plate were pooled as one sample. One insert of ciliated ALI culture was used as one sample. Cells were lysed in 400 µl RLT buffer with β-mercaptopethanol. Cell lysis was aided by scraping the culture surface using a cell lifter (Sigma). Lysed cells were further homogenized by spinning down the sample through the QiaShredder column (Qiagen) at maximum speed at 4ºC for 2 min. The filtrate was then mixed with an equal volume of 70% ethanol, and was passed through the RNA binding silica gel membrane. The bound RNA sample was washed with 350 µl RW1

buffer, followed by DNA digestion using DNaseI (Qiagen) at room temperature for 15 min. The sample was then washed once with 350 µl RW1 buffer and twice with 500 µl RPE buffer. The washed RNA sample was then eluted in 35 µl nuclease-free water. RNA quantity (A260) and purity (A260/A280) were measured using NanoDrop spectrophotometer (Thermo Scientific). RNA samples were stored at -80ºC before use.

2.12.2 Human Genome Microarrays

Human airway epithelial cell gene expression was analysed using Human Genome U133 Plus 2.0 cartridge arrays and 3' IVT Express Kit (Affymetrix, Santa Clara, CA), following the manufacturer's protocol. The total RNA extracted from HAEBC was used as the starting material.

2.12.2.1 Running the microarrays

Briefly, the integrity of the total RNA samples was first assessed using the RNA 6000 Nano Kit (Agilent Technologies, Waldbronn, Germany). The samples with an RNA Integrity Number (RIN) above 9 were chosen for the microarrays. 250 ng total RNA was used for cDNA synthesis followed by amplified RNA (aRNA) synthesis. aRNA was purified on an Ambion magnetic stand-96 (Life Technologies, Paisley) using the RNA binding beads provided. Purified aRNA was quantified using a NanoDrop spectrophotometer (Thermo Scientific). The aRNA samples were then fragmented; the fragmentation was confirmed using the RNA 6000 Nano Kit. Fragmented aRNA samples were used for hybridization in the cartridge arrays.

Hybridization and pre-scanning processing were performed using the GeneChip Hybridization, Wash, and Stain kit (Affymetrix), following the manufacturer's protocol.

12.5 µg aRNA was used for preparing the hybridization cocktails. After hybridisation, cartridge arrays were washed and stained using Affymetrix Fluidics Station 400, and scanned using GeneChip Scanner 3000 and the software GeneChip Operating System (version 1.4) (Affymetrix).

2.12.2.2 Microarray analysis

Each array must pass all quality controls in order to be included in the analysis: 1) background reading was between 20 to 100; 2) signal (3'/5') ratio of house-keeping gene GAPDH was <3; 3) signals of poly-A controls and hybridisation controls were in proportion to the input quantities. All arrays must have comparable Noise values.

Analysis was performed using Limma and SAM microarray analysis packages, and the AffyBatch parameter. A significant differential gene expression was defined as an up or down expression with a magnitude >1.6-fold, or the presence of the gene in >50% individuals with asthma/healthy control subjects versus 0 healthy control subjects/individuals with asthma.

2.12.3 Reverse Transcription-quantitative Polymerase Chain Reaction (RT-qPCR)

Specific gene expression in human airway epithelial cells was evaluated using a two-step RT-qPCR kit (Invitrogen, Paisley), following the manufacturer's protocol (**Figure 2.2**). The first step was converting the total RNA to cDNA; the second step was the qPCR.

2.12.3.1 Complementary DNA (cDNA) synthesis (step 1)

For cDNA synthesis, the reaction mix contained 4 µl of 5x VILO, 2 µl of 10x SuperScript Enzyme Mix (Invitrogen), and a maximum of 2 µg or 14 µl of total RNA. Nuclease-free water was used as the diluent. Reaction conditions were 1) 10 min, room temperature; 2) 60 min, 42ºC; 3) 5 min, 85ºC. cDNA samples were stored at -20ºC before use.

2.12.3.2 qPCR (step 2)

qPCR was performed using SYBR Green RT-qPCR (Invitrogen) and the software MJ Opticon (BioRad) as previously described (316). A 20 µl qPCR mix contained 10 µl Express SYBR GreenER qPCR Universal SuperMix (Invitrogen), 200 nM of each primer, a maximum of 2 µl cDNA, and nuclease-free water to give a final volume at 20 µl. The quantity of cDNA to be put in each reaction varied between different genes of interest. It was determined by running efficiency curves. An efficient reaction is indicated by a 90-110% efficiency, and the range of cDNA quantity that gave this efficiency could be used as the input quantity for the qPCR. Reaction conditions are shown in the corresponding chapter(s). 18S rRNA was used as the housekeeping gene for normalisation. One healthy sample was used as the reference across all qPCR runs to further normalise the variation between different runs. A melting curve with a clear single peak indicated a clean, efficient reaction. The threshold was fixed at 0.005 for all qPCR runs, where the amplification curves generally started to increase exponentially.

2.12.4 Agarose Gel Electrophoresis

Agarose gel electrophoresis was performed to look at the purity of qPCR products. Pure qPCR product should only give one clear band on the agarose gel. Samples with more

than one band, or with smears, indicate the presence of a contamination or denatured cDNA where sample exclusion should be considered.

Briefly, 2% agarose gels (**Table 2.1**) were prepared. GelRed (Biotium, Camrbidge) (1 µg /10 ml gel) was used to label the qPCR products for visualisation. 12 µl samples containing 10 µl qPCR product and 2 µl 6x restriction enzyme loading buffer were loaded into each of the 15 wells. 5 µl HyperLadder I (Bioline, London, U.K.) was used as the molecular weight marker. The electrophoresis was run at 90V (90-95 mA) for 1 h. The whole agarose gel was then removed from the gasket and placed under UV light to visualise the bands of the qPCR products. A pure and intact qPCR product should appear as a clear band at a region corresponding to its molecular weight.

2.13 Glycol Methacrylate (GMA)

GMA embedding is an immunohistochemistry technique to look at the pathological features of relatively sized specimen such as bronchial biopsies. It involves firstly an embedding process to preserve the structure and pathological status of the specimen, followed by sectioning of the specimen and immuno-staining process to mark the feature of interest for further assessment (393). 7,8-dihydro-8-oxodeoxyguanosine (8-oxo-dG) is an oxidised derivative of guanine, one of the four DNA-forming units, and was therefore used as an indicator of oxidative DNA damage (394).

2.13.1 Embedding

Bronchial biopsies were collected from human airways using bronchoscopy and were processed within 2 h. The biopsies were first immersed in 2 mM PMSF/Acetone/20 mM iodoacetamide at -20ºC overnight. They were then fixed in acetone followed by methyl

benzoate, each at room temperature for 15 min. Afterwards the biopsies were embedded in processing solution [125 µl methyl benzoate, 2.75 ml Solution A of ABComplex Mix (Vectastin Elite, Vector Laboratory, Peterborough, U.K.)] at 4ºC for 2 h. This embedding step was repeated twice. Each biopsy was then put into a TAAB capsule (Agar Scientific, Essex, U.K.) and embedded with 1 ml embedding solution [10 ml SolutionA, 250 µl Solution B, 70 mg benzoyl peroxide (Sigma)]. The capsules were left in an airtight box with silicon beads at 4ºC for 48 h before storing at -20ºC.

2.13.2 Staining

2 µm sections of each biopsy were cut using a microtome (Leica Microsystems, Milton Keynes). One uncoated microscopic slide was used for capturing 2 biopsy sections. The sections were first inhibited with 0.1% sodium azide/0.3% H_2O_2 at room temperature for 30 min. The slides were then washed thoroughly in 1x TBS. 1x TBS was used as the washing buffer and the diluent. The sections were probed with 8-oxo-dG primary antibody (1:250 dilution) (Abcam, Cambridge, UK) or its isotype control (Dako, Cambridge, UK) at room temperature overnight. After washing, sections were probed with a secondary biotinylated antibody (1:5000 dilution) at room temperature for 2 h. After washing, ABComplex mix (Vectastain Elite) was applied onto the sections, and the slides were left at room temperature for 2 h. AEC substrate (MenaPath, Berkshire, U.K.) was then applied onto the slides at room temperature for 10 min. The slides were washed under running water for 5 min, left in Mayer's haematoxylin for 10 min, in still water for 1 min, and finally mounted with SuperMount (BioGenex, Fremont CA, USA). The slides were left in the dark at room temperature overnight before use.

2.13.3 Semi-quantification

Positive 8-oxo-dG staining was observed within the nuclei. The staining intensity was quantified using a semi-quantitative method. Semi-quantitative index was assigned as the following: no staining=0, very low=1, low=2, moderate=3, high=4, and very high=5.

2.14 Statistical Analysis

2.14.1 Sample sizes

When determining sample sizes for the experiments, power calculation was performed using the following equation:

$$N = [t^2 \wedge p\,(1\text{-}p)] / m^2$$

where N is sample size, t equals to the confident level at 95% (1.95), p equals to the clinical significance, and m equals to the margin error of 5% (0.05). However, the required sample sizes were not achieved with the time available due to the high variations between donors, whilst the availability of donors was restricted. Experiments were repeated as many times as the number of samples available. This affected the power of the results. It also affected the sample sizes of the follow-up experiments that used the samples collected from previous studies.

2.14.2 Categorising asthmatic patients into subgroups

The initial approach to the recruitment of asthma patients was pooled – asthmatic subjects with different phenotypes and/or inflammatory profiles were all included in the initial studies. While asthma is a heterogeneous disease, it is believed that different pathogenic pathways are involved in different subgroups of asthma. For example, different studies in the literature have already shown that asthma subgroups have differential response to current therapies (24, 25). It is plausible that a certain stimulus

may have an effect on a specific subgroup, whilst the effect could be masked by the presence of other subgroups if the data were pooled together. It is of particular importance when exploring the maximum benefit a potential therapeutic compound that could offer to specific asthmatic subgroups. Therefore, as the studies progressed, the asthmatic subjects were divided into subgroups based on their inflammatory profiles for more in depth analyses.

2.14.3 Data analysis

All data were analysed using GraphPad Prism 5.0 (San Diego, CA). Data was presented as mean± standard error of mean (SEM). If the data set was not linear, log scales transformation was carried out before a statistical analysis was performed. T-tests were used for normally distributed data – paired data points were compared using paired t-tests; non-paired data points, such as healthy controls versus asthmatics, were compared using un-paired t-tests. For non-parametric data, Mann-Whitney U tests were used as the statistical analysis. One-way ANOVA with Tukey post-tests were used for time-course analysis. For correlation analysis, Pearson and Spearman tests were performed for parametrically and non-parametrically distributed data respectively. Statistical analysis was performed after normalisation.

Reagents	**Ingredients (Source)**	**Working Concentrations / v/v% or volume**
Bronchial Epithelial Growth Medium (BEGM)	Bronchial Epithelial Basal Medium (BEBM) (Lonza) BEGM SingleQuots Supplements Lonza) Antibiotic/Antimycotic (Gibco) Fungizone® Antimycotic (Gibco)	500 ml bottle 9 vials 1% 0.3%
Air-Liquid-Interface (ALI) medium	BEBM (Lonza)	50% (250ml)
	DMEM (with L-glutamine) (Gibco)	50% (250ml)
	BEGM SingleQuots Supplements (Lonza)	9 vials
	Antibiotic/Antimycotic (Gibco)	1%
	Fungizone® Antimycotic (Gibco)	0.2%
	Retinoic acid (Sigma)	100 nM
M199 medium (pH 7.3)	M199 medium (with HEPES) (Gibco)	500 ml bottle
	Antibiotic/Antimycotic (Gibco) (if with antibiotics)	2.5%
Acrylamide gel (10% / 12%)	30% Acrylamide Mix (ProtoFLOWGel)	1.7 ml / 2.0 ml
	1.5 M Tris pH 8.8	1.3 ml
	10% Sodium dodecyl sulfate (SDS) (Fisher Scientific)	50 µl
	10% ammonium persulfate (APS) (Fisher Scientific)	55 µl
	TEMED (Sigma)	2.5 µl
	dH_2O	1.9 ml / 1.6 ml
5% Stacking gel	30% Acrylamide Mix (ProtoFLOWGel)	670 µl
	1.5 M Tris pH 8.8 (Fisher Scientific)	500 µl
	10% SDS (Fisher Scientific)	40 µl
	10% ammonium persulfate (APS) (Fisher Scientific)	40 µl
	TEMED (Sigma)	4 µl
	dH_2O	2.7 µl
10x Tris buffered saline (TBS)	Tris base (Fisher Scientific)	0.2 M
	Sodium Chloride (Fisher Scientific)	1.37 M
	pH adjusted to 7.6 with HCl	-
	Dissolved in dH_2O	-
4x Sample Buffer	Tris-HCl pH 6.8 (Fisher Scientific)	0.25 M
	SDS (Fisher Scientific)	0.139 M
	Bromophenol blue (Fisher Scientific)	0.03 mM
	Glycerol (Sigma)	0.4%
	β-Mercaptoethanol (Sigma)	10%
10x Tris-Glycine	Tris base (Fisher Scientific)	0.25 M
	Glycine (Fisher Scientific)	1.9 M
	Dissolved in dH_2O	
Running Buffer (Western Blot) Or TGS, BioRad	10x Tris-Glycine	1x
	SDS (Fisher Scientific)	0.1%
	Diluted in dH_2O	
	n/a	n/a

Reagents	**Ingredients (Source)**	**Working Concentrations / v/v% or volume**
Semi-dry transfer buffer (Western Blot)	10x Tris-Glycine	1x
	SDS (Fisher Scientific)	0.02%
	Methanol (Fisher Scientific)	20%
	Diluted in dH_2O	
Stripping Buffer	Tris pH 6.8 (Fisher Scientific)	62.5 mM
	SDS (Fisher Scientific)	2%
	β-Mercaptoethanol (Sigma)	100 mM
	Dissolved in dH_2O	-
6x Restriction Enzyme Loading Buffer	Glycerol	50%
	EDTA	0.1 M
	SDS	1%
	Bromophenol blue	1.5 mM
	Xylene cyanol	1.86 mM
	Dissolved in dH_2O	
2% Agarose gel	Agarose	2%
	Tris-Acetate EDTA – Tris-acetate	0.04 M
	– EDTA	0.001 M

Table 2.1 Reagent recipes for primary cell culture and experiments.

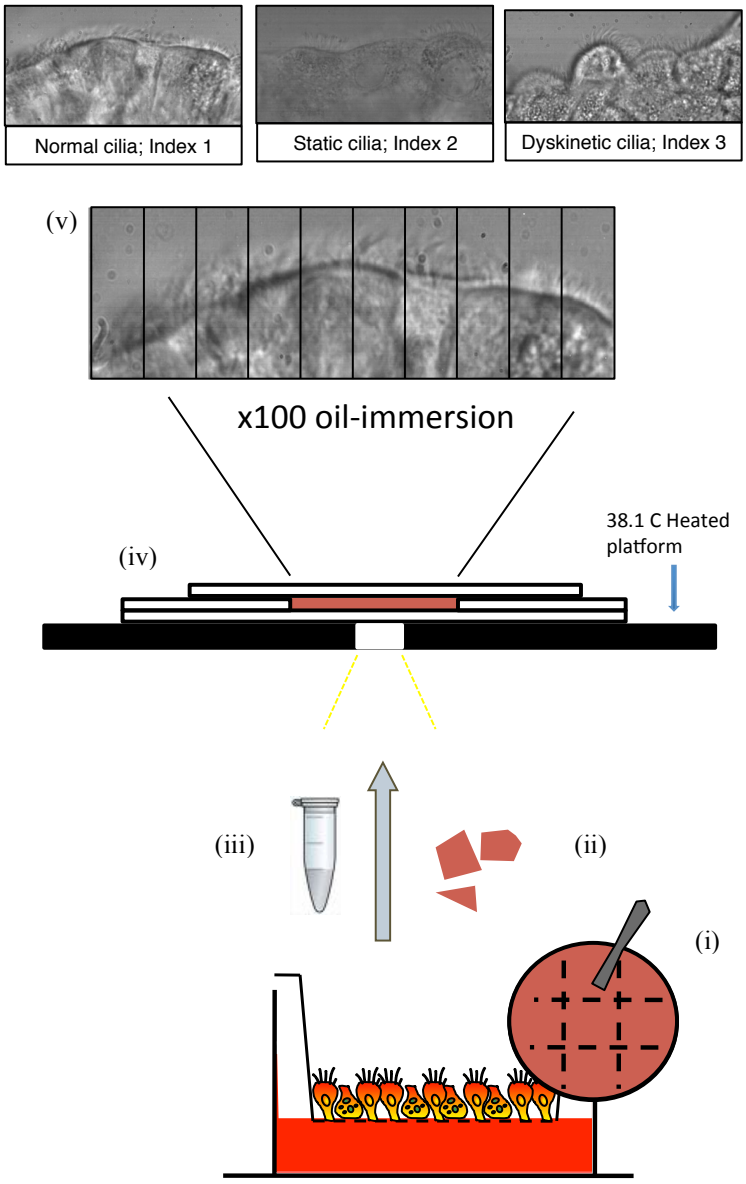

Figure 2.1 **Procedures of scraping method followed by video-microscopy.** The ciliated culture was scored into sections using a sterile spatula (i), and then scraped off from the apical surface of the Transwell insert (ii). Cell strips were resuspended in 1 ml of M199 (with antibiotics) medium (iii). 100 µl of cell suspension was added into the chamber slide (iv). Using x100 oil-immersion microscopy and high-speed camera, videos of epithelial side profiles were recorded (v).

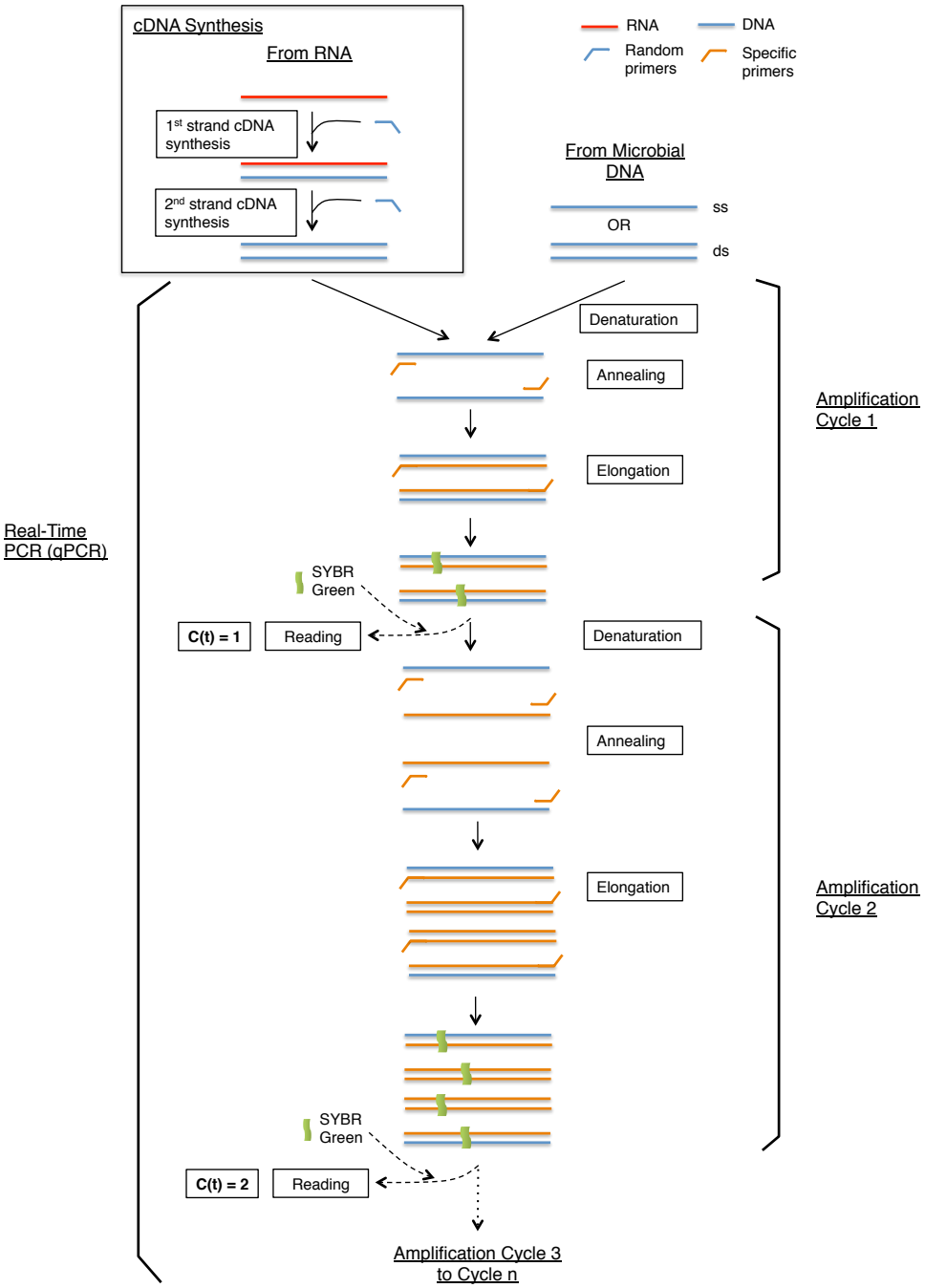

Figure 2.2 **Mechanism of real-time polymerase chain reaction (qPCR)**. Real-time PCR is also known as quantitative PCR (qPCR). If RNA is used as the input material, reverse transcriptase qPCR (RT-qPCR) is performed to convert the RNA to complementary DNA (cDNA) (box) If single- (ss-) or double-stranded (ds-) DNA is used as the input material (such as bacterial and fungal DNA), it can be used directly for the qPCR. qPCR starts with the denaturation step whilst any ds-DNA material is split into ss-DNA. Primers then anneal to the specific location on the ss-DNA material with matching sequence as the primers. The second strand of DNA material is then elongated from the site of the primer. SYBR Green is a specific cyanine dye that binds only to ds-DNA. Upon the binding, SYBR Green can be excited at 497 nm and emits green light at 520 nm. The intensity of the green light is directly proportional to the amount of ds-DNA material present in the reaction mix at the end of each amplification cycle, and is indirectly proportional to the reported C(t) value. The smaller the C(t) value, the more ds-DNA there is in the reaction mix (392).

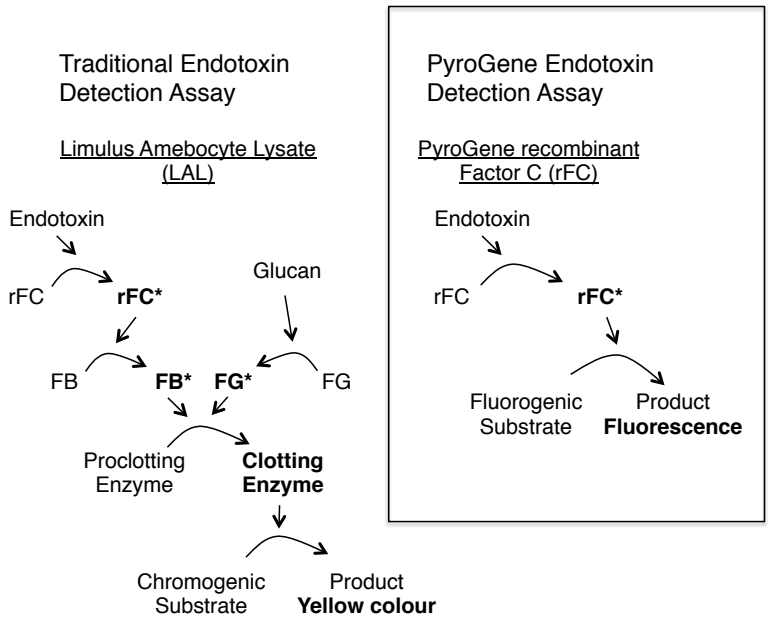

Figure 2.3 The signalling cascade of the PyroGene rFC endotoxin detection systems. The PyroGene rFC endotoxin detection system (box) uses the same signalling cascade as the tradition endotoxin detection assay, the Limulus Amebocyte Lysate (LAL) assay. rFC is a modified mimic of Factor C in the LAL cascade. It releases measurable fluorescence upon the reaction with LPS in the sample and therefore, it bypasses the downstream enzyme and substrate addition steps where fault positive arises (383).

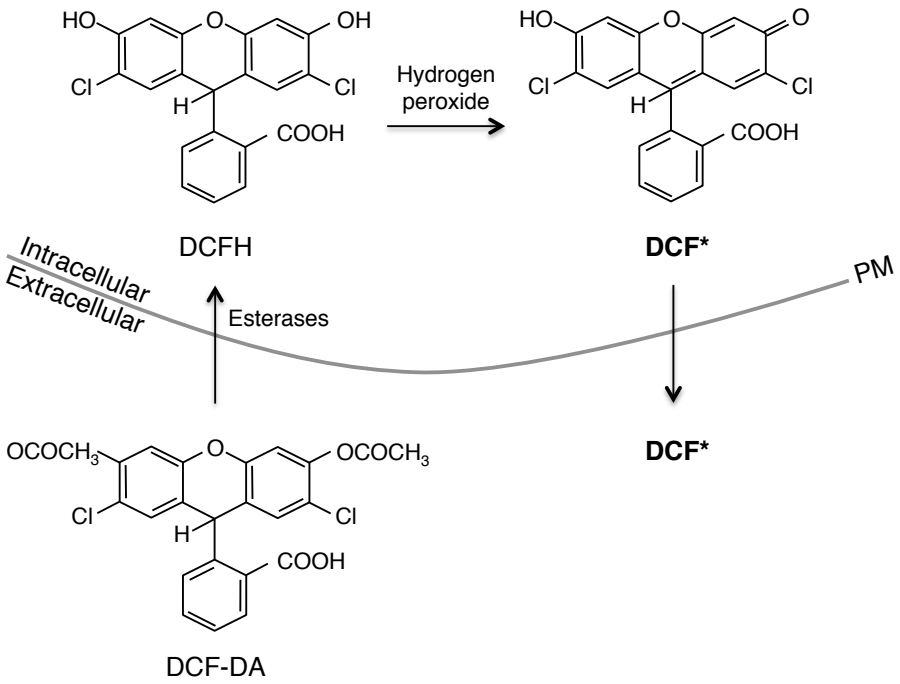

Figure 2.4 Hydrogen peroxide-induced DCF-DA molecule transition during the DCF-DA assay. The DCF-DA molecule can penetrate through plasma membrane (PM) to the cytoplasm of a cell. DCF-DA molecule then reacts with intracellular esterases to become PM-impermeable molecule DCFH. DCFH interacts with intracellular hydrogen peroxide, and is oxidised to the fluorescent DCF molecule. Fluorescent DCF molecule is PM-permeable (390).

3. Epithelial Ciliary Function in Asthma

3.1 Chapter Overview

This chapter focuses on the use of primary human airway epithelial cells as the tool to study the relationship between airway epithelium and asthma. The aims include:

1) To study the baseline characteristics of the epithelial cells *in vitro* and the potential relationship with epithelial dysfunction in asthma;
2) To determine whether ciliary dysfunction in asthma is primary or secondary;
3) To explore the epithelial function in response to asthma sputum stimulation.

Primary human airway epithelial basal cells (HAEBC) and air-liquid-interface (ALI) cultures were assessed in terms of their baseline synthetic capacity, gene expression, and the mechanical ciliary function of ciliated ALI cultures. The findings were in line with my hypothesis that the altered phenotype observed in asthma could be due to the presence of environmental factors. There was also a small indication that intrinsic factors may also play a role in this abnormal phenotype.

3.2 Introduction

Mucociliary clearance within the normal airway is important for clearing any foreign airborne substances, including allergenic particles and pathogens, that are inhaled and subsequently come into contact with the airway wall. The presence of healthy and mature cilia is pivotal in efficient mucociliary clearance. Mature cilia beat in the periciliary fluid in a continuous, organised fashion to propel the mucus with trapped particulates up and out of the airways.

Defective mucociliary clearance was first described in asthma in 1943, where abnormal cilia were found and a reduced rate of clearance was detected (395). An increased rate of infection has been found to be correlated to asthma exacerbation (242, 246), which could be partly due to the insufficient clearance of pathogens in the airways. Improvement in technology nowadays allows ciliary dysfunction to be properly quantified. Thomas *et al.* obtained fresh epithelial cell strips from bronchoscopy using bronchial brushes to enable their immediate experimental and/or clinical use (210). By using the videomicroscopy methodology, Thomas and his team showed that the asthmatic epithelial cell strips had a reduced ciliary function, which was correlated to disease severity. However, the mechanism underlying this abnormality has yet to be explored. Currently literature points toward a role of an environmental factor: exposure of ciliated epithelium to microbial materials reduced CBF *in vitro* (34, 255), and asthmatic sputa have been shown to induce ciliary immotility (396). Other studies, as revealed by gene expression studies (8, 180), suggest that the epithelium in asthmatic airways could be intrinsically abnormal. These factors could directly (e.g. disruption of the ATP/Ca^{2+} pathway) or indirectly (e.g. up-regulation of inflammation leading to

enhanced activation of the epithelium) affect the regulation of ciliary function. Based on this collective evidence, I tested the following hypotheses:

(i) The ciliary dysfunction in asthmatic epithelial cell is not due to a differential synthetic capability (in terms of cytokines and chemokines) of the epithelial cells at baseline compared to healthy controls

(ii) The ciliary dysfunction in asthmatic epithelial cells is not due to a differential gene expression of the epithelial cells at baseline

(iii) The ciliary dysfunction as observed *in vivo* persists in differentiated epithelial cultures derived from asthmatic subjects.

Differentiating epithelium *in vitro* is a recent and popular cell culture model for studying the role of epithelial cells in diseases (377). Epithelial basal cells could be differentiated *in vitro* to fully ciliated, mucus-secreting structures that highly resemble the epithelium *in vivo*. Stimuli of interest could then be added to these cultures in a controlled fashion to study their individual roles in disease development and/or progression. This model provides an invaluable tool for studying the role of airway epithelium in asthma.

3.3 Methodology

HAEBC obtained from airway epithelial cell donors were grown in BEGM; ALI cultures were differentiated from HAEBC using ALI medium with L-glutamine (**Table 2.1**). Only heavily ciliated ALI cultures (>14 d after the first visible beating cilium) were used for experiments. TEER measurement was kindly performed by Dr Rob Hirst.

Sandwich ELISA is a single protein quantification technique that utilises specific antibodies and measureable colour changes (luminescence reporter) (385). Whilst an MSD multiplex assay uses a similar sandwiching principle, it can detect multiple proteins simultaneously and uses electrochemically-stimulated SULFO-TAG labels as the measureable reporter (386). The mediators in the MSD assays were chosen based on the currently available evidence in literature that showed a linkage with asthma pathogenesis (148, 150, 181, 182, 397). Both techniques were used for studying the baseline synthetic response of HAEBC and ALI cultures.

MSD assays were done in GlaxoSmithKline Stevenage, U.K. Conditioned culture medium from HAEBC and ALI cultures was collected 24 h after refreshment and stored at -80ºC before use. Sandwich ELISA kits were used for measuring CCL5 (R&D systems; Abingdon; UK), and IFN-β (Pestka Biomedical Laboratories; Piscataway; USA). Samples were used neat. 0.1% Tween-20-PBS was used as the wash buffer. Limits of detection for the CCL5 and IFN-β ELISAs were 31.2 to 1000 pg/ml and 25 to 2000 pg/ml respectively.

Human genome microarrays measure the expression quantities of 50,000 genes simultaneously by using total RNA as the input materials. The “anti-sense”, single-

stranded RNA is converted to "sense", single-stranded genetic materials that can hybridise with specific genes on a GeneChip and releases readable fluorescence of which the intensity is directly proportional to the quantity of the input RNA (316, 391).

Human genome microarrays were used to study the baseline gene expression in HAEBC from health (n=5) and asthma (n=6). Total RNA was extracted using RNeasy mini kit plus DNaseI digestion (Qiagen). Only pure (A260/280 ratio ≈2) and intact (RIN ≈<10) total RNA samples were used for the microarrays (**Figure 3.2**). 250 ng total RNA was used as the input material. Freezing steps were minimised to prevent sample degradation.

The efficiency of mucociliary clearance could be reflected by the ciliary function of ciliated epithelium; ciliary function of ciliated ALI cultures developed from healthy and asthmatic subjects were assessed. The ciliary function of ALI cultures could be measured by the overhead method, which gave CBF and amplitude measurements (376), and by the scraping method, which gave CBF and beat pattern measurements (377). The baseline ciliary function measurement, using the overhead method, was kindly performed by Dr Rob Hirst. The ciliary beat pattern is more likely to have a significant effect on the overall ciliary function, thus the scraping method was used for the rest of the studies.

The ciliary function of the ALI cultures was measured at an un-stimulated (baseline) status and at a stimulated status after inoculating the cultures with fresh asthmatic sputa. To do that, heavily ciliated ALI cultures were incubated in either normal or antibiotic-free ALI medium for 48 h prior to the start of the experiment (at 0 h). Fresh, unprocessed asthmatic sputum plugs were diluted 1:4 in PBS. 200 µl diluted sputum or

PBS alone was added into the apical chamber. At baseline (0 h), 1 h, 4 h and 24 h, samples of apical chamber fluid (ACF) and baseolateral supernatant (ALI S/N) were collected and stored at -20ºC for further experiments (see Chapter 4). The scraped ciliated cell strips were used for ciliary function analysis. At the end of the study, the remaining cell strips were centrifuged at 10,000 rpm for 5 min and preserved in RNAlater (Qiagen) (1:0.2 PBS) at -80ºC for further experiments (see Chapter 4). To control the asthmatic sputum inoculation study, the repeatability of ciliary function measurement over 24 h was evaluated. The potential effect of antibiotics alone on the ciliary function was also evaluated by incubating the ALI cultures in an antibiotic-free ALI medium for 48 h prior to the reintroduction of antibiotics for another 48 h. The antibiotics herein consist of penicillin, gentamycin and amphotericin B. Ciliary function was measured at 48 h and 96 h.

3.4 Results

3.4.1 Overall subject characteristics

For better explanation, clinical characteristics and measurements of subjects were recorded according to the experiments they took part in each chapter. They were recorded detailing patient's physical status, lung function (predicted % of FEV_1, FEV_1/FVC ratio), blood total IgE and eosinophil levels, and atopy; airway responsiveness (PC_{20}), treatments, age of disease onset and sputum differential cell counts were covered when applicable.

Within the entire asthmatic population used in this thesis, there were 41 mild-moderate and 49 severe asthmatic subjects. Apart from the gender and blood IgE level, all the other parameters including lung function and blood eosinophils, showed correlation with disease severity. More severe subjects are likely to be older and atopic. More severe patients had higher doses of inhaled corticosteroid intakes. There was no significant difference in sputum eosinophil and neutrophil counts between the groups with mild-to-moderate and severe asthma.

3.4.2 The morphology of the cells changes from human airway epithelial basal cells (HAEBC) and Air-Liquid-Interface (ALI) ciliated cells

3.4.2.1 Morphological changes from HAEBC to ALI ciliated cells

HAEBC could be grown from the cells obtained by bronchoscopy. Ciliated epithelial cell strips were initially collected from bronchial brushes. The strips adhered to the collagen-coated surface within 24 h and only the cells with the cobblestone-shaped features expanded in BEGM (**Figure 3.1**A, Day 0). It was not clear whether the ciliated cells underwent de-differentiation or died. These cobblestone-shaped cells were also

double positive with epithelial basal cell markers cytokeratin-5/14 (375) (**Figure 3.1**B), suggesting that these cells were indeed HAEBC. The morphology of both healthy and asthmatic HAEBC were similar and remained unchanged up to passage stage 3 (P3). The cells then started to go flat, granular, and eventually became squamous. Therefore, HAEBC up to P2 were used for ALI culture differentiation and HAEBC at P3 was used for monoculture if the morphology was good.

ALI cultures were developed from HAEBC in Transwell® inserts (Corning). The 4 μm porous membrane allowed penetration of nutrients from the culture medium, located in the bottom baseolateral chamber, for cell settlement and growth. Only when the submerged culture has reached >99% confluence with no visible gaps would the cells be emerged to the air-liquid-interface. As soon as 1 day after exposing the apical surface to air, differentiating cells could be observed (**Figure 3.1**A). Mucus could be found from Day 9, indicating the differentiation of HAEBC to secretory cells. Only after this point would cells further differentiate into ciliated cells. On average, the first beating cilium could be observed on approximately Day 25. Approximately 2 weeks afterwards the cultures would become heavily ciliated. The trans-apical epithelial electrical resistance (TEER) reading of a normal healthy culture was 1,160±56 Ω/cm^2, and this would reduce in the presence of excess mucus (357±17 Ω/cm^2) (**Figure 3.1**C). The term "excess mucus" here means that the volume of the mucus layer found on the apical surface was sufficient enough to be removed by simply pipetting. In comparison, "normal mucus" means that despite of the presence of a thick mucus layer, it required an addition of 200 μl PBS in order to wash the mucus away. Differentiated ALI cultures would generally remain confluent and ciliated for over 100 days. It showed no observable morphological differences between healthy control- and asthmatic-derived

ALI cultures using light microscopy. There was also no substantial difference in the amount of observable ciliated cells between the subject groups.

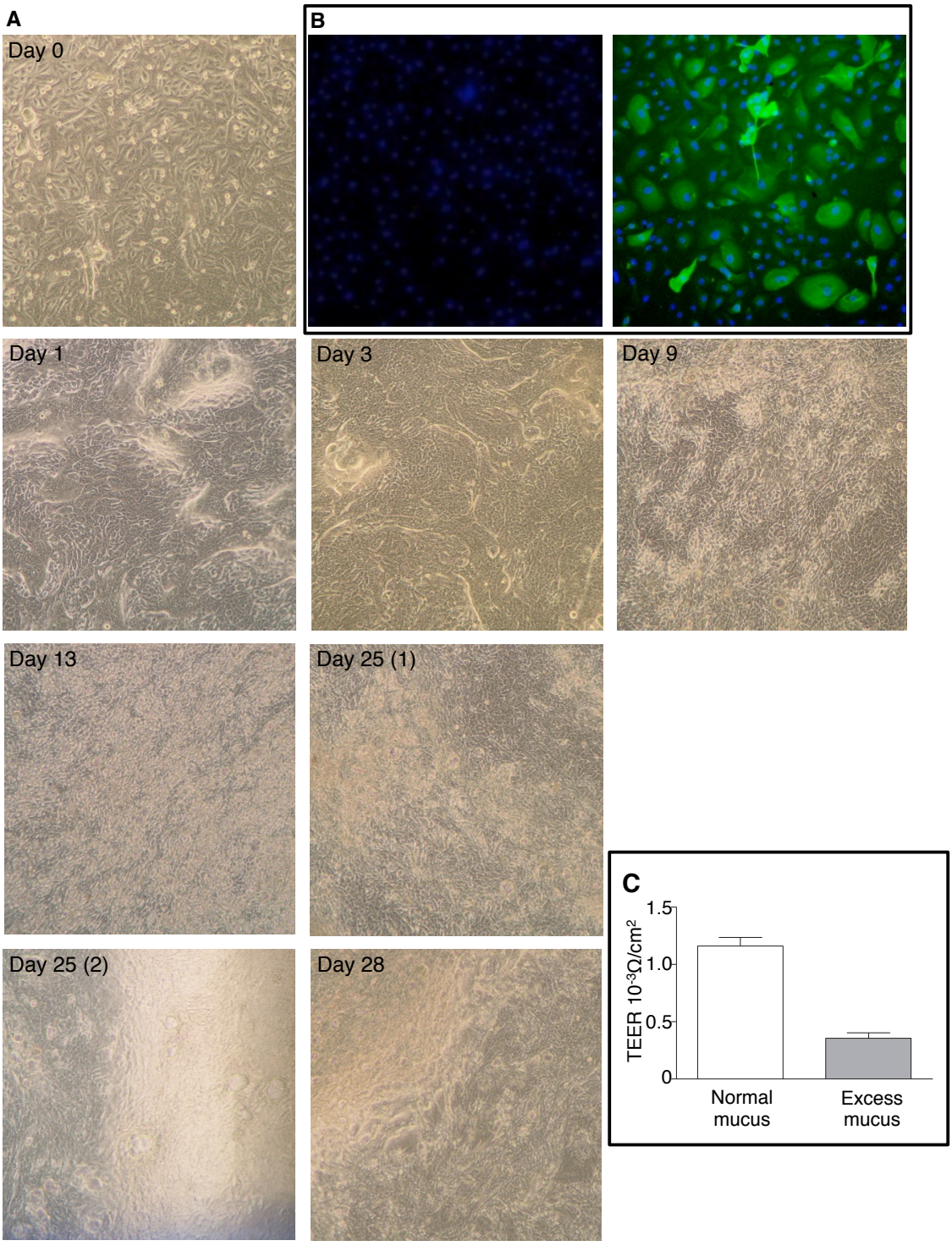

Figure 3.1 Morphological changes from HAEBC to ALI ciliated cells during cell differentiation. A shows the immunofluorescence staining of HAEBC for cytokeratins-5^{+}/14^{+} (green); cell nuclei stained with DAPI (blue). B shows the change of epithelial cell morphology of a differentiating epithelial culture of a healthy control. The morphology was observed using light microscopy: (Day 0) basal cells with cobblestone-shaped feature; (Day 9) presence of secretory cells; (Day 23-28) presence of ciliated cells. C shows the trans-apical epithelial electrical resistance (TEER) expressed as mean±SEM of fully differentiated ALI cultures developed from healthy controls.

3.4.3 Baseline synthetic response in human airway epithelial cells showed little difference between health and asthma

To evaluate if an abnormal mediator synthetic capacity is the primary cause of ciliary dysfunction in asthma, the baseline secretion of different pro-inflammatory mediators from HAEBC and ALI cultures was measured using MSD assays and ELISA.

Clinical Details	Healthy (n = 16)	Asthmatic (n = 17)	p-values
Gender (F)	6 (10)	9 (8)	0.37*
Age, yr.	39 (4)	46 (3.6)	0.17
Pack yr	1 (1)	4 (3)	0.24
% Predicted FEV_1	104 (3)	92 (5)	0.054
% FEV_1/FVC	84 (2)	75 (2)	**0.0004**
PC20 FEV_1, mg/ml †	>16	1.7 (1.0-3.0)	**<0.0001**
Blood Total IgE, kU/ml	257 (142)	992 (485)	0.33
Blood eosinophils, kU/ml	0.09 (0.02)	0.41 (0.10)	**0.02**
Treatment (mcg/24 BDP eqv.)	n/a	813 (181)	n/a
Atopy, %	25	60	0.07*
Age of Disease Onset, yr	n/a	39 (7)	n/a
Sputum Characterization			
Total cell count ($x10^6$ cells/ml)	n/a	3.4 (1.0)	n/a
Eosinophils, % ‡	n/a	5.8 (1.4-15)	n/a
Neutrophils, % ‡	n/a	43 (26-61)	n/a
Macrophages, % ‡	n/a	33 (12-47)	n/a
Epithelial cells, % ‡	n/a	1.0 (0.0-5.3)	n/a

† geometric mean (95% CI) ‡ median (interquartile range); * Chi Square test, $p<0.05$.

Table 3.1 Clinical details of the subjects for the baseline epithelial synthetic response experiment. Data are expressed as mean (SEM) unless otherwise indicated. Statistical differences were assessed using unpaired t-tests, $p<0.05$, unless otherwise indicated.

A total of 16 healthy controls and 17 asthmatic subjects were used for this experiment (**Table 3.1**). A total of 13 cytokines and chemokines released from un-stimulated HAEBC (n=17) and ALI cultures (n=21) were measured. The level of mediators measured was normalised with the number of cells and presented as pg/ml/10^6 cells. Mann-Whitney test was the statistical analysis performed after the normalisation. The pattern of release was significantly different between the two epithelial cell types,

including IFN-β, IL-1β and CCL2 (**Table 3.2**A). Interestingly, the difference in the baseline mediator release was not identified between health and asthma in either types of epithelial cell cultures (**Table 3.2**B). Therefore, the mediators measured here were not likely to be the cause of ciliary dysfunction in asthmatic epithelial cells. However, it does not exclude the possibility that these mediators may be involved in the pathogenesis of the dysfunction at a stimulated state (181, 182).

A.

Mediators	Constitutive Levels (pg/ml/10^6 cells)		p-value
	Bronchial Basal (n = 17)	ALI (n = 21)	
IFN-β	60.7 (28.8 – 127.6)	13.9 (12.5 – 15.1)	**0.0004**
CCL5	12.4 (8.9 – 17.2)	22.7 (13.3 – 38.5)	0.35
IL-1β	216.1 (81.4 – 573.9)	20.5 (7.5 – 56.2)	**0.002**
CXCL8	11205.0 (5367.0 – 23391.0)	12316.0 (8792.0 – 17251.0)	0.99
CCL2	60.3 (29.9 – 121.6)	460.7 (150.3 – 1468.0)	**0.003**
CCL13	416.7 (139.2 – 1248.0)	1037.0 (611.2 – 1761.0)	0.13
CCL4	23.3 (9.1 – 59.8)	53.9 (20.3 – 143.2)	0.07
TNF-α	146.9 (64.5 – 334.5)	121.5 (41.8 – 353.4)	0.74
CCL22	967.3 (534.5 – 1751.0)	1529.0 (965.0 – 2424.0)	0.16
CCL17	302.3 (108.3 – 844.4)	460.0 (205.2 – 1031.0)	0.31
CCL26	3137.0 (723.8 – 13594.0)	3533.0 (1842.0 – 6776.0)	0.19
CXCL10	440.5 (145.9 – 1330.0)	520.4 (230.6 – 1175.0)	0.83
CCL11	229.6 (128.5 – 410.1)	218.3 (81.0 – 588.4)	0.49

B.

Mediators	HAEBC		p-value	ALI cultures		p-value
(pg/ml/10^6 cells)	Healthy (n=7)	Asthma (n=10)		Healthy (n=10)	Asthma (n=11)	
IFN-β	73.4 (35.0 – 154.2)	53.0 (14.5 – 192.7)	0.19	12.6 (12.6 – 12.7)	14.7 (12.5 – 17.3)	0.33
CCL5	12.2 (7.3 – 23.4)	11.2 (7.7 – 17.5)	0.96	25.2 (11.1 – 75.5)	14.6 (8.7 – 27.5)	0.33
IL-1β	287.5 (63.1 – 1310.0)	177.0 (38.7 – 808.8)	0.81	8.1 (1.3 – 48.7)	44.5 (14.1 – 140.4)	0.18
CXCL8	17666.0 (5930 – 52630)	8147 (2665 – 24903)	0.42	12303 (6678 – 22666)	12326 (7846 – 19365)	0.81
CCL2	122.1 (50.6 – 294.8)	35.5 (12.8 – 98.6)	0.06	449.8 (47.7 – 4244.0)	487.0 (125.6 – 1888)	0.72
CCL13	854.4 (401.0 – 1820)	243.2 (33.9 – 1746.0)	0.35	1143.0 (455.9 – 2865)	956.8 (457.3 -2002)	0.67
CCL4	38.8 (7.7 – 194.5)	15.9 (3.9 – 61.5)	0.33	47.2 (6.8 – 326.8)	60.3 (19.2 – 189.4)	0.82
TNF-α	219.5 (61.7 – 780.8)	110.9 (31.6 – 389.6)	0.42	93.1 (10.6 – 820.8)	151.6 (47.2 – 487.1)	0.67
CCL22	1434.0 (692.4 – 2972)	719.8 (269.1 – 1925)	0.66	1622.0 (750.8 – 3503)	1457.0 (747.0 – 2840)	0.92
CCL17	586.6 (286.6 – 1201)	183.9 (29.0 – 1168)	0.41	724.4 (300.6 – 1746)	315.0 (78.9 – 1257)	0.31
CCL26	8414.0 (4393 – 16116)	1497.0 (103 – 21761)	0.28	2754.0 (1374 – 5520)	4348.0 (1386 – 13646)	0.67
CXCL10	958.7 (441.7 – 2080)	245.8 (35.5 – 1750)	0.49	739.6 (274.5 – 1993)	388.8 (98.6 – 1530)	0.45
CCL11	321.1 (132.3 – 779.5)	178.5 (71.5 – 445.4)	0.41	517.6 (216.8 – 1236)	106.3 (19.6 – 577.3)	0.16

Table 3.2 Baseline secretion of mediators from primary epithelial cells. The constitutive secretion of mediators over 24 h from primary human airway epithelial cells was investigated. Mediators CCL5 and IFN-β were measured by ELISA. The rest of the mediators were measured by MSD multiplex assay. Data are expressed as median (interquartile range). A shows the results from HAEBC (n=17) and ALI cultures (n=21). Statistical differences were assessed using Mann-Whitney U tests. B shows the results from the same set of data, with the samples divided into healthy controls and asthmatics: HAEBC (n=7 and n=10 respectively), ALI cultures (n=10 and n=11 respectively). Statistical differences were assessed using Mann-Whitney U tests.

3.4.4 Baseline gene expression in HAEBC

With no differential secretion of pro-inflammatory mediators found in epithelial cultures at baseline, the investigation of any potential primary cause of abnormality in the asthmatic epithelium was extended to the genetic level. Genome microarrays were used to capture the maximum number of genes without bias. The latest human genome microarrays allow >54,000 genes to be assessed simultaneously.

Clinical Details	Healthy (n = 5)	Asthmatic (n = 6)	p-values
Gender (F)	3 (2)	3 (3)	0.74*
Age, yr	43 (5)	52 (5)	0.24
Pack year	6 (5)	4 (2)	0.65
% Predicted FEV_1	95 (6)	76 (12)	0.21
% FEV_1/FVC	81 (4)	69 (8)	0.20
PC20 FEV_1, mg/ml †	>16	1.1 (0.1-8.4)	**0.002**
Blood Total IgE, kU/ml	17 (0.9)	86 (31)	0.18
Blood eosinophils, kU/ml	0.16 (0.04)	0.38 (0.12)	0.16
Treatment (mcg/24 BDP eqv.)	n/a	1667 (262)	n/a
Atopy, %	50	67	0.21*
Age of Disease Onset, yr	n/a	37 (9)	n/a
Sputum Characterization			
Total cell count($x10^6$ cells/ml)	n/a	3.7 (2.5)	n/a
Eosinophils, % ‡	n/a	1.8 (0-40)	n/a
Neutrophils, % ‡	n/a	84 (23-87)	n/a
Macrophages, % ‡	n/a	14 (9-34)	n/a
Epithelial cells, % ‡	n/a	1.5 (0.6-3.9)	n/a

† geometric mean (95% CI) ‡ median (inter-quartile range); * Chi square test, $p<0.05$.

Table 3.3 Clinical details of the subjects for the baseline gene expression experiment. Data are expressed as mean (SEM) unless otherwise indicated. Statistical differences were assessed using unpaired t-tests, $p<0.05$, unless otherwise indicated.

A total of 11 arrays were performed using 5 healthy controls and 6 asthmatics (**Table 3.3**). All 11 arrays passed the quality controls (**Figure 3.2**). The median of percentage (%) present was 54.1%. Using the common 2-fold difference as the cut-off (316, 398), only 5 genes were found significantly lower, and 7 genes significantly higher, in the asthmatic group. With this subtle difference in baseline gene expression, the cut-off was

therefore reduced to 1.6-fold, which was chosen because it was within the range of cut-off values (1.1-fold to 2-fold) that have previously been published (29, 180). This reduced cut-off threshold resulted in a total of 59 genes of which the expression levels were significantly different between healthy and asthmatic HAEBC (**Table 3.4**A). Their potential roles in asthma included cell survival and development (e.g. *CST6*, *EDN1*, *NEAT1*, *RGS2*, *TUBE1*), inflammation (e.g. *EGLN3*, *C1S*, *HMGB2*, *IRAK3*, *PTPRD*, *PI3*), and oxidative handling (e.g. *CYBRD1*, *CYP4F3* and *CYP4F11*, *EGLN3*, *LOX*, *PLCB1*). A low false discovery rate (18%) suggested that there was little variation between samples among each group. Some genes were specifically present (n=≥50%) or absent in asthmatic HAEBC, which are included in **Appendix 7.2**. **Table 3.4** highlights the genes that have known functions and may result in disease-related outcomes. They include cell behaviour (*LGALS4*, *EMP1*, *CAPN5, MKI67*, *PCNA and KRT75*), oxidative balance (*NOX4*, *GST* and *CYP* gene families, *HSDL2*), inflammation and signalling (*CD* gene families, *TNFRSF4*, *CLEC4M*, and *FAM* gene family), and ion transports (*ABC, SLC* and *TMEM* gene families). Some of these genes (*CHL1*, *LOX, HMGB2* and *EMP1*) have been shown to be important in HAEBC differentiation (398). These results therefore suggest that some of these genes could be the intrinsic causes that are directly or indirectly involved in the development of ciliary dysfunction. However, the low sample size reduced the power of this statement, and further investigation of these genes in HAEBC by repeating the experiment, and eventually repeats using ALI cultures and/or fresh airway ciliated cells would be required. This could be done using cheaper and more routine techniques, such as RT-qPCR.

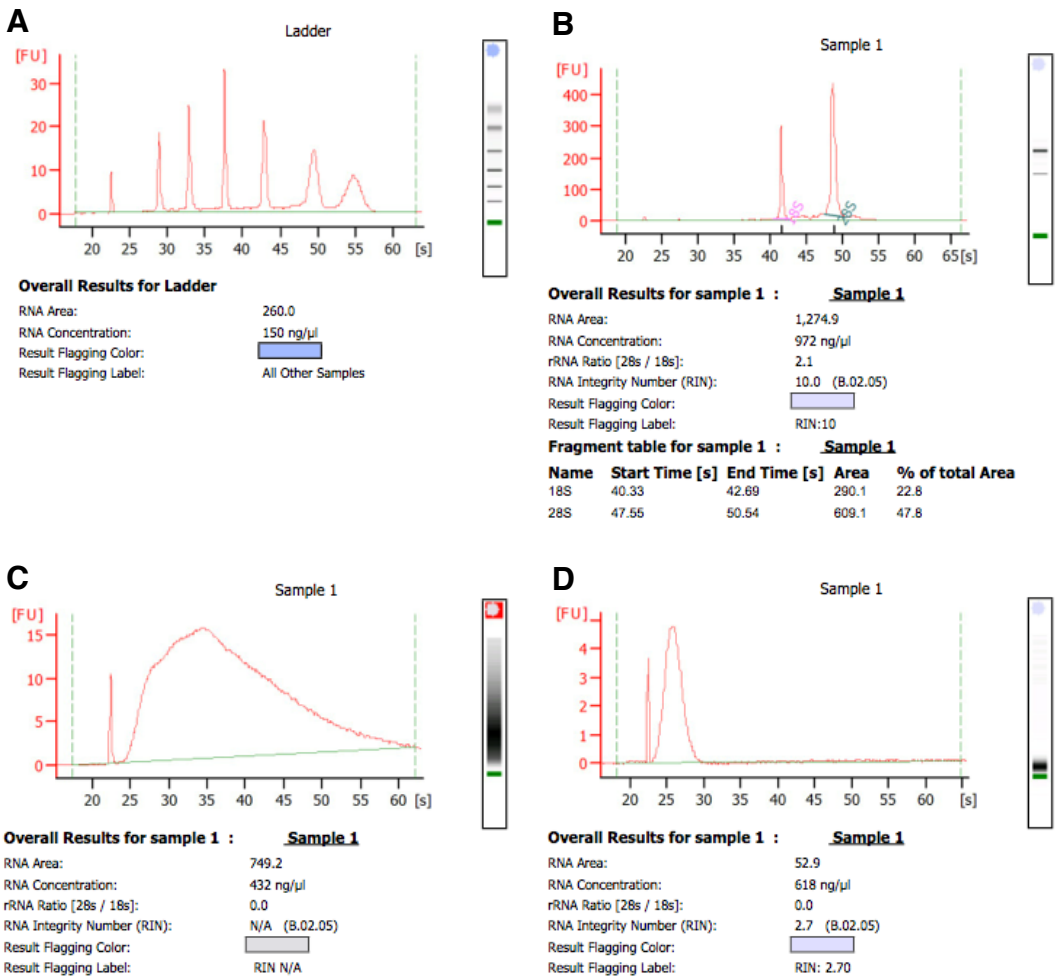

Figure 3.2 Samplequality controls for human genome microarrays. The quality control of RNA samples was done using RNA 6000 Nano Kit (Agilent). A shows the image of the ladder after electrophoresis. B shows an intact RNA sample with RNA Integrity Number (RIN) close to 10. C and D show an unfragmented and a fragmented aRNA sample respectively.

A. Genes differentially expressed in HAEBC by microarray analysis in subjects with asthma (n=6) compared with healthy controls (n=5). ≥ 1.6 fold up (+) / down (-) regulated in asthma, p <0.05 with presence calls ≥ 100% unless indicated (*). False discover rate of 1000 permutation 18%.

Affymetrix ID	Gene Symbol	Gene Name	Entrez Gene ID	Fold Difference	P value
211080_s_at	NEK2	NIMA (never in mitosis gene a)-related kinase 2	4751	2.39	0.036
204469_at	PTPRZ1	protein tyrosine phosphatase, receptor-type, Z polypeptide 1	5803	2.38	0.024
221530_s_at	BHLHE41	basic helix-loop-helix family, member e41	79365	2.07	0.022
219806_s_at	C11orf75	chromosome 11 open reading frame 75	56935	2.05	0.014
215446_s_at	LOX	lysyl oxidase	4015	2.04	0.028
213375_s_at	N4BP2L1	NEDD4 binding protein 2-like 1	90634	2.03	0.044
206515_at	CYP4F3	l P450, family 4, subfamily F, polypeptide 3	4051	2.02	0.035
223687_s_at	LY6K	lymphocyte antigen 6 complex, locus K	54742	2.00	0.025
213222_at	PLCB1	phospholipase C, beta 1 (phosphoinositide-specific)	23236	1.99	0.023
208808_s_at	HMGB2	high-mobility group box 2	3148	1.96	0.025
226181_at	TUBE1	tubulin, epsilon 1	51175	1.95	0.050
217889_s_at	CYBRD1	cytochrome b reductase 1	79901	1.94	0.015
1555229_a_at	C1S	complement component 1, s subcomponent	716	1.93	0.044
235709_at	GAS2L3	growth arrest-specific 2 like 3	283431	1.88	0.043
202375_at	SEC24D	SEC24 family, member D (S. cerevisiae)	9871	1.86	0.017
209846_s_at	BTN3A2	butyrophilin, subfamily 3, member A2	11118	1.86	0.050
205773_at	CPEB3	cytoplasmic polyadenylation element binding protein 3	22849	1.86	0.027
221911_at	ETV1	ets variant 1	2115	1.84	0.042
227379_at	MBOAT1	membrane bound O-acyltransferase domain containing 1	154141	1.82	0.028
220034_at	IRAK3	interleukin-1 receptor-associated kinase 3	11213	1.81	0.026
201853_s_at	CDC25B	cell division cycle 25 homolog B (S. pombe)	994	1.80	0.030
212503_s_at	DIP2C	DIP2 disco-interacting protein 2 homolog C (Drosophila)	22982	1.79	0.024
206153_at	CYP4F11	cytochrome P450, family 4, subfamily F, polypeptide 11	57834	1.78	0.042
1552546_a_at	LETM2	leucine zipper-EF-hand containing transmembrane protein 2	137994	1.77	0.043
215342_s_at	RABGAP1L	RAB GTPase activating protein 1-like	9910	1.76	0.032
202007_at	NID1	nidogen 1	4811	1.74	0.040
212230_at	PPAP2B	phosphatidic acid phosphatase type 2B	8613	1.74	0.038
206683_at	ZNF165	zinc finger protein 165	7718	1.72	0.045
227910_at	XPNPEP3	X-prolyl aminopeptidase (aminopeptidase P) 3, putative	63929	1.70	0.017
220334_at	RGS17	regulator of G-protein signaling 17	26575	1.70	0.010
205542_at	STEAP1	six transmembrane epithelial antigen of the prostate 1	26872	1.69	0.023
223253_at	EPDR1	ependymin related protein 1 (zebrafish)	54749	1.67	0.045
215942_s_at	GTSE1	G-2 and S-phase expressed 1	51512	1.65	0.037

Affymetrix ID	Gene Symbol	Gene Name	Entrez Gene ID	Fold Difference	P value
214774_x_at	TOX3	TOX high mobility group box family member 3	27324	1.65	0.042
203354_s_at	PSD3	pleckstrin and Sec7 domain containing 3	23362	1.65	0.044
203799_at	CD302	CD302 molecule	9936	1.65	0.019
214043_at	PTPRD	protein tyrosine phosphatase, receptor type, D	5789	1.64	0.003
220615_s_at	FAR2	fatty acyl CoA reductase 2	55711	1.63	0.040
1564630_at	EDN1	endothelin 1	1906	-1.62	0.049
219895_at	FAM70A	family with sequence similarity 70, member A	55026	-1.63	0.023
238933_at	IRS1	insulin receptor substrate 1	3667	-1.63	0.044
226145_s_at	FRAS1	Fraser syndrome 1	80144	-1.63	0.026
224454_at	ETNK1	ethanolamine kinase 1	55500	-1.63	0.025
229004_at	ADAMTS15	ADAM metallopeptidase with thrombospondin type 1 motif, 15	170689	-1.67	0.000
206595_at	CST6	cystatin E/M	1474	-1.67	0.049
207065_at	KRT75	keratin 75	9119	-1.68	0.039
222847_s_at	EGLN3	egl nine homolog 3 (C. elegans)	112399	-1.69	0.027
223544_at	TMEM79	transmembrane protein 79	84283	-1.70	0.036
235309_at	RPS15A	ribosomal protein S15a	6210	-1.71	0.034
1554026_a_at	MYO10	myosin X	4651	-1.71	0.008
215729_s_at	VGLL1	vestigial like 1 (Drosophila)	51442	-1.74	0.048
224566_at	NEAT1	nuclear paraspeckle assembly transcript 1 (non-protein coding)	283131	-1.74	0.038
233030_at	PNPLA3	patatin-like phospholipase domain containing 3	80339	-1.78	0.033
239562_at	MTHFD2L	methylenetetrahydrofolate dehydrogenase (NADP+ dependent) 2-like	441024	-1.79	0.029
203819_s_at	IGF2BP3	insulin-like growth factor 2 mRNA binding protein 3	10643	-1.89	0.022
1554966_a_at	FILIP1L	filamin A interacting protein 1-like	11259	-1.89	0.024
223210_at	CHURC1	churchill domain containing 1	91612	-1.91	0.025
202388_at	RGS2	regulator of G-protein signaling 2, 24kDa	5997	-2.16	0.033
239552_at	VWDE	von Willebrand factor D and EGF domains	221806	-2.31	0.034
219232_s_at	EGLN3	egl nine homolog 3 (C. elegans)	112399	-2.37	0.036
203691_at	PI3	peptidase inhibitor 3, skin-derived	5266	-2.46	0.005
41469_at	PI3	peptidase inhibitor 3, skin-derived	5266	-2.51	0.006
204135_at	FILIP1L	filamin A interacting protein 1-like	11259	-2.67	0.018
226736_at	CHURC1	churchill domain containing 1	91612	-2.92	0.027

B. Genes present in ≥3 asthmatics compared to 0 healthy controls

Affymetrix ID	Gene Symbol	Gene Name	Entrez Gene ID
204272_at	LGALS4	lectin, galactoside-binding, soluble, 4	3960
204418_x_at	GSTM2	glutathione S-transferase mu 2 (muscle)	2946
204683_at	ICAM2	intercellular adhesion molecule 2	3384
205439_at	GSTT2	glutathione S-transferase theta 2	2953
206637_at	P2RY14	purinergic receptor P2Y, G-protein coupled, 14	9934
206916_x_at	TAT	tyrosine aminotransferase	6898
208023_at	TNFRSF4	tumor necrosis factor receptor superfamily, member 4	7293
208462_s_at	ABCC9	ATP-binding cassette, sub-family C (CFTR/MRP), member 9	10060
209324_s_at	RGS16	regulator of G-protein signaling 16	6004
209423_s_at	PHF20	PHD finger protein 20	51230
210457_x_at	HMGA1	high mobility group AT-hook 1	3159
210836_x_at	PDE4D	phosphodiesterase 4D, cAMP-specific (phosphodiesterase E3 dunce homolog, Drosophila)	5144
212020_s_at	MKI67	antigen identified by monoclonal antibody Ki-67	4288
212080_at	MLL	Myeloid/lymphoid or mixed-lineage leukemia (trithorax homolog, Drosophila)	4297
213672_at	MARS	methionyl-tRNA synthetase	4141
214105_at	SOCS3	suppressor of cytokine signaling 3	9021
215070_x_at	RABGAP1	RAB GTPase activating protein 1	23637
215217_at	IGKC	Immunoglobulin kappa constant	3514
216325_x_at	RTEL1	regulator of telomere elongation helicase 1	51750
217889_s_at	CYBRD1	cytochrome b reductase 1	79901
219525_at	SLC47A1	solute carrier family 47, member 1	55244
219559_at	SLC17A9	solute carrier family 17, member 9	63910
219773_at	NOX4	NADPH oxidase 4	50507
220288_at	MYO15A	myosin XVA	51168
220306_at	FAM46C	family with sequence similarity 46, member C	54855
222121_at	SGEF	Src homology 3 domain-containing guanine nucleotide exchange factor	26084
224044_at	RHOT1	ras homolog gene family, member T1	55288
225654_at	NSD1	nuclear receptor binding SET domain protein 1	64324
226610_at	CENPV	centromere protein V	201161
227007_at	TMCO4	transmembrane and coiled-coil domains 4	255104
227890_at	TMEM198	transmembrane protein 198	130612
228875_at	FAM162B	family with sequence similarity 162, member B	221303
230664_at	H2BFM	H2B histone family, member M /// H2B histone family, member X, pseudogene	286436 /// 767811
230802_at	ARHGAP24	Rho GTPase activating protein 24	83478
230949_at	SLC23A3	solute carrier family 23 (nucleobase transporters), member 3	151295
231164_at	ABCA17P	ATP-binding cassette, sub-family A (ABC1), member 17 (pseudogene)	650655
231794_at	CTLA4	cytotoxic T-lymphocyte-associated protein 4	1493

Affymetrix ID	Gene Symbol	Gene Name	Entrez Gene ID
232912_at	GPR180	G protein-coupled receptor 180	160897
234818_at	TMEM108	transmembrane protein 108	66000
235339_at	SETDB2	SET domain, bifurcated 2	83852
236195_x_at	PRKCG	protein kinase C, gamma	5582
238564_at	FAM171B	Family with sequence similarity 171, member B	165215
241995_at	DGUOK	deoxyguanosine kinase	1716
242946_at	CD53	CD53 molecule	963
243301_at	COL22A1	collagen, type XXII, alpha 1	169044
244225_x_at	LMNA	Lamin A/C	4000
244691_at	SETD5	SET domain containing 5	55209
1552281_at	SLC39A5	solute carrier family 39 (metal ion transporter), member 5	283375
1555447_at	GPR114	G protein-coupled receptor 114	221188
1564796_at	EMP1	epithelial membrane protein 1	2012
1568830_at	IRAK3	interleukin-1 receptor-associated kinase 3	11213
1569504_at	LILRB4	Leukocyte immunoglobulin-like receptor, subfamily B (with TM and ITIM domains), member 4	11006
204591_at	CHL1	cell adhesion molecule with homology to L1CAM (close homolog of L1)	10752
211100_x_at	LILRA2	leukocyte immunoglobulin-like receptor, subfamily A (with TM domain), member 2	11027
215108_x_at	TOX3	TOX high mobility group box family member 3	27324
224262_at	IL1F10	interleukin 1 family, member 10 (theta)	84639
229849_at	WIPF3	WAS/WASL interacting protein family, member 3	644150
235518_at	SLC8A1	solute carrier family 8 (sodium/calcium exchanger), member 1	6546
237144_at	LTBP3	latent transforming growth factor beta binding protein 3	4054
1552787_at	HELB	helicase (DNA) B	92797
1554396_at	UEVLD	UEV and lactate/malate dehyrogenase domains	55293
1555063_at	USP6	ubiquitin specific peptidase 6 (Tre-2 oncogene)	9098
1555078_at	ZNF843	zinc finger protein 843	283933
1557223_at	RBPMS	RNA binding protein with multiple splicing /// succinate dehydrogenase complex, subunit A, flavoprotein pseudogene 2	11030 /// 727956
1559128_at	HSDL2	hydroxysteroid dehydrogenase like 2	84263
242762_s_at	FAM171B	family with sequence similarity 171, member B	165215
1563318_s_at	MAGIX	MAGI family member, X-linked	79917
205885_s_at	ITGA4	integrin, alpha 4 (antigen CD49D, alpha 4 subunit of VLA-4 receptor)	3676

C. Genes present in ≥3 healthy controls compared to 0 asthmatics

Affymetrix ID	Gene Symbol	Gene Name	Entrez Gene ID
205708_s_at	TRPM2	transient receptor potential cation channel, subfamily M, member 2	7226
205752_s_at	GSTM5	glutathione S-transferase mu 5	2949

Affymetrix ID	Gene Symbol	Gene Name	Entrez Gene ID
207004_at	BCL2	B-cell CLL/lymphoma 2	596
207095_at	SLC10A2	solute carrier family 10 (sodium/bile acid cotransporter family), member 2	6555
207309_at	NOS1	nitric oxide synthase 1 (neuronal)	4842
207995_s_at	CLEC4M	C-type lectin domain family 4, member M	10332
208147_s_at	CYP2C8	cytochrome P450, family 2, subfamily C, polypeptide 8	1558
211909_x_at	PTGER3	prostaglandin E receptor 3 (subtype EP3)	5733
216260_at	DICER1	dicer 1, ribonuclease type III	23405
217400_at	PCNA	proliferating cell nuclear antigen	5111
91703_at	EHBP1L1	EH domain binding protein 1-like 1	254102
225449_at	RDH13	retinol dehydrogenase 13 (all-trans/9-cis)	112724
226292_at	CAPN5	calpain 5	726
227222_at	FBXO10	F-box protein 10	26267
236274_at	EIF3B	eukaryotic translation initiation factor 3, subunit B	8662
238453_at	FGFBP3	fibroblast growth factor binding protein 3	143282
239607_at	GPR156	G protein-coupled receptor 156	165829
244819_x_at	PSPH	phosphoserine phosphatase	5723
1552804_a_at	TIRAP	toll-interleukin 1 receptor (TIR) domain containing adaptor protein	114609
1552912_a_at	IL23R	interleukin 23 receptor	149233
1552980_at	HAS3	hyaluronan synthase 3	3038
1558732_at	MAP4K4	mitogen-activated protein kinase kinase kinase kinase 4	9448
212803_at	NAB2	NGFI-A binding protein 2 (EGR1 binding protein 2)	4665
213338_at	TMEM158	transmembrane protein 158	25907
215769_at	TRD@	T cell receptor delta locus	6964
220663_at	IL1RAPL1	interleukin 1 receptor accessory protein-like 1	11141
237210_at	NFRKB	nuclear factor related to kappaB binding protein	4798
240063_at	LOC441046	glucuronidase, beta pseudogene	441046
1553175_s_at	PDE5A	phosphodiesterase 5A, cGMP-specific	8654
1555082_a_at	NEK11	NIMA (never in mitosis gene a)- related kinase 11	79858
1556144_at	DHX30	DEAH (Asp-Glu-Ala-His) box polypeptide 30	22907
1564386_at	TXNDC8	thioredoxin domain containing 8 (spermatozoa)	255220
216755_at	OSBPL10	oxysterol binding protein-like 10	114884
204795_at	PRR3	proline rich 3	80742

Table 3.4 Baseline gene expression in HAEBC in health and asthma. The HAEBC gene expression profile was compared between health (n=5) and asthma (n=6). A shows the gene differentially expressed at baseline with ≥1.6-fold significant difference, $p<0.05$ with presence calls ≥100%. False discovery rate of 1000 permutations is 18.0%. B highlights the genes that are present in ≥3 asthmatics compared to 0 healthy control, and are relevant in this thesis. C highlights the genes that are present in ≥3 healthy controls compared to 0 asthmatics, and are relevant in this thesis.

3.4.5 Baseline ciliary function of ALI cultures was similar between health and asthma

Abnormal ciliary function is believed to be one of the causes of the impaired mucociliary clearance in asthmatic airways (210). By using ciliated ALI cultures as a tool, it was considered whether this dysfunction persisted in *in vitro* primary cultures and represented an altered epithelial cell phenotype.

Clinical Details	Healthy (n = 17)	Asthmatic (n = 31)	p-values
Gender (F)	10 (6)	17 (14)	0.61*
Age, yr	43 (5)	45 (2)	0.56
Pack year	3 (3)	3 (2)	1.00
% Predicted FEV_1	102 (3)	88 (2)	**0.002**
% FEV_1/FVC	85 (3)	74 (2)	**0.0002**
PC20 FEV_1, mg/ml †	>16	0.8 (0.4-1.6)	**< 0.0001**
Blood Total IgE, kU/ml	106 (57)	515 (247)	0.35
Blood eosinophils, kU/ml	0.11 (0.01)	0.43 (0.07)	**0.001**
Treatment (mcg/24 BDP eqv.)	n/a	1412 (120)	n/a
Atopy, %	50	73	0.19*
Age of Disease Onset, yr	n/a	35 (4)	n/a
Sputum Characterization			
Total cell count($x10^6$ cells/ml)	n/a	2.2 (0.3)	n/a
Eosinophils, % ‡	n/a	1.6 (0.2-11)	n/a
Neutrophils, % ‡	n/a	46 (29-84)	n/a
Macrophages, % ‡	n/a	28 (12-49)	n/a
Epithelial cells, % ‡	n/a	2.0 (0.8-6.9)	n/a

† geometric mean (95% CI) ‡ median (inter-quartile range); *Chi Square test, $p<0.05$.

Table 3.5 Clinical details of the subjects in the baseline ciliary function experiment. Data are expressed as mean (SEM) unless otherwise indicated. Statistical differences were assessed using unpaired t-tests, $p<0.05$, unless otherwise indicated.

17 healthy controls and 31 asthmatic samples were used in this experiment (**Table 3.5**). Ciliary function of ALI cultures was firstly assessed by two methods. The overhead method recorded videos of the ciliary tips, leaving the ALI cultures undisturbed. The scraping method recorded videos of surface side profiles of the ALI cells that were scraped off and re-suspended in culture medium (**Figure 3.3**). Example representative

videos can be found in the disc attached as **Appendix 7.1**. The scraping method also allows the assessment of ciliary beat patterns, which was shown to be equally important as the CBF in normal mucociliary clearance (125, 126). There was no significant difference in mean±SEM CBF regardless the method used (scraping method, 9.5±0.8 Hz versus 9.4±1.0 Hz, p=0.92; overhead method, 12.7±1.4 Hz versus 13.5±0.6 Hz, p=0.58) (**Figure 3.4**A). There was also no significant difference across disease severity (scraping method, p=0.65; overhead method, p=0.42). The CBF obtained by overhead method was significantly higher than that obtained by scraping method in asthmatic cells (13.5±0.6 Hz versus 9.4±1.0 Hz, mean difference [95% CI] -4.2 [-6.4 to -1.9] Hz, p=0.001), which might be explained by the "injury" introduced to the cells during scraping. This "injury" however may not explain the similarity in the CBF between health and asthma since it was a variable that existed among all the "scraped" samples. Similar to the CBF observation, beat patterns were similar in healthy and asthmatic groups. They included the % of normal cilia (**Figure 3.4**B, health versus asthma, 48±8 % versus 41±5 %, p=0.48), the % of dyskinetic cilia (**Figure 3.4**C, 43±7 % versus 50±4 %, p=0.35) and the % of static cilia (**Figure 3.4**D, 9±3 % versus 8±2 %, p=0.69). Similarity in the levels of ciliogenesis in culture (**Figure 3.4**E, 60±7 % versus 62±3 %, p=0.78) and surface morphology (**Figure 3.4**F, 1.6±0.1 versus 1.7±0.1, p=0.57) suggests asthmatic cells had no deficiency in differentiation.

These data suggest that the abnormal ciliary function observed *in vivo* was not maintained when the cells were in culture. This phenomenon was also observed in other studies using differentiated nasal epithelial cultures (377, 399).

To further validate this experimental approach, the repeatability of the ciliary function over 24 h and long-term culture was evaluated. CBF, beat patterns, the level of ciliogenesis, and surface morphology were measured and no difference was observed, suggesting that the scraping method was repeatable (**Figure 3.5**). The observation was similar with long-term culture for up to 126 d, with no significant difference in any ciliary function parameter between the two time points. These results suggest that by using the Glenfield Hospital protocol, differentiated primary ALI cultures may last for up to 126 d after the first cilium was observed.

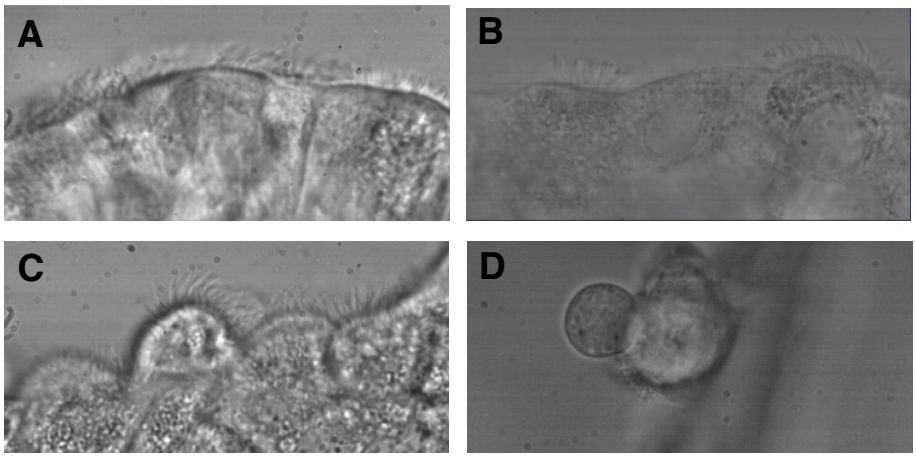

Figure 3.3 Side profiles of different ciliated epithelial surfaces observed.
A shows a side profile with a smooth surface and no cell protrusion, which is categorised as morphology index 1. It also shows the bended tips of normally beating cilia. B shows a side profile with a relatively smooth surface with some cell protrusion, which is categorised as index 2. It also shows the presence of static cilia. C shows an uneven surface with cell protrusion, which is categorised as index 3. It also shows the presence of dyskinetic cilia. D shows single cells with ciliated surfaces (for fresh cells only); this is categorised as index 4.

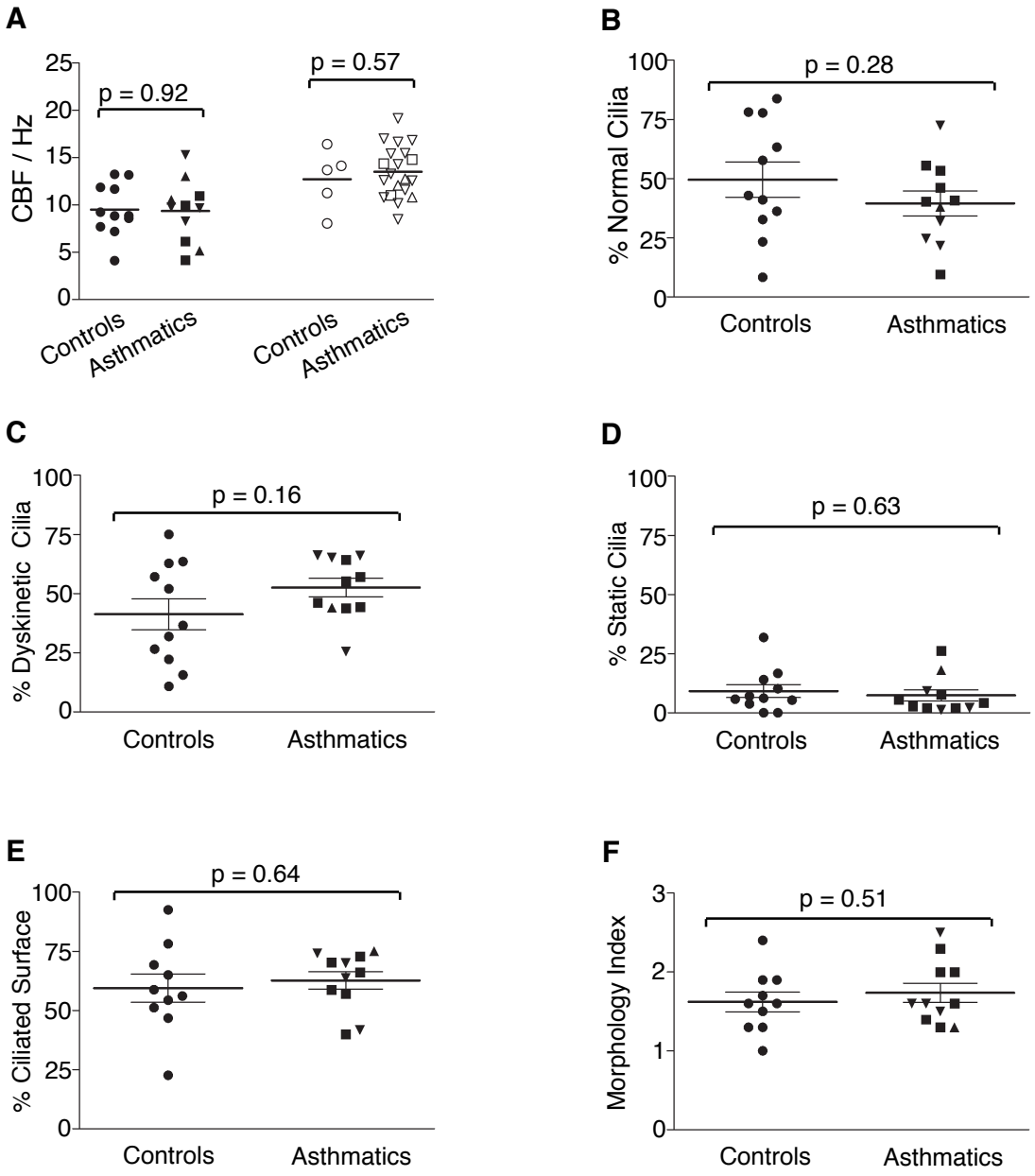

Figure 3.4 Baseline ciliary function of ciliated human primary epithelial cell cultures. Ciliary function was assessed using the parameters ciliary beat frequency (CBF) (healthy controls n=16, asthmatics n=32) and ciliary beat patterns (healthy controls n=9, asthmatics n=11). The data are presented as mean±SEM. (A) CBF of ciliated epithelial cells from controls (circles), mild asthmatics (squares), moderate asthmatics (triangles) and severe asthmatics (inverted triangles). CBF analyzed by scraping method (closed) or overhead viewing method (open), followed by high-speed video-microscopy. Ciliary beat patterns were expressed as a % of normally beating cilia (B), a % of dyskinetic cilia (C), and a % of static cilia (D). The level of ciliogenesis (E) and the ciliated surface (F) were also determined. Morphology index 1 to 3 represented smooth ciliated surfaces to uneven surfaces with cell protrusion. Statistical differences were assessed using unpaired t-tests, $p<0.05$.

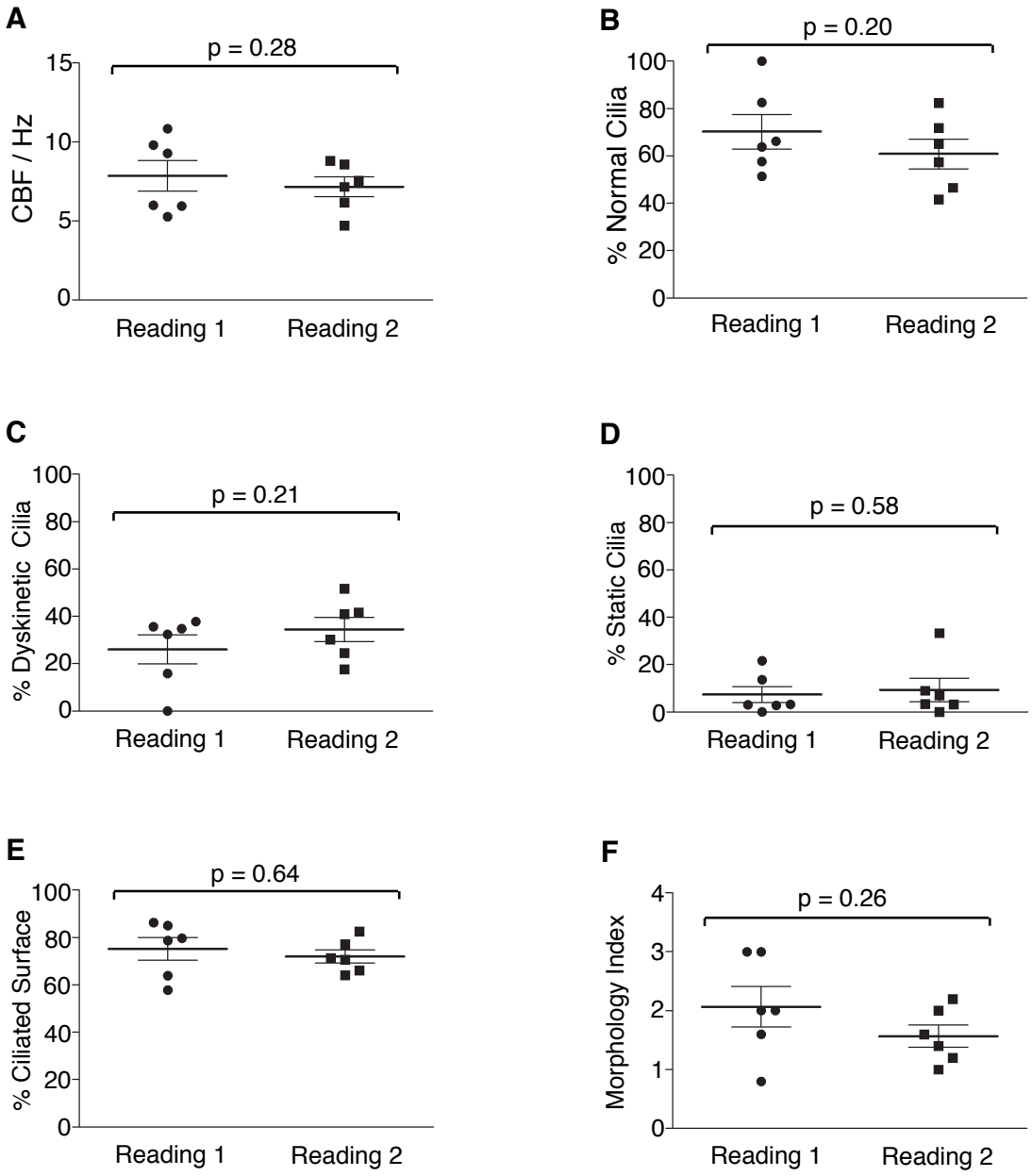

Figure 3.5 Ciliary function repeatability over 24 h. The repeatability of ciliary function analysis approach was assessed to support the sputum inoculation study. Reading 1 was taken at time zero (dots); reading 2 was taken 24 h later (squares). The data was presented in mean±SEM. Ciliary function was using the parameters CBF (A) and beat patterns, represented by a % of normal cilia (B), a % of dyskinetic cilia (C) and a % of static cilia (D). Culture surface quality was presented as % of ciliated surface (E) and surface morphology (F). Statistical differences were assessed using paired t-tests, $p<0.05$.

3.4.6 Asthmatic sputum induced ciliary dysfunction in asthmatic ALI cultures

The loss of ciliary dysfunction in asthmatic ciliated cultures implicates that an altered environment surrounding the cilia may more important to the epithelial ciliary function than expected. To test if the environment factor plays a role in ciliary dysfunction in asthma, fresh and un-processed asthmatic sputa were used as the tool to provide an asthma-specific microenvironment to the ALI cultures.

Study	**Sputum inoculation study epithelial cell donors**				**Sputum donors**
Clinical Details	**Healthy (n = 5)**	**Asthmatic (n = 6)**	**p-values**		**Asthmatic (n = 11)**
Gender (F)	1 (4)	2 (4)	0.62*		4 (7)
Age, yr	38 (7)	44 (7)	0.55		54 (6)
Pack year	0	0.8 (0.8)	0.36		0.5 (0.3)
% Predicted FEV_1	101 (8)	97 (6)	0.71		76 (7)
% FEV_1/FVC	85 (2)	75 (3)	**0.03**		69 (4)
PC20 FEV_1, mg/ml †	>16	2.2 (0.7-7.6)	**0.0007**		n/a
Blood Total IgE, kU/ml	253 (230)	52 (15)	0.17		359 (234)
Blood eosinophils, kU/ml	0.10 (0.03)	0.3 (0.1)	0.13		0.57 (0.11)
Treatment (mcg/24 BDP eqv.)	n/a	700 (309)	n/a		1662 (143)
Atopy, %	50	83	0.26		75*
Age of Disease Onset, yr	n/a	39 (9)	n/a		23 (7)
Sputum Characterization					
Total cell count($x10^6$ cells/ml)	n/a	3.2 (0.9)	n/a		9.4 (4.7)
Eosinophils, % ‡	n/a	2.8 (1.3-8.5)	n/a		1.7 (0.001-12.3)
Neutrophils, % ‡	n/a	47 (35-78)	n/a		72 (51-96)
Macrophages, % ‡	n/a	36 (15-55)	n/a		10 (3-16)
Epithelial cells, % ‡	n/a	1.8 (1.0-12.4)	n/a		8.0 (0.3-12.3)

† geometric mean (95% CI) ‡ median (inter-quartile range) * Chi Square $p<0.05$.

Table 3.6 Clinical details of subjects in sputum-inoculation experiment. This table shows the details of the subjects of which the ALI cultures were developed from (Sputum inoculation study epithelial cell donors), and the sputa were collected from (Sputum donors). Data are expressed as mean (SEM) unless otherwise indicated. Statistical differences were assessed using unpaired t-tests, $p<0.05$, unless otherwise indicated.

5 healthy controls and 6 asthmatic ALI cultures, and 11 asthmatic sputa were used in this experiment (**Table 3.6**). At baseline, there was no significant difference in CBF between the presence (8.2±0.8 Hz) and absence (8.2±1.0 Hz) of antibiotics among all samples (n=11). This remained not significant when they were divided into their healthy

and asthmatic groups (**Figure 3.6**A and B). At 1 h with the presence of antibiotics, an acute significant increase in CBF in response to asthmatic sputa (**Figure 3.6**A) was observed in the epithelial cells derived from subjects with (mean difference [95% CI] 4.2 [1.6 to 8.6] Hz, p=0.01) and without asthma (2.6 [0.05 to 5.1] Hz, p=0.05) (**Figure 3.6**C). This increase was not likely to be induced simply by the physical contact between the sputum materials and the cilia, because this phenomenon was lost in the absence of antibiotics (**Figure 3.6**B). In contrast, 24 h sputum inoculation without antibiotics significantly reduced CBF in subjects with asthma (5.4±1.3 Hz) compared to health (10.1±1.4 Hz; -4.7[-9.0 to -0.39] Hz, p=0.04; **Figure 3.6**D). This reduction was very similar to the *in vivo* observations in severe asthma (210). To look at the difference between health and asthma in response to the 24 h sputum inoculation, the area under curve (AUC) of **Figure 3.6**A and **Figure 3.6**B were calculated. The AUC values were similar between the subject groups with antibiotics (**Figure 3.6**E). In the antibiotic-free group, AUC was significantly lower in the asthmatic donors compared to healthy controls (-2.4±1.6 Hz versus 1.9±0.8 Hz, 4.3[-8.6 to 0.1] Hz; p=0.03) (**Figure 3.6**F). The repeatability of ciliary function measurement was excellent (**Table 3.8**), with an interclass correlation coefficient >0.99 within a single observer and >0.99 across observers.

As for the ciliary beat patterns, the sputum inoculation with antibiotics caused an acute reduction in the % of static cilia in all samples at 1 h (5±1 %) from baseline (9±3 %, p=0.04), which was not observed when antibiotics were absent in the culture medium. After dividing the samples into subject groups (**Figure 3.7**A and B), this acute decrease was only observed in the asthmatic ALI cells (9.1±1.6 % to 3.9±1.3 %, -5.2 [-9.8 to -0.4] %, p=0.04) (**Figure 3.7**C). With antibiotics, sputum inoculation increased the % of

static cilia in a non-significant, time-dependent manner (**Figure 3.7**A) that was not significantly different between health and disease at any time-point (**Figure 3.7**E). However without antibiotics, the sputum inoculation dramatically increased the % of static cilia in the asthmatic group from 1 h (14±9 %) to 24 h (36±14 %, p=0.01) (**Figure 3.7**B), and was significantly different from the controls at 24 h (6±3 %, p=0.02) (**Figure 3.7**D). Without antibiotics, the % static cilia AUC for asthmatic donors was significantly increased (27±13 %, p=0.03), and was significantly higher compared to the controls (-2±5 %, p=0.03) (**Figure 3.7**F). **Table 3.7** includes the results of other ciliary function parameters. Results from both healthy controls and asthmatics were combined (n=11) due to the lack of differences between the two subject groups. The % of normal cilia reduced in response to asthmatic sputum in the absence of antibiotics (**Table 3.7**A), but was not differentially difference between subject groups. There was no difference in the % of dyskinesia between subject groups in response to sputum inoculation, with or without antibiotics. There was no significant difference in the % of ciliated surface and the surface morphology between subject groups (**Table 3.7**B). The agreement within single observer was excellent ($r<0.78$, **Table 3.8**). There were no differences in ciliary function between subject groups inoculated with PBS at any time-point.

Furthermore, this reduction in ciliary function was not caused by the absence of antibiotics. The removal of antibiotics for 48 h did not induce any differential difference between healthy and asthmatic ALI cultures using any parameters of the ciliary function (CBF, p=0.55; % normal cilia, p=0.49; % dyskinetic cilia, p=0.38; % static cilia, p=0.70; % ciliated surface, p=0.08; morphology, p=0.48). There was also no difference between the subject groups after the re-introduction of antibiotics for another 48 h. The ciliary dysfunction was therefore not likely to be caused by any low profile infection embedded

within the asthmatic cells that became high profile when the cells in an antibiotic-free environment.

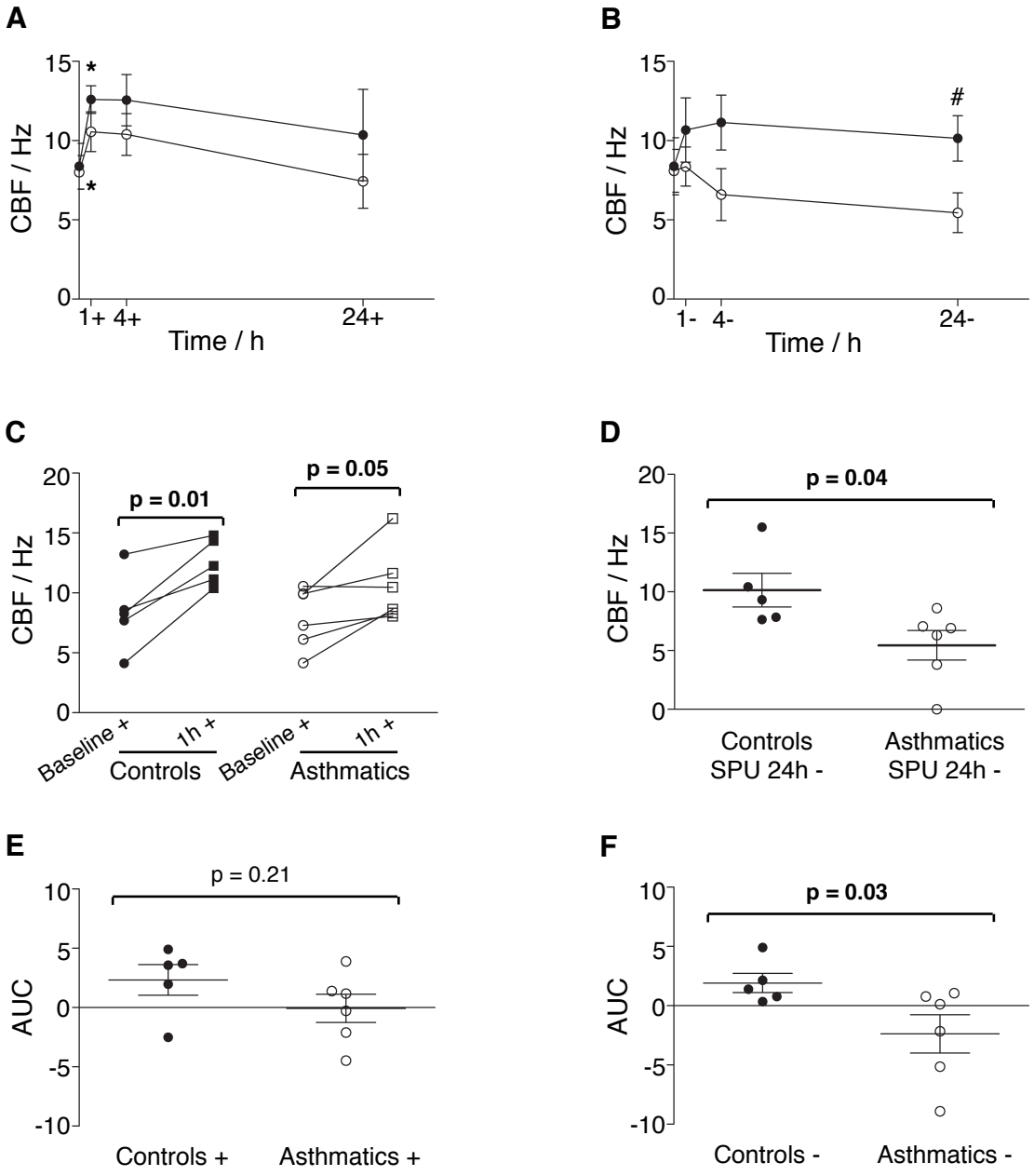

Figure 3.6 Effect of sputum inoculation with/(out) antibiotics on CBF over 24 h. Ciliated epithelial cells were first pre-incubated in medium with (+, left panel) or without (-, right panel) antibiotics. Cells were then inoculated with fresh asthmatic sputa for 0 h (baseline), 1 h, 4 h and 24 h. At the end of each time point, cells were scraped off and video-microscopy was performed. Heavily ciliated ALI cultures developed from healthy controls (n=5, closed symbols) and asthmatics (n=6, open symbols) were used. The data are presented as mean±SEM. A and B show the CBF changes upon sputum inoculation. C shows the acutely induced CBF increase in subject groups with the presence of asthmatic sputa and exogenous antibiotics at 0-1 h. D shows the sputum-induced CBF reduction at 1-24 h without antibiotics. E and F show the area under curve (AUC) of A and B. * indicates comparison with baseline using paired t-tests, $p<0.05$. # indicates comparison between subject groups using Mann-Whitney U test, $p<0.05$. § indicates comparison of AUC using Wilcoxon test compared with no change, $p<0.05$.

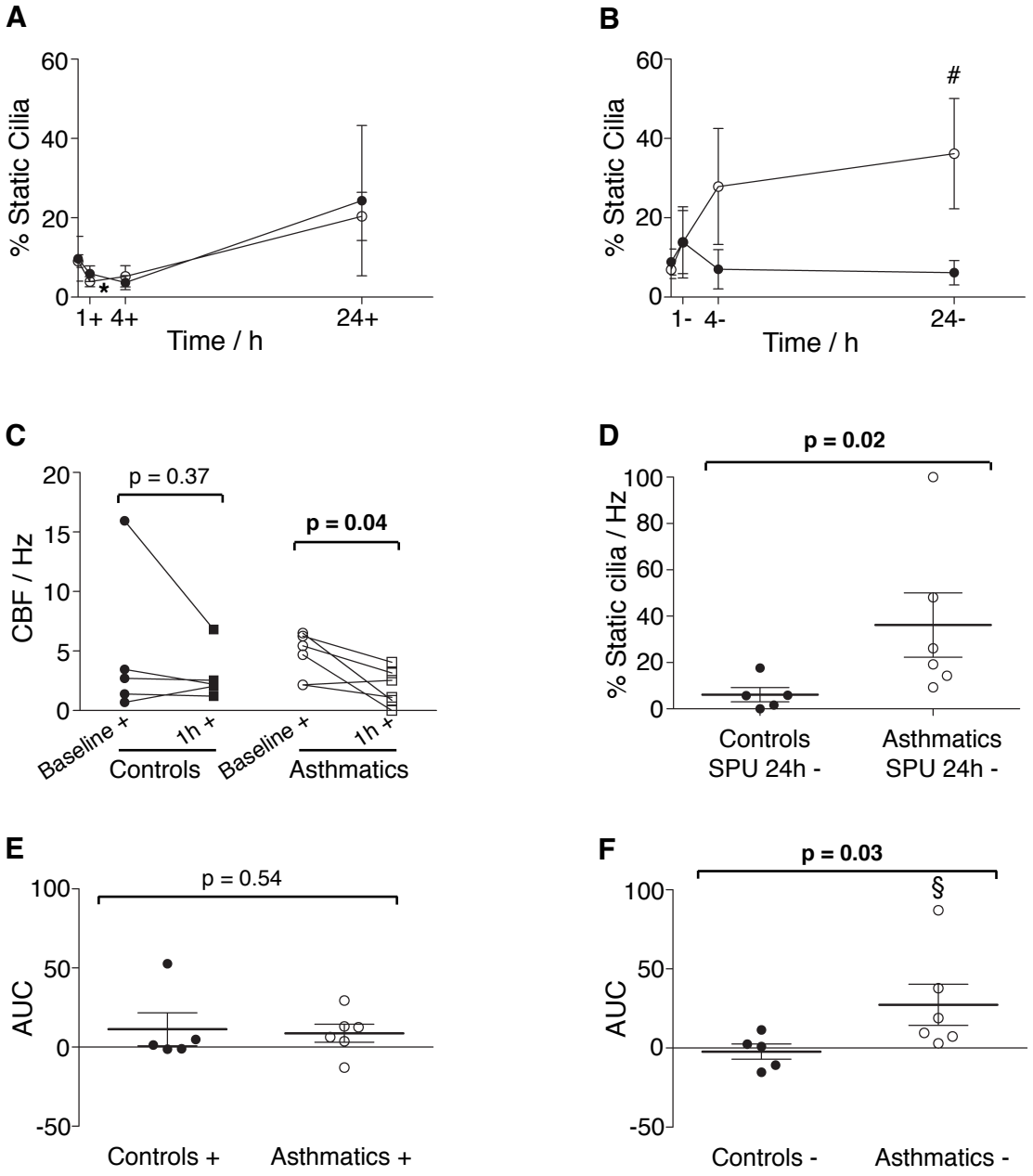

Figure 3.7 Effects of sputum inoculation with/(out) antibiotics on the % of static cilia over 24 h. Ciliated epithelial cells were first pre-incubated in medium with (+, left panel) or without (-, right panel) antibiotics. Cells were then inoculated with fresh asthmatic sputa for 0 h (baseline), 1 h, 4 h and 24 h. At the end of each time point, cells were scraped off and video-microscopy was performed. Heavily ciliated ALI cultures developed from healthy controls (n=5, closed symbols) and asthmatics (n=6, open symbols) were used. The data are presented as mean±SEM. A and B show the changes in the % of static cilia upon sputum inoculation. C shows the acutely induced reduction in the % of static cilia in subject groups with the presence of asthmatic sputa and exogenous antibiotics at 0-1 h. D shows the sputum-induced elevation in % of static cilia at 1-24 h without antibiotics. E and F show the area under curve (AUC) of A and B. * indicates comparison with baseline using paired t-tests, $p<0.05$. # indicates comparison between subject groups using Mann-Whitney U tests. § indicates comparison of AUC using Wilcoxon tests with no change, $p<0.05$.

A.

Mean (SEM)		All Samples (n=11)			
Normal Cilia / %	With antibiotics	Baseline 55 (5.4)	PBS 1 h 58 (5.2) p = 0.53	PBS 4 h 62 (4.4) p = 0.23	PBS 24 h 53 (5.2) p = 0.69
			SPU 1h 58 (3.3) p = 0.54	SPU 4h 60 (6.2) p = 0.35	SPU 24 h 46 (8.4) p = 0.14
	Without antibiotics	Baseline 55 (7.7)	PBS 1 h 62 (7.7) p = 0.41	PBS 4 h 62 (6.0) p = 0.54	PBS 24 h 56 (6.3) p = 0.86
			SPU 1h 50 (8.7) p = 0.58	SPU 4h 53 (9.0) p = 0.78	SPU 24 h 32 (7.7) **p = 0.003**
Dyskinetic Cilia / %	With antibiotics	Baseline 35 (5.2)	PBS 1 h 38 (4.9) p = 0.62	PBS 4 h 30 (4.6) p = 0.44	PBS 24 h 33 (6.0) p = 0.85
			SPU 1h 38 (3.1) p = 0.56	SPU 4h 36 (5.5) p = 0.94	SPU 24 h 32 (5.7) p = 0.59
	Without antibiotics	Baseline 37 (6.9)	PBS 1 h 32 (8.0) p = 0.54	PBS 4 h 32 (6.0) p = 0.60	PBS 24 h 34 (5.3) p = 0.40
			SPU 1h 36 (6.0) p = 0.88	SPU 4h 29 (7.0) p = 0.34	SPU 24 h 45 (8.1) p = 0.40

B.

Mean (SEM)		All Samples (n=11)			
Ciliated Surface / %	With antibiotics	Baseline 64 (5.3)	PBS 1 h 63 (5.1) p = 0.93	PBS 4 h 70 (4.6) p = 0.17	PBS 24 h 61 (4.3) p = 0.82
			SPU 1h 75 (4.8) **p = 0.004**	SPU 4h 68 (4.5) p = 0.25	SPU 24 h 63 (3.8) p = 0.80
	Without antibiotics	Baseline 65 (5.5)	PBS 1 h 66 (6.5) p = 0.88	PBS 4 h 66 (4.5) p = 0.66	PBS 24 h 64 (4.7) p = 0.62
			SPU 1h 62 (7.8) p = 0.72	SPU 4h 64 (7.0) p = 0.76	SPU 24 h 54 (7.3) **p = 0.01**
Surface Morphology / index	With antibiotics	Baseline 1.8 (0.1)	PBS 1 h 1.7 (0.1) p = 0.77	PBS 4 h 1.9 (0.1) p = 0.67	PBS 24 h 2.2 (0.1) p = 0.10
			SPU 1h 1.7 (0.1) p = 0.71	SPU 4h 1.9 (0.1) p = 0.66	SPU 24 h 1.9 (0.1) p = 0.65
	Without antibiotics	Baseline 2.1 (0.14)	PBS 1 h 1.8 (0.17) p = 0.04	PBS 4 h 2.0 (0.17) p = 0.41	PBS 24 h 2.2 (0.18) p = 0.79
			SPU 1h 1.7 (0.1) **p = 0.03**	SPU 4h 1.8 (0.1) p = 0.16	SPU 24 h 2.0 (0.2) p = 0.74

Table 3.7 Effects of sputum inoculation with/(out) antibiotics on the ciliary beat patterns and surface quality over 24 h. These tables show the results on the rest of the parameters on ciliary function analysis. Data are presented as mean (SEM). Results from both healthy controls and asthmatics were combined (n=11) due to the lack of differences between the two subject groups. A shows the change in the % of normally beating cilia and the % of dyskinetic cilia in response to asthmatic sputum inoculation with and without antibiotics. B shows the ciliated surface quality as the % of ciliated surface and surface morphology (index). Statistical differences were assessed using paired t-tests, $p<0.05$, compared with baseline.

A.

Intra-Observer Correlation	CBF / Hz	% Normal Cilia	% Dyskinetic Cilia	% Static Cilia	% Ciliated Surface	Morphology Index
Correlation coefficient (r)	0.981	0.756	0.673	0.584	0.982	0.912
p-value	**<0.0001**	**0.005**	**0.017**	**0.046**	**0.001**	**<0.0001**
Interclass correlation coefficient (Cronbach's Alpha)	0.990	0.853	0.783	0.736	0.992	0.928
p-value	**<0.0001**	**0.002**	**0.009**	**0.018**	**<0.0001**	**<0.0001**

B.

Cross-Observer Correlation	**CBF**
Correlation Coefficient (r)	0.981
p-value	<0.0001
Interclass correlation coefficient (Cronbach's Alpha)	0.991
p-value	<0.0001

Table 3.8 Repeatability of ciliary function measurement. The intra-observer (A) and cross-observers (B) correlations on ciliary function analysis using linear correlation coefficient (r) and intra-class correlation coefficient (Cronbach's alpha), $p<0.05$.

3.5 Discussion

In this chapter it has been shown that heavily ciliated ALI cultures were successfully grown at Glenfield hospital from both healthy and asthmatic subjects across different disease severity, which would remain confluent and ciliated for over 100 d. In comparison to the ALI cultures studies in literature (400-402), the ALI cultures at Glenfield Hospital took longer to become fully ciliated. This could be due to the differences in culture protocols, ingredients in the ALI medium, geographical location and source of the cells. Using the light microscopy, there was no observable difference in morphology between healthy- and asthma-derived HAEBC or the ALI cultures. Evidence in literature has shown that asthmatic epithelium has a loss of TJs and loss of cilia, with goblet cell hyperplasia and mucus hypersecretion (64, 194). To further investigate these pathological features as well as the robustness of cell differentiation, paraffin embedded tissue would be required on which immunofluorescence and/or immunohistochemical staining could be conducted.

The results from MSD assays and ELISAs supported the null hypothesis that the ciliary dysfunction in asthmatic epithelial cells is not likely to be due to a differential synthetic capability, in terms of pro-inflammatory mediators, between healthy and asthmatic epithelial cultures. In asthmatic airways, the epithelium plays a major role in contributing to persistent inflammation. It is evident in literature that the asthmatic epithelium is persistently active even at a resting state, with an increased baseline secretion of mediators such as CXCL8 and IL-6 (29, 180). However, these abnormalities were not observed in the current MSD results. This result was supported by some studies (403, 404), but not by others (180, 182). The deficiency in type I and III interferons following a viral infection has been reported to be a fundamental

impairment in the innate immune response in asthma that promotes the persistence of a viral infection and the development of an exacerbation (181, 182). This impairment is not revealed at an un-stimulated status in HAEBC as reported here. As mentioned in the Methodology section, the mediators investigated here were based on literature reviews (148, 150) as well as the technical constraints from the manufacturer. The results shown here may not necessarily and inclusively represent all the pro-inflammatory mediators involved in the innate immune system. Other cytokines such as IL-33, TSLP, and IL-25 (405), were shown to play significant roles in asthma pathogenesis, and therefore could be investigated. Apart from cytokines and chemokines, other components such as antimicrobial products β-defensins and Toll-like receptors (TLRs) also play important roles in mediating innate response, and were shown to be involved in chronic airways diseases (78, 406). Their involvement in asthma is discussed in Chapter 4. On the other hand, the results here supported the current view that different epithelial subtypes have differential functions within the epithelium (77, 407, 408). For example, the high constitutive level of IFN-β in progenitorial basal cells may help with a rapid activation of the anti-microbial immunity, and any required apoptosis, upon viral infection (64).

The result from human genome microarrays weakly opposed the null hypothesis that differential HAEBC gene expression at baseline was found between health and asthma. Differential gene expression between health and asthma at an un-stimulated level has been reported previously (8, 180). At the time of the experiment, there was no report in literature suggesting any specific genes that were responsible for the regulation of ciliary function. The genes that were found differentially expressed from the current microarrays are involved in a range of cellular functions, such as cell survival and development, inflammation and signalling, oxidative handling, and ion transports.

Specifically, some of these genes may be involved in HAEBC differentiation, such as *TUBE1* that encodes tubulin is for cilia formation (398), and *RGS2* that encodes a protein for regulating $[Ca^{2+}]_i$ and thus CBF (116), and therefore might contribute to the abnormal ciliary function. Interestingly, some of the results challenge current literature. For example, the gene of cell cycle marker Ki67 was present in ≥3 asthmatic HAEBC but absent in healthy HAEBC, and vice versa for *PCNA*. This is in agreement with some studies showing a dysregulated, fast epithelial cell proliferation (178, 180), but contradicts the others (409). However the low sample size restricted the power of these results, which was due to the high running cost of the microarrays. This low sample size also did not allow further dissection of the samples into asthma subtypes that seem to have different underlying mechanisms (25, 334). Another limitation was that no ciliated samples were used for the microarray analysis. Gene polymorphisms had also not been taken into account in the current analysis (338, 339).

To address the limitation on sample size and the cell type used, I compared the microarray result here a recent study reported by Woodruff *et al.* (8). They compared the gene expression in fresh bronchial brushes obtained from healthy controls (n=28), asthmatics (n=42) and smokers (n=16) using Affymetrix microarrays (8). They used a cut-off value of 1.1-fold change. Among the top ten genes that were shown differentially expressed in fresh brushes between health and asthma in Woodruff's study, none of which showed up in this microarray result. However, more similarities could be found when comparing healthy controls herein and smokers in Woodruff's dataset. For example, *CYP4F3* and *CYP4F11* gene expression were found upregulated in the disease groups of both studies; *AKR1C2, ABCC* gene family and *SLC* gene family were up-regulated in Woodruff's smoker group, whilst they were expressed in ≥3 out of 6

asthmatics in the asthmatic group used here. The similarity between the healthy controls/asthmatic dataset herein and Woodruff's healthy controls/smokers dataset might be explained by the similarity in the subject characteristics – the lung function of this asthma subject group was worse than Woodruff's asthma, but was similar to their smoker group; ex-smokers were included in this asthma subject group. This comparison here further illustrated that gene expression profile could be sample-dependent (77), and it changes as the basal cells differentiate into fully ciliated cells(398).

Mucociliary clearance is essential in pulmonary defence (101) and is impaired in asthma (395, 410). My group has previously demonstrated that CBF and beat pattern are abnormal in asthma and are related to disease severity (210). These abnormalities were determined in subjects without radiological evidence of bronchiectasis (210), but importantly bronchiectasis is present in 40% of severe asthmatics (411) suggesting that ciliary dysfunction in asthma may be underestimated. It was reported here that the ciliary dysfunction did not persist in ciliated cultures differentiated *in vitro*, but could be re-introduced only in the asthmatic ALI cultures by inoculating the cells with fresh, un-processed asthmatic sputa. The loss in ciliary dysfunction in the asthmatics cells could be due to the controlled, sterile growing environment *in vitro*, which further implies the importance of the presence of an asthma-specific microenvironment in driving the abnormal clinical phenotypes. This was further supported by the result from the sputum inoculation study. Sputa consist of materials that are present on the surface of the airway epithelium, including structural cells, inflammatory cells and trapped inhaled materials (243, 412), and thus they provide a cell profile that is specific to the asthmatic individual. Therefore, the asthmatic sputa were likely to be introducing an asthma-specific environment to the ALI cultures. Ciliary dysfunction was re-introduced only to

the asthmatic ALI cultures by exposing the cells to fresh, un-processed asthmatic sputa in the absence of antibiotics. In fact, it has been shown that asthmatic sputa could induce ciliary immotility (396). The materials in the asthmatic sputa were therefore very likely to be related to the induced ciliary dysfunction in asthmatic ALI cultures. The ciliary dysfunction of the asthmatic ALI cultures was only revealed in an antibiotic-free environment, implicating the potential role of microbial colonisation/infection in the induction of ciliary dysfunction. As a result, these results opposed the null hypothesis that the ciliary dysfunction persists in epithelial cultures derived form asthmatic subjects. This abnormality is likely to be associated with the asthma-specific microenvironment.

3.6 Criticism

There are several limitations present in the studies in this chapter:

Limitation 1 – The lack of quality control on HAEBC differentiation into ALI cultures

One of the main limitations in the current chapter was the lack of quality control on the robustness and consistency on HAEBC differentiation into ALI cultures up to the point where they were used for experiment. These quality controls may include the expression level and the localisation of proteins such as β-tubulin (cilium-specific marker), mucins MUC5AC (goblet cell marker), cytokeratin 5/14 (basal cell marker), α-smooth muscle actin (marker for epithelial-mesenchymal transition), Ki67 (cell proliferation marker) and Bcl (cell apoptosis marker). This quality control was not performed because the paraffin embedding technique was still under optimisation at the time of the experiment.

Nevertheless, cilia were developed from cells collected from human airways that were characterised as epithelial basal cells. These cells were able to grow and differentiate in a serum-free medium specific for bronchial epithelial cells (Lonza), but not in serum-supplemented medium (data not shown). This strongly suggested that my ALI cultures used in this thesis were indeed airway epithelial cells. Furthermore, these ALI cultures were grown for a much longer time than those reported in literature before being used for experiments (400, 401). Performing quality control on these samples would be beneficial, but was not performed due to the technical limitation as mentioned above. In spite of this, ciliary function was found stable for over 100 days, suggesting that the ALI cultures were healthy for these experiments. Pyrtherch *et al.* (413) reported that the cell layers became less compact with large inter-cellular gaps observed within the

structure 36 days after ALI (18 days after cilia were visible). However, the primary cells they used were bought commercially (414), as well s them being frozen/thawed. The cell handling and cell differentiation protocols could also be different. These differences may explain the difference in ALI cultures between the two sites.

Limitation 2 – Amplitude of beating cilia has been shown to be important in ciliary function, but was not assessed in these studies

To date there are 3 parameters to measure an overall ciliary function – CBF, beat patterns, and "amplitude" (378, 415). The most common interpretation of "amplitude" is the distance travelled by a cilium from one end to another. In literature, amplitude has been shown to be important, with its role in ciliary function independent from CBF (104, 376). Apart from CBF, the overhead method can be used for assessing beat amplitude. This approach was tested in the sputum inoculation study using 1 healthy and 1 asthmatic sample. As shown in **Figure 3.8**A, tips of cilia could be focused on when there was only PBS present in the apical chamber of a Transwell®. However, the density and the viscosity of the diluted sputum, although homogenised, made the focusing very difficult (**Figure 3.8**B). Another problem was the choice of cilia. *In vitro* basal cells within a Transwell® differentiated at different rate. The maturity of each cilium is different, thus resulting different cilia lengths. The resolution of the image captured by the camera allowed the ease in focusing on a normal cilium with bendable tip. Dyskinetic and static cilia could therefore be easily neglected. This might explain the high CBF readings recorded in both control (**Figure 3.8**C) and asthma (**Figure 3.8**D) that did not resemble the patterns observed using the scraping method. The overhead method was therefore not established as the regular protocol for ciliary function analysis.

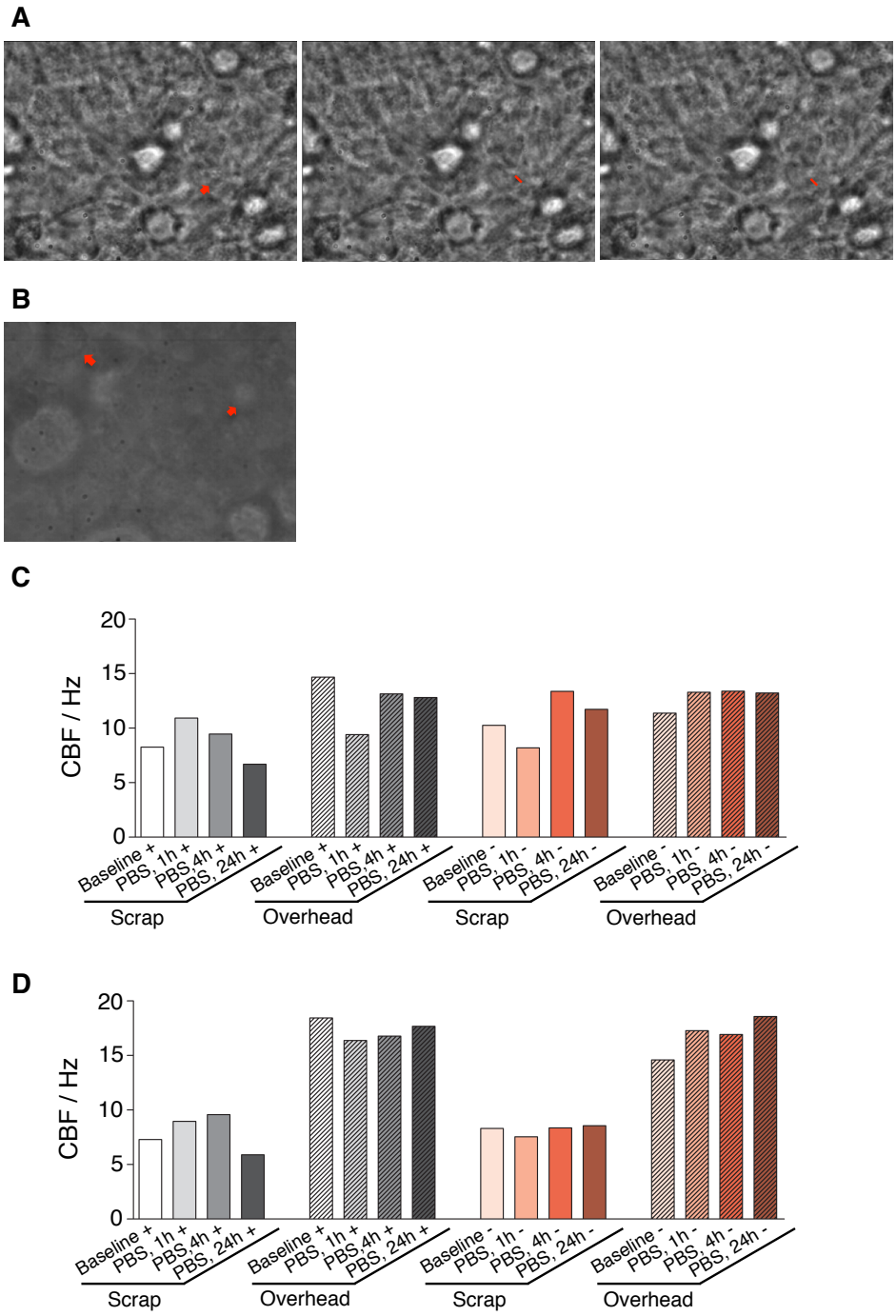

Figure 3.8 Ciliary function assessment using overhead method versus scraping method. Since the overhead method gave a different ciliary function analysis outcome from scraping method, a comparison was performed using healthy (n=1) and asthmatic (n=1) ALI cultures. A shows that with the presence of PBS in the apical chamber, tips of cilia could be focused for functional analysis (arrow). B shows that with the presence of asthmatic sputum in the apical chamber, focusing became difficult. Arrows show the presence of viscous sputum. C and D show the difference in CBF measurement using different method in a healthy and an asthmatic ALI culture respectively. Grey-scaled bars represent PBS-inoculated samples; red-scaled bars represent sputum-inoculated samples.

Limitation 3– Effect of asthmatic sputum on ciliary function might be over-/under-estimated

In the sputum inoculation study, only 1 sputum concentration was used. To confirm the role of asthmatic sputum in inducing asthmatic ciliary dysfunction in asthmatic cells, it would be beneficial to do a titration on sputum concentration to see if the induced ciliary dysfunction is retained with highly diluted sputum. It would also be beneficial if the sputum samples from healthy controls could be obtained to see if they have a similar effect on the asthmatic cells. However, this is problematic as healthy controls produce little-to-no sputum even after sputum induction. Meanwhile, the supply of asthmatic sputum samples varies over the year. The availability of fully differentiated ALI cultures was also very limited. As a result, these supporting experiments could not be performed in my project.

Limitation 4 – The lack of follow-up on the microarrays results

Apart from the lack of ALI culture samples, another major limitation of the current microarrays was the lack of follow-up on the 'hits' identified.

The result from the microarrays suggested that the baseline gene expression was fairly similar between healthy and asthmatic HAEBC, but only if a 2-fold threshold was used. The difference became more prominent if the threshold was reduced to 1.6-fold (**Table 3.4**A), which was also an acceptable cut-off for interpreting microarray results (29, 180). Besides, long lists of genes were found predominantly expressed in either subject groups (**Table 3.4**B and C). With such an enormously long list of genes, it would be difficult to prioritise which ones to test without a thorough literature reviews. The restricted time frame of my PhD limited any further investigation on these 'hits', which

would be essential in understanding the full profile of airway epithelium and its role in asthma pathogenesis.

3.7 Summary

Epithelial cells could be fully differentiated *in vitro*, which highly resemble the structure *in vivo*. The ALI cultures at Glenfield Hospital were able to stay healthy for over 100 days and remain experimentally compatible. This provides for researchers a convenient and yet reliable model to study the role of the epithelium in asthma.

MSD data revealed that epithelial basal cells and differentiated cells have different pro-inflammatory mediator secretion profiles, but the profiles were surprisingly similar between health and asthma. The microarrays result embedded with the limitation of low sample number, but revealed some differential HAEBC gene expression between health and asthma, including *TUBE1*, *EDN1* and *CST6*, and those predominantly found in asthmatic HAEBC such as *NOX4*, *TNFRSF* and *FAM*. It would be interesting to look into whether this intrinsic abnormality contributes to asthmatic ciliary dysfunction, despite the message was weak due to the low sample sizes.

By using ciliated epithelial cells differentiated *in vitro*, it has been demonstrated that the ciliary dysfunction evident in asthma does not persist in *ex vivo*. This suggests that the asthmatic airway environment is critical in the development and maintenance of this abnormality. Interestingly, this ciliary dysfunction could be re-introduced by the addition of asthmatic sputa whilst the antibiotics were absent in the culture environment. This phenomenon was, however, only observed in the asthmatic ALI cultures and not in healthy controls. It was also not caused by the absence of antibiotics itself. In addition, this observation was not caused by the artefacts of the cell model such as the length of culture and the scraping procedure before videomicroscopy. These findings support the hypothesis that ciliary dysfunction is caused by an asthma-specific microenvironment.

Additionally, the results from the microarrays suggest a weak link between ciliary dysfunction and intrinsic genetic defects that might result in higher cell susceptibility to injury. To dissect the underlying mechanism of this asthmatic abnormality, the role of infection and innate immunity of the epithelium and the role of the oxidative stress are respectively investigated and discussed in detail in Chapter 4 and 5.

4. Infection And Epithelial Ciliary Function in Asthma

4.1 Chapter Overview

In Chapter 3 it has been demonstrated that the asthmatic sputum-induced ciliary dysfunction was induced only with an absence of exogenous antibiotics, suggesting that microbes may be important in the dysfunction. This could be resulted from microbial colonisation/infection, microbial cytotoxicity and/or the presence of an abnormal innate immunity of the epithelium that facilitates microbial growth. Therefore, the aims of this chapter were 1) to explore the relationship between microbes and asthmatic ciliary dysfunction, 2) to assess the presence of any defects in anti-microbial activity in the asthmatic epithelium and, 3) to investigate if the asthmatic sputum contributed any bacterial cytotoxic effect to the induced ciliary dysfunction.

The contents of the asthmatic sputum, including bacteria, fungi and bacterial toxin, were quantified. Human β-defensins are potent anti-microbial peptides predominantly secreted by airway epithelium and were thus evaluated. The results suggested that these elements were likely to be the exogenous factors that initiated the abnormal ciliary function in asthmatic epithelium. However, they did not explain the higher susceptibility of the asthmatic cells to injuries such as pathogenic colonisation/infection.

4.2 Introduction

A normal microbiota is important for the host defence system. The beneficial effect could be due to the counter balance between the T_H2 response, which is triggered by the allergen, and the T_H1 response, which is triggered by the low profile microbial colonisation (416). It could also be simply because of a physical barrier function of the local commensals against the settlement of allergens and other pathogenic colonisation. A lack of commensal has been shown to cause a deficiency in allergen-induced inflammation (240). An altered microbiota community has also been shown to be pathogenic. The microbiota in asthmatic airways has been found abnormal, with a reduction in microbial diversity and an elevation in microbial load (243, 244). In stable asthmatics, mucus containing trapped stimuli persists in the airway lumen (249, 250), which is likely to be the consequence of mucus hypersecretion as well as a defective mucociliary clearance (417). This is likely to prolong the exposure time of these stimuli, such as excessive microbes and their pathogenic factors, to the epithelium and thus may increase the chance of colonisation and infection. This may explain the associated between infection and asthma exacerbation (241, 242, 246).

In Chapter 3, it was reported that asthmatic sputum-induced ciliary dysfunction in asthmatic ALI cultures was revealed only when there was an absence of exogenous antibiotics. These antibiotics included penicillin, gentamycin and amphotericin, which target both bacteria and fungi but not viruses. This implies that bacterial/fungal colonisation/infection might play a role in asthmatic ciliary dysfunction. It has been shown that asthmatic airways are exposed to increased pathogenic bacterial contents (243, 244, 418) and fungal contents (260, 264), and have defective in innate response

(181, 182). Viable microbes as well as their products have also been shown to directly affect CBF (252, 254, 255).

Meanwhile, the antimicrobial activity of the airway epithelium may be defective in asthma. Gene polymorphisms in toll-like receptors (214) and anti-microbial peptide encoding gene (406), and deficiency in IFN secretion (181, 182), have been reported in the literatures. For instance, airway epithelium secretes different antimicrobial proteins such as human β-defensins (hBDs) and cathelicidins (419), whilst single nucleotide polymorphisms (SNPs) on DEFB1, the gene that encodes hBD-1, have been reported to associate with asthma diagnosis (406). hBDs has a broad-spectrum of anti-microbial capacity against Gram-positive and Gram-negative bacteria, fungi and viruses (165, 167, 168). A deficiency in hBD secretion from the airway epithelium may therefore facilitate microbial growth that impacts ciliary function.

In addition, the rapid effect of the asthmatic sputa on ciliary dysfunction (~1 h) suggests that asthmatic sputa are cytotoxic (420). Both bacteria and fungi are capable of producing toxins and pathogenic molecules that are cytotoxic. Toxins are able to directly reduce CBF and induce ciliary immotility (34, 254). There is an increasing amount of evidence that supports the role of Gram-negative bacteria in asthma development and exacerbation (246, 249). Endotoxin (LPS) present on the cell walls of these bacteria is a PAMP that binds to TLR-2 and TLR-4 (**Table 1.3**). It triggers downstream signalling pathways and induces a rapid innate response. Whilst airway epithelial cells express both TLR homologues (133, 258), it is plausible that LPS may play a role in induced ciliary dysfunction.

Based on the above evidence, I tested the following hypotheses:

(i) Bacterial colonisation/infection is the cause of the asthmatic ciliary dysfunction, that antimicrobial treatments would improve ciliary function.

(ii) Fungal colonisation/infection is the cause of the asthmatic ciliary dysfunction, that antimicrobial treatments would improve ciliary function.

(iii) Bacterial cytotoxicity is the cause of the asthmatic ciliary dysfunction, that antimicrobial treatments would improve ciliary function.

(iv) Asthmatic epithelium facilitates microbial growth that leads to ciliary dysfunction.

The surface of airway epithelium contains materials such as airway structural and inflammatory cells, materials (e.g. mediators) from these cells, and any trapped inhaled particulates such as microbes (243, 412). These materials can be collected alongside the induced sputa (22, 379), and thus can be evaluated using the appropriate qualitative and quantitative methods for the target of interest. In this chapter, fresh sputa collected from healthy and asthmatic subjects, as well as the ACF, ALI S/N and the preserved ALI cell strips collected from the sputum inoculation study in Chapter 3, were used as the tools to evaluate the microbial and innate immunity profiles in health and asthma and their potential correlation with asthmatic ciliary dysfunction.

4.3 Methodology

Sputum samples from a total of 10 healthy controls and 12 asthmatic subjects were collected for evaluating any differences between healthy and asthmatic subjects in microbial profiles, namely the bacterial and fungal contents. Sputum filtrates were used for numerating bacterial culture to colony forming unit (cfu) measurement. Unprocessed sputum plugs were used for fungal culture and species identification based on the published morphology criteria (381). The remaining sputum materials were used for qPCR quantification.

qPCR is a sensitive quantitative method that allows low input materials to be used. Here it used the total DNA extracted from sputum cells as the input material. A specific sequence of DNA is amplified and is reported the number of amplification cycles it takes for the emitted fluorescence to be above the threshold (C(t)), which is indirectly proportional to the input DNA quantity (**Figure 2.2**) (392). Bacterial load was quantified by measuring the non-specific bacterial 16S copies (380); *A. fumigatus* was quantified by measuring specifically the *A. fumigatus* mitochondria (AfMITO) gene (382). The qPCR cycles are stated in **Table 4.1**. Bacterial 16S qPCR was performed using the remaining sputum samples from the culture above, as well as the ACF, ALI S/N and the preserved cell strips collected from the sputum inoculation study in Chapter 3. *A. fumigatus* qPCR was performed using only the collectables from the sputum inoculation study. These experiments were kindly performed by Dr Kairobi Haldar and Dr Catherine Pashley.

	Polymerase activation	Amplification					Holding Step	Melting Step	Hold
		Denaturation	Annealing	Elongation	Reading	Total no. of cycle			
Bacterial 16S	95ºC, 15 min	95ºC, 20s	60ºC, 30s	72ºC, 20 s	80ºC, 20s	40	72ºC, 60s	72-100ºC	4ºC
AfMITO	50ºC, 2 min	95ºC, 10min	95ºC, 15 s	65ºC, 1 min	read	50	-	-	4ºC

Table 4.1 qPCR reaction conditions for bacterial 16S and *A. fumigatus*.

hBD-1 and -2 were measured using sandwich ELISAs, a protein quantification assay that uses antibodies specifically targeting hBD-1 or hBD-2, and luminescence as the reporter (Peprotech) (385). 6 ACF samples (3 healthy and 3 asthmatics) and 6 ALI S/N samples (3 healthy and 3 asthmatics) collected from the sputum inoculation study in Chapter 3 were used as the input materials. Each sample was run in duplicate. 0.05% Tween-20-PBS was used as the wash buffer. At the end of the assay, TMB liquid substrate solution (BD Biosciences, Oxford, U.K.) was used for 15 min colour development. Without stopping the colour development sodium hydroxide, plates were read every 10 min for a 45 min period at wavelength 405 nm. The set of absorbance readings that gave a top standard below 1.2 U and a zero control above 0.3 U was chosen for each assay.

In addition, the quantity of bacterial endotoxin was quantified using Endotoxin Recombinant Factor C (rFC) detection system (Lonza). It utilises the Limulus blood coagulation cascade by using a recombinant Factor C that emits a quantifiable fluorescence after interacting with bacterial endotoxin (**Figure 2.3**) (383, 384). The assay was performed following the manufacturer's protocol. It was first optimized for a

suitable sample dilution factor and microplate reader setting. 6 ACF samples (3 healthy and 3 asthmatics) and 6 ALI S/N samples (3 healthy and 3 asthmatics) collected from the sputum inoculation study in Chapter 3 were used as the input material. Each sample was run in duplicate.

4.4 Results

4.4.1 The elevated microbial quantity was not likely to be the direct cause of ciliary dysfunction in asthma

It was reported in the previous chapter that asthmatic sputum contents might play a role in inducing ciliary dysfunction in asthma. To consider if asthmatic cultures facilitate a microenvironment that leads to ciliary dysfunction, the microbial quantities in fresh asthmatic sputa and those used in the sputum inoculation study were evaluated.

Clinical Details	Healthy (n = 10)	Asthmatic (n = 12)	p-values
Gender (F)	4 (6)	6 (6)	0.64*
Age, yr	37 (4)	38 (4)	0.97
Pack year	3 (2)	2 (1)	0.54
% Predicted FEV_1	96 (5)	78 (7)	**0.049**
% FEV_1/FVC	82 (2)	68 (4)	**0.005**
PC20 FEV_1, mg/ml †	n/a	n/a	n/a
Blood Total IgE, kU/ml	n/a	214 (98)	n/a
Blood eosinophils, kU/ml	n/a	0.28 (0.04)	n/a
Treatment (mcg/24 BDP eqv.)	n/a	1500 (261)	n/a
Atopy, %	50	58	1.0*
Age of Disease Onset, yr	n/a	21 (4)	n/a
Sputum Characterization			
Total cell count($x10^6$ cells/ml)	n/a	1.8 (0.7)	n/a
Eosinophils, % ‡	n/a	1.0 (0.5-3.8)	n/a
Neutrophils, % ‡	n/a	67 (55-79)	n/a
Macrophages, % ‡	n/a	n/a	n/a
Epithelial cells, % ‡	n/a	n/a	n/a

† geometric mean (95% CI) ‡ median (interquartile range); * Chi Square test $p<0.05$.

Table 4.2 Clinical details of the sputum donors for the baseline microbiology analysis. Data are expressed as mean±SEM unless otherwise indicated. Statistical differences were assessed using unpaired t-tests, $p<0.05$, unless otherwise indicated.

Table 4.2 shows the clinical details of 10 healthy sputum donors and 12 severe asthmatics sputum donors. The bacterial load assessment using the bacterial culture methodology was expressed as cfu count. Since the data was skewed, it was transformed to a $\log_{10}$ scale prior to the statistical analysis using unpaired t-tests to

compare the healthy and asthmatic groups. The result showed that asthmatic sputa had a bacterial load ($10^{6.5\ [5.9\ to\ 7.2]}$ cfu/ml) significantly higher than that of healthy controls ($10^{5.8\ [5.5\ to\ 6.1]}$ cfu/ml, mean difference [95% CI] $10^{0.8\ [-0.06\ to\ 1.5]}$ cfu/ml; p=0.05) (**Figure 4.1**A). The bacterial load was not biased towards the amount of inhaled corticosteroid intake (r=0.08, p=0.81) and oral corticosteroid intake (r=0.14, p=0.67) of these subjects.

Bacterial quantity was also measured using qPCR for bacterial 16S expressed as copies/ml. **Figure 4.1**B and **Figure 4.1**C show the standard curve of the 16S qPCR and the melting curves of the qPCR product with peaks at 84ºC. Since the 16S copies data points were not normally distributed, it was transformed to a Log_{10} scale prior to the corresponding statistical analyses. Among the severe asthmatic sputa used for the sputum inoculation study, the bacterial 16S load was not different between those used on the healthy ALI cultures ($10^{9.8\ [7.4\ to\ 12.2]}$ copies/ml) and on the asthmatic ALI cultures ($10^{8.5\ [6.8\ to\ 10.1]}$ copies/ml) (**Figure 4.1**D). Inoculating sputa on the ALI cultures increased the bacterial 16S load, which was significantly higher with the absence of antibiotics ($10^{10.2\ [9.5\ to\ 10.9]}$ copies/ml) versus with the presence of antibiotics ($10^{9.0\ [8.2\ to\ 9.9]}$ copies/ml) (p=0.03) (**Figure 4.1**E). However, this increase in bacterial load was not specific to asthmatic epithelial cells among the antibiotic-free group (**Figure 4.1**F). This observation was not likely to be biased towards the use of inhaled corticosteroid (r=0.12, p=0.77) and oral corticosteroid (r=0.07, p=0.86) among the sputum donors. This is also not biased towards the use of inhaled corticosteroid (with antibiotics, spearman r=0.44, p=0.38; without antibiotics, spearman r=0.73, p=0.10) among the epithelial cell donors after 24 h inoculation despite the small sample numbers being used. None of the epithelial cell donors took oral corticosteroids. The bacterial load in the ALI S/N and

within ALI cells were also assessed. The quantities were below detection limit and did not increase overtime (**Table 4.3**).

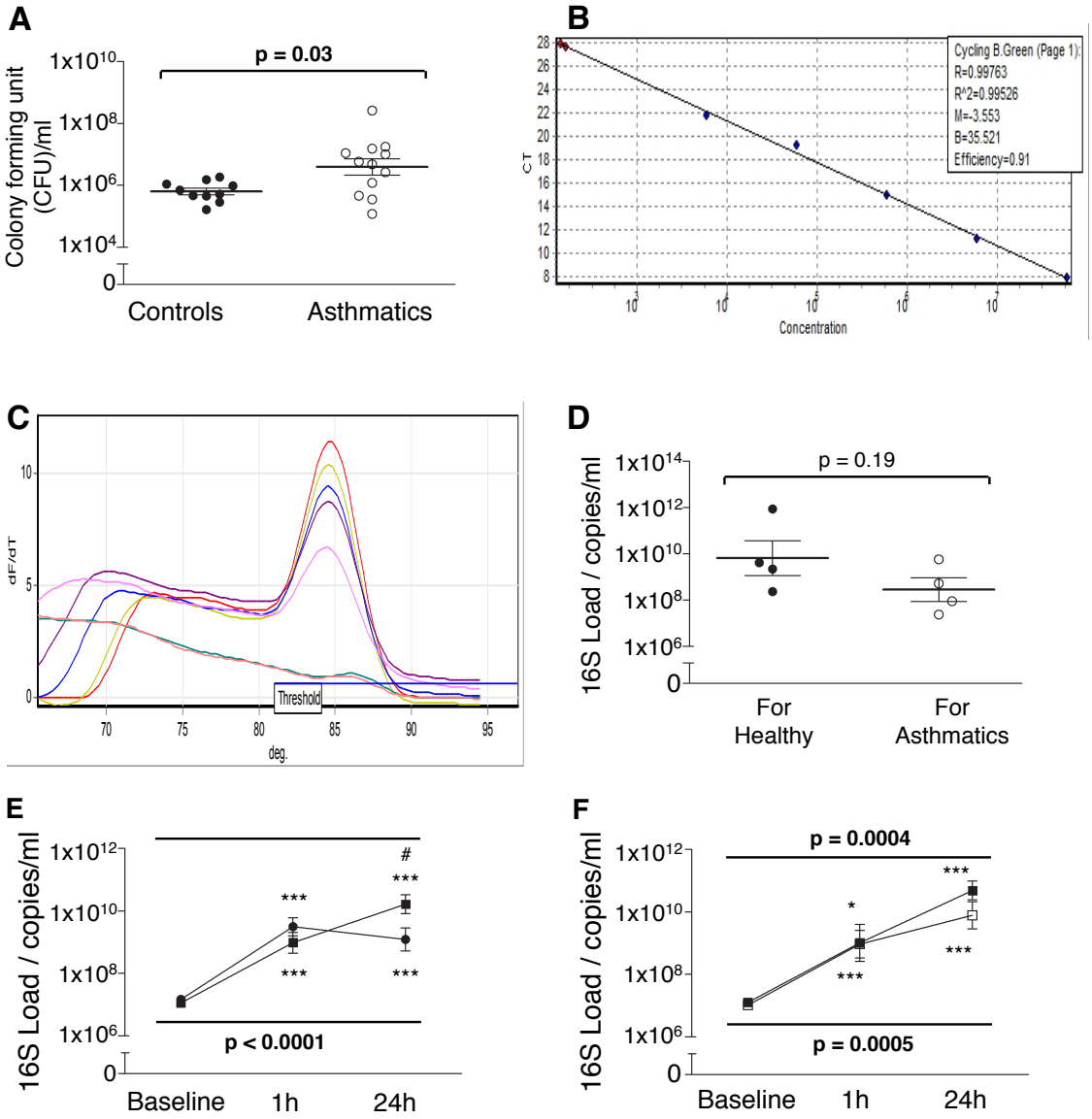

Figure 4.1 Bacterial load in fresh sputa, and the apical chamber fluid (ACF) samples from the sputum inoculation. Bacterial load (in cfu count) in fresh sputa was first investigated using samples from health (n=10) and asthma (n=12). Statistical difference was assessed using an unpaired t-test, $p<0.05$. Bacterial load represented by 16S copies was quantified by qPCR using the collectables from the sputum inoculation study. B shows standard curve generated from *E coli* standard DNA. C shows the amplification curve of bacterial 16S qPCR. D shows the 16S load present in the asthmatic sputa used for the inoculation study. E shows the change in 16S load in the ACF samples (n=8) with sputum inoculation over the 24 h, with the presence (dots) or absence (squares) of antibiotics. F shows in the absence of antibiotics, the change in 16S load in health (n=4, closed squares) and asthma (n=4, open squares) over the 24 h inoculation. * indicates comparison with baseline using One-way ANOVA with Tukey post-tests, $p<0.05$. # indicates comparison between subject groups using unpaired t-tests, $p<0.05$.

A.

ALI S/N		With antibiotics			Without antibiotics		
	Sputum	Cell	1 h	24 h	Cell	1 h	24 h
Healthy (n=4)	$10^{9.8\ [7.4\text{-}12.2]}$	$10^{7.1\ [6.7\text{-}7.5]}$	$10^{7.1\ [6.5\text{-}7.6]}$	$10^{7.1\ [6.5\text{-}7.7]}$	$10^{7.1\ [6.7\text{-}7.5]}$	$10^{9.0\ [7.1\text{-}10.9]}$	$10^{7.1\ [6.6\text{-}7.7]}$
Asthmatic (n=6)	$10^{8.5\ [6.8\text{-}10.1]}$	$10^{7.2\ [6.8\text{-}7.7]}$	$10^{7.3\ [6.8\text{-}7.7]}$	$10^{7.3\ [6.8\text{-}7.7]}$	$10^{7.0\ [6.7\text{-}7.3]}$	$10^{7.0\ [6.6\text{-}7.4]}$	$10^{7.1\ [6.7\text{-}7.4]}$

B.

(n=1, duplicate)	With antibiotics	
	1 h	24 h
Cells	$10^{7.5\ [6.7\text{-}8.3]}$	$10^{7.5\ [7.5\text{-}7.7]}$
ACF	$10^{7.6\ [5.6\text{-}9.6]}$	$10^{7.5\ [6.5\text{-}8.4]}$
ALI S/N	$10^{7.5\ [7.4\text{-}7.6]}$	$10^{7.6\ [6.8\text{-}8.4]}$

Table 4.3 Bacterial 16S load in the collectables from the sputum inoculation study. Bacterial 16S load (by qPCR) was investigated in the collectables from healthy and asthmatic cultures in the sputum inoculation study. Data are expressed as mean [95% CI]. A shows the 16S load in the baseolateral supernatants (ALI S/N) samples from health (n=4) and asthma (n=6). B shows the 16S load in the collectables from the PBS-inoculated asthmatic ALI cultures. 'Cells' represents the DNA extracted from ciliated cell strips preserved in RNA*later*.

4.4.2 Fungi were not likely to be the cause of ciliary dysfunction

Amphotericin is an antibiotic specifically targets fungi. Since it was one of the 3 antibiotics involved in the sputum-induced ciliary dysfunction in ALI cultures reported in the previous chapter, the quantity of fungi, particularly *A. fumigatus*, was assessed in asthmatic sputa and the collectables from the sputum inoculation study.

The result from the fungal culture showed that 60% of the severe asthmatic sputa were fungal positive, but was not significantly different from healthy controls, which was 50% positivity (p=0.67, **Table 4.4**). In fact, the high level of fungi in healthy airways was not surprising because of the endogenous colonisation reported previously (421, 422). Meanwhile, 33% of the asthmatic sputa were *A. Fumigatus* positive compared to the 0% in the healthy sputa (p=0.07), which was also consistent with a previous finding (264). However, using qPCR targeting AfMITO, none of the severe asthmatic sputa used for the sputum inoculation in Chapter 3 was *A. fumigatus* positive, which was in disagreement with a previous study (423). Furthermore, *A. fumigatus* was not identified in the ACF samples collected after the inoculation study. **Figure 4.2** shows that the lack of detectable *A. fumigatus* was not due to any artefact in the reaction. In fact, this could be due to the methodological approach on microbial DNA extraction (424). It could also be due to the lack of *A. fumigatus*-sensitization among these sputum donors. In fact, only 3 of the 11 donors were *A. fumigatus*-IgE-sensitized patient, and none of them were atopic to Aspergillus species. Unfortunately, the limited sample volumes and sputum supply made it difficult to validate this finding. Further repeats would be required to draw a conclusive result.

Fungal Contents	Healthy (n=8)	Asthmatic (n=12)	p-value
Fungal positive	50%	60%	0.67
- Aspergillus	0%	33%	0.07
- yeast	100%	56%	0.82
- other moulds	0%	22%	0.34

Table 4.4 Fungal contents in fresh sputa collected from health and asthma. Fungal growth was tested in fresh sputa collected from health (n=8) and asthma (n=12). Sputum cells were cultured for fungal mycology assessment. Data are expressed as a % of presence. Statistical differences were assessed using Chi-square tests, $p<0.05$.

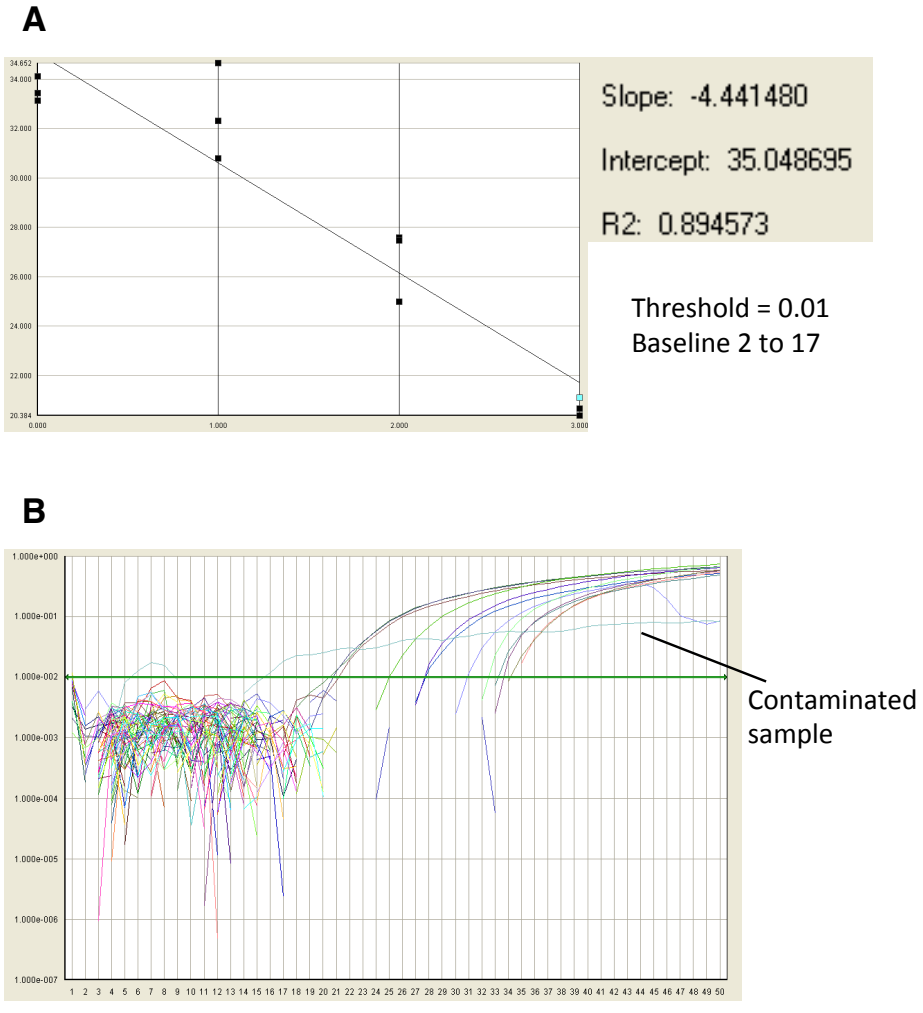

Figure 4.2 *Aspergillus fumigatus* qPCR graphs. These graphs show that the absence of detectable *A fumigatus* was not due to the artefact of the reaction. A shows the standard group generated from the amplification data as shown on B. The irregular line suggests a contamination of that particular reaction.

4.4.3 The human β-defensin secretion was similar in healthy and asthmatic cultures

To evaluate if the asthmatic epithelium provided an environment that facilitated bacterial growth, antimicrobial protein hBD-1 and hBD-2 secretion from the epithelial cells was quantified. **Figure 4.3**A and **Figure 4.3**B illustrate the secretion patterns of hBD-1 and hBD-2 respectively from different types of epithelial collectables at an un-stimulated status. hBD-1 was constitutively secreted by HAEBC (250±99 pg/ml), and by ALI cultures both basolaterally (ALI S/N, 1124±261 pg/ml) and apically (ACF, 996±278 pg/ml) (**Figure 4.3**A). In comparison, the baseline secretion of hBD-2 level was lower in all samples (**Figure 4.3**B). hBD-2 secretion was low or undetectable in HAEBC, and was low in ALI S/N (36±16 pg/ml) and in ACF (137±46.4 pg/ml). Both hBDs were measurable in all healthy controls and asthmatic samples with no differences between two subject groups.

6 ACF samples (3 healthy and 3 asthmatics) collected from the sputum inoculation study in Chapter 3 were used for measuring hBD1/2 quantities. This small sample size was due to the limited number of samples available after the microbial quantification experiments. It therefore limited the power of the statistical comparison, and thus the datasets from healthy controls and asthmatics were combined as shown in **Figure 4.4**. Both hBDs were detectable in the asthmatic sputa used for the sputum inoculation study in Chapter 3 (**Figure 4.4**A). The constitutive hBD-1 secretion in the apical surface of ALI cultures could be induced by asthmatic sputa, but not by PBS (**Figure 4.4**B). This sputum-induced increase was in a time-dependent but insignificant manner. This effect was similar between the presence (8869±2533 pg/ml) and the absence (12130±3460 pg/ml) of exogenous antibiotics. Similarly, asthmatic sputa induced the secretion of

hBD-2 in a time-dependent manner (**Figure 4.4**C), but with no significantly difference between the presence (458±352 pg/ml) and the absence (655±211 pg/ml) of antibiotics. Despite the low sample size in each subject group, paired t-tests were performed, and it showed no significant difference between health and asthma. Inhaled corticosteroid intake was not correlated to hBD-1 level ($r=0.19$, $p=0.76$), and to hBD-2 level ($r=0.05$, $p=0.94$), in the sputa. Therefore these results were not likely to be biased towards the use of steroid among the sputum donors or the epithelial cell donors despite the small sample numbers being used.

The basolateral secretion of hBD-1 and hBD-2 were also evaluated using 6 ALI S/N samples (3 healthy and 3 asthmatics) from the sputum inoculation study. Both defensins were also detectable in all ALI S/N samples (**Table 4.5**), which further supports the role of the airway epithelium in facilitating adaptive immunity via hBDs as reported previously (174). There was no difference in hBD levels in ALI S/N between health and asthma.

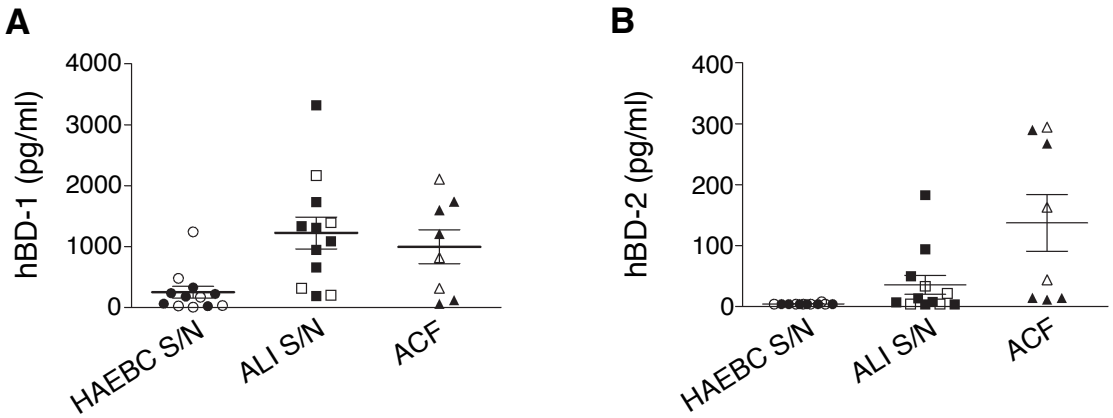

Figure 4.3 Baseline secretion of human β-defensins (hBD)-1 and -2 from human airway epithelial cells. hBD-1 and hBD-2 secretion were measured in HAEBC conditioned medium (n=12), ALI culture baseolateral supernatant (ALI S/N) (n=12) and apical chamber PBS wash (ACF) (n=8), from health (closed symbols) and asthma (open symbols), by single ELISAs. Closed and open symbols represent healthy and asthmatic samples respectively. Data are expressed as mean±SEM.

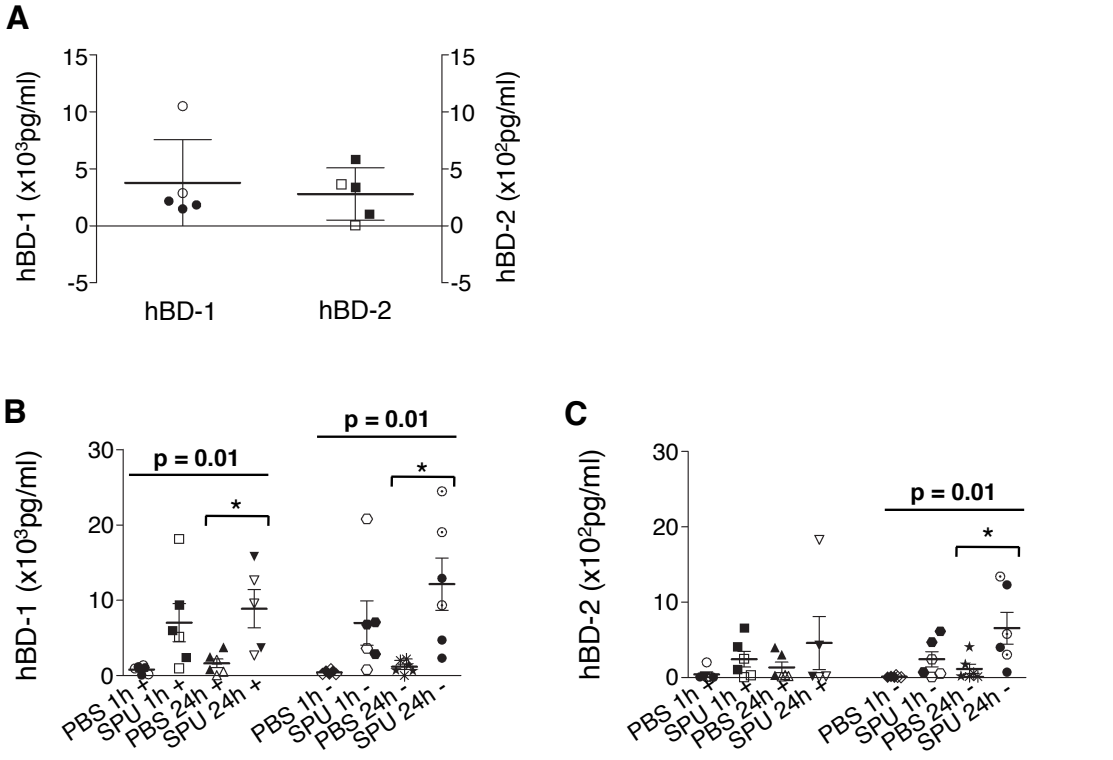

Figure 4.4 Human β-defensin (hBD)-1 and hBD-2 secretion on apical surfaces of ALI cultures upon 24 h PBS/sputum inoculation. Apical chamber fluid (ACF) samples collected from healthy (n=2-3, closed symbols) and asthmatic (n=3, open symbols) samples in the sputum inoculation study were used for this experiment. Data are expressed as mean±SEM. A shows the hBDs present in diluted sputa at baseline. B and C show the levels of hBD-1 and hBD-2, respectively, detected in ACF samples upon PBS or asthmatic sputum inoculation, with (+) or without (-) antibiotics. Statistical differences were assessed using One-way ANOVA with Tukey post-tests, $p<0.05$.

A.

hBD-1	All (n=6)	p-value*	p-value§	Healthy (n=3)	Asthmatics (n=3)	p-value#
Baseline +	1077±708	-	-	1590±1159	307±9	0.20
PBS 1h +	201±74	0.06	-	161±115	241±113	1.00
SPU 1h +	493±335	0.44	-	136±90	851±652	0.70
PBS 24h +	1610±844	0.63	-	1975±1687	1245±761	1.00
SPU 24h +	1867±750	0.81	-	1402±1167	2332±1111	0.40
Baseline -	629±272	-	0.63	850±425	299±119	0.40
PBS 1h -	185±72	0.13	0.69	95±58	276±121	0.27
SPU 1h -	177±81	0.13	0.22	58±28	296±135	0.51
PBS 24h -	1505±1156	0.31	0.59	349±152	2661±2307	0.70
SPU 24h -	1122±536	1.00	0.59	1296±942	948±718	0.70

B.

hBD-2	All (n=6)	p-value*	p-value§	Healthy (n=3)	Asthmatics (n=3)	p-value#
Baseline +	8.0±2.6	-	-	10.8±3.6	3.9±0.0	0.20
PBS 1h +	4.2±0.3	0.50	-	4.5±0.6	3.9±0.0	0.42
SPU 1h +	17.3±12.2	0.75	-	28.7±24.8	5.8±1.0	1.00
PBS 24h +	12.5±5.2	0.75	-	10.9±7.0	14.1±9.2	0.64
SPU 24h +	31.4±10.5	0.13	-	21.0±12.5	41.8±16.8	0.04
Baseline -	5.5±1.6	-	0.50	6.6±2.7	3.9±0.0	0.42
PBS 1h -	5.7±1.8	0.37	1.00	3.9±0.0	7.4±3.5	0.42
SPU 1h -	4.9±0.7	1.00	0.50	4.4±0.5	5.4±1.5	1.00
PBS 24h -	15.8±9.5	1.00	0.88	8.2±2.9	23.5±19.6	1.00
SPU 24h -	53.6±16.8	0.06	0.56	42.4±3.3	64.8±35.7	1.00

Table 4.5 Human β-defensin (hBD) secretion in the baseolateral supernatants of ALI culture (ALI S/N) upon 24 h PBS/sputum inoculation. ALI S/N samples collected from healthy (n=3) and asthmatic (n=3) samples, with (+) and without (-) antibiotics, in the sputum inoculation study were used for this experiment. Data are expressed as mean±SEM. A and B show the results of hBD-1 and hBD-2 respectively. * indicates comparison with baseline using Wilcoxon rank tests. § indicates comparison with the corresponding antibiotics control using Mann-Whitney U tests, $p<0.05$. # indicates comparison between subject groups using Mann-Whitney U tests, $p<0.05$.

4.4.4 Bacterial endotoxin was not likely to be the direct cause of ciliary dysfunction in asthma

Whilst the bacterial load has increased in the ACF samples during the sputum inoculation study, it is expected that bacterial endotoxin level may have increased as well. To evaluate the potential role of bacterial endotoxin in sputum-induced ciliary dysfunction, endotoxin quantity in the asthmatic sputa was measured using rFC assay. The assay was first optimized by obtaining a net Log [relative fluorescence unit (RFU)] value at ~3.5 for the standard concentration at 1 endotoxin unit (EU)/ml (**Figure 4.5**A). This could be adjusted by changing the sensitivity of the plate reader (determined by "Gain" value, repeatedly tested) (**Figure 4.5**B). According to U.S. Food and Drug Administration (FDA) (425), 1 EU is equivalent to 100-200 pg of endotoxin, and is equivalent to approximately 10^5*E coli*. EU is preferred as the standard unit because the potency can be defined and standardised across different endotoxin assays and in clinic. Sample dilution factor was first tested in some sputum PBS supernatants. The preliminary result suggested a dilution factor ranging from 1:200 to 1:500, which gave acceptable spike recovery ranging from 50% to 200% (**Figure 4.5**C). This dilution factor was adjusted later to 1:450 for the ACF from the PBS-inoculated cells and 1:5000 for the ACF from the sputum-inoculated cells (**Figure 4.5**D).

Bacterial endotoxin was present in a $\log_{10}$ scale because the data points were not normally distributed; statistical analysis using linear regression was performed after the data transformation. The endotoxin level in severe asthmatic sputa was at $10^{2.4\ [1.8\ to\ 3.1]}$ EU/ml (**Figure 4.6**A), a level that is compatible with the cfu count previously found ($10^{6.5\ [5.9\ to\ 7.2]}$ cfu/ml, **Figure 4.1**) and with other studies (32). In parallel to the result from the bacterial 16S qPCR, the level of endotoxin in the ACF increased from -0.5±0.5

-fold change at 1 h to 0.6±0.2-fold change at 24 h in the antibiotics-present group (linear regression coefficient r=0.44, p=0.07), and from -1.4±1.4-fold change at 1 h to 1.5±0.8-fold change at 24 h in the antibiotics-free group (linear regression coefficient r=0.46, p=0.05) (**Figure 4.6**B). Unlike the result from the 16S qPCR, the endotoxin level at 24 h showed no response to the effect of antibiotics. There was no difference in the ACF endotoxin levels between health and asthma. The result was not biased towards the use of inhaled corticosteroids (r=0.43, p=0.39), nor the use of inhaled corticosteroids (r=0.69, p=0.13), among the corresponding sputum donors.

A

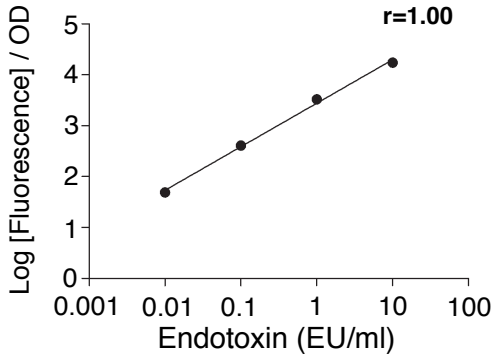

B.

	Log [net RFU] at Gain (G)								
Endotoxin	G1550		G1575		G1600		G1650		G1700
EU/ml	1	2	1	2	1	2	1	2	1
10	4.19	4.12	4.24	4.19	4.30	4.24	4.39	4.29	4.49
1	3.45	3.36	3.52	3.43	3.57	3.48	3.67	3.52	3.77
0.1	2.52	1.51	2.54	1.65	2.62	1.41	2.68	2.61	2.79
0.01	2.23	1.01	2.37	1.44	2.51	1.22	2.7	1.69	2.87

C.

	Spike Recovery %		
Dilution Factor	Sample 1	Sample 2	Sample 3
1:100	118.9	45.2	199.1
1:200	123.6	192.7	241.9
1:500	233.6	220.7	236.4

D.

	Spike Recovery %		
Dilution Factor	Sputum	ACF of spu sample	ACF of pbs samples
1:400	-282.8	-284.7	127 - 196
1:450	-	-	102 - 174
1:5000	102.0	69.2	-

Figure 4.5 **Bacterial endotoxin (rFC) assay optimization.** A shows the endotoxin standard curve in the rFC assay. B shows the optimization of plate reader sensitivity by choosing the gain that gives a net RFU ~3.5 for the 1 EU/ml standard. C and D show the optimization of the sample dilution factors. C shows the result from the preliminary test. D shows the results using some samples collected from the sputum inoculation study (spu, sputum-inoculated sample; pbs, PBS-inoculated sample).

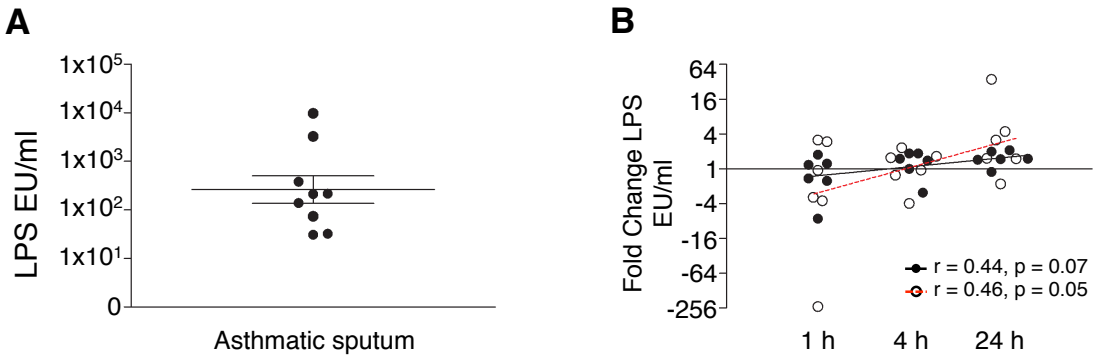

Figure 4.6 Endotoxin quantity in sputum or ACF samples before and after inoculation with ALI cultures. A shows the level of bacterial LPS present in the cell-free supernatant of asthmatic sputa before the inoculation with ALI cultures. B shows the fold change of bacterial endotoxin present in the ACF from the antibiotic-present group (n=6, close dots) and from the antibiotic-free group (n=5-6, open dots) of the sputum inoculation study. Statistical differences were assessed using linear regression, $p<0.05$.

4.5 Discussion

The current results did not support the null hypotheses that bacteria were the cause of ciliary dysfunction in asthma. In Chapter 3, it was reported that the use of exogenous antibiotics prevented the induction of ciliary dysfunction caused by sputum inoculation, suggesting bacterial load and its effects upon the local milieu are important in the development of ciliary dysfunction. However no differential bacterial quantity was found between healthy and asthmatic ACF samples among the antibiotic-free group. These finding therefore could not explain the difference in ciliary function between asthmatic and healthy cells.

Interestingly, the bacterial level in the severe asthmatic sputa was comparable to the sputa from COPD patients (380) – 36% of asthmatic samples arose a bacterial growth of $\geq 10^7$ cfu/ml compared to 0% in healthy controls ($p=0.03$). The relationship between COPD pathogenesis and bacterial colonisation has been well documented (426, 427). This result suggests that the role of bacterial infection/colonization should not be underestimated in asthma.

Apart from bacterial contents, an abnormal fungal colonization is common in chronic airway diseases such as cystic fibrosis (428) and asthma (260). In particular, *A. fumigatus* has been shown to correlate to the reduced lung function in asthma (264). The results reported here also showed a higher fungal culture and *A. fumigatus* positivity in the asthmatic sputa compared to those from healthy controls. It has been demonstrated that *A. fumigatus* metabolites may have ciliary inhibitory effect (429). However no *A. fumigatus* was detected in any of the severe asthmatic sputa used for the inoculation study. This was likely to be because of the lack of *A. fumigatus* allergy and sensitisation

among these sputum donors. Nevertheless, based on the results reported here, it did not support the null hypothesis that fungal content is a cause of asthmatic ciliary dysfunction. An increase in sample sizes will be required to draw a reliable conclusion.

The similarity in hBD1 and hBD2 secretion between health and asthma did not support the null hypothesis that the asthmatic epithelium has a defective anti-microbial activity that facilitates microbial growth and leads to ciliary dysfunction. The airway epithelium secretes various anti-microbial peptides, including different homologues of hBDs and cathelicidins (419), to act against abnormal microbial colonisation/infection. hBD-1 and hBD-2 were specifically chosen because 1) both of them have been extensively reviewed; 2) single nucleotide polymorphisms (SNPs) on defensin β-1 locus (DEFB1), which encodes hBD-1, has been reported to associate with asthma diagnosis (406); 3) hBD-2 is an inducible defensin that is highly responsive to microbes (161, 166, 167); and 4) restricted assays for other hBD isotypes at the time of the study. DEFB genes encode different hBD isoforms (158), and gene polymorphism was reported in asthma, predominantly in female subjects (406). However, no deficiency in hBD secretion at baseline, in either the female subjects or in the asthmatic group, was reported here. Despite the small sample sizes, the secretion of hBD1/2 both at the baseline level and at a sputum-induced level were similar between health and asthma. These findings suggest that the hBD-1/2 quantity may not be the cause of ciliary dysfunction induced by asthmatic sputa, regardless the presence or absence of exogenous antibiotics. However, the involvement other deficiency that may lead to a defective innate response against microbes cannot be justified.

It is noteworthy that the asthmatic sputa contain a range of detectable components including inflammatory cells, microbes and molecules mediating innate and adaptive immune systems (379, 430). This includes a substantial amount of anti-microbial peptides such as hBD-1 and hBD-2 as shown in the result here. Although it has been shown that macrophages produce hBDs (431), it only counts towards 10-20% of the total sputum cell count and was comparable with previous studies (379, 432). Similarly, the epithelial cells present in the sputum samples herein (~3-10%) were likely to be squamous or dead cells (26, 379), and thus may not contribute to the hBD generation detected *in vitro*. As a result, the presence of viable sputum inflammatory cells may not necessarily explain the substantial increase in hBDs present in ACF after 24 h inoculation.

In addition, the result suggests that hBD-1 could be induced by asthmatic sputum inoculation, instead of simply being a constitutive antimicrobial peptide secreted by the airway epithelium. Furthermore, it has been previously shown that overexpressing hBD-2 is cytotoxic to airway epithelium (433). Therefore, it is plausible that the overexpression of hBD-1 might have a similar effect. It is also noteworthy that ELISAs only quantified the level of hBD secretion and gave no indication on the activities of the proteins. Further investigation would be required to justify these.

Apart from viable cells, microbial toxins such as Gram-negative bacterial endotoxin (LPS) (254) and *A. fumigatus* derived gliotoxin (429) may also affect ciliary function. The lack of detectable *A. fumigatus* and the lack of a reliable quantification assay for gliotoxin restricted these evaluations. Whilst a high level of bacterial 16S was measured in asthmatic sputa, it is plausible that the associated toxins, such a bacterial endotoxin,

may induce ciliary dysfunction. LPS are conserved structures that can be found on the surface of Gram-negative bacteria, which are common in asthmatic airways (243, 434). LPS has been shown to directly reduce CBF in airway epithelium, whilst their effects were independent from the bacterial viability (254, 255, 435). rFC assay was chosen over the traditional Limulus Amebocyte Lysate (LAL) assay for endotoxin quantification because of its simplicity, its wider range of standard concentrations and, most importantly, its low false positive rate (383, 384, 425). Unlike the result from the 16S qPCR, the endotoxin level in the ACF samples increased overtime, but showed no difference between health and asthma at 24 h. The use of steroid was not correlated to the endotoxin level nor the bacterial level measured. Therefore bacterial endotoxin is not likely to have a direct contribution to the ciliary dysfunction in asthma. As a result, these findings did not support the null hypothesis that bacterial cytotoxicity is the cause of asthmatic ciliary dysfunction. However, the use of exogenous antibiotics did suppress the sputum-induced ciliary dysfunction in ALI cultures, suggesting that bacterial endotoxin could be an environmental trigger of the abnormality.

4.6 Criticism

Limitation 1: Sputum contents and differences between healthy and asthmatic samples were not dissected in detail

The assessment of the sputum components was limited to the general bacterial load, fungal load, differential inflammatory cell counts and hBD-1/2 quantity. The viability of the microbes may be evident in the microbial cultures (cfu for bacteria; species identification for fungi). However, measuring bacterial 16S was a broad quantification approach that included both live and dead bacteria. This might mask the importance of certain low profile microbes that could be important to the induction of ciliary dysfunction. Asthma-specific microbial species have been identified previously (243, 244). Identifying individual bacteria could be done using mass spectrometry-based proteomics, which allow the identification of a broad spectrum of bacteria simultaneously (436, 437). However, it demands time and specific sample processing, and thus it was not pursued in my project. Furthermore, differential inflammatory cell counts did not reflect the viability or the activity of these inflammatory cells. hBD ELISAs could only measure the quantity but not the anti-microbial activity of these peptides. Other contents that were present in the sputum and their activities are yet to be studied.

Another limitation was that the sputum contents were not compared extensively between health and asthma. Some sputum samples (n=10) were successfully collected from healthy controls. Whilst some healthy sputum samples were collected after many attempts, the sample volumes were generally very low. There were not enough materials for both bacterial and fungal analysis. Collecting enough sputum volume for the sputum inoculation study would be even more difficult. Therefore, no further

comparison between healthy and asthmatic sputum samples were performed in this thesis.

Limitation 2: The role of Aspergillus might be underestimated

Fungal culture revealed that only 33% of the severe asthmatic sputum was *A. fumigatus* positive compared to 0% in health controls, but with a lack of significance (p=0.07). Of the sputa used for the sputum inoculation study, the sputum donors were coincidently all non-atopic to *A. fumigatus*. The majority of them were also non-sensitized to this fungal species. Therefore, the quantity of *A. fumigatus* in these sputa was already low to assert any effect on the ciliary function during the sputum inoculation period. Furthermore, recent findings have suggested an association between *A. fumigatus* colonisation and specific inflammatory profiles in asthma (263), although the aetiology was contentious. As a result, it would be beneficial to further investigate the role of fungi in asthmatic ciliary dysfunction by using sputum samples from specific groups of asthma including asthmatics with ABPA and/or with neutrophilia.

Limitation 3: Colonisation versus Infection

It is important to distinguish infection from colonisation. Colonisation is the growth of microbes without any clinical outcomes. It could refer to both a normal microbiota and a pathogenic microbial community. In comparison, infection is likely to be symptomatic and involves the presence of pathogenic factors. The techniques used in the project herein, such as microbial culture and qPCR, only revealed the quantity of the microbes, (colonisation) and may not reflect the case of infection. Therefore, the results reported here may only be used to conclude an association between microbial quantity and asthma. Incidence of infection may be assessed by real time clinical studies (438), or

using *in situ* immunohistochemistry in animal models, bronchial biopsies, *ex vivo* tissue (69) and cell models (439). However, more conclusive findings are needed before moving on to any in vivo studies, which can be achieved by increasing the sample sizes.

Limitation 4: Small sample numbers may affect justifications

As mentioned throughout this chapter, another major limitation that restricted a clear conclusion to be drawn was the small sample numbers in the experiments. Most of the experiments performed utilised the apical and basolateral fluids from the ALI cultures of the sputum inoculation study. Each of these collectables contained 200 μl and 700 μl in volume, which were very limited amount of samples. This resulted in the small sample numbers for some experiments including the hBDs and LPS assessments, and thus the donor-to-donor variation and the lack of significance. The conclusion being drawn so far on the similarity between health and disease subject groups may not be reliable. To justify that, increasing the sample numbers would be beneficial.

4.7 Summary

In this chapter the roles of pathogens and epithelial innate immunity in driving asthmatic ciliary dysfunction have been evaluated. The absence of antibiotics provided an environment for pathogens in the asthmatic sputa to flourish, as reflected by the increase in bacterial load during the 24 h inoculation with epithelial ALI cultures.

However, this bacteria-favoured environment may not be contributed from a defective secretion of human β-defensin 1 and 2 from the epithelial cells. The ciliary function of asthmatic ALI cultures responded negatively to asthmatic sputum within 1 h. Such a rapid response implies that the asthmatic sputa may have a cytotoxic effect on the ALI cultures. However, despite the elevated bacterial 16S copies and bacterial endotoxin during the 24 h sputum inoculation, there was no significant difference between health and asthma among the antibiotic-free subgroup. In the meantime, Aspergillus may not be involved in asthmatic ciliary dysfunction.

Both bacterial load and LPS quantity were increased, which was in coherence with the absence of antibiotics and the presence of ciliary dysfunction. It is therefore reasonable to believe that bacteria may be an environmental factor that induced the ciliary dysfunction in asthmatic ALI cultures in the sputum inoculation study. Increase the sample sizes of the experiments will improve the conclusiveness of this finding.

5. Oxidative Stress and Epithelial Ciliary Function in Asthma

5.1 Chapter Overview

The results from Chapter 3 and Chapter 4 suggested that bacterial infection/colonisation was likely to be an environmental factor that was associated with the asthmatic sputum-induced ciliary dysfunction, but was not directly correlated to the reduction in ciliary function. Whilst a cytotoxic effect from the asthmatic sputa could be the cause of ciliary dysfunction, data suggested it was not caused by bacterial endotoxin. In fact, there may be other cytotoxic factors such as oxidants that are present in the asthmatic sputum and could contribute to the asthmatic ciliary dysfunction. Therefore, the aims in this chapter were 1) to evaluate if abnormalities in oxidative handling are present in asthmatic epithelium, and 2) to evaluate if there is a link between these abnormalities and epithelial ciliary function.

To do that, the presence of oxidative DNA damage was revealed using an immunohistological approach. Using HAEBC, an abnormal oxidative burden following stimulation was found using a ROS quantification assay. Expression of specific genes and proteins was quantified using qPCR and Western Blots, and it became evident that there may be an upregulation of NOX4 gene expression in asthma that may be associated with neutrophilic inflammation. Blocking NOX4 activity showed an improvement in intracellular oxidative burden in HAEBC, and an improvement in ciliary dysfunction in fresh asthmatic epithelial cells that was also associated with neutrophilic inflammation. These findings not only suggested that NOX4 may play a significant role in regulating ciliary dysfunction in asthma, but also that the role of NOX4 may be particularly prevalent in neutrophilic asthma. It opens new avenues with regards to research into potential novel therapeutic targets for treating corticosteroid-insensitive asthmatic patients, the majority of whom have neutrophilic inflammation.

5.2 Introduction

The link between age and oxidative stress (440), and between age and ciliary function (441), implies a possible relationship between oxidative stress and ciliary dysfunction. In fact, oxidative imbalance has been reported in diseased lung cells. Lung fibroblasts with excessive NADPH oxidase (NOX) 4 activity are associated with lung fibrosis (312). Airway smooth muscle cells from asthmatic airways show increased NOX4 gene expression that is associated with airflow obstruction in asthma (316). A direct application of H_2O_2 causing disruption of ciliated ependyma (252, 420) suggests a direct relationship between ROS toxicity and ciliary dysfunction. The association between bacteria and reactive species implies an altered oxidative balance in the host cells that leads to a cytotoxic effect. For instance, *Streptococcus pneumoniae*, a common pathogen found in the airways of patients with asthma and COPD, is able to generate ROS (252). On the other hand, the virulent factors of *Pseudomonas aeruginosa*, a common pathogen found in bronchiectasis patients, have been shown to activate the downstream signalling molecules in the oxidative pathways that cause ciliary immotility, which could be modulated by oxidants and antioxidants (34). Meanwhile, microbial colonisation/infection is thought to be associated with neutrophil activity in the airways (32, 263). Asthmatic subjects with infection-induced exacerbations may also be associated with an activated T_H1 signalling pathway and neutrophil-dominant inflammatory profile (32, 142, 442, 443). Activated neutrophils generate an abundant amount of ROS during the oxidative burst associated with microbial phagocytosis. This could increase the oxidative burden in the surrounding environment. Moreover, the activity of reactive peroxynitrite has been found in asthmatic sputa (444). As a result, it is plausible that the asthmatic sputa itself can act as an oxidative stimulus due to the abundant bacterial and inflammatory cell contents, to induce ciliary dysfunction in

asthmatic cells as shown in Chapter 3. I therefore considered that oxidative stress might be important in increasing the susceptibility of asthmatic epithelial cells to develop ciliary dysfunction.

Based on the above evidence, I tested the following sub-hypotheses:

(i) Oxidative mishandling is not the cause of the asthmatic ciliary dysfunction, and that an anti-oxidative treatment would not improve ciliary function

(ii) The anti-oxidative treatment has the same effect on ciliary function across different asthma subtypes

5.3 Methodology

The presence of oxidative stress was assessed in the different types of airway epithelial cells using different approaches: an *ex vivo* approach using bronchial biopsies, and an *in vitro* approach using HAEBC.

8-oxo-dG is an oxidised derivative of guanine, one of the four DNA-forming units, and is commonly used as an indicator of an oxidative DNA damage (394). The presence of 8-oxo-dG in epithelial cells was assessed by staining the epithelium region of the GMA-embedded bronchial biopsies with the anti-8-oxo-dG antibody or its isotype control, followed by a semi-quantification method (316). The 8-oxo-dG staining and analysis were kindly performed by Miss Camille Doe and Prof. Chris Brightling.

The DCF-DA assay is a quantitative assay for measuring intracellular reactive oxygen species generation (iROS). The DCF-DA molecules penetrate the cell plasma membrane, and subsequently emit a quantifiable fluorescence that is directly proportional to the quantity of iROS present intracellularly (390). The DCF-DA assay was first optimised for sensitivity (Gain value at 1100) and sample dilution. The iROS level in healthy and asthmatic HAEBC was measured at an un-stimulated (baseline) status and a stimulated status. H_2O_2 at concentrations ranging from 50 mM to 50 μM were used as the stimulus. Black 96-well plates were specifically used to prevent fluorescence contamination across adjacent wells. Only the wells that reached ≥90% cell confluence were used for the assays.

Coomassie Bradford assay is a quantification assay that measures protein levels in cell lysates. The assay reagent provides an acidic environment for the coomassie dye to

change from brown to blue upon protein binding, of which the intensity is in proportion to the protein quantity in the sample (387). It was performed to measure the HAEBC protein levels at the end of each DCF-DA assay

NOX4 and SOD2 were potential players in the epithelial oxidative pathways in asthma (316), thus they were specifically measured using a genetic approach (RT-qPCR) and a protein approach (Western Blot). RT-qPCR is a two-step gene quantification method, where initial synthesis of cDNA from total RNA samples, followed by the amplification of the cDNA of interest. This amplification is measured by a fluorescent reporter (SYBR Green) of which the C(t) reading is indirectly proportional to the input RNA quantity (392). Samples of total RNA were prepared from HAEBC and ALI cultures: HAEBC were prepared in 6-well plates. After reaching >80% confluence 2 wells were combined as 1 sample; 50 to 100 % of a Transwell® of ALI culture was used as 1 sample. Total RNA was extracted using Qiagen RNeasy mini kit plus DNaseI digestion. Only the RNA samples with an A260/A280 ratio ≈2 were used for the RT-qPCR. RT-qPCR was performed following the manufacturer's protocol. The primers and reaction conditions are stated in **Table 5.2**. The size and purity of the qPCR products were analysed using 2 % agarose gel electrophoresis. As for the data analysis, the C(t) value of each sample was first corrected with its own housekeeping gene (18S) C(t) value followed by a normalisation with a reference sample. This same reference sample was used for the normalisation of all RT-qPCR runs. Statistical analysis was performed after the normalisation.

Western Blot is the one of the most common protein analytical assay that uses gel electrophoresis to first separate proteins according to their molecular weight, followed

by recognition of the protein of interest using a specific antibody which can be picked up fluorescently and can be quantified using densitometry (388, 389). Whole cell lysates were prepared from HAEBC and ALI cultures for protein samples. 10 % and 12 % acrylamide running gels were used for resolving NOX4 and SOD2 proteins respectively. **Table 5.1** shows the antibodies used for each target protein. A human airway smooth muscle cell (HASMC) lysates were used as a positive control. The intensity of each densitometry measurement was normalised with the corresponding housekeeping protein β-actin.

Protein of Interest	1° antibody	Dilution factor	2° antibody	Dilution Factor	Blot Development
SOD2	Polyclonal rabbit anti-SOD2 (ab13533, Abcam, Cambridge)	1:5000	Anti-rabbit HRP-conjugated (Cell Signaling Technology)	1:3000	ECL (Amersham, Little Chalfont, U.K.)
NOX4	Polyclonal rabbit anti-NOX4 (ab60940, Abcam)	1:1000	Anti-rabbit HRP-conjugated (Cell Signaling Technology)	1:3000	UptiLight™(Interchim, MontluconCedex, France)
NOX4	Polyclonal rabbit anti-NOX4 (NB110-58851, Novus Biological, Cambridge)	1:500	Anti-rabbit HRP-conjugated (Cell Signaling Technology)	1:3000	
β-actin	HRP-conjugated human anti-β-actin 9	1:20,000	-	-	ECL (Amersham)

Table 5.1 Antibodies used for Western Blot for NOX4 and SOD2. One SOD2 antibody, and two NOX4 antibodies were used for detecting NOX4 protein in cell lysates from HAEBC and ALI cultures. β-actin was used as the housekeeping reference protein. Both SOD2 and β-actin were highly expressed thus ECL western blot analysis reagent was used for the blot development. NOX4 protein expression was low, thus a more sensitive, UptiLight™ reagent was used.

A.

Gene	Primers	Volume in rxn mix	Source
NOX4	4598-forward 5'-TGGCTGCCCATCTGGTGAATG-3'	1 µl	Operon MWG Biotech
	4878-reverse 5'-GCATCGTTTATGGTCGGAAC-3'	1 µl	
SOD2	Forward 5'-CGACCTGCCCTACGACTAC-3'	0.4 µl	PrimerDesign
	Reverse 5'-AACGCCTCCTGGTACTTCTC-3'	0.4 µl	
18S	Forward 5'-GTTGGTTTTCGGAACTGAGG-3'	1 µl	Operon MWG Biotech
	Reverse 5'-GCATCGTTTATGGTCGGAAC-3'	1 µl	

B.

			Amplification							
	DNA Glycosylase inactivation	Polymerase activation	Denaturation	Annealing	Elongation	Reading	Total no. of cycle	Holding Step	Melting Step	Hold
SOD2 qPCR	50ºC, 2 min	95ºC, 20 s	95ºC, 20 s	59ºC, 30s	72ºC, 30 s	read	36	-	-	4ºC
NOX4 qPCR	50ºC, 2 min	95ºC, 20 s	95ºC, 20 s	60ºC, 30s	72ºC, 30 s	read	37	-	-	4ºC

Table 5.2 RT-qPCR for NOX4, SOD2 and housekeeping gene 18S rRNA. A shows the primers used for the reactions. B shows the reaction conditions of qPCR for each target gene.

To further investigate the role of NOX4 in oxidative handling in airway epithelial cells, NOX4 protein activity was blocked by GKT137831 (NOX4i), is a NOX1/NOX4 duo protein inhibitor donated from GenKyoTex, Switzerland (**Figure 5.1**). The inhibitory effect of GKT137831 in HAEBC and ciliated cultures was evaluated using the DCF-DA assay and ciliary function analysis respectively.

To assess the effect of GKT137831 on oxidative handling in HABEC, the cells were incubated with 100 µl of the following reagents: GKT137831 alone (1 µM, 5 µM or 20 µM.), H_2O_2 alone (at 10 mM, 1 mM), or GKT137831 (20 µM) plus H_2O_2 (at 10 mM, 1

mM). The incubation time was 0.5 h and 1 h. iROS generation was measured using the DCF-DA assay. After the assay protein levels were measured by Coomassie Bradford assays. Furthermore, the effect of NOX4i on HAEBC survival was evaluated using trypan blue to enumerate viable adherent cells. To do this, the supernatant was removed from each well at the end of the DCF-DA assay. 30 µl filtered, sterile trypan blue stain (diluted in PBS in 1:1 ratio) was added into each well for 2 to 6 min. The stain was then completely removed. Each well was refilled with 30 µl PBS. As illustrated in **Figure 5.2**, a grid was placed at the bottom of the 96-well plate, dividing each well into 4 regions of squares. 4 photos at x20 magnification were taken at the top left corner of each of the squares. Cells were categorized as healthy cell with negative staining, cells negatively stained but with abnormal morphology, and cells with positive staining. The known length of a square of a haemocytometer was photographed at the same magnification as the images and then measured using Image J software, in order to enable calculation of the area of the images in μm^2.

After the DCF-DA assay, the number of concentrations of GKT137831 was reduced to 5 µM and 20 µM only for testing the effect of the compound on the ciliary function of fresh epithelial cell strips. Bronchial brushes (n=13) freshly obtained from the airways were used <1.5 h after bronchoscopy. Cell strips from each brush were resuspended in 2 ml M199 medium by vigorous shaking. Each suspension was split into 99 µl or 198 µl aliquots depending on the original size of the tissue collected. Compounds were prepared in M199 medium with antibiotics and: GKT137831 at 500 µM and 2 mM; NAC at 500 mM as the positive control of GKT137831; equivalent DMSO as in 20 µM GKT137831 condition (NOX4i diluent) as the negative control. 1 µl or 2 µl of the compounds was added into the corresponding aliquots to give working concentrations

of GKT137831 at 5 μM and 20 μM; NAC at 5 mM. Incubation took place at 37°C for 0.5 h or 1 h prior to side-profile video-microscopy.

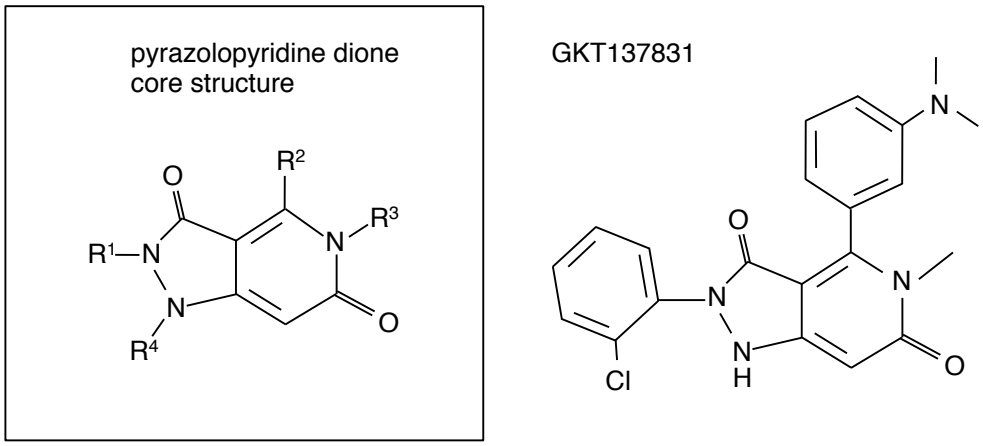

Figure 5.1 Structure of NOX inhibitors. A shows the structure of pyrazolopyridine dione core, the core of anti-NOX small molecules (370). B shows the molecular structure of NOX1/NOX4 inhibitor GKT137831 (320).

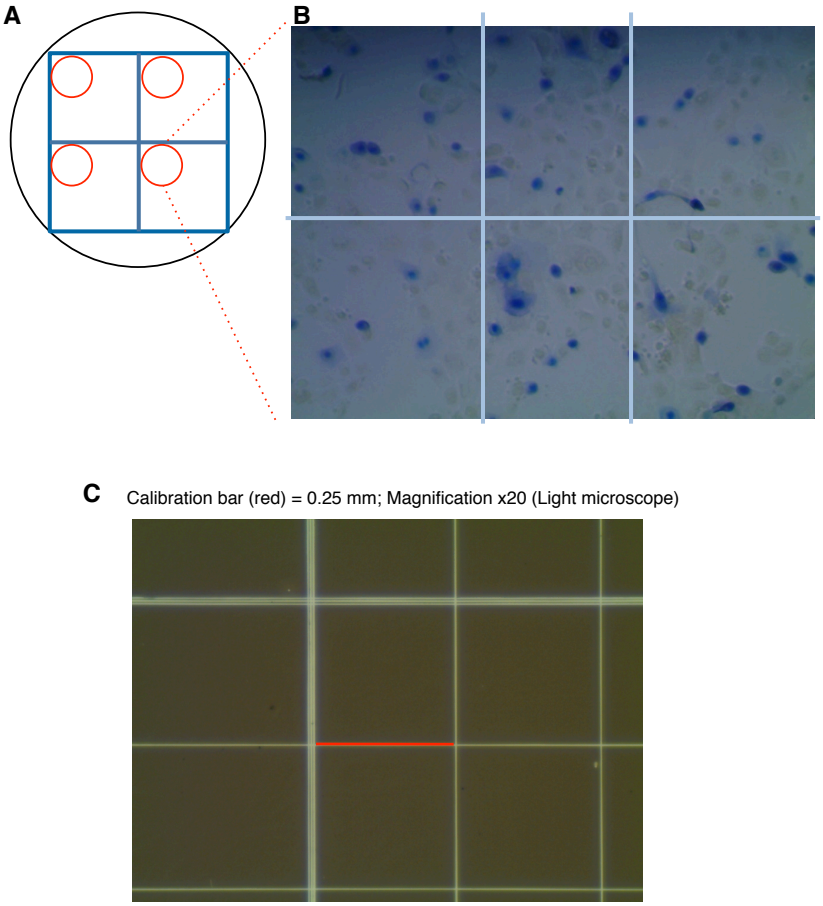

Figure 5.2 Illustration on cell viability assessment using trypan blue staining on adherent cells. A shows a schematic well from a 96-well plate with a grid place at the bottom. 4 pictures were taken per well as indicated by the red circles. B shows a sample picture of adherent HAEBC stained with trypan blue at x20 magnification. Each picture was divided into regions for accurate cell count. C shows a haemocytometer grid taken at x20 magnification using the same light microscope.

5.4 Results

5.4.1 Oxidative mishandling is present in asthmatic epithelium

Oxidative stress was found to be increased in the epithelial cells from asthmatics, but not in healthy controls. The bronchial biopsies from 9 healthy and 27 asthmatics (16 mild-moderate, 11 severe) were used (**Table 5.3**A). Oxidative stress-induced DNA damage, as represented by 8-oxo-dG expression, was increased in the asthmatic epithelium (**Figure 5.3**A). Compared with isotype control (**Figure 5.3**A, left), the asthmatic epithelial biopsy showed a strong positively staining with 8-oxo-dG with different intensities (**Figure 5.3**A, middle and right). This DNA damage was correlated to disease severity (p=0.04) (**Figure 5.3**B). The 8-oxo-dG expression was also correlated to airflow obstruction (p=0.001) (**Figure 5.3**C) and the % of sputum neutrophils (p=0.02) (**Figure 5.3**D). This DNA damage is likely to be due to an abnormal oxidative handling in asthmatic epithelial cells. To confirm this, the DCF-DA assay was used to measure the iROS generation in HAEBC with or without H_2O_2 stimulation.

The DCF-DA assay was first tested using different reagents as the DCF-DA diluent because of the prolonged incubation/stimulation time. PBS is normally used as the diluent for the assay. However, HBSS contains essential ions that may help with maintaining cell survival and adjusting pH value (445). To test if HBSS would be a suitable diluent for the prolonged DCF-DA assays, it was used in a 2 h preliminary test. The result suggested that the use of HBSS resulted in an auto-fluorescence. Therefore, PBS remained as the diluent for the DCF-DA assay. The sensitivity of the microplate reader was also tested using Gain values ranging from 1000 to 1800. A Gain at 1100

gave a window that allowed the biggest changes in fluorescence, and thus it was used for the rest of the DCF-DA assay.

Exogenous H_2O_2-induced oxidative stress was evaluated in HAEBC from 8 healthy and 13 asthmatics (4 non-neutrophilic, 9 neutrophilic) (**Table 5.3**B). The asthmatic group was further divided into non-neutrophilic and neutrophilic sub-groups because of the correlation between 8-oxo-dG staining and sputum neutrophil counts (**Figure 5.3**). At an un-stimulated level, there was no significant difference in iROS generation (i.e. fluorescence intensity, OD) between all subject groups (One-way ANOVA p=0.9, data not shown). H_2O_2 stimulation caused an increase in iROS generation in all subject groups (

Figure 5.4A). The mean [95% CI] EC_{50} was similar between health (0.04 [0.002 to 0.8] mM) and non-neutrophilic asthma (0.1 [0.005 to 1.9] mM). The EC_{50} of the neutrophilic asthma subgroup (0.3 [0.1 to 0.7] mM) was significantly higher than that of healthy controls (p=0.02), although this may be driven by an increase in the maximal response to H_2O_2 as the response to H_2O_2 at concentrations within the EC_{50} range was not significantly different. Interestingly, when comparing the maximum dose effect of the H_2O_2 stimulation, only the neutrophilic asthma subgroup (3380±270 OD, n=9), but not the non-neutrophilic subgroup (2542±398 OD, n=4), produced a significantly higher iROS compared to healthy controls (2371±252 OD, p=0.02, n=8) (

Figure 5.4B). This H_2O_2-induced maximum dose effect was associated with the % sputum neutrophil with a significant value at p=0.052 (

Figure 5.4C), and was in coherence with the correlation between 8-oxo-dG positivity and sputum neutrophil count (**Figure 5.3**E). Despite the lower n number for the non-neutrophilic sub-group, these collective results provide strong evidence for the presence of abnormalities in ROS handling within the subpopulation of asthmatics with neutrophilic inflammation.

In addition, H_2O_2 significantly reduced the protein levels in a concentration-dependent manner (

Figure 5.4D), which was likely to be due to the cytotoxic effect of the stimulus. The protein levels of the adherent cells were measured at the end of the DCF-DA assay using Bradford assay, because it was thought to provide an indirect assessment of cell viability. However adherent dead cells would have also been counted using this

approach. Furthermore, it has been shown previously that certain types of stimulation could increase intracellular protein expression (446, 447). The validation of Bradford assay and the reliability of the results will be discussed later.

A.

Study	Bronchial Biopsy 8-oxo-dG immunohistology			
Clinical Details	**Healthy (n = 9)**	**Mild-Moderate Asthmatic (n = 16)**	**Severe Asthmatic (n = 11)**	**1way-ANOVA p-values**
Gender (F)	5 (4)	6 (10)	4 (7)	0.62*
Age, yr	42 (5)	51 (3)	51 (3)	0.23
Pack year	0.1 (0.1)	3.3 (1.4)	2.5 (1.1)	
% Predicted FEV_1	94 (3)	86 (6)	79 (7)	0.56
% FEV_1/FVC	83 (2)	73 (2)	74 (3)	**0.03**
PC20 FEV_1, mg/ml †	>16	0.8 (0.3-1.8)	0.9 (0.3-2.7)	**< 0.0001**
Blood Total IgE, kU/ml	23 (n/a)	75 (24)	67 (44)	n/a
Blood eosinophils, kU/ml	0.15 (0.05)	0.26 (0.04)	0.23 (0.03)	0.25
Treatment (mcg/24 BDP eqv.)	n/a	594 (157)	1251 (134)	n/a
Atopy, %	33	69	73	0.14*
Age of Disease Onset, yr	n/a	37 (9)	54 (9)	n/a
Sputum Characterization				
Total cell count($x10^6$ cells/ml)	n/a	2.5 (0.4)	4.5 (1.0)	n/a
Eosinophils, % ‡	n/a	1.0 (0.2-5.7)	1.5 (0.3-8.6)	n/a
Neutrophils, % ‡	n/a	58 (22-75)	71 (52-88)	n/a
Macrophages, % ‡	n/a	28 (16-59)	24 (10-32)	n/a
Epithelial cells, % ‡	n/a	4.0 (0.3-6.9)	1.0 (0.6-4.4)	n/a

B.

Study	DCF-DA assay (H_2O_2 stimulation)			
Clinical Details	**Healthy (n = 8)**	**Non-neutrophilic Asthmatic (n = 4)**	**Neutrophilic Asthmatic (n = 9)**	**1way-ANOVA p-values**
Gender (F)	5 (2)	3 (1)	7 (2)	0.96*
Age, yr	46 (7)	55 (5)	57 (5)	0.35
Pack year	3 (3)	30 (16)	11 (5)	0.08
% Predicted FEV_1	105 (6)	66 (8)	80 (6)	**0.005**
% FEV_1/FVC	79 (3)	56 (7)	66 (6)	0.059
PC20 FEV_1, mg/ml †	>16	1.2 (0)	2.3 (0.1-69)	**<0.0001**
Blood Total IgE, kU/ml	45 (31)	65 (26)	123 (54)	0.44
Blood eosinophils, kU/ml	0.15 (0.03)	0.25 (0.09)	0.27 (0.07)	0.39
Treatment (mcg/24 BDP eqv.)	n/a	1867 (133)	1100 (217)	n/a
Atopy, %	0	33	50	0.44*
Age of Disease Onset, yr	n/a	41 (2)	38 (7)	n/a
Sputum Characterization				
Total cell count($x10^6$ cells/ml)	n/a	2.4 (1.2)	5.3 (1.4)	n/a
Eosinophils, % ‡	n/a	15.3 (3.7-25.3)	1 (0.0-2.4)	n/a
Neutrophils, % ‡	n/a	41 (30-52)	84 (72-93)	n/a
Macrophages, % ‡	n/a	10 (5-16)	9 (3-17)	n/a
Epithelial cells, % ‡	n/a	4.4 (2.9-27.4)	1.8 (0.6-4.5)	n/a

† geometric mean (95% CI) ‡ median (inter-quartile range); * Chi Square test $p<0.05$.

Table 5.3 Clinical details of the subjects in the oxidative stress assessment. A, the bronchial biopsy donors; B, epithelial cell donors for the DCF-DA assay with H_2O_2 stimulation. Data are expressed as mean±SEM unless otherwise indicated. Statistical difference were assessed using unpaired t-tests, $p<0.05$ unless otherwise indicated.

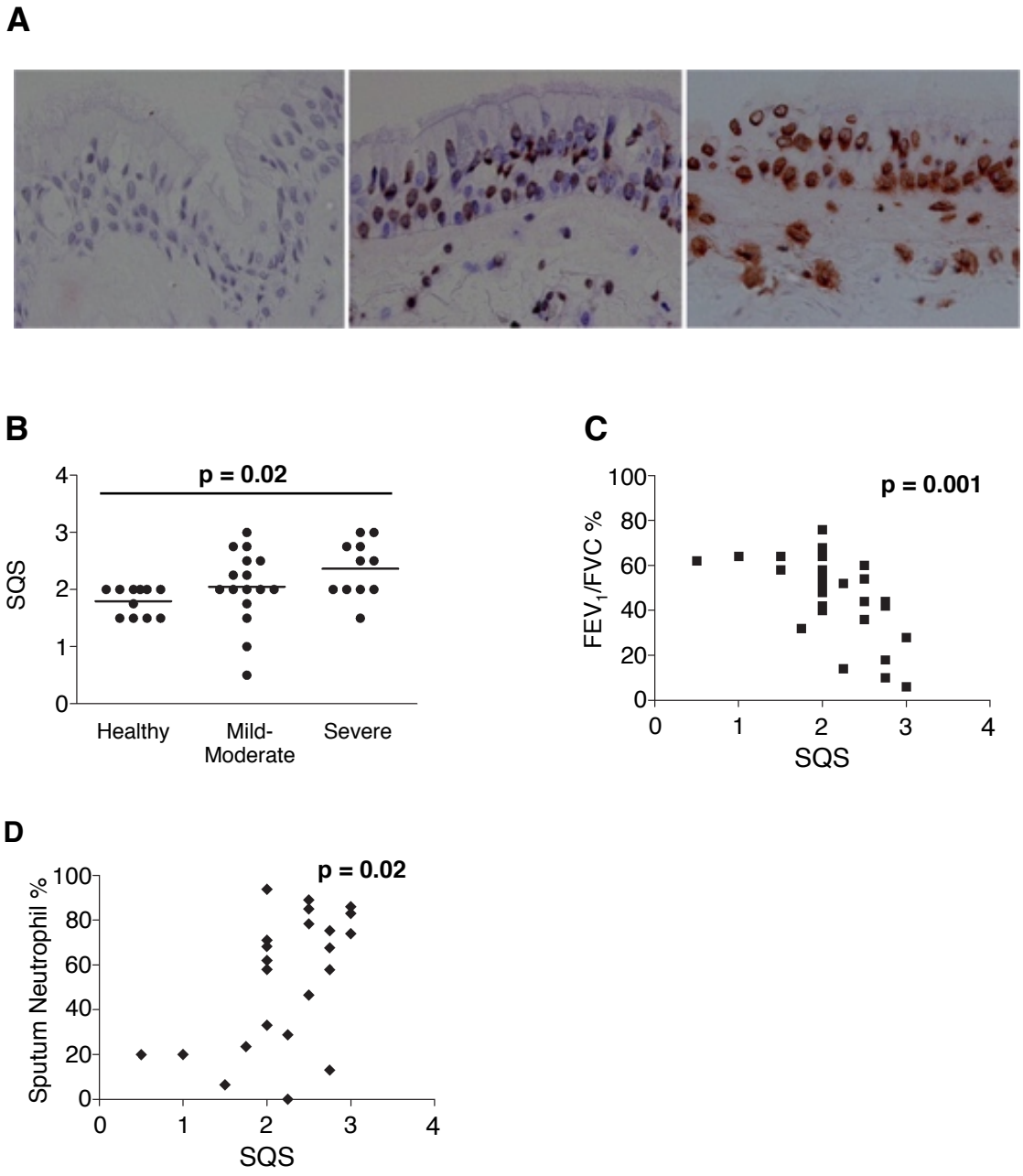

Figure 5.3 Epithelium positively stained with 8-oxo-7,8-dihydro- 2'-deoxyguanosine (8-oxo-dG) in asthmatic bronchial biopsies. Oxidative DNA damage in the asthmatic epithelium in human bronchial biopsies was indicated by the presence of 8-oxo-dG positive staining in brown. A shows GMA-embedded bronchial biopsies that were immuno-stained with isotype control (left) and 8-oxo-dG with medium intensity (middle) and high intensity (right). Semi-quantitative scoring (SQS) was used to assess 8-oxo-dG staining intensity. B shows the SQS across asthma severity. Data are expressed as mean. Statistical analysis was performed using the Kruskal-Wallis test, $p<0.05$.C and D show the correlation between 8-oxo-dG staining intensity and airflow obstruction (C), and sputum neutrophil count (D), respectively. Statistical analysis was performed using Spearman correlation, $p<0.05$.

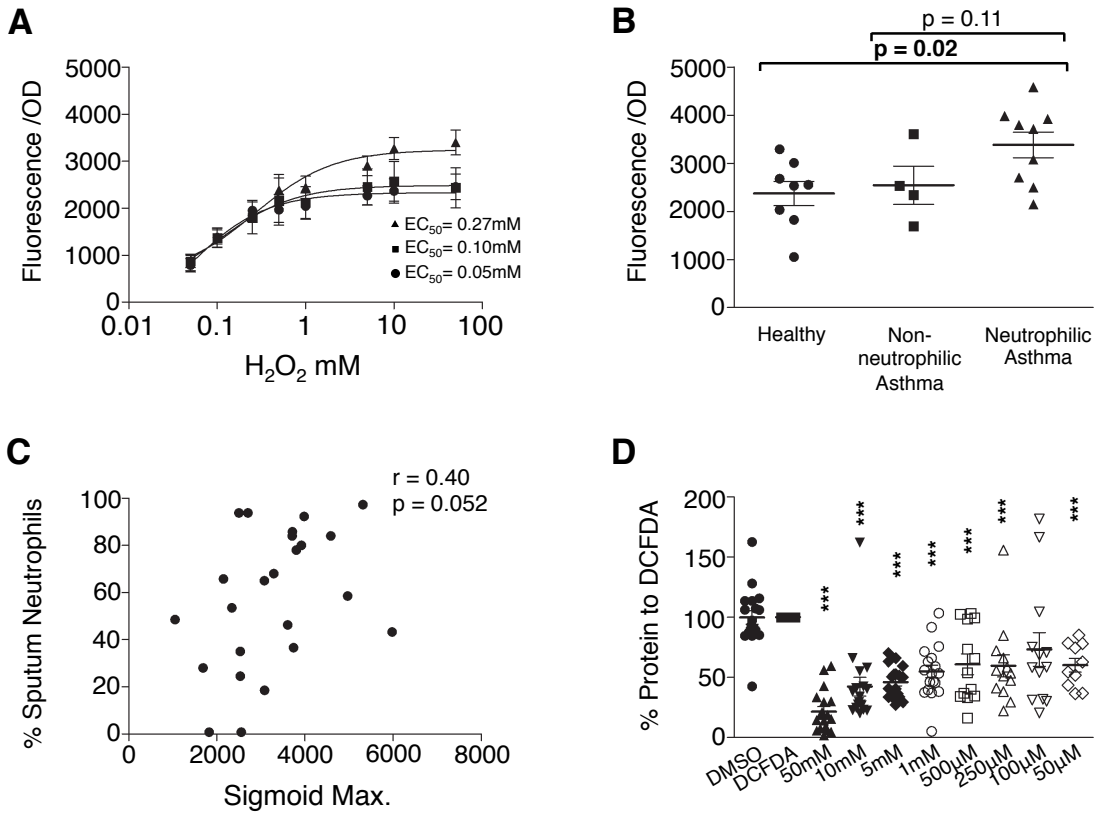

Figure 5.4 Intracellular reactive oxygen species (iROS) generation in response to hydrogen peroxide (H_2O_2) stimulation in HAEBC. To look at oxidative handling, HAEBC were stimulated by H_2O_2 ranging from 50 mM to 50 µM for 1 h. H_2O_2-induced iROS generation, reflected by the amount of fluorescence, was measured using the DCF-DA assay. Cells from healthy controls (n=8, dots), non-neutrophilic (n=4, squares) and neutrophilic (n=9, triangles) asthmatics were used for this experiment. Data are expressed as mean±SEM. A shows the dose response and EC_{50} of iROS generation in the epithelial basal cells upon H_2O_2 stimulation. B shows the fluorescence in response to the maximum dose of H_2O_2 (sigmoid max.). Statistical differences were assessed using unpaired t-tests. C shows the sigmoid maximum dose correlated to the % sputum neutrophils. Statistical analysis was performed using Spearman correlation, $p<0.05$. D shows the % of HAEBC protein level after H_2O_2 stimulation. Statistical differences were assessed using paired t-tests, *** = $p<0.05$ compared to DCF-DA controls.

5.4.2 NOX4 may be involved in the asthmatic oxidative stress

Despite the low sample size, the preliminary data of the microarrays from Chapter 3 identified NOX4 as one of the few genes that may be differentially expressed in asthmatic HAEBC, and were related to oxidative handling. At normal condition, NOX4 is likely to be involved in oxidative handling and was thus investigated further using protein and gene quantification. Because DNA damage and iROS mishandling in HAEBC were associated with the level of neutrophilic inflammation, the asthmatic group was subdivided into those with neutrophilic asthma and those with non-neutrophilic asthma.

NOX4 protein expression could not be quantified using Western Blot due to a technical issue. In spite of the clear and dense bands for NOX4 protein detected at the correct molecular weight in the HASMC samples using the Abcam antibody ab60940, in the epithelial samples it resulted in a number of non-specific bands in the low molecular weight region of the blot, but with none at 60 kDa corresponding to the molecular weight of NOX4. The experiment was repeated using another NOX4 antibody from Novus Biological (360, 448), but it gave a similar result. These bands were not likely to represent any NOX4 variants, whose the molecular weights range from 59 kDa to 64 kDa (309).

A.

Study	NOX4 gene expression (HAEBC)			
Clinical Details	**Healthy (n = 7)**	**Non-neutrophilic Asthmatic (n = 4)**	**Neutrophilic Asthmatic (n = 8)**	**1way-ANOVA p-values**
Gender (F)	5 (3)	1 (3)	6 (2)	0.25
Age, yr	45 (5)	51 (7)	58 (5)	0.26
Pack year	4 (3)	19 (16)	13 (7)	0.48
% Predicted FEV_1	101 (7)	58 (9)	86 (8)	**0.01**
% FEV_1/FVC	79 (3)	55 (5)	69 (5)	**0.02**
PC20 FEV_1, mg/ml †	>16	2.0 (0.0) ‡	3.3 (0.6-11.6) ‡	**0.02**
Blood Total IgE, kU/ml	76 (36)	60 (27)	116 (55)	0.69
Blood eosinophils, kU/ml	0.13 (0.03)	0.32 (0.09)	0.23 (0.06)	0.18
Treatment (mcg/24 BDP eqv.)	n/a	1533 (291)	967 (352)	n/a
Atopy, %	0	50	33	0.63
Age of Disease Onset, yr	n/a	32 (10)	32 (10)	n/a
Sputum Characterization				
Total cell count($x10^6$ cells/ml)	n/a	1.6 (1.0)	5.3 (1.7)	n/a
Eosinophils, % ‡	n/a	23.2 (2.5-48)	1.0 (0.0-2.9)	n/a
Neutrophils, % ‡	n/a	40 (35-54)	88 (72-93)	n/a
Macrophages, % ‡	n/a	39 (12-39)	7 (1-13)	n/a
Epithelial cells, % ‡	n/a	2.5 (0.0-2.8)	1.4 (0.6-4.4)	n/a

B.

Study	NOX4 gene expression (ALI)			
Clinical Details	**Healthy (n = 7)**	**Non-neutrophilic Asthmatic (n = 4)**	**Neutrophilic Asthmatic (n = 4)**	**1way-ANOVA p-values**
Gender (F)	4 (3)	3 (1)	3 (1)	0.77*
Age, yr	54 (7)	46 (10)	54 (7)	0.76
Pack year	8 (6)	0 (0)	8 (3)	0.47
% Predicted FEV_1	103 (4)	92 (7)	95 (7)	0.32
% FEV_1/FVC	80 (2)	71 (5)	65 (2)	**0.01**
PC20 FEV_1, mg/ml †	>16	2.1 (1-16) ‡	7.2 (0.8-16) ‡	0.08
Blood Total IgE, kU/ml	140 (114)	109 (79)	162 (90)	0.94
Blood eosinophils, kU/ml	0.11 (0.02)	0.77 (0.29)	0.27 (0.08)	**0.01**
Treatment (mcg/24 BDP eqv.)	n/a	700 (473)	850 (435)	n/a
Atopy, %	2 (3)	3 (1)	1 (3)	0.34*
Age of Disease Onset, yr	n/a	45 (9)	30 (13)	n/a
Sputum Characterization				
Total cell count($x10^6$ cells/ml)	n/a	2.6 (0.5)	2.0 (1.0)	n/a
Eosinophils, % ‡	n/a	10 (7-27)	0 (0)	n/a
Neutrophils, % ‡	n/a	37 (32-60)	94 (91-96)	n/a
Macrophages, % ‡	n/a	55 (12-56)	2 (0.3-4.1)	n/a
Epithelial cells, % ‡	n/a	1.0 (1.0-1.0)	0.9 (0.8-1.6)	n/a

† geometric mean (95% CI) ‡ median (inter-quartile range); * Chi square test $p<0.05$.

Table 5.4 Clinical details of the subjects in the NOX4 gene expression experiment. Data are expressed as mean±SEM unless otherwise indicated. Statistical differences were assessed using unpaired t-tests, and considered to be significant when $p<0.05$ unless otherwise indicated.

In comparison, NOX4 gene expression could be detected and quantified using RT-qPCR. HAEBC from 8 healthy controls and 13 asthmatics (4 non-neutrophilic, 8 neutrophilic) (**Table 5.4**A), and ALI cultures from 7 healthy controls and 8 asthmatics (4 non-neutrophilic, 4 neutrophilic) (**Table 5.4**B), were used. The C(t) value of the gene of interest was normalised with the corresponding C(t) value of the housekeeping gene, followed by a second normalisation with a reference healthy sample used across different qPCR runs. Because of relative quantity of NOX4 was not normally distributed, the data was transformed into $\log_2$ scale. Statistical analyses were performed after the normalisation and transformation.

An efficiency curve was first performed using a healthy HAEBC sample. The efficiency was 94.9% using cDNA ranging from 1 ng to 50 ng (**Figure 5.5**A). The amount of cDNA used in subsequent reactions for both HAEBC and ALI cultures was therefore chosen at 10ng/reaction. The efficiency curve for 18S was performed using an input material ranging from 0.001 ng to 10 ng, and the result can be found in **Figure 5.8**B. It was not repeated using a higher range of input material as for NOX4 because the high 18S expression in the cells limits the input cDNA quantity to 1ng/reaction. A quantity higher than 1ng/reaction is likely to push the C(t) values of 18S closer to 1, and thus it may arise unreliable results. The amplification curves showed low threshold cycle (C(t)) values for 18S rRNA and higher C(t) values for NOX4 (**Figure 5.5**B). The C(t) values for NOX4 were high for HAEBC samples and were even higher for some ALI cultures. The melting curves of the HAEBC samples gave clear single peaks (**Figure 5.5**C). Among the ALI samples, some of the melting curves contained double-peaks (**Figure 5.5**D). These double-peaks could be caused by 1) RNA/cDNA contamination, and 2) primer dimerization due to a low RNA input. The latter one was more likely to be the

cause since all the RNA samples had the A260/A280 ratios at ~2, were always handled below 4°C, and have undergone minimal re-freezing steps. The apparatus and materials were also kept sterile throughout the process. Therefore, sample contamination and degradation were not likely to be the cause. A second efficiency curve was performed using a healthy ALI sample as the reference. The efficiency was 95.2 % using cDNA ranging from 10 ng to 100 ng/reaction (**Figure 5.5**E). The amount of cDNA used in subsequent reactions was therefore chosen at 20 ng/reaction for ALI cultures. The improvement in the shape of the melting curve supported the use of a higher cDNA quantity (**Figure 5.5**F). The amount of cDNA used for HAEBC samples was also increased to prevent any potential primer dimerisation. The available HAEBC samples allowed an increase to 25 ng/reaction.

NOX4 gene expression has been found significantly higher in the asthma neutrophilic subgroup compared to healthy controls, but was only in the differentiated epithelial cells and not in the undifferentiated basal cells (HAEBC). In the HAEBC, the relative quantity (RQ) of NOX4 RNA in the neutrophilic asthmatics (n=8, 1.5±1.1 RQ) was not significantly different from the RQ in healthy controls (n=8, 0.00±0.6 RQ, p=0.51), but was significantly higher than the RQ in the non-neutrophilic asthmatics (n=4, -1.5±0.03 RQ, p=0.046) (**Figure 5.6**A). The NOX4 RNA expression level among the neutrophilic asthma subgroup was more variable. This result is in coherence with the microarray result in Chapter 3: 1) there was no significant difference in the level of NOX4 gene expression between healthy and asthmatic HAEBC, and 2) NOX4 gene expression was not seen in healthy HAEBC, but was seen in some but not all asthmatic HAEBC. In comparison, ALI cultures developed from neutrophilic asthmatics expressed significantly higher NOX4 RNA (n=4, 2.1±0.5 RQ) compared to healthy controls (n=7,

0.0±0.3, mean difference [95% CI] 2.1 [0.8 to 3.3] RQ, p=0.02), but this was not significantly higher than the non-neutrophilic asthmatics (n=4, -0.4±0.5 RQ, p=0.06) (**Figure 5.6**B). Similar to the oxidative DNA damage shown by the 8-oxo-dG staining (**Figure 5.3**), this NOX4 RNA expression in ALI cultures was correlated to airflow obstruction (r=0.54, p=0.04) (**Figure 5.6**C). The consistent 18S expression level in HAEBC and ALI cultures in both subject groups confirmed the suitability of its use as a housekeeping gene (**Figure 5.6**D). The low sample size among the asthmatic subgroups may have reduced the power of the effect, thus this result should be treated as a preliminary data. Despite the high RNA input quantity (20ng/reaction) and the high C(t) values (~33) obtained for NOX4 gene expression, these factors are unlikely to have affected the reliability of the results presented here because 1) the maximum C(t) value allowed here was the number of amplification cycles, 37 cycles (449), and 2) increasing the amount of cDNA used in the reactions improved the quality of the qPCR performance (**Figure 5.5**). Agarose gel electrophoresis also confirmed the efficiency of the reaction and the purity of the target products (**Figure 5.6**E). The smear of one ALI culture sample, as shown on Lane 6, may suggest RNA degradation; the initial RNA quantity of this sample was pure but low. This sample was excluded from the analysis. Very fade bands could be seen towards the bottom of the gel. It is likely to be due to the colour of the dye. Clear bands can be seen in the RT negative controls of 18S qPCR products. It is likely to be due to the high level of this housekeeping gene present in the RNA samples. This gene was replicated extensively over the qPCR cycles and was picked up towards the end of the amplification. This however cannot be regarded as a fault positive.

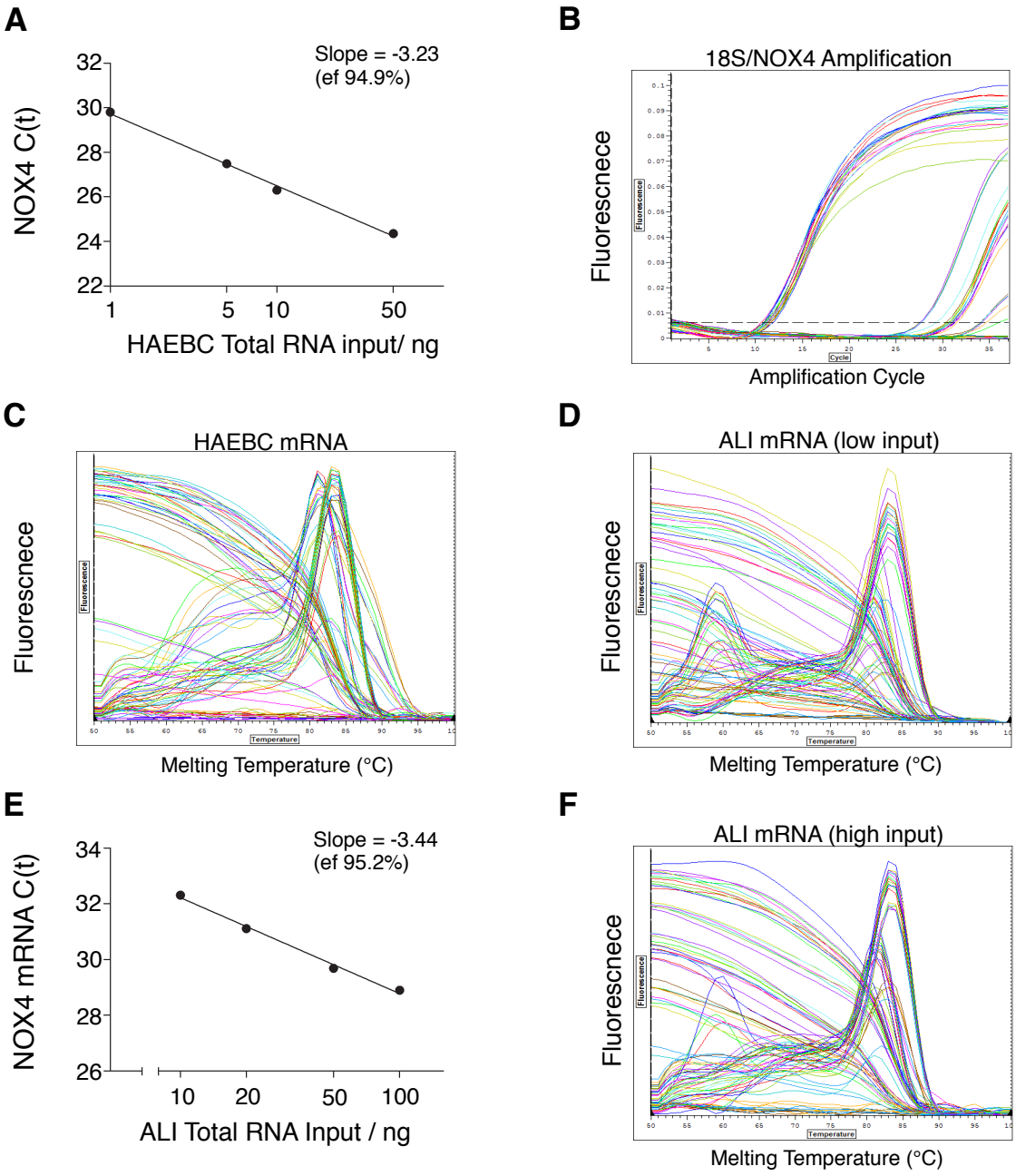

Figure 5.5 **RT-qPCR optimisation for NOX4 gene expression.** RT-qPCR quality control and repeatability were measured by looking at efficiency curves, amplification curves and qPCR product melting curves. A shows the efficiency curve for NOX4 using a healthy HAEBC sample as the reference. B shows the amplification curves of 18S rRNA (left group) and NOX4 (right group) qPCR using 10ng RNA. C and D show the melting curves of 18S rRNA (~82°C) and NOX4 (~84°C) of HAEBC and ALI culture samples respectively. E shows the efficiency curve for NOX4 using an ALI culture as the reference. F shows the improved melting curves of ALI cultures using 20 ng RNA.

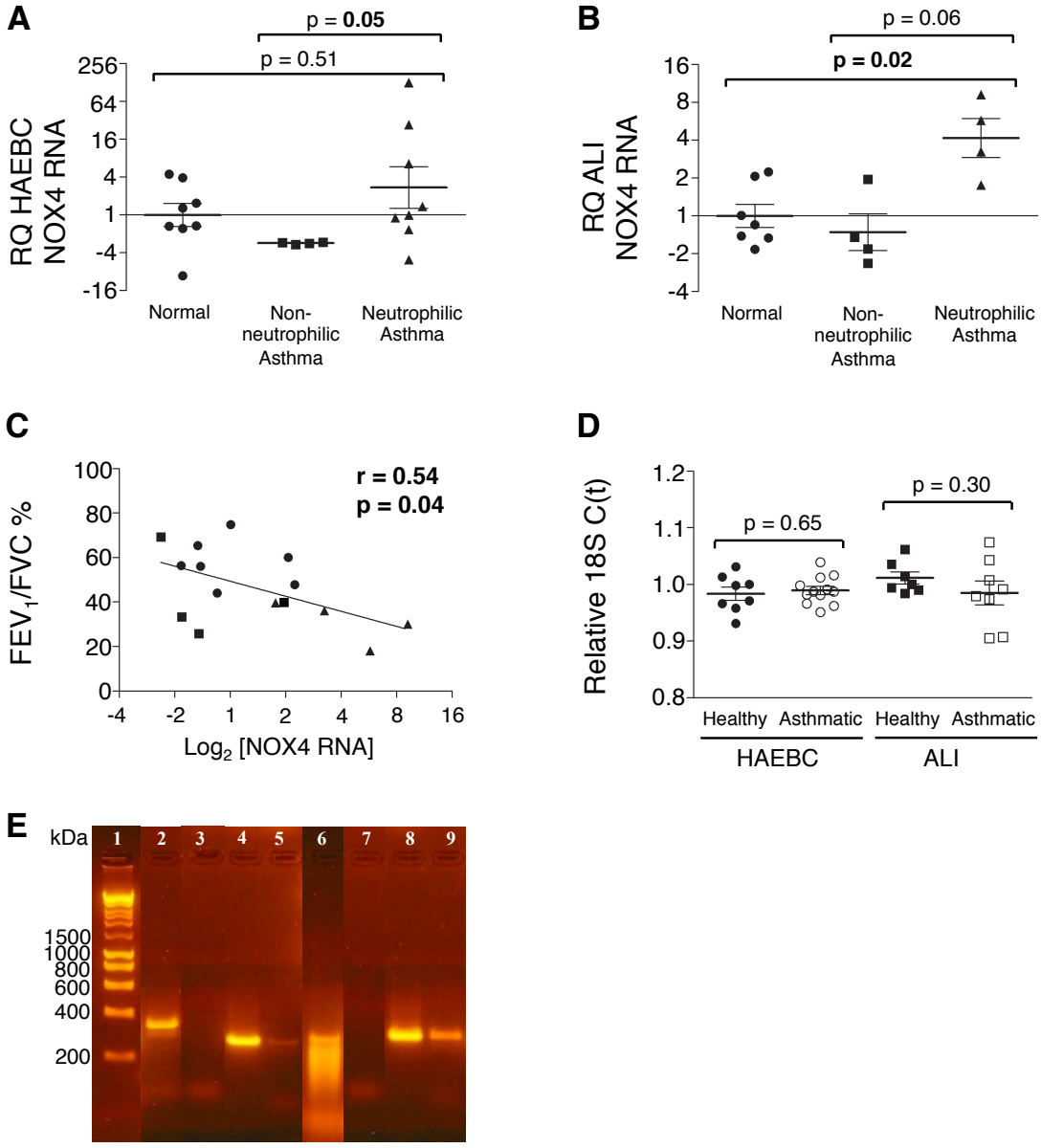

Figure 5.6 **NOX4 gene expression in airway epithelial cells assessed by RT-qPCR.** NOX4 gene expression was quantified in HAEBC (dots), non-neutrophilic asthmatics (square) and neutrophilic asthmatics (triangle), using RT-qPCR. Data are expressed as relative quantity (RQ) mean±SEM. A shows the NOX4 gene expression measured in HABEC from healthy controls (n=8), non-neutrophilic (n=4) and neutrophilic (n=8) asthma subgroups. B shows the expression in ALI cultures from healthy controls (n=7), non-neutrophilic (n=4) and neutrophilic (n=4) asthma subgroups. Statistical differences were assessed using Mann Whitney U tests, $p<0.05$, compared to healthy controls. C shows the correlation between NOX4 gene expression and airflow obstruction (% FEV_1/FVC). Statistically differences were assessed using Spearman correlation, $p<0.05$. D shows the 18S mRNA expression relative to the reference healthy sample of HAEBC and ALI culture. E shows the products from NOX4 qPCR, with molecular weight marker (1), HAEBC NOX4 (2) and its negative control (3), HAEBC18S (4) and its negative control (5), ALI culture NOX4 (6) and its negative control (7), ALI culture 18S (8) and its negative control (9).

5.4.3 SOD2 is not likely to be involved in the asthmatic epithelial oxidative stress

SOD2 is an antioxidant located in the mitochondria, which is responsible for dismutating $O_2^{\bullet-}$ to H_2O_2. Despite the fact that SOD2 was not identified as differentially expressed in the microarrays in Chapter, its gene and protein expression in airway epithelial cells were assessed using the same approaches as for the NOX4 expression, as it may work in concert with NOX4 within the mitochondrial compartment (306, 307) to regulate the intracellular oxidative balance.

Clinical Details	Healthy (n = 11)	Non-neutrophilic asthmatic (n=4)	Neutrophilic Asthmatic (n = 8)	One-way ANOVA p-values
Gender (F)	8 (4)	2 (2)	6 (2)	0.69*
Age, yr	45 (4)	43 (11)	62 (5)	0.06
Pack year	5 (3)	17 (17)	19 (7)	0.25
% Predicted FEV_1	103 (5)	72 (11)	82 (6)	**0.01**
% FEV_1/FVC	79 (2)	65 (8)	66 (6)	**0.06**
PC20 FEV_1, mg/ml ‡	>16	2.1 (2.0-2.1)	7.2 (0.5-16)	n/a
Blood Total IgE, kU/ml	39 (21)	34 (4)	99 (57)	0.47
Blood eosinophils, kU/ml	0.16 (0.02)	0.42 (0.13)	0.38 (0.15)	0.16
Treatment (mcg/24 BDP eqv.)	n/a	1000 (577)	767 (285)	n/a
Atopy, %	50	50	20	0.64*
Age of Disease Onset, yr	n/a	26 (10)	34 (8)	n/a
Sputum Characterization				
Total cell count($x10^6$ cells/ml)	n/a	2.0 (1.0)	4.0 (1.9)	n/a
Eosinophils, % ‡	n/a	10 (2.5-48)	0 (0.0-1.6)	n/a
Neutrophils, % ‡	n/a	40 (32-54)	91 (84-94)	n/a
Macrophages, % ‡	n/a	39 (12-56)	5 (2-13)	n/a
Epithelial cells, % ‡	n/a	1.0 (0.0-4.8)	0.9 (0.6-4.2)	n/a

† geometric mean (95% CI) ‡ median (inter-quartile range); * Chi square test p<0.05.

Table 5.5 Clinical details of the subjects in the SOD2 expression experiment. Data are expressed as mean±SEM unless otherwise indicated. Statistical differences were assessed using One-way ANOVA, $p<0.05$, unless otherwise indicated.

A total of 11 healthy controls and 12 asthmatics (4 non-neutrophilic asthmatics, 8 neutrophilic asthmatics) were used for this experiment (**Table 5.5**). Using Western Blot, SOD2 protein expression was detected in both ALI cultures and HAEBC, and in both health (lanes 1) and asthma (lanes 2) (**Figure 5.7**A). The intensity of the bands were

measured using densitometry; the values of SOD2 were normalised with values the corresponding β-actin and presented as relative quantity (RQ). Mann-Whitney U test was performed after the normalisation to compare different subject groups. There was no difference in the SOD2 protein expression in HAEBC derived from healthy controls (n=8, 1.7±0.5 RQ), non-neutrophilic asthmatics (n=3, 1.2±0.2 RQ), and neutrophilic asthma (n=4, 1.7±0.5 RQ) (**Figure 5.7**B). There was also no significant difference in SOD2 expression in ALI cultures derived from healthy controls (n=3, 0.9±0.1 RQ) and neutrophilic asthmatic (n=3, 1.0±0.1 RQ) (**Figure 5.7**C). There were no non-neutrophilic asthmatic ALI cultures available at the time of this study. Although in ALI cultures only n=3 was done in each subject group, the expression levels were very similar among the samples within each group. Therefore no repeats were performed.

Meanwhile, SOD2 gene expression was quantified using RT-qPCR. Efficiency curves for SOD2 and 18S were first performed using a HAEBC sample. The efficiency was 104.6 % for SOD2 using input material ranging from 0.01 ng to 10 ng per reaction (**Figure 5.8**A), and was 98.3 % for 18S rRNA using input material ranging from 0.001ng to 10ng per reaction (**Figure 5.8**B). 1 ng RNA was therefore chosen as the input quantity per reaction. Similar to the NOX4 expression, the amplification curves showed two distinct populations (**Figure 5.8**C). The two distinct peaks of the melting curves for both genes reflected on the purity of the qPCR products and the efficiency of the reactions (**Figure 5.8**D). The relative quantity of SOD2 in relation to 18S rRNA expression was calculated followed by further normalisation using a reference healthy sample that was used across all qPCR runs. Mann-Whitney U test was then performed after the normalisations. The result showed that there was no significant difference in SOD2 gene expression between healthy controls, non-neutrophilic and neutrophilic

asthmatic subgroups in HABEC (**Figure 5.8**E) and in ALI cultures (**Figure 5.8**F). The limited ALI culture supply at the time restricted the sample size and thus no further repeats could be done. Therefore these results should be treated as preliminary data, and further repeats should be done to confirm this finding. All samples expressed a similar level of 18S rRNA (**Figure 5.8**G). The efficiency of the qPCR, and the purity of the qPCR products, was further confirmed by agarose gel electrophoresis (**Figure 5.8**H). It is noteworthy that the very faint band present in the 18S rRNA negative control (lane 5) was due to the excessive qPCR product obtained at the end of the amplification cycle, and was in keeping with its C(t) value approaching the maximum number of amplification cycle (37 cycles). This is a common phenomenon with housekeeping genes and thus was not classified as a contamination. Very fade bands could be seen towards the bottom of the gel, and are likely to be due to the colour of the dye. Some smear could be seen with ALI culture SOD2 positive samples. It was more likely to be due to the degradation of the qPCR product rather than a contamination since the melting curve of each sample was clean (**Figure 5.8**D).

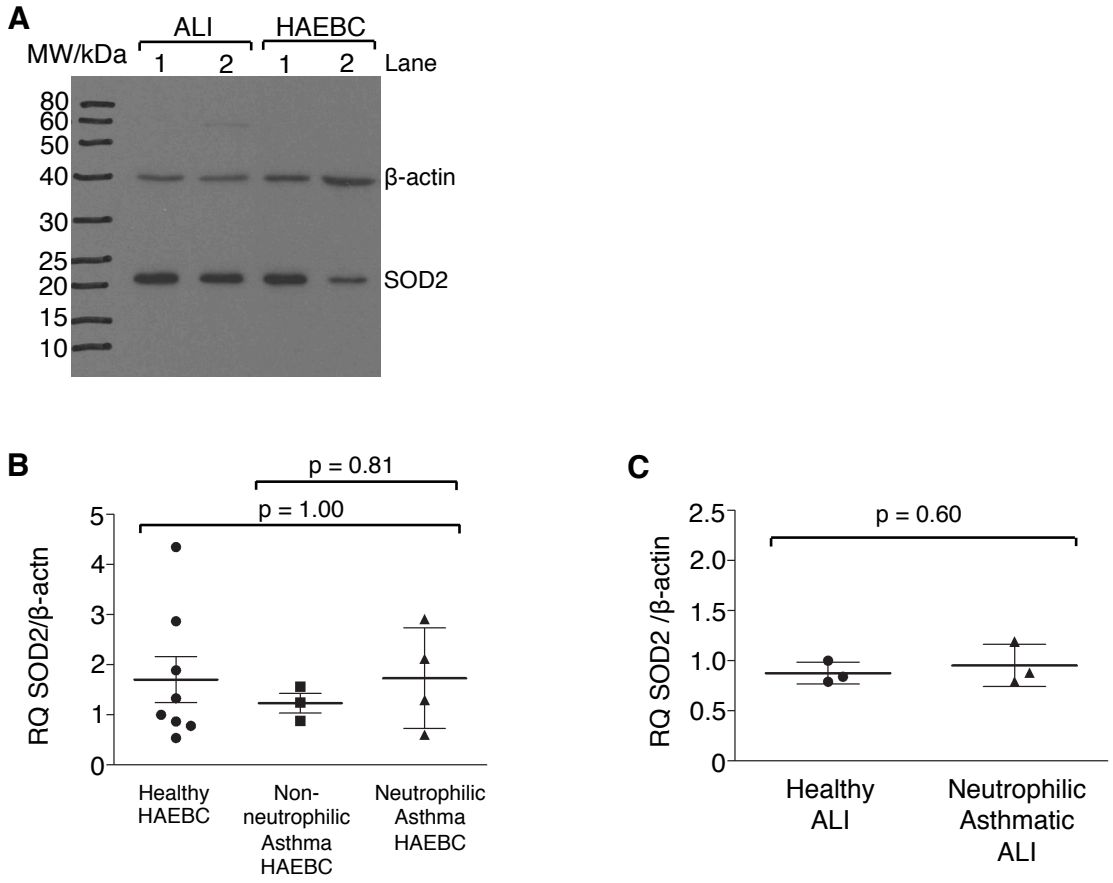

Figure 5.7 SOD2 protein expression in airway epithelial cells. Expression of SOD2 protein (25 kDa) and reference protein β-actin (42 kDa) were assessed by Western Blot. A shows that SOD2 protein was detectable using the Western blot approach, and was present in both healthy (1) and asthmatic (2) ALI cultures and HAEBC. The intensity of the bands was quantified using densitometry and the software ImageJ. Data are expressed as mean±SEM relative quantity (RQ) to housekeeping protein β-actin. B shows the SOD2 protein expression in HAEBC from healthy controls (n=8, dots) and non-neutrophilic (n=3, squares) and neutrophilic (n=4, triangles) asthma subgroups. C shows the SOD2 expression in ALI cultures from healthy controls (n=3) and neutrophilic asthma subgroup (n=3). Statistical differences were assessed using Mann-Whitney U tests, $p<0.05$.

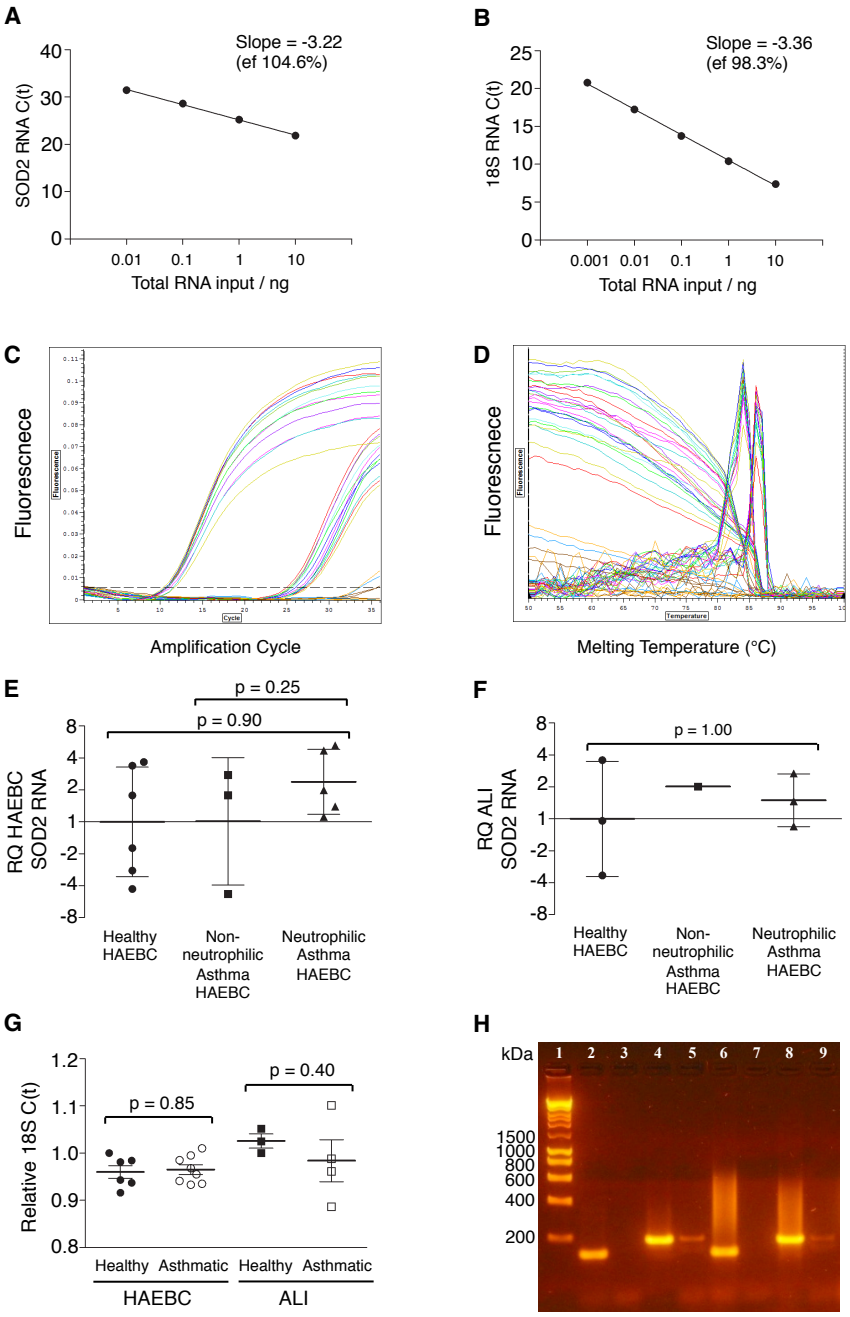

Figure 5.8 SOD2 gene expression in airway epithelial cells assessed by RT-qPCR. RT-qPCR quality control and repeatability were measured by looking at efficiency curves, amplification curves and qPCR product melting curves. A and B show the efficiency curve for SOD2 and 18S using a healthy HAEBC sample as the reference. C shows the amplification curves of 18S rRNA (left group) and SOD2 (right group) qPCRs using 1ng cDNA/reaction. D shows the melting curves of 18S rRNA (~82°C) and SOD2 (~87°C). SOD2 gene expression was quantified in HAEBC and ALI cultures. Data are expressed as relative quantity (RQ) mean±SEM. E shows the SOD2 gene expression measured in HAEBC as healthy controls (n=6, dots), non-neutrophilic asthmatics (n=3, squares) and neutrophilic asthmatics (n=5, triangles), using RT-qPCR. F shows the SOD2 gene expression measured in ALI cultures from healthy controls (n=3, dots), non-neutrophilic asthmatics (n=1, squares) and neutrophilic asthmatics (n=3, triangles). Statistical differences were assessed using Mann Whitney U tests, $p<0.05$, compared with healthy controls. G shows the 18S rRNA expression relative to the reference healthy sample of HAEBC and ALI culture. H shows the products from SOD2 qPCR, with molecular weight marker (1), HAEBC SOD2 (2) and its negative control (3), HAEBC 18S (4) and its negative control (5), ALI culture SOD2 (6) and its negative control (7), ALI 18S (8) and its negative control (9).

5.4.4 NOX4 inhibition using GKT137831 reduced intracellular ROS generation in HAEBC without affecting cell viability

The preliminary data on NOX4 gene expression in ALI cultures suggested that NOX4 might be involved in the abnormal oxidative pathway in asthma. To see if NOX4 plays a role in asthmatic epithelial cell ciliary dysfunction, NOX4 activity was inhibited using GKT137831, a NOX1/NOX4 specific inhibitor developed by GenKyoTex, Switzerland (320). With reference to past studies done by GenKyoTex and collaborators, GKT137831 at 20 μM, 5 μM and 1 μM were used as the starting concentrations for the experiments on airway epithelial cells.

Clinical Details	Healthy (n = 3)	Non-neutrophilic Asthmatic (n=3)	Neutrophilic Asthmatic (n = 3)	One-way ANOVA p-values
Gender (F)	2 (1)	2 (1)	2 (1)	1.0*
Age, yr	43 (10)	56 (5)	57 (5)	0.35
Pack year	7 (7)	3 (3)	10 (3)	0.57
% Predicted FEV_1	101 (3)	74 (18)	89 (6)	0.30
% FEV_1/FVC	85 (5)	56 (9)	68 (6)	0.07
PC20 FEV_1, mg/ml †	n/a	n/a	n/a	n/a
Blood Total IgE, kU/ml	n/a	112 (25)	178 (128)	n/a
Blood eosinophils, kU/ml	0.13 (0.04)	0.30 (0.16)	0.31 (0.08)	0.46
Treatment (mcg/24 BDP eqv.)	n/a	1533 (291)	600 (200)	n/a
Atopy, %	0	33	100	0.15*
Age of Disease Onset, yr	n/a	45 (6)	42 (2)	n/a
Sputum Characterization				
Total cell count($x10^6$ cells/ml)	n/a	3.9 (1.6)	1.1 (0.7)	n/a
Eosinophils, % ‡	n/a	23 (7.3-23.5)	0 (0.0-1.75)	n/a
Neutrophils, % ‡	n/a	46 (35-65)	94 (84-94)	n/a
Macrophages, % ‡	n/a	12 (10-39)	4.4 (0.4-14)	n/a
Epithelial cells, % ‡	n/a	2.5 (2.0-35)	0.8 (0.0-8.8)	n/a

† Geometric mean (95% CI) ‡ median (inter-quartile range); * Chi square p<0.05.

Table 5.6 Clinical details of the subjects in the DCF-DA assay experiments testing the effect of NOX4i. Data are expressed as mean±SEM unless otherwise indicated. Statistical differences were assessed using One-way ANOVA, $p<0.05$, unless otherwise indicated.

HAEBC from 3 healthy controls and 6 asthmatics (3 non-neutrophilic and 3 neutrophilic) were used this experiment (**Table 5.6**). The asthmatic group was split into

neutrophilic and non-neutrophilic subgroups because DNA damage and high NOX4 expression were predominantly found in the neutrophilic subgroup.

At an un-stimulated level, with GKT137831 at 5 μM and 1 μM there was a small but significantly reduction in iROS generation a 4 h time course (One-way ANOVA, p=0.02 and p=0.002 respectively) (**Figure 5.9**A). There was no concentration-dependent difference between 20 μM and 5 μM. NAC (5 mM) was used as the positive control of GKT137831 due to its antioxidant activity. It also significantly reduced the baseline iROS generation (p=0.002). GKT137831 at 20 μM did not give any significant time-dependent effect compared to other GKT137831 concentrations, suggesting it could be regarded as the maximum dose of this compound. This is in line with other GenKyoTex *in vitro* studies in which GKT137831 at 20 μM was used as the maximum dose. Assessment of protein levels with the Coomassie Bradford assay showed that when compared to baseline, the protein levels were reduced slightly after 4 h, but not after 1 h (**Figure 5.9**B). A 1 h time course was therefore chosen for the next stage of the experiment. Whilst it was shown in Section 5.4.1 that the Coomassie Bradford assay might not truly reflect the viability of the adherent cells after the DCF-DA assays, trypan blue cell counts were performed on these adherent cells to confirm that they were alive. 3 asthmatic samples were used for this preliminary evaluation. **Figure 5.9**C shows a sample picture of the stained adherent HAEBC, with healthy cells that were negatively stained, dead cells that were positively stained, and cells that were negatively stained but with abnormal morphology. Abnormal cell morphology is regarded as squamous, non-cobblestone shaped or with disturbed and/or blebbing surface membrane. The total cell count showed no difference across different GKT137831 concentrations, NAC, and the corresponding diluents (**Figure 5.9**D). The differential viable cell count

also showed that none of these reagents caused any significant cell death compared to the DCF-DA control at 0.5 h (**Figure 5.9**E) and 1 h (**Figure 5.9**F).

Having established the maximal dose of GKT137831 to be 20 μM and the optimum time points to be the 0.5 h and 1 h incubation, these conditions were used for the rest of the experiments. To test the potential role of NOX4 in H_2O_2-induced iROS generation, HAEBC (n=9) were incubated for 0.5 to 1 h with a cocktail containing 20 μM GKT137831 plus 10 mM or 1 mM H_2O_2. The presence of GKT137831 significantly reduced the 10mM H_2O_2 induced iROS generation at 0.5 h (mean difference [95% CI] 947 [718 to 1176] OD, p<0.0001) and at 1 h (1159 [922 to 1396] OD, p<0.0001) (**Figure 5.10**A). GKT137831 showed a similar and significant effect on the cells stimulated with 1 mM H_2O_2 (**Figure 5.10**B). NAC at 5 mM reduced iROS upon stimulation using 10 mM H_2O_2 (mean difference [95% CI] 896 [700 to 1091] OD, p<0.0001) (**Figure 5.10**A) and 1 mM H_2O_2 (983 [757 to 1209] OD, p<0.0001) (**Figure 5.10**B). Its inhibitory effect on iROS generation was comparable to the effect of GKT137831 at 20 μM. The H_2O_2-induced iROS was generally higher in the asthmatic samples, but was not significantly different from that of healthy controls (**Figure 5.10**C). This might be explained by the higher iROS generated in these cells in response to H_2O_2 (

Figure 5.4). The effect of GKT137831 and NAC on the H_2O_2-induced iROS reduction over time was further illustrated by looking at the AUC (**Figure 5.10**D). There was no significant difference in AUC between healthy controls (n=3), non-neutrophilic (n=3) and neutrophilic asthmatics (n=3) in any individual stimulation condition. NAC at 5 mM was generally used as the maximum effective dose in the literature (450, 451). Interestingly, the inhibition on H_2O_2-induced iROS generation at 1 h seemed to be more effective using 20 μM GKT137831 compared to 5 mM NAC (**Figure 5.10**E). However the small sample size restricted the power of the statistical analysis. These results should therefore be regarded as preliminary data. Nevertheless, it would be difficult to directly compare their effects without looking into their pharmacokinetics.

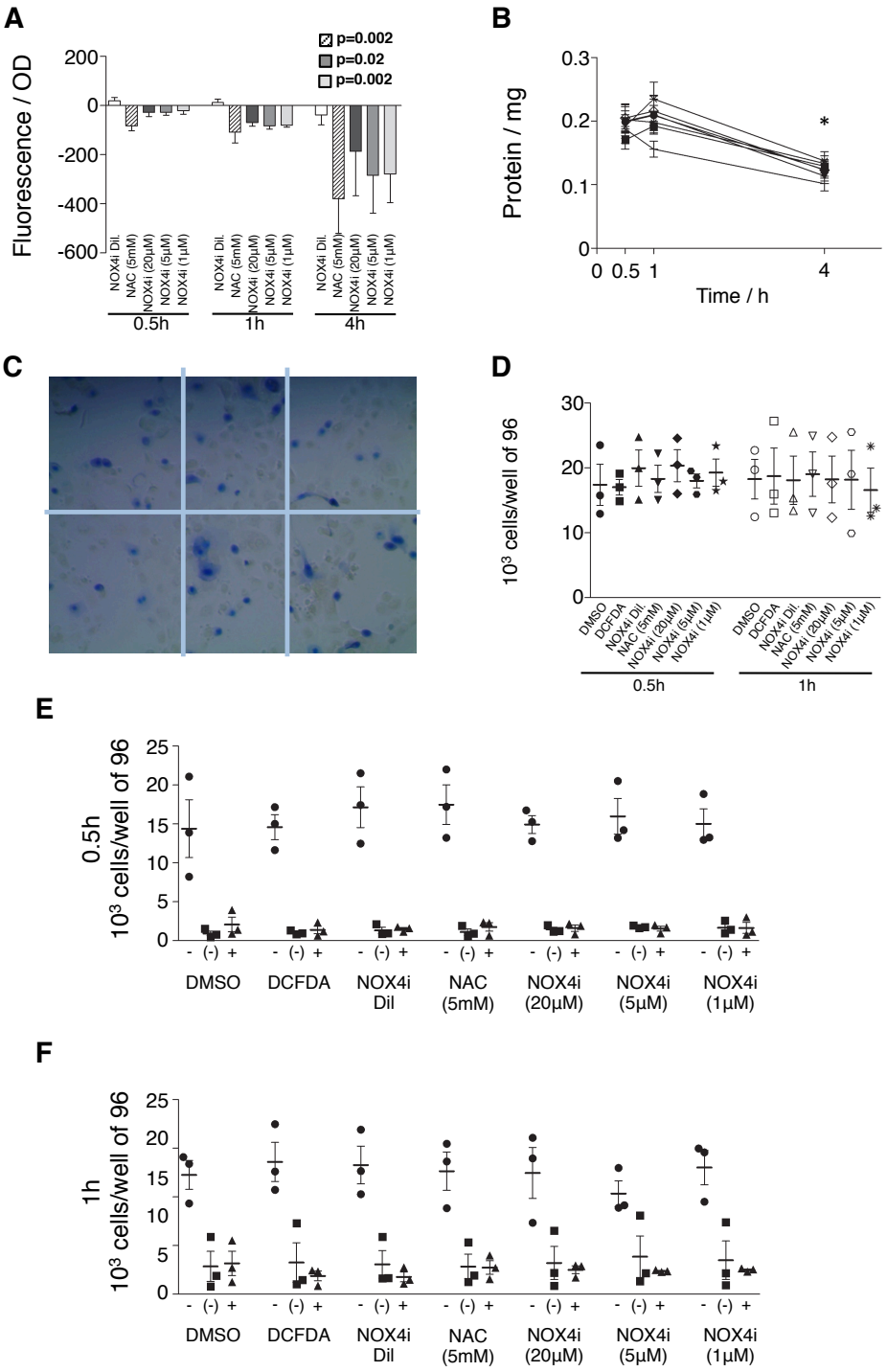

Figure 5.9 Effect of NOX4 inhibition on iROS generation and cell viability in HAEBC at baseline. NOX4 protein in HAEBC (n=9) was inhibited using NOX1/NOX4 duo inhibitor GKT137831 (NOX4i). Its effect on iROS generation (A) and protein level (B) were observed over a 4 h incubation period. Statistical differences were assessed using Tukey post-test, $p<0.05$, compared with time 0. The effect of GKT137831 on cell viability was also assessed using trypan blue viable cell count on adherent cells. C shows a sample picture of trypan blue stained-adherent HAEBC. D shows the total number of cells per one well of a 96 well plate after 0.5 h and 1 h GKT137831 incubation. Cells were categorised as negatively stained cells (-, expressed in dots), positively stained cells but with abnormal morphology ((-), expressed in squares) and positively stained cells (+, expressed in triangles). E and F show the viable cell count at 0.5 h and 1 h respectively.

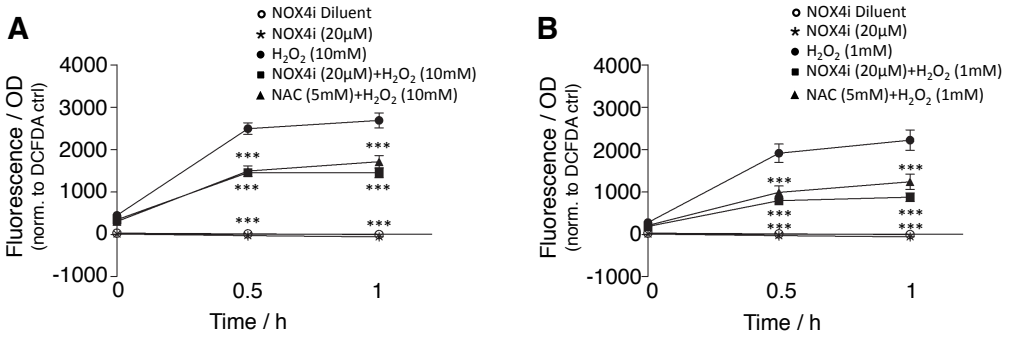

C.

Mean±SEM	0.5 h			1 h		
	Health (n=3)	Asthma (n=6)	p-value	Health (n=3)	Asthma (n=6)	p-value
NOX4i (20 μM) + 10 mM H_2O_2	1213±141	1540±135	0.18	1129±142	1588±170	0.13
NAC (5 mM) + 10 mM H_2O_2	1347±170	1640±207	0.39	1565±217	1906±221	0.37
NOX4i (20 μM) + 1 mM H_2O_2	593±33	888±113	0.12	596±64	983±136	0.10
NAC (5 mM) + 1 mM H_2O_2	784±177	1125±260	0.42	915±172	1429±261	0.24

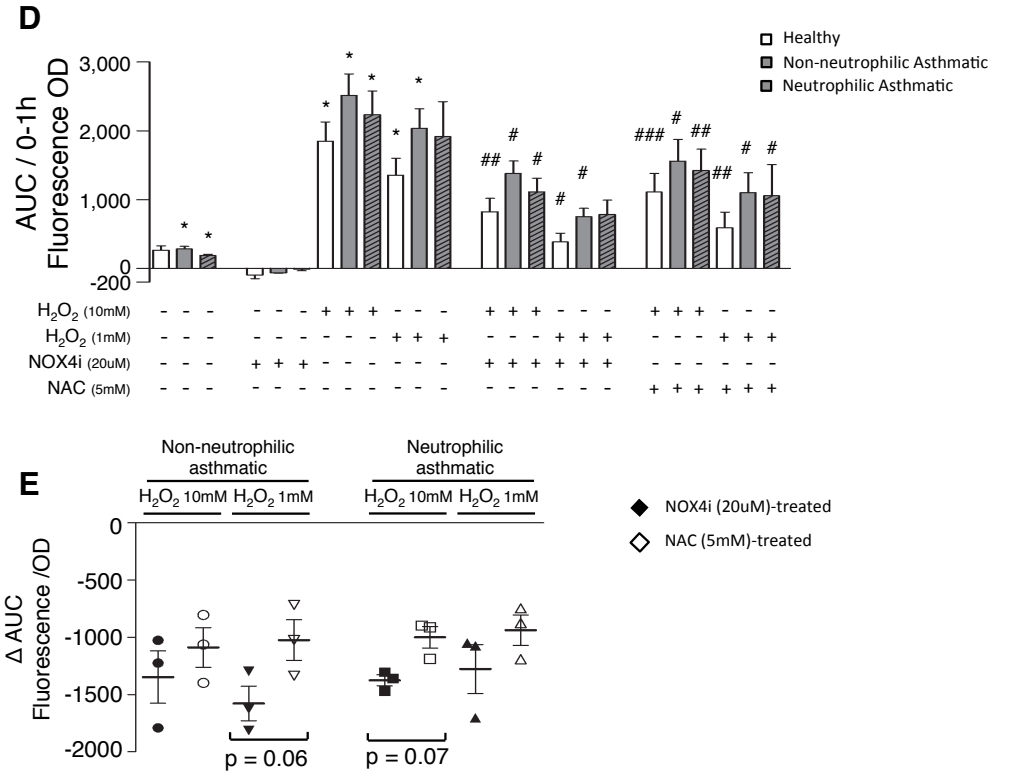

Figure 5.10 The effect of NOX4 inhibition on H_2O_2-induced iROS generation. The effect of NOX4 inhibition using NOX1/NOX4 duo inhibitor GKT137831 (NOX4i) on the oxidative handling of HAEBC (n=9) was investigated. Data are expressed as mean±SEM. H_2O_2 at 10 mM (A) and 1 mM (B) were used to stimulate iROS production. Statistical differences were assessed using paired t-tests, *** = $p<0.001$, compared with H_2O_2 stimulation. C compares the absolute fluorescence values (OD) between healthy (n=3) and asthmatic (n=6) HAEBC. Statistical differences were assessed using unpaired t-tests, $p<0.05$. D shows the area under curves (AUC) of A and B, but expressed as healthy (n=3), and non-neutrophilic (n=3) and neutrophilic (n=3) asthma subgroups. Statistical differences were assessed using paired t-tests, * = $p<0.05$ compared with GKT137831 alone, # = $p<0.05$; ## = $p<0.01$; ### = $p<0.001$ compared with H_2O_2 stimulation alone. E shows the absolute reduction in AUC fluorescence (subtracted from H_2O_2 stimulation-only group) upon GKT137831 or NAC treatment among the asthmatic subgroups. Statistical analysis was performed using paired t-tests.

5.4.5 NOX4 inhibition using GKT137831 improved ciliary dysfunction in fresh asthmatic epithelial cells

To further explore the role of oxidative stress, and potentially NOX4, in epithelial function, fresh epithelial cell strips from asthmatic human airways were obtained by bronchial brushes and used for NOX4 inhibition using GKT137831. No fresh cell strips from healthy controls were tested in my project due to resources and time constraints.

Inhibiting NOX4 using GKT137831 significantly improved ciliary dysfunction in asthmatic epithelium. At baseline, the asthmatic fresh epithelial cells possessed abnormal ciliary function as previously described (178, 210), including low CBF measurements (6.4±0.5 Hz), abnormal beat patterns with a low % of normal cilia (39±5 %), a high % of dyskinetic cilia (47±4 %) and a high % of static cilia (14±2 %), and the presence of abnormal epithelial surface morphologies (morphology index 2.5±1). GKT137831 at 5 μM and 20 μM were used at the start of the study but there was no concentration-dependent response. This suggests GKT137831 at 5 μM may be approaching the maximum dose effect. Whilst the epithelial cell strips consist of multiple layers of cells, to ensure the effect of NOX4 inhibition was distributed across different cell layers, GKT137831 at 20 μM was used as the single concentration for the rest of the experiment.

Clinical Details	Non-neutrophilic Asthmatic (n = 10)	Neutrophilic Asthmatic (n = 3)	p-values
Gender (F)	3 (7)	1 (2)	0.91*
Age, yr	57 (2)	68 (8)	0.08
Pack year	0.9 (0.8)	19 (12)	**0.01**
% Predicted FEV_1	71 (7)	61 (11)	0.49
% FEV_1/FVC	63 (3)	51 (9)	0.18
PC20 FEV_1, mg/ml †	n/a	n/a	n/a
Blood Total IgE, kU/ml	n/a	n/a	n/a
Blood eosinophils, kU/ml	0.32 (0.07)	0.31 (0.13)	0.93
Treatment (mcg/24 BDP eqv.)	1460 (158)	1267 (371)	0.59
Atopy, %	n/a	n/a	n/a
Age of Disease Onset, yr	36 (4)	59 (10)	**0.02**
Sputum Characterization			
Total cell count($x10^6$ cells/ml)	3.5 (0.8)	5.6 (2.1)	0.27
Eosinophils, % ‡	10 (4.3-23.3)	2 (0.3-2.8)	0.08
Neutrophils, % ‡	46 (38-52)	80 (78-87)	**0.0002**
Macrophages, % ‡	35 (21-50)	14 (12-17)	0.07
Epithelial cells, % ‡	4.5 (2.4-8.8)	1.8 (0.5-3.8)	0.35

† geometric mean (95% CI) ‡ median (inter-quartile range); * Chi square test p<0.05.

Table 5.7 Clinical details of the fresh bronchial brush donors. Data are expressed as mean±SEM unless otherwise indicated. Statistical differences were assessed using unpaired t-tests, p<0.05, unless otherwise indicated.

Fresh epithelial strips from a total of 13 asthmatic donors were used in this experiment (**Table 5.7**). 20 μM GKT137831 at 1 h significantly increased the CBF (10.9±0.6 Hz) compared to the GKT137831 diluent (8.9±0.9 Hz) (mean difference [95% CI] 2.0 [0.6 to 3.4] Hz, p=0.01) (**Figure 5.11**A). Although the GKT137831 diluent significantly increased the CBF compared to baseline (2.5 [0.9 to 4.1] Hz, p=0.005), the magnitude was substantially lower than the effect of GKT137831. NAC also significantly increased the CBF compared to its control at 1 h (1.6 [0.4 to 2.9] Hz, p=0.01). Using 20 μM GKT137831 the % of normal cilia increased from 28±5 % (GKT137831 diluent) to 45±5 % (20 μM GKT137831) (mean difference [95% CI] 17 [6 to 27] %, p=0.01) at 1 h (**Figure 5.11**B), and the % of dyskinetic cilia reduced from 57±4 % (GKT137831 diluent) to 50±5 % (20 μM GKT137831) (-7 [-14 to 0.3] %, p=0.04) at 0.5 h (**Figure 5.11**C). The improvement in CBF in response to NOX4 inhibition was in fact due to the

reduction in cilia immotility: NOX4 inhibition significantly reduced the % of static cilia at 0.5 h (2±1.0 %) and 1 h (2±0.6 %) compared to GKT137831 diluent at 0.5 h (11±4%) (mean difference [95% CI] -9 [-16 to -2] %, p=0.01) and 1 h (17±7 %) (-15 [-29 to -0.6] %, p=0.04) (**Figure 5.11**D). Remarkably, the sputum neutrophil count was correlated to the GKT137831 -induced improvement in the % of normal cilia (Pearson's correlation coefficient r=0.55, p=0.05, **Figure 5.11**E). The GKT137831-induced improvement in the % of static cilia was not normally distributed, thus was expressed to a $\log_{10}$ scale before performing a Pearson correlation test. The sputum neutrophil count was also correlated to the improvement in the % of static cilia (r=0.61, p=0.03, **Figure 5.11**F). The improvements in ciliary function in the presence of GKT137831 were predominantly found in the fresh cells from neutrophilic asthmatics (**Figure 5.11**G), suggesting the oxidative stress could be a pathophysiological pathway specific to this asthma subtype. It is noteworthy that despite a sample size of n=13 was used to produce this data; the variation among human samples suggests that it should be regarded as preliminary data. Further repeats should be done to validate this finding.

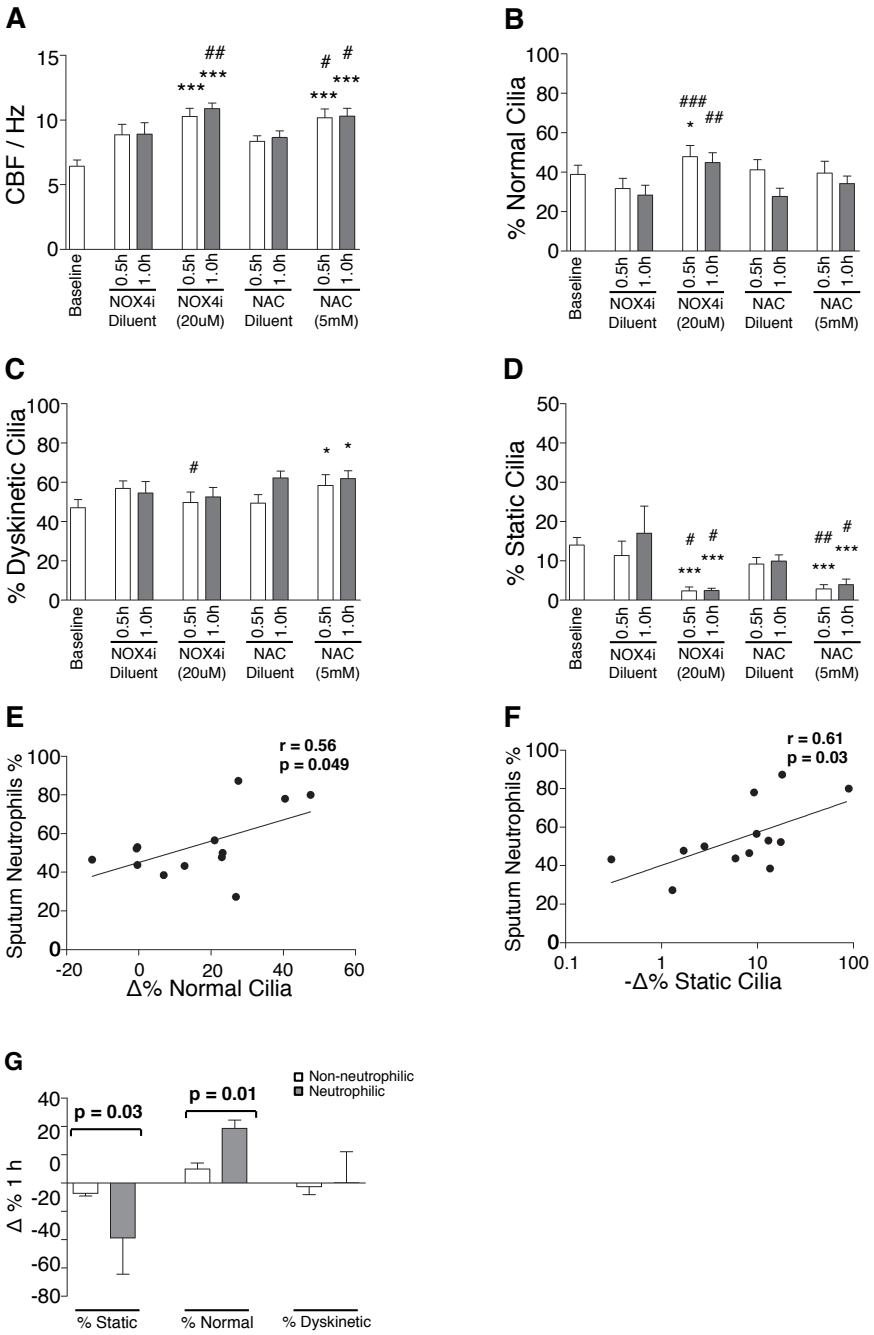

Figure 5.11 The effect of NOX4 inhibition on the ciliary function of fresh asthmatic epithelial cells. The effect of 20 μM GKT137831 (NOX4i) on the ciliary function was assessed using fresh asthmatic epithelial strips (n=13) obtained from bronchoscopy. The effect was assessed following incubation with GKT137831 for up to 1 h. Data are expressed as mean±SEM. Ciliary function was expressed as CBF (Hz) (A), and beat patterns as a % of normal cilia (B), % of dyskinetic cilia (C) and % of static cilia (D). * indicates comparison with baseline and # with corresponding diluent controls. Statistical differences were assessed using paired t-tests, $p<0.05$. The effect of GKT137831 incubation for 1 h on the absolute change in % of normal cilia (E) and % of static cilia (F) was correlated to the % of sputum neutrophil count. Statistical differences were assessed using Pearson's correlation, $p<0.05$. G compares the GKT137831-induced improvement in beat patterns in non-neutrophilic and neutrophilic asthma subtypes. Statistical differences were assessed using unpaired t-tests.

5.5 Discussion

The relationship between oxidative stress and asthma has been well documented (219, 277, 323). The inhibitory effect of reactive radicals on ciliary function has also been repeatedly reported (34, 252, 349, 354). However, none of the reports directly linked the oxidative stress to ciliary dysfunction in asthma. The results presented in this chapter are the first to explore this possibility. Oxidative mis-handling was observed in the asthmatic epithelium, with a correlation to disease severity as indicated by the oxidative DNA damage in bronchial biopsies (8-oxo-dG staining intensity). This mishandling was also correlated to the level of neutrophilic inflammation in the airways. Oxidative mishandling also persisted in the epithelial cultures - asthmatic HAEBC stimulated by H_2O_2 released a significantly higher amount of iROS. This H_2O_2-induced iROS generation was also found to correlate to neutrophilic inflammation.

To enable further investigation into whether oxidative mishandling is an intrinsic defect of asthmatic epithelial cells that contributes to ciliary dysfunction, gene expression analysis was used to identify potential candidates may contribute to this oxidative mishandling. Despite the low sample size of the microarrays that reduced the power of the result, abnormal gene expression of several of the components of the oxidative pathways were identified, such as GST subunits, cytochrome subunits and NOX4, which were in keeping with other studies (289, 316, 323). For instance, the preliminary data from the microarrays showed that NOX4 gene expression was absent in all of the 5 healthy HAEBC samples (**Appendix 7.2**). A role for NOX4 in asthma supported by studies in which it has been shown to be involved in the increased contractility of (316), and the release of inflammatory mediators by (315), human airway smooth muscle cells.

Therefore further studies were performed in which to assess the role of NOX4 in epithelial cells in asthma.

To date there are 4 confirmed NOX4 variants, encoding 3 functional NOX4 protein isoforms in human cells (309). None of these isoforms could be identified by Western Blot, suggesting they are expressed at low levels. More sensitive methods, such as flow cytometry, could be used for further protein analysis. Nevertheless, the preliminary data on gene expression assessed by RT-qPCR was found to be significantly elevated among the neutrophilic asthmatics compared to healthy controls in ALI cultures, and compared to the non-neutrophilic asthmatics in the HAEBC. Although the low sample size of the non-neutrophilic asthmatic sub-group may have reduced the power of the result in general, it is in agreement with the result obtained from the microarrays gene expression analysis. The results suggest that the elevated NOX4 gene expression seen in HAEBC may persist as they differentiate into ciliated ALI cultures. Therefore NOX4 has the potential to contribute to the oxidative mishandling in the asthmatic epithelial cultures.

In contrast, no difference in the expression of SOD2, which is also involved in oxidative handling in mitochondria, was seen in the HAEBC or ALI cultures between healthy controls and asthmatic subgroups preliminarily, and at both the RNA and protein level. Despite the low sample sizes, this concurrence between gene and protein expression suggests that the results are likely to be representative of a larger population. This result is contradictory to other studies in the literature: a reduction in SOD2 activity in asthmatic lung cells has been reported by Mak *et al.* (338) and Smith *et al.* (452). Interestingly in the latter study, the SOD2 activity was measured by the cytochrome *c* reduction rate, whereas the results from my microarray gene expression analyses

suggest abnormal gene expression of the cytochrome b and c subunits *per se* in the asthmatic HAEBC.

In the literature it has been suggested that DUOX1 and DUOX2 are the NOX homologues for regulating local oxidative balance in the lungs (321, 453). NOX4, in comparison, has been shown to be expressed at a very low level at baseline, but can be highly induced upon stimulation (297, 302). DUOX1 and DUOX2 have been suggested to regulate the oxidative balance in epithelial cells (454); DUOX2 may be substituted by NOX4 (302). Therefore it is plausible upregulation of NOX4 expression alone may be sufficient to induce an oxidative imbalance via an increased generation of ROS. Indeed, the increased NOX4 gene expression in asthmatic epithelial cells reported in the preliminary study in this chapter, that appears to be most prominently expressed in neutrophilic asthma, suggests a potential role for NOX4 in oxidative handling in epithelial cells; inhibition of NOX4 activity will help to determine its functional role in asthmatic epithelium. To inhibit NOX4 activity, gene expression can be knocked down using small interfering RNA (siRNA) as shown previously (279, 316). However, the use of this technique is limited to being used on monolayers of cells – the small "genomic constructs" has been shown not to be able to penetrate to the middle layers of a multi-layered epithelium (455, 456). Therefore other approaches are required to inhibit NOX4 function in the multi-layered epithelial cells. GKT137831 is a NOX1/NOX4 specific small molecule that has good cell penetration. In keeping with current literature, the preliminary results here showed that NOX4 gene expression and, very likely, NOX4 protein activity were very low at baseline, but the inhibition of NOX4 activity using GKT137831 caused a substantial reduction in the H_2O_2-induced iROS generation in HAEBC. GKT137831 also significantly improved the ciliary function of fresh asthmatic

epithelial cells. Fresh cells were used instead of ALI cultures because 1) ALI cultures normally take at least a month to become heavily differentiated; 2) HAEBC differentiation varies between donors, which could unexpectedly lengthen the time of the study; and most importantly 3) fresh cells from asthmatic airways were already "injured" due to the presence of the asthma-specific microenvironment, which has been proven to be an important factor in asthmatic ciliary dysfunction as shown in Chapter 3. It would be reasonable to believe that this model is as close to the *in vivo* situation as animal models. In fact, this current methodology has an advantage over the use of animal models due to the differences in the airway epithelial structures between humans and other species (457). Therefore the improvement in the *ex vivo* ciliary function upon the GKT137831 application may suggest that GKT137831 could have beneficial effects in the clinical setting. However, the preliminary nature of the result presented herein suggested that further repeats should be done to validate this finding before moving onto human studies. It should also be noted that there are many more interactions between different cells and the surrounding microenvironment *in vivo*. Moreover, there is a lack of information in the literature to associate CBF and ciliary beat pattern to clinical outcomes. There is currently one report suggesting that ±1 Hz in CBF may be translated to a clinical significance (210). However how significant this change of 1 Hz would be on clinical outcomes, such as the rate of mucociliary clearance and hence the prevalence of infection and exacerbation, is yet to be evaluated. As a result, the physiological significance of the effect of GKT137831 on ciliary function has yet to be determined. If the proposed "±1 Hz gives clinical significance" approach proves to be valid, the effect of GKT137831 on improving the ciliary dysfunction in asthma may have a significant role in thus on reversing the impaired mucociliary clearance that could prevent or slow down the progression of the disease.

The improvement in CBF and the % of static cilia upon NOX4 inhibition were intercalated. However it is noteworthy that the reduction in the % of static cilia upon NOX4i treatment may not only improve the overall CBF reading. A recent study has suggests that motile cilia possess a mechanical and/or chemical sensory function (458). This sensory function may contribute to a regulatory function between cilia of adjacent cells in an autocrine manner as reported previously (459). When the cilia become static or immotile, this sensory function may be lost, and thus the epithelium may become less responsive to external stimulations. This dysregulated ciliary response that may partly contribute to the reduction in CBF, together with the changes in the composition of the mucus (460) and the periciliary fluid (231), may result in the impaired mucociliary clearance as observed in asthmatic airways in a cumulative manner.

NAC has been suggested as an anti-oxidant therapy (365, 366), but is not generally used for treating asthma due to the predictable side effects – most notably its ubiquitous effect on inhibiting oxidant activities as well as promiscuous scavenging of reactive oxygen and nitrogen species that are essential in signalling pathways (279, 280). In comparison, GKT137831 specifically targets NOX4 and NOX1 activities without affecting the production of reactive species that is normal and essential to the cells (320). Herein the improvement of some ciliary function parameters, such as the % of normal cilia at 1 h, was more significant using GKT137831 compared to NAC (-10 [-20 to -0.4] %, p=0.04). The effect of NOX4i on inhibiting HAEBC iROS generation was also more profound (**Figure 5.10**). It is worth noting that whilst GKT137831 is a NOX1/NOX4 inhibitor, the effect of NOX1 inhibition on iROS generation and ciliary function was not evaluated. However GKT137831 has a 1.5-fold lower potency and 1.7-fold lower

affinity towards NOX1 compared to NOX4. NOX1 to date was found to be correlated to apoptosis (461), but has a low constitutive and induced activity in airway epithelial cells (296, 297). As GKT137831 has not shown to reduce epithelial cell viability, it is therefore plausible that it was predominantly acting via the inhibition of NOX4 as opposed to NOX1 in epithelial cells, which further supports its use as an anti-oxidant therapy.

To summarise, the current findings strongly suggested that oxidative damage is present in the asthmatic epithelium, which persisted when the epithelial cells were cultured and differentiated *in vitro*. This intrinsic abnormality might be linked to the ciliary dysfunction in asthma as suggested in the preliminary studies in this chapter. In fact, an elevation in NOX4 gene expression implicates an abnormal, increased NOX4 protein activity (295). This suggests that NOX4 may play a role in the abnormal oxidative handling in asthma. Whether NOX4 is the only component involved in regulating the oxidative balance in airway epithelial cells that is dysregulated, or whether other NOX homologues, such as DUOX1/2, are also involved as previously shown (300), requires further investigation with an increase in sample size. Although the evidence suggesting that the increase in NOX4 gene expression is specific to neutrophilic asthmatic epithelial cultures is limited, The data is supported by the use of GKT137831 to inhibit NOX4 protein activity in fresh epithelial cells, which results in improves ciliary function in terms of CBF and beat patterns. This collective evidence opposes the null hypotheses outlined at the beginning of the chapter, to suggest that oxidative mishandling could indeed be the cause of asthmatic ciliary dysfunction, that use of a specific anti-oxidative treatment targeting NOX4 may improve ciliary function, and that

the effect of this anti-oxidative treatment may be more profound in the neutrophilic asthma subtype.

5.6 Criticism

Limitation 1 – The method of DCF-DA assay optimisation might not be correct

Unlike the rFC assay used in Chapter 4, there was not much information in literature reporting the correct way to optimise a DCF-DA assay. The optimisation I performed was therefore based on colleagues' experience and common sense: 1) fluorescence of the DCF-DA stain on its own should not increase overtime; 2) at baseline, the cells stained with DCF-DA should not have a dramatic increase in fluorescence across time; 3) there should be a time-dependent increase and concentration-dependent increase in response to an increasing concentration of H_2O_2, with substantial differences between time points and between concentrations to allow standard errors; 4) the range of fluorescence measured should be within the limit of the microplate reader (0 to 60,000). All these points were crosschecked between array repeats. Furthermore it was realised later on that the "% increase" was an invalid parameter for DCF-DA assay analysis since the reactions had different 'starting points'. Absolute change in fluorescence reading (OD) was therefore used throughout the DCF-DA assay analysis.

Limitation 2 –Western blot: detection limit and densitometry

Western blot analysis can be carried out in different ways, although densitometry is the most commonly method that is used for publication. Commercial densitometers are commonly used in research that allow blot development and electronic scanning to happen at the same time, followed by digital density measurements (389). For the analysis here, an office scanner was used for capturing images of the films, and bands were analysed using the software ImageJ. This has been proved to be a valid method. Measurement by a single observer was repeatable. Within densitometry there are also

different analytical approaches (389). None of these methods showed any difference to the results herein.

Limitation 3 – Penetration of the NOX4i small molecules to the inner layers of the epithelium was not evaluated.

Despite using the high concentration of GKT137831, it was uncertain whether the small molecules would have penetrated into the inner layers of the epithelial cell strips. This may be assessed by tagging the molecules with fluorescence tags or "golden" magnetic beads, followed by confocal imaging or electron-microscopy to visualise the location of the molecules within the cells. Either method would require a substantial amount of time for synthesis and optimisation. It has been shown previously that the GKT137831 molecule is very small with good permeability (370). Previous Genkyotex studies have already validated the use of the molecule at 5-10 μM GKT137831 and data herein showed that a 1 h incubation time was effective for iROS reduction at a range of concentrations. Therefore it would be reasonable to presume that with a concentration as high as 20 μM, 1 h incubation would be sufficient enough to neutralise the NOX4 activity in the cells among the middle layers of the epithelium.

5.7 Summary

In this chapter, the possible role of oxidative stress in contributing to the impairment of epithelial ciliary function in asthma was evaluated. An intrinsic abnormality in oxidative handling was found in asthmatic airway epithelium, as shown by the strong 8-oxo-dG positive staining in the asthmatic bronchial biopsies, and the substantially higher H_2O_2-stimulated iROS generation in asthmatic HAEBC. Both phenomena were associated with neutrophilic inflammation. The power of the data was limited by small sample sizes, but the results suggest a possible association between increased NOX4 expression and oxidative mishandling in the epithelial cells from asthmatics with a neutrophilic inflammatory profile. GKT137831, which is a small molecule inhibitory compound that specifically inhibits NOX4 and NOX1 activity. GKT137831 was shown to reduce iROS production in HAEBC from both health and asthma, suggesting a role for NOX4 in iROS generation in airway epithelial cells. Furthermore, inhibition of NOX4 protein activity using GKT137831 resulted in an improvement in the ciliary dysfunction observed in fresh epithelial strips obtained from asthmatics, particularly those from the neutrophilic subgroup.

Interestingly, neutrophilia in the airway has been linked to infection-related asthma (32) whilst airway pathogens have been shown to directly (252, 255), and indirectly (254, 435), induce an impairment of ciliary function via ROS generation (34). Therefore, in addition to the dysregulation of oxidative handling intrinsic to the epithelial cells presented herein, the source of oxidative stress in the epithelial cells in the asthmatic environment could be due to bacterial colonisation/infection. These different lines of evidence, in combination with the data presented herein, suggest a plausible link between infection, neutrophilia, oxidative stress and ciliary function which may be specific to the neutrophilic asthma subtype, and warrants further investigation with

regards to possible identification of therapeutic targets for drug development. Appropriate combination of therapies targeting both microbes and NOX4 may be beneficial for treating epithelial ciliary dysfunction in neutrophilic asthmatics.

6. Overall Discussion

6.1 Overall Discussion and Criticism

The data presented in this thesis have tested and provide support for my hypothesis – asthmatic ciliary dysfunction in epithelial cell culture is likely to be triggered by the presence of exogenous environmental factors, which may be caused by an intrinsic factor embedded within the epithelial cells that results in its increased susceptibility to injury, such as infection and oxidative challenge.

Characterisation of unstipulated healthy and asthmatic ALI cultures revealed a number of similarities between health and disease that could indicate that epithelial ciliary dysfunction in asthma is likely to be triggered by an exogenous factor. These similarities included the capacity to synthesise pro-inflammatory mediators and the baseline ciliary function. This was in disagreement with some studies, but in line with others, although the majority of studies in the literature reported an abnormal pro-inflammatory mediator profile in unstipulated asthmatic epithelial cells (176, 184). Interestingly the results herein showed a differential secretion of mediators between bronchial basal cells HAEBC and ALI cultures, but with no differences between asthmatic and healthy samples. This could be due to the inclusion of atopic healthy controls and non-atopic asthmatic subjects as suggested by Bayram *et al.* (223) and/or the inclusion of smokers as suggested by Freishtat *et al.* (404). Other differences reported in the literature in cells from healthy controls compared to those from asthmatics include the persistence of structural abnormalities in asthmatic ALI cultures, such as changes in basement membrane and epithelial thickness, goblet cell hyperplasia and mucus hypersecretion (176, 184). These features could not be evaluated in my ALI cultures due to the histological technique not being available at the time of the study. Despite the above similarities, the results from the human genome microarrays

suggested that, although only small differences exist in the baseline gene expression between the HAEBC from healthy and asthmatic subjects, these differences could affect cell differentiation and function.

In line with some previous studies, asthmatic ALI cultures did not possess the ciliary abnormalities (223, 377, 399) that are observed *in vivo* (210). There was also no difference in CBF between cultures derived from males and females as previously reported (236), which was likely to be due to the lack of sex hormones in the *in vitro* environment. The lack of differences in the inflammatory mediator profiles between healthy and asthmatic cultures as shown in my study could at least in part explain the lack of differences in the ciliary function of my unstipulated cultures. Inflammatory mediators have been shown to affect mucociliary clearance: eosinophil-derived major basic protein (BMP) has been shown to induce ciliary immotility by inhibiting the ATPase on the ciliary axenomes (462). In addition high concentrations of leukotrienes (233, 234), T_H2 cytokines, such as IL-4 and IL-13 (217), and mast cell mediators (194) have been shown to reduce CBF and thus reduce the rate of clearance. Interestingly, Bayram *et al.* have demonstrated that asthmatic epithelial cells were more sensitive to challenges (223), raising the possibility that epithelial ciliary dysfunction in asthma may be triggered by an exogenous factor found in the asthmatic environment. Interestingly, the exposure of the ALI cultures to asthmatic sputa in combination with the removal of antibiotics produced a similar effect to the Bayrum study with re-establishment of the impairment of ciliary dysfunction in the asthmatic ALI cultures. In support of this observation, Delano *et al.* demonstrated the potential effect of asthmatic sputa on ciliary function (396). They showed that only “slurry” sputa were able to induce ciliary immotility. These “slurry” sputa were usually obtained during exacerbations. As asthma

exacerbations are usually associated with microbial infection (242, 246), it is plausible that the ciliary dyskinetic/static factor(s) present in these sputa is microbe-associated. Interestingly, airway pathogens have been shown to directly (252, 255) induce an impairment of ciliary function via ROS generation (34). On the whole, these results support the hypothesis that the asthmatic abnormality in the epithelium is revealed only in an altered microenvironment.

However, there could also be intrinsic abnormalities in the epithelial cells that make them more susceptible to behavioural changes in this asthmatic microenvironment, e.g. an intrinsic defect in oxidative handling. It has been shown previously that exposure to oxidants can result in a reduction in CBF (223, 463) and defective cell differentiation (463), which persisted even after the removal of the oxidants. This could be due to the fact that oxidative stimulation induces further generation of reactive species (463). My results showed the presence of oxidative DNA damage and intracellular oxidative miss-handling in the asthmatic epithelium, particularly in the neutrophilic asthma subgroup. This raises the possibility that dysregulation of the pathway involved in oxidative handling could potentially increase the susceptibility of asthmatic epithelial cells to stimulation, such as microbial challenges, resulting in the impaired ciliary function seen *in vivo*. Asthma is a heterogeneous disease that can be divided into subgroups by the means of assessment of inflammatory profiles (26), assessment of the correlation between inflammatory profiles and clinical characteristics (334), and transcriptomic profiling (37). Regardless of which method is used, the evidence suggests the presence of a sizable population of asthmatic subjects with a low T_H2 and high neutrophilic inflammatory profile. This population is not well controlled due to corticosteroid insensitivity and the lack of other effective drugs. This asthma subgroup is usually

associated with microbial colonisation/infection (32, 34), however the effectiveness of anti-microbial treatments in relieving asthma symptoms has been shown to be controversial (254, 273, 274). Further studies to enable recognition of the mechanistic differences between different asthma subtypes will help in the development of specific and effective treatments. From the evidence discussed above, it is plausible that infection, neutrophilia and oxidative stress could act in concert to promote ciliary dysfunction in asthma, warranting further investigation into identification of potential therapeutic targets for drug development.

High throughput approaches, such as microarrays (8, 9, 464), may help with understanding the underlying mechanisms of the disease phenotypes and the clinical outcomes observed. Although limited by sample number and the use of HAEBC as the only tested cell type, the microarrays analysis presented in this thesis has revealed a list of genes that might be specifically expressed subject groups. NOX4, which is involved in ROS generation, is among these genes, and has been investigated further in the airway epithelial cultures using RT-qPCR. The results were in coherence with the microarrays. The results suggested that increased expression of NOX4 was associated with the neutrophilic asthma subgroup. In the presence of a NOX4 inhibitor, GKT137831, iROS generation in HAEBC was reduced and ciliary function in fresh asthmatic bronchial ciliated cells was improved, providing support for a potential role for NOX4 in the abnormal oxidative handling and impaired ciliary function in asthmatic airway epithelium.

It is important to point out that GKT137831 is a NOX1/NOX4 duo inhibitor, in spite of the lower potency (1.5-fold) and affinity (1.7-fold) towards NOX1. One of the

limitations in my thesis is that the role of NOX1 in airway epithelium function was not evaluated. The lack of differential NOX1 gene expression between health and asthma from the microarray analysis presented gives credence to the idea that the effect of GKT137831 on NOX1 inhibition towards ciliary dysfunction is minimal in the current study. However, high constitutive NOX1 gene expression in airway epithelial cells has been reported in some studies (298). A recent study also suggested that NOX1 might regulate NOX4 expression upon interaction with SOD1 in renal cells (320). Therefore this NOX homologue should not simply be ignored. In addition, it has been shown that NOX1 may regulate epithelial cell apoptosis via inhibition of inhibitor of κB kinase (IKK) in a TNF-R1-dependent manner (318, 465). My group has recently published that blocking IKK could have a corticosteroid "sparing" effect on corticosteroid insensitive human airway epithelial cells (466). Combining GKT137831 and an IKK inhibitor could be an effective therapeutic regimen in treating asthmatic patients with a neutrophilic inflammation profile who are also steroid insensitive.

Another major limitation of my study would be the lack of evaluation of: 1) from a scientific aspect, how NOX4 expression is linked to the regulation of ciliary function; and 2) from a clinical aspect, whether the changes in epithelial cell behaviour associated with regulation of NOX4 activity are sufficient to result in improved clinical outcomes. For the former point, I believe there are two plausible pathways. When NOX4 oxidises NADPH to $NADP^+$, one electron is transported to the outer side of the membrane (**Figure 1.7**). To balance the change in ionic charges, a H^+ ion is transported to the outside concurrently. A higher NOX4 expression would imply a higher NOX4 activity (295) that leads to an accumulation of H^+ ions around the outer membrane and causes a change in pH of the surrounding environment. An increase in extracellular acidity

caused by NOX activity has in fact been reported previously (296). The reduction in pH could therefore reduce the ciliary function of the epithelium (108, 109). Another potential mechanism could involve changes in the Ca^{2+} homeostasis. It has been shown that H_2O_2 can activate Ca^{2+} signalling by manipulating IP_3-sensitive intracellular Ca^{2+} stores(467). In vascular cells it has been shown that hypoxia-induced NOX-generated iROS are associated with $[Ca^{2+}]_i$ (468, 469), which acts via the mitochondrial PKCε pathway(468). A mitochondria-driven increase in $[Ca^{2+}]_i$ could therefore facilitate the PKA signalling pathway (**Figure 1.6**). In fact, the relationship between ageing and oxidative stress(440), aging and ciliary function (441), and interlink between mitochondria, ageing and asthma (323) have been previously discussed. The exact involvement of each/both pathway(s), together with the localisation of functional NOX4 isoforms in airway epithelial mitochondria, would require further investigation.

As for the latter point, evidence from literature as well as the results in this thesis suggests a relationship between ciliary function, mucociliary clearance and infection-induced asthma exacerbation, thus highlighting the possibility in the improvement of asthma management by targeting ciliary dysfunction. Current asthma therapies have been showed to non-specifically improve CBF (217, 233, 234). These treatments, however, were inefficient in certain subgroups of asthmatic patients, such as those with a neutrophilic inflammatory profile. The preliminary findings of this thesis showed that the inhibition of NOX4 might specifically improve ciliary function of the epithelial cells obtained from the neutrophilic asthmatics. The sample numbers of some of the studies here were limited, and thus would require more repeats of the corresponding experiment in order to validate these findings. If the same conclusion could be drawn with the increased sample sizes, the clinical benefit of NOX4 inhibition could then be evaluated using animal models and clinical trials.

6.2 Future Studies

The findings from various chapters in this thesis could open up several possible future studies. Some of these studies have already been mentioned in the criticism section of the corresponding chapters. Whilst some of these findings were based on relative low sample numbers, future studies should focus on increasing the n number in order to validate the current findings and to draw more conclusive results:

6.2.1 Project 1: The role of NOX4 in epithelial ciliary function in asthma

In this thesis I have suggested that NOX4 inhibition may have an impact on restoring the ciliary function of airway epithelial cells from asthmatic subjects. The choice of NOX4 was based on the preliminary data from the HAEBC microarrays, as well as the qPCR of HAEBC and ALI cultures with the limited sample numbers. In order to validate my findings, the first step would be to increase the sample numbers of the qPCR to show that NOX4 gene expression is indeed elevated in the neutrophilic asthma sub-group, but not in healthy controls and the non-neutrophilic subgroup. Once this has been validated, it can then move on to validating at the effect of GKT137831 on the restoring ciliary function in fresh ciliated epithelial cells model. I believe this model is the closest *ex vivo* model to the *in vivo* approach. Despite the fact that these cells were assessed outside the human body, they retained the ciliary dysfunction and the microenvironment that was observed in asthmatic airways. These fresh samples were used within a minimal period of time after the bronchoscopy being performed (<1.5 h). It is therefore reasonable to believe that this approach could represent the clinical situation to a certain and realistic degree. Only if these follow-up experiments have confirmed the role of NOX4/GKT137831 in the *in vitro*/*ex vivo* environment could the study be moved on to *in vivo* studies. The potential *in vivo* experiments would be NOX4

knockout mouse models (313, 360), or the pneumonia mouse model that was developed recently(470), or clinical trials in human. However as discussed early on, the limited indication on how relevant the current ciliary function parameters (such as ±CBF) is to the efficiency in mucociliary clearance and the prevention of disease progression is unclear.

6.2.2 Project 2: Microarray follow-up

Microarray using fresh bronchial brushes and/or differentiated ALI cultures upon stimulation

The microarray result presented here was based on low HAEBC sample numbers in both healthy and asthmatic subject groups. To increase the reliability of the current result, it is essential to increase the sample numbers to a desirable level. Despite the constitutive gene expression showed similarity between HAEBC (**Table 3.4**) and ALI cultures(398), the primary objective of this thesis is to investigate the underlying mechanism of ciliary dysfunction in asthma. Microarrays should ideally be done using fresh brushes and/or ALI cultures, and after challenges, such as incubation with asthmatic sputum, if possible. This may help to identify additional genes, which are associated with the high susceptibility of asthmatic epithelial cells to development of ciliary dysfunction, whose use as therapeutic targets could then be further explored.

Microarray analysis and follow-up on differentiation gene expression

Besides the sample numbers and the epithelial samples being used, the current microarray analysis was the first step to explore the baseline gene expression profile of airway epithelial cells. A proper analysis using bioinformatic packages would help with identifying the pathway(s) that might be involved in the ciliary dysfunction in asthma.

For instance, the regulator of G-protein signalling (RGS) 2 molecule regulates $[Ca^{2+}]_i$ by modulating G-protein signalling pathways and was shown to correlate to hyperresponsiveness (471) and to regulate CBF (116). The preliminary result here reported a >2.0-fold down-regulation in asthmatic HAEBC might therefore explain the reduced ciliary function in asthmatic cells. On the other hand, RGS16 has been reported to modulate pulmonary inflammation (475). The preliminary result here showed that RGS16 was specifically expressed in the asthmatic HAEBC. As a result, the role of RGS protein family in asthmatic epithelial function warrants further investigation. PLC is downstream of the cAMP pathway in CBF upregulation (**Figure 1.6**). Interestingly, phospholipase C beta 1 (PLCB1) was found ~2.0-fold upregulated in the asthmatic HAEBC, and thus might be involved in the cAMP/PLC signalling pathway. Another gene HMGB2 was reported to be expressed only during embryogenesis (476). Its homologue HMGB1, however, acts as a DAMP as well as a mitochondria modulator (136) to facilitate innate immunity, and has been reported to be involved in asthma pathogenesis (477, 478), in particular among those subjects with neutrophilia (479, 480). Tubulin ε 1 (TUBE1) is an intracellular component required for centriole duplication(481); its upregulation in asthmatic HAEBC might imply a dysregulated ciliogenesis that may increase the susceptibility to secondary ciliary dyskinesia. Various cytochrome family members were also picked up by the current microarrays, and may be involved in the oxidative handling in asthmatic epithelium. Therefore, it is important to further validate these findings by increasing the sample sizes in order to support further, more detailed investigation of these genes. These results may help with understanding the underlying mechanism of asthma and asthmatic ciliary dysfunction, and thus help with identifying therapeutic targets for asthma treatment.

6.3 Thesis Conclusion

To summarise, there are four novel findings in this thesis. Firstly, the ciliary dysfunction evident in asthma did not persist in *ex vivo* ALI epithelial cultures. There was also no differentiation in the baseline synthetic capacity in different asthmatic epithelial cell subtypes. This suggests that the asthmatic airway environment is critical in the development and maintenance of these abnormalities in ciliary function. Secondly, the asthmatic sputum-induced ciliary dysfunction was only revealed in the absence of antibiotics. However, the microbial levels in the collectables from the sputum-inoculation study were not different between health and asthma. This suggests that, in addition to the asthmatic environment, there is an intrinsic susceptibility of epithelial cells to damage in asthma that is involved in the development of ciliary dysfunction. Thirdly, the asthmatic epithelial cells are likely to be under oxidative stress, and the modulation of oxidative handling via inhibition of NOX4 might improve ciliary function. This suggests that the oxidative mis-handling, due to an increased expression of NOX4, may be the driver of the intrinsic susceptibility in the epithelial cells in asthma. Finally, NOX4 inhibition predominantly improved the epithelial ciliary function of the neutrophilic asthmatic individuals. This suggests that the NOX4-derived oxidative pathway may be specific to the neutrophilic asthma subgroup. Further investigation of the involvement of NOX4 and oxidative handling on the regulation of epithelial ciliary dysfunction is required, primarily by increasing the sample numbers of the qPCR and NOX4 inhibitor studies.

To conclude, the mechanism underlying the asthmatic ciliary dysfunction may involve a defect in intrinsic NOX4-related oxidative handling. This intrinsic factor may contribute

to the high susceptibility of these cells to any environmental stimuli, such as microbial loads, which may then trigger ciliary dysfunction and potentially promotes asthma progression that leads to exacerbation. Targeting the abnormal asthmatic microenvironment as well as the intrinsic NOX4 defect in the epithelial cells as an appropriate strategy for treating asthma, especially the neutrophilic subtype, is worthy of further investigation. The right combination of current and new treatments to address the patient-specific conditions may be the most appropriate way for future asthma management.

7. Appendix

Appendix 7.1 Videos of side profiles equivalent to Figure 3.3.

A. Genes present in ≥3 asthmatics compared to 0 healthy controls

Affymetrix ID	Gene Symbol	Gene Name	Entrez Gene ID
201430_s_at	DPYSL3	dihydropyrimidinase-like 3	1809
201578_at	PODXL	podocalyxin-like	5420
202175_at	CHPF	chondroitin polymerizing factor	79586
204002_s_at	ICA1	islet cell autoantigen 1, 69kDa	3382
204272_at	LGALS4	lectin, galactoside-binding, soluble, 4	3960
204317_at	GTSE1	G-2 and S-phase expressed 1	51512
204418_x_at	GSTM2	glutathione S-transferase mu 2 (muscle)	2946
204683_at	ICAM2	intercellular adhesion molecule 2	3384
205439_at	GSTT2	glutathione S-transferase theta 2	2953
206611_at	C2orf27A	chromosome 2 open reading frame 27A	29798
206637_at	P2RY14	purinergic receptor P2Y, G-protein coupled, 14	9934
206839_at	C22orf31	chromosome 22 open reading frame 31	25770
206916_x_at	TAT	tyrosine aminotransferase	6898
208023_at	TNFRSF4	tumor necrosis factor receptor superfamily, member 4	7293
208060_at	PAX7	paired box 7	5081
208462_s_at	ABCC9	ATP-binding cassette, sub-family C (CFTR/MRP), member 9	10060
208987_s_at	KDM2A	lysine (K)-specific demethylase 2A	22992
209170_s_at	GPM6B	glycoprotein M6B	2824
209324_s_at	RGS16	regulator of G-protein signaling 16	6004
209423_s_at	PHF20	PHD finger protein 20	51230
210103_s_at	FOXA2	forkhead box A2	3170
210457_x_at	HMGA1	high mobility group AT-hook 1	3159
210595_at	ZNF235	zinc finger protein 235	9310
210836_x_at	PDE4D	phosphodiesterase 4D, cAMP-specific (phosphodiesterase E3 dunce homolog, Drosophila)	5144
212020_s_at	MKI67	antigen identified by monoclonal antibody Ki-67	4288
212080_at	MLL	Myeloid/lymphoid or mixed-lineage leukemia (trithorax homolog, Drosophila)	4297
213672_at	MARS	methionyl-tRNA synthetase	4141
214068_at	BEAN	brain expressed, associated with Nedd4	146227
214105_at	SOCS3	suppressor of cytokine signaling 3	9021
214852_x_at	VPS13A	vacuolar protein sorting 13 homolog A (S. cerevisiae)	23230
215070_x_at	RABGAP1	RAB GTPase activating protein 1	23637
215217_at	IGKC	Immunoglobulin kappa constant	3514
215463_at	OR7E24	olfactory receptor, family 7, subfamily E, member 24	26648

Affymetrix ID	Gene Symbol	Gene Name	Entrez Gene ID
215509_s_at	BUB1	budding uninhibited by benzimidazoles 1 homolog (yeast)	699
215711_s_at	WEE1	WEE1 homolog (S. pombe)	7465
216203_at	SPTLC2	serine palmitoyltransferase, long chain base subunit 2	9517
216325_x_at	RTEL1	regulator of telomere elongation helicase 1	51750
216344_at	NPHP4	nephronophthisis 4	261734
216417_x_at	HOXB9	homeobox B9	3219
216661_x_at	MUTYH	mutY homolog (E. coli)	4595
217560_at	GGA1	golgi associated, gamma adaptin ear containing, ARF binding protein 1	26088
217889_s_at	CYBRD1	cytochrome b reductase 1	79901
218308_at	TACC3	transforming, acidic coiled-coil containing protein 3	10460
219509_at	MYOZ1	myozenin 1	58529
219525_at	SLC47A1	solute carrier family 47, member 1	55244
219559_at	SLC17A9	solute carrier family 17, member 9	63910
219773_at	NOX4	NADPH oxidase 4	50507
220288_at	MYO15A	myosin XVA	51168
220306_at	FAM46C	family with sequence similarity 46, member C	54855
220908_at	CCDC33	coiled-coil domain containing 33	80125
221261_x_at	MAGED4	melanoma antigen family D, 4 /// melanoma antigen family D, 4B	728239 /// 81557
222121_at	SGEF	Src homology 3 domain-containing guanine nucleotide exchange factor	26084
223763_at	DTNBP1	dystrobrevin binding protein 1	84062
223837_at	GULP1	GULP, engulfment adaptor PTB domain containing 1	51454
224016_at	HIPK2	homeodomain interacting protein kinase 2	28996
224044_at	RHOT1	ras homolog gene family, member T1	55288
224940_s_at	PAPPA	pregnancy-associated plasma protein A, pappalysin 1	5069
225628_s_at	MLLT6	myeloid/lymphoid or mixed-lineage leukemia (trithorax homolog, Drosophila); translocated to, 6	4302
225654_at	NSD1	nuclear receptor binding SET domain protein 1	64324
226141_at	CCDC149	coiled-coil domain containing 149	91050
226210_s_at	MEG3	maternally expressed 3 (non-protein coding)	55384
226610_at	CENPV	centromere protein V	201161
226731_at	PELO	Pelota homolog (Drosophila)	53918
227007_at	TMCO4	transmembrane and coiled-coil domains 4	255104
227104_x_at	ZNF800	zinc finger protein 800	168850
227258_at	C10orf46	chromosome 10 open reading frame 46	143384
227677_at	JAK3	Janus kinase 3	3718
227742_at	CLIC6	chloride intracellular channel 6	54102
227890_at	TMEM198	transmembrane protein 198	130612
228161_at	RAB32	RAB32, member RAS oncogene family	10981
228193_s_at	C13orf15	Chromosome 13 open reading frame 15	28984

Affymetrix ID	Gene Symbol	Gene Name	Entrez Gene ID
228226_s_at	ZNF775	zinc finger protein 775	285971
228320_x_at	CCDC64	coiled-coil domain containing 64	92558
228547_at	NRXN1	neurexin 1	9378
228875_at	FAM162B	family with sequence similarity 162, member B	221303
229867_at	BTBD9	BTB (POZ) domain containing 9	114781
230360_at	GLDN	gliomedin	342035
230664_at	H2BFM	H2B histone family, member M /// H2B histone family, member X, pseudogene	286436 /// 767811
230802_at	ARHGAP24	Rho GTPase activating protein 24	83478
230949_at	SLC23A3	solute carrier family 23 (nucleobase transporters), member 3	151295
230992_at	BTNL9	butyrophilin-like 9	153579
231164_at	ABCA17P	ATP-binding cassette, sub-family A (ABC1), member 17 (pseudogene)	650655
231315_at	NKX2-1	NK2 homeobox 1	7080
231794_at	CTLA4	cytotoxic T-lymphocyte-associated protein 4	1493
231860_at	BRWD1	bromodomain and WD repeat domain containing 1	54014
231971_at	FANCM	Fanconi anemia, complementation group M	57697
232167_at	MIF	macrophage migration inhibitory factor (glycosylation-inhibiting factor) /// solute carrier family 2 (facilitated glucose transporter), member 11	4282 /// 66035
232514_at	KIF27	kinesin family member 27	55582
232844_at	IFT140	Intraflagellar transport 140 homolog (Chlamydomonas)	9742
232912_at	GPR180	G protein-coupled receptor 180	160897
232953_at	C20orf69	chromosome 20 open reading frame 69 /// similar to hypothetical protein LOC284701 /// similar to hCG1984118 /// similar to Putative uncharacterized protein C20orf69 /// hypothetical protein LOC100288169 /// hypothetical LOC728323 /// protein-L-isoaspartate (D-aspartate) O-methyltransferase domain containing 2 /// hypothetical LOC402483	100287060 /// 100287654 /// 100288169 /// 140849 /// 402483 /// 55251 /// 642780 /// 728323
234818_at	TMEM108	transmembrane protein 108	66000
235330_at	CCDC117	coiled-coil domain containing 117	150275
235339_at	SETDB2	SET domain, bifurcated 2	83852
236126_at	ACVR2B	activin A receptor, type IIB	93
236195_x_at	PRKCG	protein kinase C, gamma	5582
236840_at	C12orf56	chromosome 12 open reading frame 56	115749
236863_at	C17orf67	chromosome 17 open reading frame 67	339210
237054_at	ENPP5	ectonucleotide pyrophosphatase/phosphodiesterase 5 (putative function)	59084
238564_at	FAM171B	Family with sequence similarity 171, member B	165215
239446_x_at	DCBLD2	discoidin, CUB and LCCL domain containing 2	131566
240199_x_at	ZNF345	zinc finger protein 345	25850
241995_at	DGUOK	deoxyguanosine kinase	1716

Affymetrix ID	Gene Symbol	Gene Name	Entrez Gene ID
242946_at	CD53	CD53 molecule	963
243099_at	NFAM1	NFAT activating protein with ITAM motif 1	150372
243301_at	COL22A1	collagen, type XXII, alpha 1	169044
244225_x_at	LMNA	Lamin A/C	4000
244691_at	SETD5	SET domain containing 5	55209
1552281_at	SLC39A5	solute carrier family 39 (metal ion transporter), member 5	283375
1552889_a_at	EXOC3L2	exocyst complex component 3-like 2	90332
1552946_at	ZNF114	zinc finger protein 114	163071
1553736_at	ZFC3H1	zinc finger, C3H1-type containing	196441
1553967_at	ADAT3	adenosine deaminase, tRNA-specific 3, TAD3 homolog (S. cerevisiae)	113179
1554742_at	PMS1	PMS1 postmeiotic segregation increased 1 (S. cerevisiae)	5378
1554785_at	CCDC82	coiled-coil domain containing 82	79780
1555131_a_at	PER3	period homolog 3 (Drosophila)	8863
1555235_s_at	IQCF3	IQ motif containing F3	401067
1555447_at	GPR114	G protein-coupled receptor 114	221188
1558322_a_at	PAQR9	progestin and adipoQ receptor family member IX	344838
1558706_a_at	ATOH8	Atonal homolog 8 (Drosophila)	84913
1558754_at	ZNF763	zinc finger protein 763	284390
1559266_s_at	C10orf140	chromosome 10 open reading frame 140	387640
1559982_s_at	AKR1CL2	aldo-keto reductase family 1, member C-like 2	83592
1562256_at	NLRP1	NLR family, pyrin domain containing 1	22861
1562381_at	RP3-377H14.5	hypothetical LOC285830	285830
1562446_at	ZNF391	zinc finger protein 391	346157
1562717_at	C2orf46	chromosome 2 open reading frame 46	339789
1564356_at	ZNF568	zinc finger protein 568	374900
1564796_at	EMP1	epithelial membrane protein 1	2012
1568554_x_at	C6orf142	Chromosome 6 open reading frame 142	90523
1568830_at	IRAK3	interleukin-1 receptor-associated kinase 3	11213
1568849_at	C21orf135	chromosome 21 open reading frame 135	727701
1569076_a_at	ZNF836	zinc finger protein 836	162962
1569296_a_at	LOC493754	RAB guanine nucleotide exchange factor (GEF) 1 pseudogene	493754
1569504_at	LILRB4	Leukocyte immunoglobulin-like receptor, subfamily B (with TM and ITIM domains), member 4	11006
1569701_at	PER3	Period homolog 3 (Drosophila)	8863
204591_at	CHL1	cell adhesion molecule with homology to L1CAM (close homolog of L1)	10752
208386_x_at	DMC1	DMC1 dosage suppressor of mck1 homolog, meiosis-specific homologous recombination (yeast)	11144
210219_at	SP100	SP100 nuclear antigen	6672
211100_x_at	LILRA2	leukocyte immunoglobulin-like receptor, subfamily A (with TM domain), member 2	11027
211740_at	ICA1	islet cell autoantigen 1, 69kDa	3382

Affymetrix ID	Gene Symbol	Gene Name	Entrez Gene ID
214713_at	YLPM1	YLP motif containing 1	56252
215041_s_at	DOCK9	dedicator of cytokinesis 9	23348
215108_x_at	TOX3	TOX high mobility group box family member 3	27324
216131_at	FRMD4B	FERM domain containing 4B	23150
216480_x_at	MLLT10	Myeloid/lymphoid or mixed-lineage leukemia (trithorax homolog, Drosophila); translocated to, 10	8028
216623_x_at	TOX3	TOX high mobility group box family member 3	27324
217546_at	MT1M	metallothionein 1M	4499
218110_at	XAB2	XPA binding protein 2	56949
220149_at	C2orf54	chromosome 2 open reading frame 54	79919
224262_at	IL1F10	interleukin 1 family, member 10 (theta)	84639
226355_at	WDR51A	WD repeat domain 51A	25886
229381_at	C1orf64	chromosome 1 open reading frame 64	149563
229849_at	WIPF3	WAS/WASL interacting protein family, member 3	644150
235210_s_at	C8orf84	chromosome 8 open reading frame 84	157869
235518_at	SLC8A1	solute carrier family 8 (sodium/calcium exchanger), member 1	6546
236386_at	SUZ12P	Suppressor of zeste 12 homolog pseudogene	440423
236805_at	C9orf96	chromosome 9 open reading frame 96	169436
237144_at	LTBP3	latent transforming growth factor beta binding protein 3	4054
238158_at	MEIG1	meiosis expressed gene 1 homolog (mouse)	644890
238753_at	FREQ	frequenin homolog (Drosophila)	23413
241383_at	ZNF385C	zinc finger protein 385C	201181
1552705_at	DUSP19	dual specificity phosphatase 19	142679
1552787_at	HELB	helicase (DNA) B	92797
1563919_a_at	CCDC123	coiled-coil domain containing 123	84902
1554396_at	UEVLD	UEV and lactate/malate dehyrogenase domains	55293
1555063_at	USP6	ubiquitin specific peptidase 6 (Tre-2 oncogene)	9098
1555078_at	ZNF843	zinc finger protein 843	283933
1555238_at	PTH2	parathyroid hormone 2	113091
1557223_at	RBPMS	RNA binding protein with multiple splicing /// succinate dehydrogenase complex, subunit A, flavoprotein pseudogene 2	11030 /// 727956
1559128_at	HSDL2	hydroxysteroid dehydrogenase like 2	84263
1568606_at	C11orf88	chromosome 11 open reading frame 88	399949
242762_s_at	FAM171B	family with sequence similarity 171, member B	165215
1563318_s_at	MAGIX	MAGI family member, X-linked	79917
205885_s_at	ITGA4	integrin, alpha 4 (antigen CD49D, alpha 4 subunit of VLA-4 receptor)	3676

B. Genes present in ≥3 healthy controls compared to 0 asthmatics

Affymetrix ID	Gene Symbol	Gene Name	Entrez Gene ID
204795_at	PRR3	proline rich 3	80742
205216_s_at	APOH	apolipoprotein H (beta-2-glycoprotein I)	350
205245_at	PARD6A	par-6 partitioning defective 6 homolog alpha (C. elegans)	50855
205708_s_at	TRPM2	transient receptor potential cation channel, subfamily M, member 2	7226
205752_s_at	GSTM5	glutathione S-transferase mu 5	2949
207004_at	BCL2	B-cell CLL/lymphoma 2	596
207095_at	SLC10A2	solute carrier family 10 (sodium/bile acid cotransporter family), member 2	6555
207309_at	NOS1	nitric oxide synthase 1 (neuronal)	4842
207995_s_at	CLEC4M	C-type lectin domain family 4, member M	10332
208147_s_at	CYP2C8	cytochrome P450, family 2, subfamily C, polypeptide 8	1558
210611_s_at	DTNA	dystrobrevin, alpha	1837
210936_at	WDR1	WD repeat domain 1	9948
211909_x_at	PTGER3	prostaglandin E receptor 3 (subtype EP3)	5733
216260_at	DICER1	dicer 1, ribonuclease type III	23405
217400_at	PCNA	proliferating cell nuclear antigen	5111
217622_at	RHBDD3	rhomboid domain containing 3	25807
219846_at	GON4L	gon-4-like (C. elegans)	54856
219908_at	DKK2	dickkopf homolog 2 (Xenopus laevis)	27123
220774_at	DYM	dymeclin	54808
221272_s_at	C1orf21	chromosome 1 open reading frame 21	81563
91703_at	EHBP1L1	EH domain binding protein 1-like 1	254102
225449_at	RDH13	retinol dehydrogenase 13 (all-trans/9-cis)	112724
226292_at	CAPN5	calpain 5	726
227222_at	FBXO10	F-box protein 10	26267
229775_s_at	MLLT4	myeloid/lymphoid or mixed-lineage leukemia (trithorax homolog, Drosophila); translocated to, 4	4301
229914_at	FLJ38717	FLJ38717 protein	401261
234055_s_at	GZF1	GDNF-inducible zinc finger protein 1	64412
235496_at	HRCT1	histidine rich carboxyl terminus 1	646962
236274_at	EIF3B	eukaryotic translation initiation factor 3, subunit B	8662
236847_at	C19orf18	chromosome 19 open reading frame 18	147685
238453_at	FGFBP3	fibroblast growth factor binding protein 3	143282
239607_at	GPR156	G protein-coupled receptor 156	165829
240510_at	NBN	Nibrin	4683
244819_x_at	PSPH	phosphoserine phosphatase	5723
244829_at	C6orf218	chromosome 6 open reading frame 218	221718
1552804_a_at	TIRAP	toll-interleukin 1 receptor (TIR) domain containing adaptor protein	114609
1552912_a_at	IL23R	interleukin 23 receptor	149233

Affymetrix ID	Gene Symbol	Gene Name	Entrez Gene ID
1552980_at	HAS3	hyaluronan synthase 3	3038
1553021_s_at	BICD2	bicaudal D homolog 2 (Drosophila)	23299
1558331_at	SIRT2	Sirtuin (silent mating type information regulation 2 homolog) 2 (S. cerevisiae)	22933
1558732_at	MAP4K4	mitogen-activated protein kinase kinase kinase kinase 4	9448
1559682_at	TRIM16L	Tripartite motif-containing 16-like	147166
1559756_at	DKFZp667F0711	hypothetical protein DKFZp667F0711	399716
212803_at	NAB2	NGFI-A binding protein 2 (EGR1 binding protein 2)	4665
213338_at	TMEM158	transmembrane protein 158	25907
215769_at	TRD@	T cell receptor delta locus	6964
220663_at	IL1RAPL1	interleukin 1 receptor accessory protein-like 1	11141
237210_at	NFRKB	nuclear factor related to kappaB binding protein	4798
240063_at	LOC441046	glucuronidase, beta pseudogene	441046
241478_at	MICALL2	MICAL-like 2	79778
242949_x_at	CCDC157	Coiled-coil domain containing 157	550631
1553175_s_at	PDE5A	phosphodiesterase 5A, cGMP-specific	8654
1555082_a_at	NEK11	NIMA (never in mitosis gene a)- related kinase 11	79858
1556144_at	DHX30	DEAH (Asp-Glu-Ala-His) box polypeptide 30	22907
1559507_at	LOC100130357	similar to hCG2038897	100130357
1564386_at	TXNDC8	thioredoxin domain containing 8 (spermatozoa)	255220
216755_at	OSBPL10	oxysterol binding protein-like 10	114884
204795_at	PRR3	proline rich 3	80742

Appendix 7.2 Difference in baseline gene expression in HAEBC between health and asthma. A shows all the genes present in ≥3 asthmatics compared to 0 healthy control. C shows all the genes present in ≥3 healthy controls compared to 0 asthmatics.

8. References

References

(1) Bousquet J, Khaltaev N, editors. Global surveillance, prevention and control of chronic respiratory diseases: a comprhensive approach. WHO Press: World Health Organization; 2007.

(2) Masoli M, Fabian D, Holt S, Beasley R. The global burden of asthma: Executive summary of the GINA Dissemination Committee Report. *Allergy: European Journal of Allergy and Clinical Immunology* 2004;59:469-478.

(3) Asthma U. Facts for journalists. 2012.

(4) BTS BTS, editor. British Guideline on the Management of Asthma: A national clinical guideline. ; 2009.

(5) O'Byrne PM. Global guidelines for asthma management: summary of the current status and future challenges. *Pol Arch Med Wewn* 2010;120:511-517.

(6) Hargreave FE, Dolovich J, Newhouse MT. The assessment and treatment of asthma: a conference report. *J Allergy Clin Immunol* 1990;85:1098-1111.

(7) Reddel HK, Taylor DR, Bateman ED, Boulet LP, Boushey HA, Busse WW, Casale TB, Chanez P, Enright PL, Gibson PG, de Jongste JC, Kerstjens HA, Lazarus SC, Levy ML, O'Byrne PM, Partridge MR, Pavord ID, Sears MR, Sterk PJ, Stoloff SW, Sullivan SD, Szefler SJ, Thomas MD, Wenzel SE, American Thoracic Society/European Respiratory Society Task Force on Asthma Control and Exacerbations. An official American Thoracic Society/European Respiratory Society statement: asthma control and exacerbations: standardizing endpoints for clinical asthma trials and clinical practice. *Am J Respir Crit Care Med* 2009;180:59-99.

(8) Woodruff PG, Boushey HA, Dolganov GM, Barker CS, Yee HY, Donnelly S, Ellwanger A, Sidhu SS, Dao-Pick TP, Pantoja C, Erle DJ, Yamamoto KR, Fahy JV. Genome-wide profiling identifies epithelial cell genes associated with asthma and with treatment response to corticosteroids. *Proc Natl Acad Sci U S A* 2007;104:15858-15863.

(9) Wenzel SE, Balzar S, Ampleford E, Hawkins GA, Busse WW, Calhoun WJ, Castro M, Chung KF, Erzurum S, Gaston B, Israel E, Teague WG, Curran-Everett D, Meyers DA, Bleecker ER. IL4R alpha mutations are associated with asthma exacerbations and mast cell/IgE expression. *Am J Respir Crit Care Med* 2007;175:570-576.

(10) Moffatt MF, Kabesch M, Liang L, Dixon AL, Strachan D, Heath S, Depner M, von Berg A, Bufe A, Rietschel E, Heinzmann A, Simma B, Frischer T, Willis-Owen SA, Wong KC, Illig T, Vogelberg C, Weiland SK, von Mutius E, Abecasis GR, Farrall M, Gut IG, Lathrop GM, Cookson WO. Genetic variants regulating ORMDL3 expression contribute to the risk of childhood asthma. *Nature* 2007;448:470-473.

(11) Gudbjartsson DF, Bjornsdottir US, Halapi E, Helgadottir A, Sulem P, Jonsdottir GM, Thorleifsson G, Helgadottir H, Steinthorsdottir V, Stefansson H, Williams C, Hui J, Beilby J, Warrington NM, James A, Palmer LJ, Koppelman GH, Heinzmann A, Krueger M, Boezen HM, Wheatley A, Altmuller J, Shin HD, Uh ST, Cheong HS, Jonsdottir B, Gislason D, Park CS, Rasmussen LM, Porsbjerg C, Hansen JW, Backer V, Werge T, Janson C, Jonsson UB, Ng MC, Chan J, So WY, Ma R, Shah SH, Granger CB, Quyyumi AA, Levey AI, Vaccarino V, Reilly MP, Rader DJ, Williams MJ, van Rij AM, Jones GT, Trabetti E, Malerba G, Pignatti PF, Boner A, Pescollderungg L, Girelli D, Olivieri O, Martinelli N, Ludviksson BR, Ludviksdottir D, Eyjolfsson GI, Arnar D, Thorgeirsson G, Deichmann K, Thompson PJ, Wjst M, Hall IP, Postma DS, Gislason T, Gulcher J, Kong A, Jonsdottir I, Thorsteinsdottir U, Stefansson K. Sequence variants affecting eosinophil numbers associate with asthma and myocardial infarction. *Nat Genet* 2009;41:342-347.

(12) Moffatt MF, Gut IG, Demenais F, Strachan DP, Bouzigon E, Heath S, von Mutius E, Farrall M, Lathrop M, Cookson WO, GABRIEL Consortium. A large-scale, consortium-based genomewide association study of asthma. *N Engl J Med* 2010;363:1211-1221.

(13) Li X, Howard TD, Zheng SL, Haselkorn T, Peters SP, Meyers DA, Bleecker ER. Genome-wide association study of asthma identifies RAD50-IL13 and HLA-DR/DQ regions. *J Allergy Clin Immunol* 2010;125:328-335.e11.

(14) Torgerson DG, Ampleford EJ, Chiu GY, Gauderman WJ, Gignoux CR, Graves PE, Himes BE, Levin AM, Mathias RA, Hancock DB, Baurley JW, Eng C, Stern DA, Celedon JC, Rafaels N, Capurso D, Conti DV, Roth LA, Soto-Quiros M, Togias A, Li X, Myers RA, Romieu I, Van Den Berg DJ, Hu D, Hansel NN, Hernandez RD, Israel E, Salam MT, Galanter J, Avila PC, Avila L, Rodriquez-Santana JR, Chapela R, Rodriguez-Cintron W, Diette GB, Adkinson NF, Abel RA, Ross KD, Shi M, Faruque MU, Dunston GM, Watson HR, Mantese VJ, Ezurum SC, Liang L, Ruczinski I, Ford JG, Huntsman S, Chung KF, Vora H, Li X, Calhoun WJ, Castro M, Sienra-Monge JJ, del Rio-Navarro B, Deichmann KA, Heinzmann A, Wenzel SE, Busse WW, Gern JE, Lemanske RF,Jr, Beaty TH, Bleecker ER, Raby BA, Meyers DA, London SJ, Mexico City Childhood Asthma Study (MCAAS), Gilliland FD, Children's Health Study (CHS) and HARBORS study, Burchard EG, Genetics of Asthma in Latino Americans (GALA) Study, Study of Genes-Environment and Admixture in Latino Americans (GALA2) and Study of African Americans, Asthma, Genes & Environments (SAGE), Martinez FD, Childhood Asthma Research and Education (CARE) Network, Weiss ST, Childhood Asthma Management Program (CAMP), Williams LK, Study of Asthma Phenotypes and Pharmacogenomic Interactions by Race-Ethnicity (SAPPHIRE), Barnes KC, Genetic Research on Asthma in African Diaspora (GRAAD) Study, Ober C, Nicolae DL. Meta-analysis of genome-wide association studies of asthma in ethnically diverse North American populations. *Nat Genet* 2011;43:887-892.

(15) Wan YI, Shrine NR, Soler Artigas M, Wain LV, Blakey JD, Moffatt MF, Bush A, Chung KF, Cookson WO, Strachan DP, Heaney L, Al-Momani BA, Mansur AH, Manney S, Thomson NC, Chaudhuri R, Brightling CE, Bafadhel M, Singapuri A, Niven R, Simpson A, Holloway JW, Howarth PH, Hui J, Musk AW, James AL, the Australian Asthma Genetics Consortium, Brown MA, Baltic S, Ferreira MA, Thompson PJ, Tobin MD, Sayers I, Hall IP. Genome-wide association study to identify genetic determinants of severe asthma. *Thorax* 2012;67:762-768.

(16) Repapi E, Sayers I, Wain LV, Burton PR, Johnson T, Obeidat M, Zhao JH, Ramasamy A, Zhai G, Vitart V, Huffman JE, Igl W, Albrecht E, Deloukas P, Henderson J, Granell R, McArdle WL, Rudnicka AR, Wellcome Trust Case Control Consortium, Barroso I, Loos RJ, Wareham NJ, Mustelin L, Rantanen T, Surakka I, Imboden M, Wichmann HE, Grkovic I, Jankovic S, Zgaga L, Hartikainen AL, Peltonen L, Gyllensten U, Johansson A, Zaboli G, Campbell H, Wild SH, Wilson JF, Glaser S, Homuth G, Volzke H, Mangino M, Soranzo N, Spector TD, Polasek O, Rudan I, Wright AF, Heliovaara M, Ripatti S, Pouta A, Naluai AT, Olin AC, Toren K, Cooper MN, James AL, Palmer LJ, Hingorani AD, Wannamethee SG, Whincup PH, Smith GD, Ebrahim S, McKeever TM, Pavord ID, MacLeod AK, Morris AD, Porteous DJ, Cooper C, Dennison E, Shaheen S, Karrasch S, Schnabel E, Schulz H, Grallert H, Bouatia-Naji N, Delplanque J, Froguel P, Blakey JD, NSHD Respiratory Study Team, Britton JR, Morris RW, Holloway JW, Lawlor DA, Hui J, Nyberg F, Jarvelin MR, Jackson C, Kahonen M, Kaprio J, Probst-Hensch NM, Koch B, Hayward C, Evans DM, Elliott P, Strachan DP, Hall IP, Tobin MD. Genome-wide association study identifies five loci associated with lung function. *Nat Genet* 2010;42:36-44.

(17) Van Eerdewegh P, Little RD, Dupuis J, Del Mastro RG, Falls K, Simon J, Torrey D, Pandit S, McKenny J, Braunschweiger K, Walsh A, Liu Z, Hayward B, Folz C, Manning SP, Bawa A, Saracino L, Thackston M, Benchekroun Y, Capparell N, Wang M, Adair R, Feng Y, Dubois J, FitzGerald MG, Huang H, Gibson R, Allen KM, Pedan A, Danzig MR, Umland SP, Egan RW, Cuss FM, Rorke S, Clough JB, Holloway JW, Holgate ST, Keith TP. Association of the ADAM33 gene with asthma and bronchial hyperresponsiveness. *Nature* 2002;418:426-430.

(18) Wu J, Kobayashi M, Sousa EA, Liu W, Cai J, Goldman SJ, Dorner AJ, Projan SJ, Kavuru MS, Qiu Y, Thomassen MJ. Differential proteomic analysis of bronchoalveolar lavage fluid in asthmatics following segmental antigen challenge. *Mol Cell Proteomics* 2005;4:1251-1264.

(19) Brightling CE, Gupta S, Gonem S, Siddiqui S. Lung damage and airway remodelling in severe asthma. *Clin Exp Allergy* 2012;42:638-649.

(20) Gupta S, Siddiqui S, Haldar P, Entwisle JJ, Mawby D, Wardlaw AJ, Bradding P, Pavord ID, Green RH, Brightling CE. Quantitative analysis of high-resolution computed tomography scans in severe asthma subphenotypes. *Thorax* 2010;65:775-781.

(21) Pavord ID, Brightling CE, Woltmann G, Wardlaw AJ. Non-eosinophilic corticosteroid unresponsive asthma. *Lancet* 1999;353:2213-2214.

(22) Brightling CEFCCP. Clinical Applications of Induced Sputum. *Chest* 2006;130:1626-1627.

(23) Berry M, Morgan A, Shaw DE, Parker D, Green R, Brightling C, Bradding P, Wardlaw AJ, Pavord ID. Pathological features and inhaled corticosteroid response of eosinophilic and non-eosinophilic asthma. *Thorax* 2007;62:1043-1049.

(24) Wenzel SE, Schwartz LB, Langmack EL, Halliday JL, Trudeau JB, Gibbs RL, Chu HW. Evidence that severe asthma can be divided pathologically into two inflammatory subtypes with distinct physiologic and clinical characteristics. *American Journal of Respiratory and Critical Care Medicine* 1999;160:1001-1008.

(25) Green RH, Brightling CE, Woltmann G, Parker D, Wardlaw AJ, Pavord ID. Analysis of induced sputum in adults with asthma: identification of subgroup with isolated sputum neutrophilia and poor response to inhaled corticosteroids. *Thorax* 2002;57:875-879.

(26) Simpson JL, Scott R, Boyle MJ, Gibson PG. Inflammatory subtypes in asthma: Assessment and identification using induced sputum. *Respirology* 2006;11:54-61.

(27) McGrath KW, Icitovic N, Boushey HA, Lazarus SC, Sutherland ER, Chinchilli VM, Fahy JV, Asthma Clinical Research Network of the National Heart, Lung, and Blood Institute. A large subgroup of mild-to-moderate asthma is persistently noneosinophilic. *Am J Respir Crit Care Med* 2012;185:612-619.

(28) Woodruff PG, Khashayar R, Lazarus SC, Janson S, Avila P, Boushey HA, Segal M, Fahy JV. Relationship between airway inflammation, hyperresponsiveness, and obstruction in asthma. *J Allergy Clin Immunol* 2001;108:753-758.

(29) Fahy JV, Kim KW, Liu J, Boushey HA. Prominent neutrophilic inflammation in sputum from subjects with asthma exacerbation. *J Allergy Clin Immunol* 1995;95:843-852.

(30) Turner MO, Hussack P, Sears MR, Dolovich J, Hargreave FE. Exacerbations of asthma without sputum eosinophilia. *Thorax* 1995;50:1057-1061.

(31) Gibson PG, Simpson JL, Saltos N. Heterogeneity of airway inflammation in persistent asthma : evidence of neutrophilic inflammation and increased sputum interleukin-8. *Chest* 2001;119:1329-1336.

(32) Simpson JL, Grissell TV, Douwes J, Scott RJ, Boyle MJ, Gibson PG. Innate immune activation in neutrophilic asthma and bronchiectasis. *Thorax* 2007;62:211-218.

(33) Cox G. Glucocorticoid treatment inhibits apoptosis in human neutrophils. Separation of survival and activation outcomes. *J Immunol* 1995;154:4719-4725.

(34) Jackowski JT, Szepfalusi Z, Wanner DA, Seybold Z, Sielczak MW, Lauredo IT, Adams T, Abraham WM, Wanner A. Effects of P. aeruginosa-derived bacterial products on tracheal ciliary function: role of O2 radicals. *Am J Physiol* 1991;260:L61-7.

(35) Gupta S, Siddiqui S, Haldar P, Raj JV, Entwisle JJ, Wardlaw AJ, Bradding P, Pavord ID, Green RH, Brightling CE. Qualitative analysis of high-resolution CT scans in severe asthma. *Chest* 2009;136:1521-1528.

(36) Haldar P, Pavord ID. Noneosinophilic asthma: A distinct clinical and pathologic phenotype. *J Allergy Clin Immunol* 2007;119:1043-1052.

(37) Woodruff PG, Modrek B, Choy DF, Jia G, Abbas AR, Ellwanger A, Koth LL, Arron JR, Fahy JV. T-helper type 2-driven inflammation defines major subphenotypes of asthma. *Am J Respir Crit Care Med* 2009;180:388-395.

(38) Rhen T, Cidlowski JA. Antiinflammatory action of glucocorticoids--new mechanisms for old drugs. *N Engl J Med* 2005;353:1711-1723.

(39) Barnes PJ. Glucocorticosteroids: current and future directions. *Br J Pharmacol* 2011;163:29-43.

(40) Cooper PR, Panettieri RA,Jr. Steroids completely reverse albuterol-induced beta(2)-adrenergic receptor tolerance in human small airways. *J Allergy Clin Immunol* 2008;122:734-740.

(41) Hasani A, Toms N, O'Connor J, Dilworth JP, Agnew JE. Effect of salmeterol xinafoate on lung mucociliary clearance in patients with asthma. *Respir Med* 2003;97:667-671.

(42) Hasani A, Toms N, Agnew JE, Lloyd J, Dilworth JP. Mucociliary clearance in COPD can be increased by both a D2/beta2 and a standard beta2 agonists. *Respir Med* 2005;99:145-151.

(43) Devalia JL, Sapsford RJ, Rusznak C, Toumbis MJ, Davies RJ. The effects of salmeterol and salbutamol on ciliary beat frequency of cultured human bronchial epithelial cells, in vitro. *Pulm Pharmacol* 1992;5:257-263.

(44) Barnes PJ. Corticosteroid resistance in airway disease. *Proc Am Thorac Soc* 2004;1:264-268.

(45) Haney S, Hancox RJ. Rapid onset of tolerance to beta-agonist bronchodilation. *Respir Med* 2005;99:566-571.

(46) Storms W, Bowdish MS, Farrar JR. Omalizumab and asthma control in patients with moderate-to-severe allergic asthma: a 6-year pragmatic data review. *Allergy Asthma Proc* 2012;33:172-177.

(47) Riccio AM, Dal Negro RW, Micheletto C, De Ferrari L, Folli C, Chiappori A, Canonica GW. Omalizumab modulates bronchial reticular basement membrane thickness and eosinophil infiltration in severe persistent allergic asthma patients. *Int J Immunopathol Pharmacol* 2012;25:475-484.

(48) Rodrigo GJ, Neffen H, Castro-Rodriguez JA. Efficacy and safety of subcutaneous omalizumab vs placebo as add-on therapy to corticosteroids for children and adults with asthma: a systematic review. *Chest* 2011;139:28-35.

(49) Haldar P, Brightling CE, Hargadon B, Gupta S, Monteiro W, Sousa A, Marshall RP, Bradding P, Green RH, Wardlaw AJ, Pavord ID. Mepolizumab and exacerbations of refractory eosinophilic asthma. *N Engl J Med* 2009;360:973-984.

(50) Nair P, Pizzichini MM, Kjarsgaard M, Inman MD, Efthimiadis A, Pizzichini E, Hargreave FE, O'Byrne PM. Mepolizumab for prednisone-dependent asthma with sputum eosinophilia. *N Engl J Med* 2009;360:985-993.

(51) Wills-Karp M, Chiaramonte M. Interleukin-13 in asthma. *Curr Opin Pulm Med* 2003;9:21-27.

(52) Wenzel S, Wilbraham D, Fuller R, Getz EB, Longphre M. Effect of an interleukin-4 variant on late phase asthmatic response to allergen challenge in asthmatic patients: results of two phase 2a studies. *Lancet* 2007;370:1422-1431.

(53) Singh D, Kane B, Molfino NA, Faggioni R, Roskos L, Woodcock A. A phase 1 study evaluating the pharmacokinetics, safety and tolerability of repeat dosing with a human IL-13 antibody (CAT-354) in subjects with asthma. *BMC Pulm Med* 2010;10:3.

(54) Hodsman GP, Ashman C, Cahn A, De Boever E, Locantore N, Serone A, Pouliquen I. A Phase 1, Randomized, Placebo-Controlled, Dose-Escalation Study of an Anti-IL-13 Monoclonal Antibody in Healthy Subjects and Mild Asthmatics. *Br J Clin Pharmacol* 2012.

(55) Ying S, Robinson DS, Varney V, Meng Q, Tsicopoulos A, Moqbel R, Durham SR, Kay AB, Hamid Q. TNF alpha mRNA expression in allergic inflammation. *Clin Exp Allergy* 1991;21:745-750.

(56) Bradding P, Roberts JA, Britten KM, Montefort S, Djukanovic R, Mueller R, Heusser CH, Howarth PH, Holgate ST. Interleukin-4, -5, and -6 and tumor necrosis factor-alpha in normal and asthmatic airways: evidence for the human mast cell as a source of these cytokines. *Am J Respir Cell Mol Biol* 1994;10:471-480.

(57) Baines KJ, Simpson JL, Wood LG, Scott RJ, Gibson PG. Transcriptional phenotypes of asthma defined by gene expression profiling of induced sputum samples. *J Allergy Clin Immunol* 2011;127:153-60, 160.e1-9.

(58) Desai D, Brightling C. TNF-alpha antagonism in severe asthma? *Recent Pat Inflamm Allergy Drug Discov* 2010;4:193-200.

(59) Kraft M, Cassell GH, Pak J, Martin RJ. Mycoplasma pneumoniae and Chlamydia pneumoniae in asthma: effect of clarithromycin. *Chest* 2002;121:1782-1788.

(60) Beigelman, Avraham Gunsten, Sean Mikols,Cassandra L., Vidavsky IC,Carolyn L., Brody SL, Walter MJ. Azithromycin Attenuates Airway Inflammation in a Noninfectious Mouse Model of Allergic Asthma. *Chest* 2009;136:498-506.

(61) Garey KW, Rubinstein I, Gotfried MH, Khan IJ, Varma S, Danziger LH. Long-term clarithromycin decreases prednisone requirements in elderly patients with prednisone-dependent asthma. *Chest* 2000;118:1826-1827.

(62) Jeffrey PK. The development of large and small airways. *Am J Respir Crit Care Med* 1998;157:S174-80.

(63) Lee SL, Adams WP, Li BV, Conner DP, Chowdhury BA, Yu LX. In vitro considerations to support bioequivalence of locally acting drugs in dry powder inhalers for lung diseases. *AAPS J* 2009;11:414-423.

(64) Holgate ST. Epithelium dysfunction in asthma. *J Allergy Clin Immunol* 2007;120:1233-1244.

(65) Godde NJ, Galea RC, Elsum IA, Humbert PO. Cell polarity in motion: redefining mammary tissue organization through EMT and cell polarity transitions. *J Mammary Gland Biol Neoplasia* 2010;15:149-168.

(66) Hajj R, Baranek T, Le Naour R, Lesimple P, Puchelle E, Coraux C. Basal cells of the human adult airway surface epithelium retain transit-amplifying cell properties. *Stem Cells* 2007;25:139-148.

(67) Coraux C, Roux J, Jolly T, Birembaut P. Epithelial cell-extracellular matrix interactions and stem cells in airway epithelial regeneration. *Proceedings of the American Thoracic Society* 2008;5:689-694.

(68) Wanner A, Salathe M, O'Riordan TG. Mucociliary clearance in the airways. *Am J Respir Crit Care Med* 1996;154:1868-1902.

(69) Chilvers MA, McKean M, Rutman A, Myint BS, Silverman M, O'Callaghan C. The effects of coronavirus on human nasal ciliated respiratory epithelium. *European Respiratory Journal* 2001;18:965-970.

(70) Ebnet K. Organization of multiprotein complexes at cell-cell junctions. *Histochem Cell Biol* 2008;130:1-20.

(71) AntibodyAndBeyond. Epithelial Cell Markers. 2007.

(72) Damjanovich L, Albelda SM, Mette SA, Buck CA. Distribution of integrin cell adhesion receptors in normal and malignant lung tissue. *Am J Respir Cell Mol Biol* 1992;6:197-206.

(73) Paulsson M. Basement membrane proteins: structure, assembly, and cellular interactions. *Crit Rev Biochem Mol Biol* 1992;27:93-127.

(74) Knight DA, Holgate ST. The airway epithelium: structural and functional properties in health and disease. *Respirology* 2003;8:432-446.

(75) Jeffrey PK. The development of large and small airways. *Am J Respir Crit Care Med* 1998;157:S174-80.

(76) Evans CM, Koo JS. Airway mucus: The good, the bad, the sticky. *Pharmacology and Therapeutics* 2009;121:332-348.

(77) Crystal RG, Randell SH, Engelhardt JF, Voynow J, Sunday ME. Airway epithelial cells: current concepts and challenges. *Proc Am Thorac Soc* 2008;5:772-777.

(78) Parker D, Prince A. Innate immunity in the respiratory epithelium. *Am J Respir Cell Mol Biol* 2011;45:189-201.

(79) Evans CM, Kim K, Tuvim MJ, Dickey BF. Mucus hypersecretion in asthma: Causes and effects. *Curr Opin Pulm Med* 2009;15:4-11.

(80) Knowles MR, Boucher RC. Mucus clearance as a primary innate defense mechanism for mammalian airways. *J Clin Invest* 2002;109:571-577.

(81) Tarran R, Button B, Boucher RC. Regulation of normal and cystic fibrosis airway surface liquid volume by phasic shear stress. *Annu Rev Physiol* 2006;68:543-561.

(82) Widdicombe JG. Airway liquid: a barrier to drug diffusion? *Eur Respir J* 1997;10:2194-2197.

(83) Thornton DJ, Rousseau K, McGuckin MA. Structure and function of the polymeric mucins in airways mucus. *Annu Rev Physiol* 2008;70:459-486.

(84) Wang K, Wen F-, Xu D. Mucus hypersecretion in the airway. *Chin Med J* 2008;121:649-652.

(85) Girod S, Zahm JM, Plotkowski C, Beck G, Puchelle E. Role of the physiochemical properties of mucus in the protection of the respiratory epithelium. *Eur Respir J* 1992;5:477-487.

(86) Sleigh MA, Blake JR, Liron N. The propulsion of mucus by cilia. *Am Rev Respir Dis* 1988;137:726-741.

(87) Jain R, Pan J, Driscoll JA, Wisner JW, Huang T, Gunsten SP, You Y, Brody SL. The Temporal Relationship Between Primary and Motile Ciliogenesis in Airway Epithelial Cells. *Am J Respir Cell Mol Biol* 2010.

(88) Dai D, Li L, Huebner A, Zeng H, Guevara E, Claypool DJ, Liu A, Chen J. Planar cell polarity effector gene Intu regulates cell fate-specific differentiation of keratinocytes through the primary cilia. *Cell Death Differ* 2012.

(89) Wallingford JB, Mitchell B. Strange as it may seem: the many links between Wnt signaling, planar cell polarity, and cilia. *Genes Dev* 2011;25:201-213.

(90) Heijink IH, Brandenburg SM, Noordhoek JA, Postma DS, Slebos DJ, van Oosterhout AJ. Characterisation of cell adhesion in airway epithelial cell types using electric cell-substrate impedance sensing. *Eur Respir J* 2010;35:894-903.

(91) Parker J, Sarlang S, Thavagnanam S, Williamson G, O'donoghue D, Villenave R, Power U, Shields M, Heaney L, Skibinski G. A 3-D well-differentiated model of pediatric bronchial epithelium demonstrates unstimulated morphological differences between asthmatic and nonasthmatic cells. *Pediatr Res* 2010;67:17-22.

(92) Oshima T, Gedda K, Koseki J, Chen X, Husmark J, Watari J, Miwa H, Pierrou S. Establishment of esophageal-like non-keratinized stratified epithelium using normal human bronchial epithelial cells. *Am J Physiol Cell Physiol* 2011;300:C1422-9.

(93) Rhodin JA. The ciliated cell. Ultrastructure and function of the human tracheal mucosa. *Am Rev Respir Dis* 1966;93:Suppl:1-15.

(94) Breeze RG, Wheeldon EB. The cells of the pulmonary airways. *Am Rev Respir Dis* 1977;116:705-777.

(95) Houtmeyers E, Gosselink R, Gayan-Ramirez G, Decramer M. Regulation of mucociliary clearance in health and disease. *Eur Respir J* 1999;13:1177-1188.

(96) Satir P, Sleigh MA. The physiology of cilia and mucociliary interactions. *Annu Rev Physiol* 1990;52:137-155.

(97) Busuttil A, More IA, McSeveney D. A reappraisal of the ultrastructure of the human respiratory nasal mucosa. *J Anat* 1977;124:445-458.

(98) Foliguet B, Puchelle E. Apical structure of human respiratory cilia. *Bull Eur Physiopathol Respir* 1986;22:43-47.

(99) Dirksen ER. Centriole and basal body formation during ciliogenesis revisited. *Biol Cell* 1991;72:31-38.

(100) Thomas B. Ciliated epithelium in respiratory diseases. 2010.

(101) Chilvers MA, O'Callaghan C. Local mucociliary defence mechanisms. *Paediatr Respir Rev* 2000;1:27-34.

(102) Mizuno N, Taschner M, Engel BD, Lorentzen E. Structural studies of ciliary components. *J Mol Biol* 2012;422:163-180.

(103) Teff Z, Priel Z, Gheber LA. Forces applied by cilia measured on explants from mucociliary tissue. *Biophys J* 2007;92:1813-1823.

(104) Teff Z, Priel Z, Gheber LA. The forces applied by cilia depend linearly on their frequency due to constant geometry of the effective stroke. *Biophys J* 2008;94:298-305.

(105) Chilvers MA, Rutman A, O'Callaghan C. Functional analysis of cilia and ciliated epithelial ultrastructure in healthy children and young adults. *Thorax* 2003;58:333-338.

(106) Clary-Meinesz CF, Cosson J, Huitorel P, Blaive B. Temperature effect on the ciliary beat frequency of human nasal and tracheal ciliated cells. *Biol Cell* 1992;76:335-338.

(107) Kilgour E, Rankin N, Ryan S, Pack R. Mucociliary function deteriorates in the clinical range of inspired air temperature and humidity. *Intensive Care Med* 2004;30:1491-1494.

(108) Clary-Meinesz C, Mouroux J, Cosson J, Huitorel P, Blaive B. Influence of external pH on ciliary beat frequency in human bronchi and bronchioles. *Eur Respir J* 1998;11:330-333.

(109) Sutto Z, Conner GE, Salathe M. Regulation of human airway ciliary beat frequency by intracellular pH. *J Physiol (Lond)* 2004;560:519-532.

(110) Horstmann G, Iravani J, Norris Melville G, Richter HG. Influence of temperature and decreased water content of inspired air on the ciliated bronchial epithelium. A physiological and electron microscopical study. *Acta Otolaryngol* 1977;84:124-131.

(111) Mercke U, Toremalm NG. Air humidity and mucociliary activity. *Ann Otol Rhinol Laryngol* 1976;85:32-37.

(112) Luk CK, Dulfano MJ. Effect of pH, viscosity and ionic-strength changes on ciliary beating frequency of human bronchial explants. *Clin Sci (Lond)* 1983;64:449-451.

(113) van de Donk HJ, Zuidema J, Merkus FW. The influence of the pH and osmotic pressure upon tracheal ciliary beat frequency as determined with a new photo-electric registration device. *Rhinology* 1980;18:93-104.

(114) Braiman A, Priel Z. Intracellular stores maintain stable cytosolic Ca(2+) gradients in epithelial cells by active Ca(2+) redistribution. *Cell Calcium* 2001;30:361-371.

(115) Lansley AB, Sanderson MJ, Dirksen ER. Control of the beat cycle of respiratory tract cilia by Ca2+ and cAMP. *Am J Physiol* 1992;263:L232-42.

(116) Nlend MC, Bookman RJ, Conner GE, Salathe M. Regulator of G-protein signaling protein 2 modulates purinergic calcium and ciliary beat frequency responses in airway epithelia. *American Journal of Respiratory Cell & Molecular Biology* 2002;27:436-445.

(117) Lansley AB, Sanderson MJ. Regulation of airway ciliary activity by Ca2+: simultaneous measurement of beat frequency and intracellular Ca2+. *Biophys J* 1999;77:629-638.

(118) Zhang L, Sanderson MJ. Oscillations in ciliary beat frequency and intracellular calcium concentration in rabbit tracheal epithelial cells induced by ATP. *J Physiol* 2003;546:733-749.

(119) Lorenzo IM, Liedtke W, Sanderson MJ, Valverde MA. TRPV4 channel participates in receptor-operated calcium entry and ciliary beat frequency regulation in mouse airway epithelial cells. *Proc Natl Acad Sci U S A* 2008;105:12611-12616.

(120) Ma W, Korngreen A, Weil S, Cohen EB, Priel A, Kuzin L, Silberberg SD. Pore properties and pharmacological features of the P2X receptor channel in airway ciliated cells. *J Physiol* 2006;571:503-517.

(121) Uzlaner N, Priel Z. Interplay between the NO pathway and elevated [Ca2+]i enhances ciliary activity in rabbit trachea. *J Physiol* 1999;516 (Pt 1):179-190.

(122) Zhang L, Sanderson MJ. The role of cGMP in the regulation of rabbit airway ciliary beat frequency. *J Physiol* 2003;551:765-776.

(123) Jiao J, Han D, Meng N, Jin S, Zhang L. Regulation of tracheal ciliary beat frequency by nitric oxide synthase substrate L-arginine. *ORL J Otorhinolaryngol Relat Spec* 2010;72:6-11.

(124) Reddy MM, Kopito RR, Quinton PM. Cytosolic pH regulates GCl through control of phosphorylation states of CFTR. *Am J Physiol* 1998;275:C1040-7.

(125) Maurer DR, Sielczak M, Oliver W,Jr, Abraham WM, Wanner A. Role of ciliary motility in acute allergic mucociliary dysfunction. *J Appl Physiol* 1982;52:1018-1023.

(126) Moller W, Haussinger K, Ziegler-Heitbrock L, Heyder J. Mucociliary and long-term particle clearance in airways of patients with immotile cilia. *Respir Res* 2006;7:10.

(127) Greenstone M, Rutman A, Dewar A, Mackay I, Cole PJ. Primary ciliary dyskinesia: cytological and clinical features. *Q J Med* 1988;67:405-423.

(128) Chilvers MAMRCPCH, Rutman A, O'Callaghan CFRCPCH. Ciliary Beat Pattern is Associated with Specific Ultrastructural Defects in Primary Ciliary Dyskinesia. *Journal of Allergy & Clinical Immunology* 2003;112:518-524.

(129) Mygind N, Pedersen M, Nielsen MH. Primary and secondary ciliary dyskinesia. *Acta Otolaryngol* 1983;95:688-694.

(130) Bertrand B, Collet S, Eloy P, Rombaux P. Secondary ciliary dyskinesia in upper respiratory tract. *Acta Otorhinolaryngol Belg* 2000;54:309-316.

(131) Pifferi, Massimo Caramella, Davide Cangiotti,Angela M., Ragazzo, Vincenzo Macchia, Pierantonio Boner,Attilio L. Nasal Nitric Oxide in Atypical Primary Ciliary Dyskinesia*. *Chest* 2007;131:870-873.

(132) O'Callaghan CL, Sikand K, Rutman A, Hirst RA. The effect of viscous loading on brain ependymal cilia. *Neurosci Lett* 2008;439:56-60.

(133) Dziarski R, Wang Q, Miyake K, Kirschning CJ, Gupta D. MD-2 enables Toll-like receptor 2 (TLR2)-mediated responses to lipopolysaccharide and enhances TLR2-mediated responses to Gram-positive and Gram-negative bacteria and their cell wall components. *J Immunol* 2001;166:1938-1944.

(134) Govindaraj RG, Manavalan B, Lee G, Choi S. Molecular modeling-based evaluation of hTLR10 and identification of potential ligands in Toll-like receptor signaling. *PLoS One* 2010;5:e12713.

(135) Moresco EM, LaVine D, Beutler B. Toll-like receptors. *Curr Biol* 2011;21:R488-93.

(136) Tang D, Kang R, Coyne CB, Zeh HJ, Lotze MT. PAMPs and DAMPs: signal 0s that spur autophagy and immunity. *Immunol Rev* 2012;249:158-175.

(137) Lin CF, Tsai CH, Cheng CH, Chen YS, Tournier F, Yeh TH. Expression of Toll-like receptors in cultured nasal epithelial cells. *Acta Otolaryngol* 2007;127:395-402.

(138) Winder AA, Wohlford-Lenane C, Scheetz TE, Nardy BN, Manzel LJ, Look DC, McCray PB,Jr. Differential effects of cytokines and corticosteroids on toll-like receptor 2 expression and activity in human airway epithelia. *Respir Res* 2009;10:96.

(139) Hammad H, Chieppa M, Perros F, Willart MA, Germain RN, Lambrecht BN. House dust mite allergen induces asthma via Toll-like receptor 4 triggering of airway structural cells. *Nat Med* 2009;15:410-416.

(140) Walter MJ, Kajiwara N, Karanja P, Castro M, Holtzman MJ. Interleukin 12 p40 production by barrier epithelial cells during airway inflammation. *J Exp Med* 2001;193:339-351.

(141) Lordan JL, Bucchieri F, Richter A, Konstantinidis A, Holloway JW, Thornber M, Puddicombe SM, Buchanan D, Wilson SJ, Djukanovic R, Holgate ST, Davies DE. Cooperative effects of Th2 cytokines and allergen on normal and asthmatic bronchial epithelial cells. *J Immunol* 2002;169:407-414.

(142) Simpson JL, Brooks C, Douwes J. Innate immunity in asthma. *Paediatr Respir Rev* 2008;9:263-270.

(143) Matsukura S, Stellato C, Georas SN, Casolaro V, Plitt JR, Miura K, Kurosawa S, Schindler U, Schleimer RP. Interleukin-13 upregulates eotaxin expression in airway epithelial cells by a STAT6-dependent mechanism. *Am J Respir Cell Mol Biol* 2001;24:755-761.

(144) Stirling RG, van Rensen EL, Barnes PJ, Chung KF. Interleukin-5 induces CD34(+) eosinophil progenitor mobilization and eosinophil CCR3 expression in asthma. *Am J Respir Crit Care Med* 2001;164:1403-1409.

(145) Sukkar MB, Xie S, Khorasani NM, Kon OM, Stanbridge R, Issa R, Chung KF. Toll-like receptor 2, 3, and 4 expression and function in human airway smooth muscle. *J Allergy Clin Immunol* 2006;118:641-648.

(146) Segal AW. The antimicrobial role of the neutrophil leukocyte. *J Infect* 1981;3:3-17.

(147) Xu PC, Hao J, Yang XW, Chang DY, Chen M, Zhao MH. C-reactive protein enhances the respiratory burst of neutrophils-induced by antineutrophil cytoplasmic antibody. *Mol Immunol* 2012;52:148-154.

(148) Barnes PJ. The cytokine network in asthma and chronic obstructive pulmonary disease. *J Clin Invest* 2008;118:3546-3556.

(149) Takeda N, Sumi Y, Prefontaine D, Al Abri J, Al Heialy N, Al-Ramli W, Michoud M-, Martin JG, Hamid Q. Epithelium-derived chemokines induce airway smooth muscle cell migration. *Clinical and Experimental Allergy* 2009;39:1018-1026.

(150) Lambrecht BN, Hammad H. The airway epithelium in asthma. *Nat Med* 2012;18:684-692.

(151) Ckless K, Hodgkins SR, Ather JL, Martin R, Poynter ME. Epithelial, dendritic, and CD4(+) T cell regulation of and by reactive oxygen and nitrogen species in allergic sensitization. *Biochim Biophys Acta* 2011;1810:1025-1034.

(152) Duszyk M. Regulation of anion secretion by nitric oxide in human airway epithelial cells. *Am J Physiol Lung Cell Mol Physiol* 2001;281:L450-7.

(153) Sauer H, Wartenberg M, Hescheler J. Reactive oxygen species as intracellular messengers during cell growth and differentiation. *Cell Physiol Biochem* 2001;11:173-186.

(154) Forman HJ, Maiorino M, Ursini F. Signaling functions of reactive oxygen species. *Biochemistry* 2010;49:835-842.

(155) Wang Y, Bai C, Li K, Adler KB, Wang X. Role of airway epithelial cells in development of asthma and allergic rhinitis. *Respir Med* 2008;102:949-955.

(156) Holgate ST. The airway epithelium is central to the pathogenesis of asthma. *Allergol Int* 2008;57:1-10.

(157) Selsted ME, Tang YQ, Morris WL, McGuire PA, Novotny MJ, Smith W, Henschen AH, Cullor JS. Purification, primary structures, and antibacterial activities of beta-defensins, a new family of antimicrobial peptides from bovine neutrophils. *J Biol Chem* 1993;268:6641-6648.

(158) Kao CY, Chen Y, Zhao YH, Wu R. ORFeome-based search of airway epithelial cell-specific novel human [beta]-defensin genes. *Am J Respir Cell Mol Biol* 2003;29:71-80.

(159) McCray PB,Jr, Bentley L. Human airway epithelia express a beta-defensin. *Am J Respir Cell Mol Biol* 1997;16:343-349.

(160) Chen PH, Fang SY. Expression of human beta-defensin 2 in human nasal mucosa. *Eur Arch Otorhinolaryngol* 2004;261:238-241.

(161) Harder J, Meyer-Hoffert U, Teran LM, Schwichtenberg L, Bartels J, Maune S, Schroder J-. Mucoid Pseudomonas aeruginosa, TNF-alpha, and IL-beta, but not IL-6, induce human beta-defensin-2 in respiratory epithelia. *American Journal of Respiratory Cell and Molecular Biology* 2000;22:ate of Pubaton: 2000.

(162) Garcia JR, Krause A, Schulz S, Rodriguez-Jimenez FJ, Kluver E, Adermann K, Forssmann U, Frimpong-Boateng A, Bals R, Forssmann WG. Human beta-defensin 4: a novel inducible peptide with a specific salt-sensitive spectrum of antimicrobial activity. *FASEB J* 2001;15:1819-1821.

(163) Duits LA, Nibbering PH, van Strijen E, Vos JB, Mannesse-Lazeroms SP, van Sterkenburg MA, Hiemstra PS. Rhinovirus increases human beta-defensin-2 and -3 mRNA expression in cultured bronchial epithelial cells. *FEMS Immunol Med Microbiol* 2003;38:59-64.

(164) Selsted ME, Ouellette AJ. Mammalian defensins in the antimicrobial immune response. *Nat Immunol* 2005;6:551-557.

(165) Pazgier M, Hoover DM, Yang D, Lu W, Lubkowski J. Human beta-defensins. *Cell Mol Life Sci* 2006;63:1294-1313.

(166) Krishnakumari V, Rangaraj N, Nagaraj R. Antifungal activities of human beta-defensins HBD-1 to HBD-3 and their C-terminal analogs Phd1 to Phd3. *Antimicrob Agents Chemother* 2009;53:256-260.

(167) Alekseeva L, Huet D, Femenia F, Mouyna I, Abdelouahab M, Cagna A, Guerrier D, Tichanne-Seltzer V, Baeza-Squiban A, Chermette R, Latge JP, Berkova N. Inducible expression of beta defensins by human respiratory epithelial cells exposed to Aspergillus fumigatus organisms. *BMC Microbiol* 2009;9:33.

(168) Gropp R, Frye M, Wagner TO, Bargon J. Epithelial defensins impair adenoviral infection: implication for adenovirus-mediated gene therapy. *Hum Gene Ther* 1999;10:957-964.

(169) Kluver E, Adermann K, Schulz A. Synthesis and structure-activity relationship of beta-defensins, multi-functional peptides of the immune system. *J Pept Sci* 2006;12:243-257.

(170) Goldman MJ, Anderson GM, Stolzenberg ED, Kari UP, Zasloff M, Wilson JM. Human beta-defensin-1 is a salt-sensitive antibiotic in lung that is inactivated in cystic fibrosis. *Cell* 1997;88:ate of Pubaton: 21 Feb 1997.

(171) Bals R, Wang X, Wu Z, Freeman T, Bafna V, Zasloff M, Wilson JM. Human beta-defensin 2 is a salt-sensitive peptide antibiotic expressed in human lung. *J Clin Invest* 1998;102:874-880.

(172) Soruri A, Grigat J, Forssmann U, Riggert J, Zwirner J. beta-Defensins chemoattract macrophages and mast cells but not lymphocytes and dendritic cells: CCR6 is not involved. *Eur J Immunol* 2007;37:2474-2486.

(173) Yang D, Chertov O, Bykovskaia SN, Chen Q, Buffo MJ, Shogan J, Anderson M, Schroder JM, Wang JM, Howard OM, Oppenheim JJ. Beta-defensins: linking innate and adaptive immunity through dendritic and T cell CCR6. *Science* 1999;286:525-528.

(174) Funderburg N, Lederman MM, Feng Z, Drage MG, Jadlowsky J, Harding CV, Weinberg A, Sieg SF. Human -defensin-3 activates professional antigen-presenting cells via Toll-like receptors 1 and 2. *Proc Natl Acad Sci U S A* 2007;104:18631-18635.

(175) Hertz CJ, Wu Q, Porter EM, Zhang YJ, Weismuller KH, Godowski PJ, Ganz T, Randell SH, Modlin RL. Activation of Toll-like receptor 2 on human tracheobronchial epithelial cells induces the antimicrobial peptide human beta defensin-2. *J Immunol* 2003;171:6820-6826.

(176) Hackett TL, Singhera GK, Shaheen F, Hayden P, Jackson GR, Hegele RG, Van Eeden S, Bai TR, Dorscheid DR, Knight DA. Intrinsic phenotypic differences of asthmatic epithelium and its inflammatory responses to respiratory syncytial virus and air pollution. *Am J Respir Cell Mol Biol* 2011;45:1090-1100.

(177) Masuyama K, Morishima Y, Ishii Y, Nomura A, Sakamoto T, Kimura T, Mochizuki M, Uchida Y, Sekizawa K. Sputum E-cadherin and asthma severity. *J Allergy Clin Immunol* 2003;112:208-209.

(178) Cohen L, E X, Tarsi J, Ramkumar T, Horiuchi TK, Cochran R, DeMartino S, Schechtman KB, Hussain I, Holtzman MJ, Castro M, and the NHLBI Severe Asthma Research Program (SARP). Epithelial cell proliferation contributes to airway remodeling in severe asthma. *Am J Respir Crit Care Med* 2007;176:138-145.

(179) Benayoun L, Druilhe A, Dombret MC, Aubier M, Pretolani M. Airway structural alterations selectively associated with severe asthma. *American Journal of Respiratory & Critical Care Medicine* 2003;167:1360-1368.

(180) Kicic A, Sutanto EN, Stevens PT, Knight DA, Stick SM. Intrinsic biochemical and functional differences in bronchial epithelial cells of children with asthma. *Am J Respir Crit Care Med* 2006;174:1110-1118.

(181) Wark PA, Johnston SL, Bucchieri F, Powell R, Puddicombe S, Laza-Stanca V, Holgate ST, Davies DE. Asthmatic bronchial epithelial cells have a deficient innate immune response to infection with rhinovirus. *J Exp Med* 2005;201:937-947.

(182) Contoli M, Message SD, Laza-Stanca V, Edwards MR, Wark PA, Bartlett NW, Kebadze T, Mallia P, Stanciu LA, Parker HL, Slater L, Lewis-Antes A, Kon OM, Holgate ST, Davies DE, Kotenko SV, Papi A, Johnston SL. Role of deficient type III interferon-lambda production in asthma exacerbations. *Nat Med* 2006;12:1023-1026.

(183) Xiao C, Puddicombe SM, Field S, Haywood J, Broughton-Head V, Puxeddu I, Haitchi HM, Vernon-Wilson E, Sammut D, Bedke N, Cremin C, Sones J, Djukanovic R, Howarth PH, Collins JE, Holgate ST, Monk P, Davies DE. Defective epithelial barrier function in asthma. *J Allergy Clin Immunol* 2011;128:549-56.e1-12.

(184) Gras D, Bourdin A, Vachier I, de Senneville L, Bonnans C, Chanez P. An ex vivo model of severe asthma using reconstituted human bronchial epithelium. *J Allergy Clin Immunol* 2012;129:1259-1266.e1.

(185) Kicic A, Hallstrand TS, Sutanto EN, Stevens PT, Kobor MS, Taplin C, Pare PD, Beyer RP, Stick SM, Knight DA. Decreased fibronectin production significantly contributes to dysregulated repair of asthmatic epithelium. *Am J Respir Crit Care Med* 2010;181:889-898.

(186) Hackett T, Warner SM, Stefanowicz D, Shaheen F, Pechkovsky DV, Murray LA, Argentieri R, Kicic A, Stick SM, Bai TR, Knight DA. Induction of Epithelial-Mesenchymal Transition in Primary Airway Epithelial Cells from Patients with Asthma by Transforming Growth Factor-beta 1. *American Journal of Respiratory and Critical Care Medicine* 2009;180:122-133.

(187) Kim KK, Kugler MC, Wolters PJ, Robillard L, Galvez MG, Brumwell AM, Sheppard D, Chapman HA. Alveolar epithelial cell mesenchymal transition develops in vivo during pulmonary fibrosis and is regulated by the extracellular matrix. *Proc Natl Acad Sci U S A* 2006;103:13180-13185.

(188) Torrego A, Hew M, Oates T, Sukkar M, Fan Chung K. Expression and activation of TGF-beta isoforms in acute allergen-induced remodelling in asthma. *Thorax* 2007;62:307-313.

(189) Mukhopadhyay S, Hoidal JR, Mukherjee TK. Role of TNFalpha in pulmonary pathophysiology. *Respir Res* 2006;7:125.

(190) Hays SR, Fahy JV. The role of mucus in fatal asthma. *Am J Med* 2003;115:68-69.

(191) Jenkins HA, Cool C, Szefler SJ, Covar R, Brugman S, Gelfand EW, Spahn JD. Histopathology of severe childhood asthma: a case series. *Chest* 2003;124:32-41.

(192) Ordonez CL, Khashayar R, Wong HH, Ferrando R, Wu R, Hyde DM, Hotchkiss JA, Zhang Y, Novikov A, Dolganov G, Fahy JV. Mild and moderate asthma is associated with airway goblet cell hyperplasia and abnormalities in mucin gene expression. *Am J Respir Crit Care Med* 2001;163:517-523.

(193) Jinnai M, Niimi A, Ueda T, Matsuoka H, Takemura M, Yamaguchi M, Otsuka K, Oguma T, Takeda T, Ito I, Matsumoto H, Mishima M. Induced sputum concentrations of mucin in patients with asthma and chronic cough. *Chest* 2010;137:1122-1129.

(194) Del Donno M, Bittesnich D, Chetta A, Olivieri D, Lopez-Vidriero MT. The effect of inflammation on mucociliary clearance in asthma: an overview. *Chest* 2000;118:1142-1149.

(195) Fahy JV, Steiger DJ, Liu J, Basbaum CB, Finkbeiner WE, Boushey HA. Markers of mucus secretion and DNA levels in induced sputum from asthmatic and from healthy subjects. *Am Rev Respir Dis* 1993;147:1132-1137.

(196) Sheehan JK, Richardson PS, Fung DC, Howard M, Thornton DJ. Analysis of respiratory mucus glycoproteins in asthma: a detailed study from a patient who died in status asthmaticus. *Am J Respir Cell Mol Biol* 1995;13:748-756.

(197) Zhen G, Park SW, Nguyenvu LT, Rodriguez MW, Barbeau R, Paquet AC, Erle DJ. IL-13 and epidermal growth factor receptor have critical but distinct roles in epithelial cell mucin production. *Am J Respir Cell Mol Biol* 2007;36:244-253.

(198) Broide DH, Lotz M, Cuomo AJ, Coburn DA, Federman EC, Wasserman SI. Cytokines in symptomatic asthma airways. *J Allergy Clin Immunol* 1992;89:958-967.

(199) Lappalainen U, Whitsett JA, Wert SE, Tichelaar JW, Bry K. Interleukin-1beta causes pulmonary inflammation, emphysema, and airway remodeling in the adult murine lung. *Am J Respir Cell Mol Biol* 2005;32:311-318.

(200) Bry K, Whitsett JA, Lappalainen U. IL-1beta disrupts postnatal lung morphogenesis in the mouse. *Am J Respir Cell Mol Biol* 2007;36:32-42.

(201) Song KS, Lee WJ, Chung KC, Koo JS, Yang EJ, Choi JY, Yoon JH. Interleukin-1 beta and tumor necrosis factor-alpha induce MUC5AC overexpression through a mechanism involving ERK/p38 mitogen-activated protein kinases-MSK1-CREB activation in human airway epithelial cells. *J Biol Chem* 2003;278:23243-23250.

(202) Gibson PG, Zlatic K, Scott J, Sewell W, Woolley K, Saltos N. Chronic cough resembles asthma with IL-5 and granulocyte-macrophage colony-stimulating factor gene expression in bronchoalveolar cells. *J Allergy Clin Immunol* 1998;101:320-326.

(203) Lee JJ, Dimina D, Macias MP, Ochkur SI, McGarry MP, O'Neill KR, Protheroe C, Pero R, Nguyen T, Cormier SA, Lenkiewicz E, Colbert D, Rinaldi L, Ackerman SJ, Irvin CG, Lee NA. Defining a link with asthma in mice congenitally deficient in eosinophils. *Science* 2004;305:1773-1776.

(204) Long AJ, Sypek JP, Askew R, Fish SC, Mason LE, Williams CM, Goldman SJ. Gob-5 contributes to goblet cell hyperplasia and modulates pulmonary tissue inflammation. *Am J Respir Cell Mol Biol* 2006;35:357-365.

(205) Shim JJ, Dabbagh K, Ueki IF, Dao-Pick T, Burgel PR, Takeyama K, Tam DC, Nadel JA. IL-13 induces mucin production by stimulating epidermal growth factor receptors and by activating neutrophils. *Am J Physiol Lung Cell Mol Physiol* 2001;280:L134-40.

(206) Messina MS, O'Riordan TG, Smaldone GC. Changes in mucociliary clearance during acute exacerbations of asthma. *Am Rev Respir Dis* 1991;143:993-997.

(207) Pavia D, Bateman JR, Sheahan NF, Agnew JE, Clarke SW. Tracheobronchial mucociliary clearance in asthma: impairment during remission. *Thorax* 1985;40:171-175.

(208) Foster WM, Langenback EG, Bergofsky EH. Lung mucociliary function in man: interdependence of bronchial and tracheal mucus transport velocities with lung clearance in bronchial asthma and healthy subjects. *Ann Occup Hyg* 1982;26:227-244.

(209) O'Riordan TG, Zwang J, Smaldone GC. Mucociliary clearance in adult asthma. *Am Rev Respir Dis* 1992;146:598-603.

(210) Thomas B, Rutman A, Hirst RA, Haldar P, Wardlaw AJ, Bankart J, Brightling CE, O'Callaghan C. Ciliary dysfunction and ultrastructural abnormalities are features of severe asthma. *J Allergy Clin Immunol* 2010.

(211) Valverde MA, Cantero-Recasens G, Garcia-Elias A, Jung C, Carreras-Sureda A, Vicente R. Ion channels in asthma. *J Biol Chem* 2011;286:32877-32882.

(212) Innes AL, Carrington SD, Thornton DJ, Kirkham S, Rousseau K, Dougherty RH, Raymond WW, Caughey GH, Muller SJ, Fahy JV. Ex vivo sputum analysis reveals impairment of protease-dependent mucus degradation by plasma proteins in acute asthma. *Am J Respir Crit Care Med* 2009;180:203-210.

(213) Harada M, Hirota T, Jodo AI, Hitomi Y, Sakashita M, Tsunoda T, Miyagawa T, Doi S, Kameda M, Fujita K, Miyatake A, Enomoto T, Noguchi E, Masuko H, Sakamoto T, Hizawa N, Suzuki Y, Yoshihara S, Adachi M, Ebisawa M, Saito H, Matsumoto K, Nakajima T, Mathias RA, Rafaels N, Barnes KC, Himes BE, Duan QL, Tantisira KG, Weiss ST, Nakamura Y, Ziegler SF, Tamari M. Thymic stromal lymphopoietin gene promoter polymorphisms are associated with susceptibility to bronchial asthma. *Am J Respir Cell Mol Biol* 2011;44:787-793.

(214) Hussein YM, Awad HA, Shalaby SM, Ali AS, Alzahrani SS. Toll-like receptor 2 and Toll-like receptor 4 polymorphisms and susceptibility to asthma and allergic rhinitis: a case-control analysis. *Cell Immunol* 2012;274:34-38.

(215) Ritz SA, Stampfli MR, Davies DE, Holgate ST, Jordana M. On the generation of allergic airway diseases: from GM-CSF to Kyoto. *Trends Immunol* 2002;23:396-402.

(216) Prefontaine D, Nadigel J, Chouiali F, Audusseau S, Semlali A, Chakir J, Martin JG, Hamid Q. Increased IL-33 expression by epithelial cells in bronchial asthma. *J Allergy Clin Immunol* 2010;125:752-754.

(217) Laoukili J, Perret E, Willems T, Minty A, Parthoens E, Houcine O, Coste A, Jorissen M, Marano F, Caput D, Tournier F. IL-13 alters mucociliary differentiation and ciliary beating of human respiratory epithelial cells. *J Clin Invest* 2001;108:1817-1824.

(218) Thannickal VJ, Fanburg BL. Reactive oxygen species in cell signaling. *Am J Physiol Lung Cell Mol Physiol* 2000;279:L1005-28.

(219) Nadeem A, Masood A, Siddiqui N. Oxidant--antioxidant imbalance in asthma: scientific evidence, epidemiological data and possible therapeutic options. *Ther Adv Respir Dis* 2008;2:215-235.

(220) Duszyk M, Radomski MW. The role of nitric oxide in the regulation of ion channels in airway epithelium: implications for diseases of the lung. *Free Radic Res* 2000;33:449-459.

(221) Rahman I, MacNee W. Role of transcription factors in inflammatory lung diseases. *Thorax* 1998;53:601-612.

(222) Breton CV, Byun HM, Wang X, Salam MT, Siegmund K, Gilliland FD. DNA methylation in the arginase-nitric oxide synthase pathway is associated with exhaled nitric oxide in children with asthma. *Am J Respir Crit Care Med* 2011;184:191-197.

(223) Bayram H, Devalia JL, Khair OA, Abdelaziz MM, Sapsford RJ, Sagai M, Davies RJ. Comparison of ciliary activity and inflammatory mediator release from bronchial epithelial cells of nonatopic nonasthmatic subjects and atopic asthmatic patients and the effect of diesel exhaust particles in vitro. *J Allergy Clin Immunol* 1998;102:771-782.

(224) Lopez-Guisa JM, Powers C, File D, Cochrane E, Jimenez N, Debley JS. Airway epithelial cells from asthmatic children differentially express proremodeling factors. *J Allergy Clin Immunol* 2012;129:990-7.e6.

(225) Huang SK, Xiao HQ, Kleine-Tebbe J, Paciotti G, Marsh DG, Lichtenstein LM, Liu MC. IL-13 expression at the sites of allergen challenge in patients with asthma. *J Immunol* 1995;155:2688-2694.

(226) Elias JA, Lee CG. IL-13 in asthma. The successful integration of lessons from mice and humans. *Am J Respir Crit Care Med* 2011;183:957-958.

(227) Bartlett NW, Walton RP, Edwards MR, Aniscenko J, Caramori G, Zhu J, Glanville N, Choy KJ, Jourdan P, Burnet J, Tuthill TJ, Pedrick MS, Hurle MJ, Plumpton C, Sharp NA, Bussell JN, Swallow DM, Schwarze J, Guy B, Almond JW, Jeffery PK, Lloyd CM, Papi A, Killington RA, Rowlands DJ, Blair ED, Clarke NJ, Johnston SL. Mouse models of rhinovirus-induced disease and exacerbation of allergic airway inflammation. *Nat Med* 2008;14:199-204.

(228) Wu Q, Lu Z, Verghese MW, Randell SH. Airway epithelial cell tolerance to Pseudomonas aeruginosa. *Respir Res* 2005;6:26.

(229) Sont JK, Willems LN, Bel EH, van Krieken JH, Vandenbroucke JP, Sterk PJ. Clinical control and histopathologic outcome of asthma when using airway hyperresponsiveness as an additional guide to long-term treatment. The AMPUL Study Group. *Am J Respir Crit Care Med* 1999;159:1043-1051.

(230) Ward C, Pais M, Bish R, Reid D, Feltis B, Johns D, Walters EH. Airway inflammation, basement membrane thickening and bronchial hyperresponsiveness in asthma. *Thorax* 2002;57:309-316.

(231) Toledo AC, Arantes-Costa FM, Macchione M, Saldiva PH, Negri EM, Lorenzi-Filho G, Martins MA. Salbutamol improves markers of epithelial function in mice with chronic allergic pulmonary inflammation. *Respir Physiol Neurobiol* 2011;177:155-161.

(232) Salathe M. Effects of beta-agonists on airway epithelial cells. *J Allergy Clin Immunol* 2002;110:S275-81.

(233) Piatti G, Ceriotti L, Cavallaro G, Ambrosetti U, Mantovani M, Pistone A, Centanni S. Effects of zafirlukast on bronchial asthma and allergic rhinitis. *Pharmacol Res* 2003;47:541-547.

(234) Joki S, Saano V, Koskela T, Toskala E, Bray MA, Nuutinen J. Effect of leukotriene D4 on ciliary activity in human, guinea-pig and rat respiratory mucosa. *Pulm Pharmacol* 1996;9:231-238.

(235) Sabater JR, Wanner A, Abraham WM. Montelukast prevents antigen-induced mucociliary dysfunction in sheep. *Am J Respir Crit Care Med* 2002;166:1457-1460.

(236) Jain R, Ray JM, Pan JH, Brody SL. Sex hormone-dependent regulation of cilia beat frequency in airway epithelium. *Am J Respir Cell Mol Biol* 2012;46:446-453.

(237) Ege MJ, Mayer M, Normand AC, Genuneit J, Cookson WO, Braun-Fahrlander C, Heederik D, Piarroux R, von Mutius E, GABRIELA Transregio 22 Study Group. Exposure to environmental microorganisms and childhood asthma. *N Engl J Med* 2011;364:701-709.

(238) Bochner BR, Giovannetti L, Viti C. Important discoveries from analysing bacterial phenotypes. *Mol Microbiol* 2008;70:274-280.

(239) Edwards MR, Bartlett NW, Hussell T, Openshaw P, Johnston SL. The microbiology of asthma. *Nat Rev Microbiol* 2012;10:459-471.

(240) Herbst T, Sichelstiel A, Schar C, Yadava K, Burki K, Cahenzli J, McCoy K, Marsland BJ, Harris NL. Dysregulation of allergic airway inflammation in the absence of microbial colonization. *Am J Respir Crit Care Med* 2011;184:198-205.

(241) Nicholson KG, Kent J, Ireland DC. Respiratory viruses and exacerbations of asthma in adults. *BMJ* 1993;307:982-986.

(242) Johnston SL, Pattemore PK, Sanderson G, Smith S, Lampe F, Josephs L, Symington P, O'Toole S, Myint SH, Tyrrell DA. Community study of role of viral infections in exacerbations of asthma in 9-11 year old children. *BMJ* 1995;310:1225-1229.

(243) Hilty M, Burke C, Pedro H, Cardenas P, Bush A, Bossley C, Davies J, Ervine A, Poulter L, Pachter L, Moffatt MF, Cookson WO. Disordered microbial communities in asthmatic airways. *PLoS One* 2010;5:e8578.

(244) Huang YJ, Nelson CE, Brodie EL, Desantis TZ, Baek MS, Liu J, Woyke T, Allgaier M, Bristow J, Wiener-Kronish JP, Sutherland ER, King TS, Icitovic N, Martin RJ, Calhoun WJ, Castro M, Denlinger LC, Dimango E, Kraft M, Peters SP, Wasserman SI, Wechsler ME, Boushey HA, Lynch SV, National Heart, Lung, and Blood Institute's Asthma Clinical Research Network. Airway microbiota and bronchial hyperresponsiveness in patients with suboptimally controlled asthma. *J Allergy Clin Immunol* 2011;127:372-381.e1-3.

(245) Martin C, Uhlig S, Ullrich V. Cytokine-induced bronchoconstriction in precision-cut lung slices is dependent upon cyclooxygenase-2 and thromboxane receptor activation. *Am J Respir Cell Mol Biol* 2001;24:139-145.

(246) Cosentini R, Tarsia P, Canetta C, Graziadei G, Brambilla AM, Aliberti S, Pappalettera M, Tantardini F, Blasi F. Severe asthma exacerbation: role of acute Chlamydophila pneumoniae and Mycoplasma pneumoniae infection. *Respir Res* 2008;9:48.

(247) Bisgaard H, Hermansen MN, Buchvald F, Loland L, Halkjaer LB, Bonnelykke K, Brasholt M, Heltberg A, Vissing NH, Thorsen SV, Stage M, Pipper CB. Childhood asthma after bacterial colonization of the airway in neonates. *N Engl J Med* 2007;357:1487-1495.

(248) ten Brinke A, van Dissel JT, Sterk PJ, Zwinderman AH, Rabe KF, Bel EH. Persistent airflow limitation in adult-onset nonatopic asthma is associated with serologic evidence of Chlamydia pneumoniae infection. *J Allergy Clin Immunol* 2001;107:449-454.

(249) Martin RJ, Kraft M, Chu HW, Berns EA, Cassell GH. A link between chronic asthma and chronic infection. *J Allergy Clin Immunol* 2001;107:595-601.

(250) Harju TH, Leinonen M, Nokso-Koivisto J, Korhonen T, Raty R, He Q, Hovi T, Mertsola J, Bloigu A, Rytila P, Saikku P. Pathogenic bacteria and viruses in induced sputum or pharyngeal secretions of adults with stable asthma. *Thorax* 2006;61:579-584.

(251) Wu Q, Martin RJ, LaFasto S, Chu HW. A low dose of Mycoplasma pneumoniae infection enhances an established allergic inflammation in mice: the role of the prostaglandin E2 pathway. *Clin Exp Allergy* 2009;39:1754-1763.

(252) Feldman C, Anderson R, Cockeran R, Mitchell T, Cole P, Wilson R. The effects of pneumolysin and hydrogen peroxide, alone and in combination, on human ciliated epithelium in vitro. *Respir Med* 2002;96:580-585.

(253) Wilson R, Pitt T, Taylor G, Watson D, MacDermot J, Sykes D, Roberts D, Cole P. Pyocyanin and 1-hydroxyphenazine produced by Pseudomonas aeruginosa inhibit the beating of human respiratory cilia in vitro. *J Clin Invest* 1987;79:221-229.

(254) Mallants R, Jorissen M, Augustijns P. Beneficial effect of antibiotics on ciliary beat frequency of human nasal epithelial cells exposed to bacterial toxins. *J Pharm Pharmacol* 2008;60:437-443.

(255) Wilson R, Roberts D, Cole P. Effect of bacterial products on human ciliary function in vitro. *Thorax* 1985;40:125-131.

(256) Raoust E, Balloy V, Garcia-Verdugo I, Touqui L, Ramphal R, Chignard M. Pseudomonas aeruginosa LPS or flagellin are sufficient to activate TLR-dependent signaling in murine alveolar macrophages and airway epithelial cells. *PLoS One* 2009;4:e7259.

(257) Hajjar AM, Ernst RK, Tsai JH, Wilson CB, Miller SI. Human Toll-like receptor 4 recognizes host-specific LPS modifications. *Nat Immunol* 2002;3:354-359.

(258) Guillot L, Medjane S, Le-Barillec K, Balloy V, Danel C, Chignard M, Si-Tahar M. Response of human pulmonary epithelial cells to lipopolysaccharide involves Toll-like receptor 4 (TLR4)-dependent signaling pathways: evidence for an intracellular compartmentalization of TLR4. *J Biol Chem* 2004;279:2712-2718.

(259) Greenberger PA. Allergic bronchopulmonary aspergillosis. *J Allergy Clin Immunol* 2002;110:685-692.

(260) Eaton T, Garrett J, Milne D, Frankel A, Wells AU. Allergic bronchopulmonary aspergillosis in the asthma clinic. A prospective evaluation of CT in the diagnostic algorithm. *Chest* 2000;118:66-72.

(261) Hendrick DJ, Davies RJ, D'Souza MF, Pepys J. An analysis of skin prick test reactions in 656 asthmatic patients. *Thorax* 1975;30:2-8.

(262) Denning DW, O'Driscoll BR, Hogaboam CM, Bowyer P, Niven RM. The link between fungi and severe asthma: a summary of the evidence. *Eur Respir J* 2006;27:615-626.

(263) Gibson PG, Wark PA, Simpson JL, Meldrum C, Meldrum S, Saltos N, Boyle M. Induced sputum IL-8 gene expression, neutrophil influx and MMP-9 in allergic bronchopulmonary aspergillosis. *Eur Respir J* 2003;21:582-588.

(264) Fairs A, Agbetile J, Hargadon B, Bourne M, Monteiro WR, Brightling CE, Bradding P, Green RH, Mutalithas K, Desai D, Pavord ID, Wardlaw AJ, Pashley CH. IgE sensitization to Aspergillus fumigatus is associated with reduced lung function in asthma. *Am J Respir Crit Care Med* 2010;182:1362-1368.

(265) Retsema J, Fu W. Macrolides: structures and microbial targets. *Int J Antimicrob Agents* 2001;18 Suppl 1:S3-10.

(266) Giamarellos-Bourboulis EJ. Macrolides beyond the conventional antimicrobials: a class of potent immunomodulators. *Int J Antimicrob Agents* 2008;31:12-20.

(267) Johnston SL, Blasi F, Black PN, Martin RJ, Farrell DJ, Nieman RB, TELICAST Investigators. The effect of telithromycin in acute exacerbations of asthma. *N Engl J Med* 2006;354:1589-1600.

(268) Halldorsson S, Gudjonsson T, Gottfredsson M, Singh PK, Gudmundsson GH, Baldursson O. Azithromycin maintains airway epithelial integrity during Pseudomonas aeruginosa infection. *Am J Respir Cell Mol Biol* 2010;42:62-68.

(269) Kostadima E, Tsiodras S, Alexopoulos EI, Kaditis AG, Mavrou I, Georgatou N, Papamichalopoulos A. Clarithromycin reduces the severity of bronchial hyperresponsiveness in patients with asthma. *Eur Respir J* 2004;23:714-717.

(270) Fonseca-Aten M, Okada PJ, Bowlware KL, Chavez-Bueno S, Mejias A, Rios AM, Katz K, Olsen K, Ng S, Jafri HS, McCracken GH, Ramilo O, Hardy RD. Effect of clarithromycin on cytokines and chemokines in children with an acute exacerbation of recurrent wheezing: a double-blind, randomized, placebo-controlled trial. *Ann Allergy Asthma Immunol* 2006;97:457-463.

(271) Yalcin E, Kiper N, Ozcelik U, Dogru D, Firat P, Sahin A, Ariyurek M, Mocan G, Gurcan N, Gocmen A. Effects of claritromycin on inflammatory parameters and clinical conditions in children with bronchiectasis. *J Clin Pharm Ther* 2006;31:49-55.

(272) Abe S, Nakamura H, Inoue S, Takeda H, Saito H, Kato S, Mukaida N, Matsushima K, Tomoike H. Interleukin-8 gene repression by clarithromycin is mediated by the activator protein-1 binding site in human bronchial epithelial cells. *Am J Respir Cell Mol Biol* 2000;22:51-60.

(273) Strunk RC, Bacharier LB, Phillips BR, Szefler SJ, Zeiger RS, Chinchilli VM, Martinez FD, Lemanske RF,Jr, Taussig LM, Mauger DT, Morgan WJ, Sorkness CA, Paul IM, Guilbert T, Krawiec M, Covar R, Larsen G, CARE Network. Azithromycin or montelukast as inhaled corticosteroid-sparing agents in moderate-to-severe childhood asthma study. *J Allergy Clin Immunol* 2008;122:1138-1144.e4.

(274) Fost DA, Leung DY, Martin RJ, Brown EE, Szefler SJ, Spahn JD. Inhibition of methylprednisolone elimination in the presence of clarithromycin therapy. *J Allergy Clin Immunol* 1999;103:1031-1035.

(275) Gore RB. The utility of antifungal agents for asthma. *Curr Opin Pulm Med* 2010;16:36-41.

(276) Stevens DA, Schwartz HJ, Lee JY, Moskovitz BL, Jerome DC, Catanzaro A, Bamberger DM, Weinmann AJ, Tuazon CU, Judson MA, Platts-Mills TA, DeGraff AC,Jr. A randomized trial of itraconazole in allergic bronchopulmonary aspergillosis. *N Engl J Med* 2000;342:756-762.

(277) Kirkham P, Rahman I. Oxidative stress in asthma and COPD: antioxidants as a therapeutic strategy. *Pharmacol Ther* 2006;111:476-494.

(278) Geiszt M, Leto TL. The Nox family of NAD(P)H oxidases: host defense and beyond. *J Biol Chem* 2004;279:51715-51718.

(279) Park HS, Chun JN, Jung HY, Choi C, Bae YS. Role of NADPH oxidase 4 in lipopolysaccharide-induced proinflammatory responses by human aortic endothelial cells. *Cardiovasc Res* 2006;72:447-455.

(280) Goldblatt D, Thrasher AJ. Chronic granulomatous disease. *Clin Exp Immunol* 2000;122:1-9.

(281) Moldovan L, Moldovan NI. Oxygen free radicals and redox biology of organelles. *Histochem Cell Biol* 2004;122:395-412.

(282) Simon HU, Haj-Yehia A, Levi-Schaffer F. Role of reactive oxygen species (ROS) in apoptosis induction. *Apoptosis* 2000;5:415-418.

(283) Brodska B, Holoubek A. Generation of reactive oxygen species during apoptosis induced by DNA-damaging agents and/or histone deacetylase inhibitors. *Oxid Med Cell Longev* 2011;2011:253529.

(284) Zimmermann N, Rothenberg ME. The arginine-arginase balance in asthma and lung inflammation. *Eur J Pharmacol* 2006;533:253-262.

(285) Moinard C, Caldefie-Chezet F, Walrand S, Vasson MP, Cynober L. Evidence that glutamine modulates respiratory burst in stressed rat polymorphonuclear cells through its metabolism into arginine. *Br J Nutr* 2002;88:689-695.

(286) Bannister JV, Bannister WH, Rotilio G. Aspects of the structure, function, and applications of superoxide dismutase. *CRC Crit Rev Biochem* 1987;22:111-180.

(287) Antonyuk SV, Strange RW, Marklund SL, Hasnain SS. The structure of human extracellular copper-zinc superoxide dismutase at 1.7 A resolution: insights into heparin and collagen binding. *J Mol Biol* 2009;388:310-326.

(288) Chelikani P, Fita I, Loewen PC. Diversity of structures and properties among catalases. *Cell Mol Life Sci* 2004;61:192-208.

(289) Comhair SA, Bhathena PR, Farver C, Thunnissen FB, Erzurum SC. Extracellular glutathione peroxidase induction in asthmatic lungs: evidence for redox regulation of expression in human airway epithelial cells. *FASEB J* 2001;15:70-78.

(290) Martyn KD, Frederick LM, von Loehneysen K, Dinauer MC, Knaus UG. Functional analysis of Nox4 reveals unique characteristics compared to other NADPH oxidases. *Cell Signal* 2006;18:69-82.

(291) Kawahara T, Lambeth JD. Molecular evolution of Phox-related regulatory subunits for NADPH oxidase enzymes. *BMC Evol Biol* 2007;7:178.

(292) von Lohneysen K, Noack D, Jesaitis AJ, Dinauer MC, Knaus UG. Mutational analysis reveals distinct features of the Nox4-p22 phox complex. *J Biol Chem* 2008;283:35273-35282.

(293) Schroder K. Isoform specific functions of Nox protein-derived reactive oxygen species in the vasculature. *Curr Opin Pharmacol* 2010;10:122-126.

(294) Ambasta RK, Kumar P, Griendling KK, Schmidt HH, Busse R, Brandes RP. Direct interaction of the novel Nox proteins with p22phox is required for the formation of a functionally active NADPH oxidase. *J Biol Chem* 2004;279:45935-45941.

(295) Serrander L, Cartier L, Bedard K, Banfi B, Lardy B, Plastre O, Sienkiewicz A, Forro L, Schlegel W, Krause KH. NOX4 activity is determined by mRNA levels and reveals a unique pattern of ROS generation. *Biochem J* 2007;406:105-114.

(296) Schwarzer C, Machen TE, Illek B, Fischer H. NADPH oxidase-dependent acid production in airway epithelial cells. *J Biol Chem* 2004;279:36454-36461.

(297) Kim HJ, Park YD, Moon UY, Kim JH, Jeon JH, Lee JG, Bae YS, Yoon JH. The role of Nox4 in oxidative stress-induced MUC5AC overexpression in human airway epithelial cells. *Am J Respir Cell Mol Biol* 2008;39:598-609.

(298) Kolarova H, Bino L, Pejchalova K, Kubala L. The expression of NADPH oxidases and production of reactive oxygen species by human lung adenocarcinoma epithelial cell line A549. *Folia Biol (Praha)* 2010;56:211-217.

(299) Harper RW, Xu C, Eiserich JP, Chen Y, Kao CY, Thai P, Setiadi H, Wu R. Differential regulation of dual NADPH oxidases/peroxidases, Duox1 and Duox2, by Th1 and Th2 cytokines in respiratory tract epithelium. *FEBS Lett* 2005;579:4911-4917.

(300) Kim HJ, Kim CH, Ryu JH, Joo JH, Lee SN, Kim MJ, Lee JG, Bae YS, Yoon JH. Crosstalk between platelet-derived growth factor-induced Nox4 activation and MUC8 gene overexpression in human airway epithelial cells. *Free Radic Biol Med* 2011;50:1039-1052.

(301) Li Q, Lei RX, Zhou XD, Kolosov VP, Perelman JM. Regulation of PMA-induced MUC5AC expression by heparin in human bronchial epithelial cells. *Mol Cell Biochem* 2012;360:383-391.

(302) Gattas MV, Forteza R, Fragoso MA, Fregien N, Salas P, Salathe M, Conner GE. Oxidative epithelial host defense is regulated by infectious and inflammatory stimuli. *Free Radic Biol Med* 2009;47:1450-1458.

(303) Geiszt M, Witta J, Baffi J, Lekstrom K, Leto TL. Dual oxidases represent novel hydrogen peroxide sources supporting mucosal surface host defense. *FASEB J* 2003;17:1502-1504.

(304) Geiszt M, Kopp JB, Varnai P, Leto TL. Identification of renox, an NAD(P)H oxidase in kidney. *Proc Natl Acad Sci U S A* 2000;97:8010-8014.

(305) Pendyala S, Natarajan V. Redox regulation of Nox proteins. *Respir Physiol Neurobiol* 2010;174:265-271.

(306) Graham KA, Kulawiec M, Owens KM, Li X, Desouki MM, Chandra D, Singh KK. NADPH oxidase 4 is an oncoprotein localized to mitochondria. *Cancer Biol Ther* 2010;10:223-231.

(307) Block K, Gorin Y, Abboud HE. Subcellular localization of Nox4 and regulation in diabetes. *Proc Natl Acad Sci U S A* 2009;106:14385-14390.

(308) Wu RF, Ma Z, Liu Z, Terada LS. Nox4-derived H2O2 mediates endoplasmic reticulum signaling through local Ras activation. *Mol Cell Biol* 2010;30:3553-3568.

(309) The National Center for Biotechnology Information (NCBI). NOX4 NADPH oxidase 4 [Homo sapiens]. 2012.

(310) Goyal P, Weissmann N, Rose F, Grimminger F, Schafers HJ, Seeger W, Hanze J. Identification of novel Nox4 splice variants with impact on ROS levels in A549 cells. *Biochem Biophys Res Commun* 2005;329:32-39.

(311) McCrann DJ, Yang D, Chen H, Carroll S, Ravid K. Upregulation of Nox4 in the aging vasculature and its association with smooth muscle cell polyploidy. *Cell Cycle* 2009;8:902-908.

(312) Hecker L, Vittal R, Jones T, Jagirdar R, Luckhardt TR, Horowitz JC, Pennathur S, Martinez FJ, Thannickal VJ. NADPH oxidase-4 mediates myofibroblast activation and fibrogenic responses to lung injury. *Nat Med* 2009;15:1077-1081.

(313) Carnesecchi S, Deffert C, Donati Y, Basset O, Hinz B, Preynat-Seauve O, Guichard C, Arbiser JL, Banfi B, Pache JC, Barazzone-Argiroffo C, Krause KH. A key role for NOX4 in epithelial cell death during development of lung fibrosis. *Antioxid Redox Signal* 2011;15:607-619.

(314) Sturrock A, Huecksteadt TP, Norman K, Sanders K, Murphy TM, Chitano P, Wilson K, Hoidal JR, Kennedy TP. Nox4 mediates TGF-beta1-induced retinoblastoma protein phosphorylation, proliferation, and hypertrophy in human airway smooth muscle cells. *Am J Physiol Lung Cell Mol Physiol* 2007;292:L1543-55.

(315) Michaeloudes C, Sukkar MB, Khorasani NM, Bhavsar PK, Chung KF. TGF-beta regulates Nox4, MnSOD and catalase expression, and IL-6 release in airway smooth muscle cells. *Am J Physiol Lung Cell Mol Physiol* 2011;300:L295-304.

(316) Sutcliffe A, Hollins F, Gomez E, Saunders R, Doe C, Cooke M, Challiss RA, Brightling CE. Increased nicotinamide adenine dinucleotide phosphate oxidase 4 expression mediates intrinsic airway smooth muscle hypercontractility in asthma. *Am J Respir Crit Care Med* 2012;185:267-274.

(317) Shao MX, Nadel JA. Dual oxidase 1-dependent MUC5AC mucin expression in cultured human airway epithelial cells. *Proc Natl Acad Sci U S A* 2005;102:767-772.

(318) Pantano C, Anathy V, Ranjan P, Heintz NH, Janssen-Heininger YM. Nonphagocytic oxidase 1 causes death in lung epithelial cells via a TNF-RI-JNK signaling axis. *Am J Respir Cell Mol Biol* 2007;36:473-479.

(319) Peshavariya H, Dusting GJ, Jiang F, Halmos LR, Sobey CG, Drummond GR, Selemidis S. NADPH oxidase isoform selective regulation of endothelial cell proliferation and survival. *Naunyn Schmiedebergs Arch Pharmacol* 2009;380:193-204.

(320) Aoyama T, Paik YH, Watanabe S, Laleu B, Gaggini F, Fioraso-Cartier L, Molango S, Heitz F, Merlot C, Szyndralewiez C, Page P, A Brenner D. Nicotinamide adenine dinucleotide phosphate oxidase (nox) in experimental liver fibrosis: GKT137831 as a novel potential therapeutic agent. *Hepatology* 2012.

(321) Griffith B, Pendyala S, Hecker L, Lee PJ, Natarajan V, Thannickal VJ. NOX enzymes and pulmonary disease. *Antioxid Redox Signal* 2009;11:2505-2516.

(322) Park HS, Jung HY, Park EY, Kim J, Lee WJ, Bae YS. Cutting edge: direct interaction of TLR4 with NAD(P)H oxidase 4 isozyme is essential for lipopolysaccharide-induced production of reactive oxygen species and activation of NF-kappa B. *J Immunol* 2004;173:3589-3593.

(323) Reddy PH. Mitochondrial Dysfunction and Oxidative Stress in Asthma: Implications for Mitochondria-Targeted Antioxidant Therapeutics. *Pharmaceuticals (Basel)* 2011;4:429-456.

(324) Saleh D, Ernst P, Lim S, Barnes PJ, Giaid A. Increased formation of the potent oxidant peroxynitrite in the airways of asthmatic patients is associated with induction of nitric oxide synthase: effect of inhaled glucocorticoid. *FASEB J* 1998;12:929-937.

(325) Comhair SA, Bhathena PR, Dweik RA, Kavuru M, Erzurum SC. Rapid loss of superoxide dismutase activity during antigen-induced asthmatic response. *Lancet* 2000;355:624.

(326) Comhair SA, Ricci KS, Arroliga M, Lara AR, Dweik RA, Song W, Hazen SL, Bleecker ER, Busse WW, Chung KF, Gaston B, Hastie A, Hew M, Jarjour N, Moore W, Peters S, Teague WG, Wenzel SE, Erzurum SC. Correlation of systemic superoxide dismutase deficiency to airflow obstruction in asthma. *Am J Respir Crit Care Med* 2005;172:306-313.

(327) Nadeem A, Chhabra SK, Masood A, Raj HG. Increased oxidative stress and altered levels of antioxidants in asthma. *J Allergy Clin Immunol* 2003;111:72-78.

(328) Sackesen C, Ercan H, Dizdar E, Soyer O, Gumus P, Tosun BN, Buyuktuncer Z, Karabulut E, Besler T, Kalayci O. A comprehensive evaluation of the enzymatic and nonenzymatic antioxidant systems in childhood asthma. *J Allergy Clin Immunol* 2008;122:78-85.

(329) Wood LG, Gibson PG, Garg ML. Biomarkers of lipid peroxidation, airway inflammation and asthma. *Eur Respir J* 2003;21:177-186.

(330) Nadeem A, Raj HG, Chhabra SK. Increased oxidative stress in acute exacerbations of asthma. *J Asthma* 2005;42:45-50.

(331) Fitzpatrick AM, Brown LA, Holguin F, Teague WG, National Institutes of Health/National Heart, Lung, and Blood Institute Severe Asthma Research Program. Levels of nitric oxide oxidation products are increased in the epithelial lining fluid of children with persistent asthma. *J Allergy Clin Immunol* 2009;124:990-6.e1-9.

(332) Thomassen MJ, Raychaudhuri B, Dweik RA, Farver C, Buhrow L, Malur A, Connors MJ, Drazba J, Hammel J, Erzurum SC, Kavuru MS. Nitric oxide regulation of asthmatic airway inflammation with segmental allergen challenge. *J Allergy Clin Immunol* 1999;104:1174-1182.

(333) Horvath I, Donnelly LE, Kiss A, Kharitonov SA, Lim S, Chung KF, Barnes PJ. Combined use of exhaled hydrogen peroxide and nitric oxide in monitoring asthma. *Am J Respir Crit Care Med* 1998;158:1042-1046.

(334) Haldar P, Pavord ID, Shaw DE, Berry MA, Thomas M, Brightling CE, Wardlaw AJ, Green RH. Cluster analysis and clinical asthma phenotypes. *Am J Respir Crit Care Med* 2008;178:218-224.

(335) Das DK, George A, Liu XK, Rao PS. Detection of hydroxyl radical in the mitochondria of ischemic-reperfused myocardium by trapping with salicylate. *Biochem Biophys Res Commun* 1989;165:1004-1009.

(336) Sadek HA, Nulton-Persson AC, Szweda PA, Szweda LI. Cardiac ischemia/reperfusion, aging, and redox-dependent alterations in mitochondrial function. *Arch Biochem Biophys* 2003;420:201-208.

(337) Kelly FJ, Mudway I, Blomberg A, Frew A, Sandstrom T. Altered lung antioxidant status in patients with mild asthma. *Lancet* 1999;354:482-483.

(338) Mak JC, Leung HC, Ho SP, Ko FW, Cheung AH, Ip MS, Chan-Yeung MM. Polymorphisms in manganese superoxide dismutase and catalase genes: functional study in Hong Kong Chinese asthma patients. *Clin Exp Allergy* 2006;36:440-447.

(339) Mak JC, Ho SP, Leung HC, Cheung AH, Law BK, So LK, Chan JW, Chau CH, Lam WK, Ip MS, Chan-Yeung M. Relationship between glutathione S-transferase gene polymorphisms and enzyme activity in Hong Kong Chinese asthmatics. *Clin Exp Allergy* 2007;37:1150-1157.

(340) Lander HM, Ogiste JS, Teng KK, Novogrodsky A. P21ras as a Common Signaling Target of Reactive Free Radicals and Cellular Redox Stress. *J Biol Chem* 1995;270:21195-21198.

(341) Roveri A, Coassin M, Maiorino M, Zamburlini A, van Amsterdam FT, Ratti E, Ursini F. Effect of hydrogen peroxide on calcium homeostasis in smooth muscle cells. *Arch Biochem Biophys* 1992;297:265-270.

(342) Kuipers I, Guala AS, Aesif SW, Konings G, Bouwman FG, Mariman EC, Wouters EF, Janssen-Heininger YM, Reynaert NL. Cigarette smoke targets glutaredoxin 1, increasing s-glutathionylation and epithelial cell death. *Am J Respir Cell Mol Biol* 2011;45:931-937.

(343) Mossman BT, Lounsbury KM, Reddy SP. Oxidants and signaling by mitogen-activated protein kinases in lung epithelium. *Am J Respir Cell Mol Biol* 2006;34:666-669.

(344) Goldkorn T, Balaban N, Matsukuma K, Chea V, Gould R, Last J, Chan C, Chavez C. EGF-Receptor phosphorylation and signaling are targeted by H2O2 redox stress. *Am J Respir Cell Mol Biol* 1998;19:786-798.

(345) Singh M, Moniri NH. Reactive oxygen species are required for beta2 adrenergic receptor-beta-arrestin interactions and signaling to ERK1/2. *Biochem Pharmacol* 2012;84:661-669.

(346) Wood LG, Simpson JL, Hansbro PM, Gibson PG. Potentially pathogenic bacteria cultured from the sputum of stable asthmatics are associated with increased 8-isoprostane and airway neutrophilia. *Free Radic Res* 2010;44:146-154.

(347) Rochelle LG, Fischer BM, Adler KB. Concurrent production of reactive oxygen and nitrogen species by airway epithelial cells in vitro. *Free Radic Biol Med* 1998;24:863-868.

(348) Yamaya M, Sekizawa K, Masuda T, Morikawa M, Sawai T, Sasaki H. Oxidants affect permeability and repair of the cultured human tracheal epithelium. *Am J Physiol* 1995;268:L284-93.

(349) Bayram H, Rusznak C, Khair OA, Sapsford RJ, Abdelaziz MM. Effect of ozone and nitrogen dioxide on the permeability of bronchial epithelial cell cultures of non-asthmatic and asthmatic subjects. *Clin Exp Allergy* 2002;32:1285-1292.

(350) Ercan H, Birben E, Dizdar EA, Keskin O, Karaaslan C, Soyer OU, Dut R, Sackesen C, Besler T, Kalayci O. Oxidative stress and genetic and epidemiologic determinants of oxidant injury in childhood asthma. *J Allergy Clin Immunol* 2006;118:1097-1104.

(351) Kinnula VL, Crapo JD. Superoxide dismutases in the lung and human lung diseases. *Am J Respir Crit Care Med* 2003;167:1600-1619.

(352) Hulsmann AR, Raatgeep HR, den Hollander JC, Stijnen T, Saxena PR, Kerrebijn KF, de Jongste JC. Oxidative epithelial damage produces hyperresponsiveness of human peripheral airways. *Am J Respir Crit Care Med* 1994;149:519-525.

(353) Merendino AM, Paul C, Vignola AM, Costa MA, Melis M, Chiappara G, Izzo V, Bousquet J, Arrigo AP. Heat shock protein-27 protects human bronchial epithelial cells against oxidative stress-mediated apoptosis: possible implication in asthma. *Cell Stress Chaperones* 2002;7:269-280.

(354) Feldman C, Anderson R, Kanthakumar K, Vargas A, Cole PJ, Wilson R. Oxidant-mediated ciliary dysfunction in human respiratory epithelium. *Free Radic Biol Med* 1994;17:1-10.

(355) Lener B, Koziel R, Pircher H, Hutter E, Greussing R, Herndler-Brandstetter D, Hermann M, Unterluggauer H, Jansen-Durr P. The NADPH oxidase Nox4 restricts the replicative lifespan of human endothelial cells. *Biochem J* 2009;423:363-374.

(356) Burman WJ, Martin WJ,2nd. Oxidant-mediated ciliary dysfunction. Possible role in airway disease. *Chest* 1986;89:410-413.

(357) Alberty J, Stoll W, Rudack C. The effect of endogenous nitric oxide on mechanical ciliostimulation of human nasal mucosa. *Clin Exp Allergy* 2006;36:1254-1259.

(358) Duchen MR. Mitochondria and calcium: from cell signalling to cell death. *J Physiol* 2000;529 Pt 1:57-68.

(359) Kahles T, Brandes RP. NADPH oxidases as therapeutic targets in ischemic stroke. *Cell Mol Life Sci* 2012;69:2345-2363.

(360) Jiang JX, Chen X, Serizawa N, Szyndralewiez C, Page P, Schroder K, Brandes RP, Devaraj S, Torok NJ. Liver fibrosis and hepatocyte apoptosis are attenuated by GKT137831, a novel NOX4/NOX1 inhibitor in vivo. *Free Radic Biol Med* 2012;53:289-296.

(361) Bonner MY, Arbiser JL. Targeting NADPH oxidases for the treatment of cancer and inflammation. *Cell Mol Life Sci* 2012;69:2435-2442.

(362) Hecker L, Cheng J, Thannickal VJ. Targeting NOX enzymes in pulmonary fibrosis. *Cell Mol Life Sci* 2012;69:2365-2371.

(363) Carnesecchi S, Pache JC, Barazzone-Argiroffo C. NOX enzymes: potential target for the treatment of acute lung injury. *Cell Mol Life Sci* 2012;69:2373-2385.

(364) Dickinson DA, Forman HJ. Cellular glutathione and thiols metabolism. *Biochem Pharmacol* 2002;64:1019-1026.

(365) Suter PM, Domenighetti G, Schaller MD, Laverriere MC, Ritz R, Perret C. N-acetylcysteine enhances recovery from acute lung injury in man. A randomized, double-blind, placebo-controlled clinical study. *Chest* 1994;105:190-194.

(366) Moradi M, Mojtahedzadeh M, Mandegari A, Soltan-Sharifi MS, Najafi A, Khajavi MR, Hajibabayee M, Ghahremani MH. The role of glutathione-S-transferase polymorphisms on clinical outcome of ALI/ARDS patient treated with N-acetylcysteine. *Respir Med* 2009;103:434-441.

(367) Syrkina O, Jafari B, Hales CA, Quinn DA. Oxidant stress mediates inflammation and apoptosis in ventilator-induced lung injury. *Respirology* 2008;13:333-340.

(368) Gvozdjakova A, Kucharska J, Bartkovjakova M, Gazdikova K, Gazdik FE. Coenzyme Q10 supplementation reduces corticosteroids dosage in patients with bronchial asthma. *Biofactors* 2005;25:235-240.

(369) Schroder K, Wandzioch K, Helmcke I, Brandes RP. Nox4 acts as a switch between differentiation and proliferation in preadipocytes. *Arterioscler Thromb Vasc Biol* 2009;29:239-245.

(370) Laleu B, Gaggini F, Orchard M, Fioraso-Cartier L, Cagnon L, Houngninou-Molango S, Gradia A, Duboux G, Merlot C, Heitz F, Szyndralewiez C, Page P. First in class, potent, and orally bioavailable NADPH oxidase isoform 4 (Nox4) inhibitors for the treatment of idiopathic pulmonary fibrosis. *J Med Chem* 2010;53:7715-7730.

(371) GenKyoTex. GenKyoTex Starts Phase I Trial with First in Class NOX inhibitor GKT137831. 2011.

(372) Green DE, Murphy TC, Kang BY, Kleinhenz JM, Szyndralewiez C, Page P, Sutliff RL, Hart CM. The Nox4 Inhibitor, GKT137831, Attenuates Hypoxia-Induced Pulmonary Vascular Cell Proliferation. *Am J Respir Cell Mol Biol* 2012.

(373) GINA. Global Initiative For Asthma - Global Strategy for Asthma Management and Prevention Asthma. 2009:112.

(374) BTS BTS, editor. Guidelines on diagnostic flexible bronchoscopy. ; 2008.

(375) Hicks W, Hall L, Sigurdson L, Stewart C, Hard R, Winston J, Lwebuga-Mukasa J. Isolation and characterization of basal cells from human upper respiratory epithelium. *Exp Cell Res* 1997;237:357-363.

(376) Fadaee-Shohada MJ, Hirst RA, Rutman A, Roberts IS, O'Callaghan C, Andrew PW. The behaviour of both Listeria monocytogenes and rat ciliated ependymal cells is altered during their co-culture. *PLoS One* 2010;5:e10450.

(377) Hirst RA, Rutman A, Williams G, O'Callaghan C. Ciliated air-liquid cultures as an aid to diagnostic testing of Primary Ciliary Dyskinesia (PCD). *Chest* 2010.

(378) Chilvers MA, O'Callaghan C. Analysis of ciliary beat pattern and beat frequency using digital high speed imaging: comparison with the photomultiplier and photodiode methods. *Thorax* 2000;55:314-317.

(379) Pizzichini E, Pizzichini MM, Efthimiadis A, Evans S, Morris MM, Squillace D, Gleich GJ, Dolovich J, Hargreave FE. Indices of airway inflammation in induced sputum: reproducibility and validity of cell and fluid-phase measurements. *Am J Respir Crit Care Med* 1996;154:308-317.

(380) Bafadhel M, McKenna S, Terry S, Mistry V, Reid C, Haldar P, McCormick M, Haldar K, Kebadze T, Duvoix A, Lindblad K, Patel H, Rugman P, Dodson P, Jenkins M, Saunders M, Newbold P, Green RH, Venge P, Lomas DA, Barer MR, Johnston SL, Pavord ID, Brightling CE. Acute exacerbations of chronic obstructive pulmonary disease: identification of biologic clusters and their biomarkers. *Am J Respir Crit Care Med* 2011;184:662-671.

(381) Campbell CK, Johnson EM, Philpot CM, Warnock DW, editors. Identification of pathogenic fungi. London: Public Health Laboratory Service; 1996.

(382) Costa C, Vidaud D, Olivi M, Bart-Delabesse E, Vidaud M, Bretagne S. Development of two real-time quantitative TaqMan PCR assays to detect circulating Aspergillus fumigatus DNA in serum. *J Microbiol Methods* 2001;44:263-269.

(383) Lonza. PyroGene Recombinant Factor C Endotoxin Detection System. Catalog Number: 50-658U, 50-658NV. 2012:22.

(384) Thorne PS, Perry SS, Saito R, O'Shaughnessy PT, Mehaffy J, Metwali N, Keefe T, Donham KJ, Reynolds SJ. Evaluation of the Limulus amebocyte lysate and recombinant factor C assays for assessment of airborne endotoxin. *Appl Environ Microbiol* 2010;76:4988-4995.

(385) R&D Systems. ELISA development guide - a guide for the use of antibodies in ELISA development. ; http://www.rndsystems.com/Resources/images/5670.pdf. Accessed January 2013.

(386) Meso Scale Discovery. Meso Scale Discovery clinical immunology applications. ; http://www.meso-scale.com/CatalogSystemWeb/WebRoot/literature/brochures/pdf/immunologyBrochure.pdf. Accessed January 2013.

(387) Thermo Scientific. Coomassie Plus (Bradford) Protein Assay. ; http://www.piercenet.com/browse.cfm?fldID=02020104. Accessed January 2013.

(388) Bio-Rad Laboratories. Protein Blotting Guide. ; http://www.bio-rad.com/LifeScience/pdf/Bulletin_2895.pdf. Accessed January 2013.

(389) Gassmann M, Grenacher B, Rohde B, Vogel J. Quantifying Western blots: pitfalls of densitometry. *Electrophoresis* 2009;30:1845-1855.

(390) Wang H, Joseph JA. Quantifying cellular oxidative stress by dichlorofluorescein assay using microplate reader. *Free Radic Biol Med* 1999;27:612-616.

(391) Affymetrix. How Affymetric GeneChip DNA microarrays works. ; http://public.tgen.org/tgen.org/downloads/autism/Genotypingessentials.pdf. Accessed January 2013.

(392) Dharmaraj SaI. The Basic: RT-qPCR. ; http://www.invitrogen.com/site/us/en/home/References/Ambion-Tech-Support/rtpcr-analysis/general-articles/rt--pcr-the-basics.html. Accessed January 2013.

(393) De Jonge HW, De Bakker MA, Verbeek FJ, Weijs WA. Embedding of large specimens in glycol methacrylate: prerequisites for multi-signal detection and high-resolution imaging. *Microsc Res Tech* 2005;66:25-30.

(394) Machella N, Regoli F, Cambria A, Santella RM. Application of an immunoperoxidase staining method for detection of 7,8-dihydro-8-oxodeoxyguanosine as a biomarker of chemical-induced oxidative stress in marine organisms. *Aquat Toxicol* 2004;67:23-32.

(395) Bateman JR, Pavia D, Sheahan NF, Agnew JE, Clarke SW. Impaired tracheobronchial clearance in patients with mild stable asthma. *Thorax* 1983;38:463-467.

(396) Dulfano MJ, Luk CK. Sputum and ciliary inhibition in asthma. *Thorax* 1982;37:646-651.

(397) Berry M, Brightling C, Pavord I, Wardlaw A. TNF-alpha in asthma. *Current Opinion in Pharmacology* 2007;7:279-282.

(398) Ross AJ, Dailey LA, Brighton LE, Devlin RB. Transcriptional profiling of mucociliary differentiation in human airway epithelial cells. *Am J Respir Cell Mol Biol* 2007;37:169-185.

(399) Jorissen MARK, Willems TOM. The Secondary Nature of Ciliary (Dis)Orientation in Secondary and Primary Ciliary Dyskinesia. *Acta Otolaryngol* 2004;124:527-531.

(400) Choe MM, Tomei AA, Swartz MA. Physiological 3D tissue model of the airway wall and mucosa. *Nature Protocols* 2006;1:357-362.

(401) Malavia NK, Raub CB, Mahon SB, Brenner M, Panettieri RA,Jr, George SC. Airway epithelium stimulates smooth muscle proliferation. *Am J Respir Cell Mol Biol* 2009;41:297-304.

(402) Cao J, Wong CK, Yin Y, Lam CW. Activation of human bronchial epithelial cells by inflammatory cytokines IL-27 and TNF-alpha: implications for immunopathophysiology of airway inflammation. *J Cell Physiol* 2010;223:788-797.

(403) Lopez-Souza N, Favoreto S, Wong H, Ward T, Yagi S, Schnurr D, Finkbeiner WE, Dolganov GM, Widdicombe JH, Boushey HA, Avila PC. In vitro susceptibility to rhinovirus infection is greater for bronchial than for nasal airway epithelial cells in human subjects. *J Allergy Clin Immunol* 2009;123:1384-90.e2.

(404) Freishtat RJ, Watson AM, Benton AS, Iqbal SF, Pillai DK, Rose MC, Hoffman EP. Asthmatic Airway Epithelium is Intrinsically Inflammatory and Mitotically Dyssynchronous. *Am J Respir Cell Mol Biol* 2010.

(405) Saenz SA, Taylor BC, Artis D. Welcome to the neighborhood: epithelial cell-derived cytokines license innate and adaptive immune responses at mucosal sites. *Immunol Rev* 2008;226:172-190.

(406) Levy H,b, Raby BAb, Lake S, Tantisira KGb, Kwiatkowski, Davidb,d,e, Lazarus R, Silverman EKb, Richter B, Klimecki WTc, Vercelli D, Martinez FDc, Weiss STb,d. Association of defensin [beta]-1 gene polymorphisms with asthma. *Journal of Allergy & Clinical Immunology* 2005;115:252-258.

(407) Hong KU, Reynolds SD, Watkins S, Fuchs E, Stripp BR. Basal cells are a multipotent progenitor capable of renewing the bronchial epithelium. *Am J Pathol* 2004;164:577-588.

(408) Hackett TL, Knight DA. The role of epithelial injury and repair in the origins of asthma. *Curr Opin Allergy Clin Immunol* 2007;7:63-68.

(409) Fedorov IA, Wilson SJ, Davies DE, Holgate ST. Epithelial stress and structural remodelling in childhood asthma. *Thorax* 2005;60:389-394.

(410) Daviskas E, Anderson SD, Shaw J, Eberl S, Seale JP, Yang IA, Young IH. Mucociliary clearance in patients with chronic asthma: effects of beta agonists. *Respirology* 2005;10:426-435.

(411) Gupta S, Siddiqui S, Haldar P, Raj JV, Entwisle JJ, Wardlaw AJ, Bradding P, Pavord ID, Green RH, Brightling CE. Qualitative analysis of high-resolution CT scans in severe asthma. *Chest* 2009;136:1521-1528.

(412) Brightling CE, Mbbs FCCP. Chronic Cough Due to Nonasthmatic Eosinophilic Bronchitis: ACCP Evidence-Based Clinical Practice Guidelines. *Chest.Diagnosis and Management of Cough: ACCP Evidence-Based Clinical Practice Guidelines* 2006;129:116S-121S.

(413) Prytherch Z. An*in vitro*NHBE model of the human bronchial epithelium for toxicological testing. 2010.

(414) Prytherch Z, Job C, Marshall H, Oreffo V, Foster M, BeruBe K. Tissue-Specific stem cell differentiation in an in vitro airway model. *Macromol Biosci* 2011;11:1467-1477.

(415) Rossman CM, Lee RM, Forrest JB, Newhouse MT. Nasal ciliary ultrastructure and function in patients with primary ciliary dyskinesia compared with that in normal subjects and in subjects with various respiratory diseases. *Am Rev Respir Dis* 1984;129:161-167.

(416) Wills-Karp M, Santeliz J, Karp CL. The germless theory of allergic disease: revisiting the hygiene hypothesis. *Nat Rev Immunol* 2001;1:69-75.

(417) Voynow JA, Rubin BK. Mucins, mucus, and sputum. *Chest* 2009;135:505-512.

(418) Miravitlles M, Marin A, Monso E, Vila S, de la Roza C, Hervas R, Esquinas C, Garcia M, Millares L, Morera J, Torres A. Colour of sputum is a marker for bacterial colonisation in chronic obstructive pulmonary disease. *Respir Res* 2010;11:58.

(419) Tecle T, Tripathi S, Hartshorn KL. Defensins and cathelicidins in lung immunity. *Innate Immunity* 2010;16:ate of Pubaton: June 2010.

(420) Hirst RA, Rutman A, O'Callaghan C. Hydrogen peroxide at a concentration used during neurosurgery disrupts ciliary function and causes extensive damage to the ciliated ependyma of the brain. *Childs Nerv Syst* 2009;25:559-561.

(421) Lass-Florl C, Salzer GM, Schmid T, Rabl W, Ulmer H, Dierichi MP. Pulmonary Aspergillus colonization in humans and its impact on management of critically ill patients. *Br J Haematol* 1999;104:745-747.

(422) Sellart-Altisent M, Torres-Rodriguez JM, Gomez de Ana S, Alvarado-Ramirez E. Nasal fungal microbiota in allergic and healthy subjects. *Rev Iberoam Micol* 2007;24:125-130.

(423) O'Driscoll BR, Powell G, Chew F, Niven RM, Miles JF, Vyas A, Denning DW. Comparison of skin prick tests with specific serum immunoglobulin E in the diagnosis of fungal sensitization in patients with severe asthma. *Clin Exp Allergy* 2009;39:1677-1683.

(424) Baxter CG, Jones AM, Webb K, Denning DW. Homogenisation of cystic fibrosis sputum by sonication--an essential step for Aspergillus PCR. *J Microbiol Methods* 2011;85:75-81.

(425) The U.S. Food and Drug Administration (FDA). Guideline on validation of the limulus amebocyte lysate test as an end-product endotoxin test for human and animal parenteral drugs, biological products, and medical devices. 1987.

(426) Cabello H, Torres A, Celis R, El-Ebiary M, Puig de la Bellacasa J, Xaubet A, Gonzalez J, Agusti C, Soler N. Bacterial colonization of distal airways in healthy subjects and chronic lung disease: a bronchoscopic study. *Eur Respir J* 1997;10:1137-1144.

(427) Wilkinson TM, Patel IS, Wilks M, Donaldson GC, Wedzicha JA. Airway bacterial load and FEV1 decline in patients with chronic obstructive pulmonary disease. *Am J Respir Crit Care Med* 2003;167:1090-1095.

(428) Kraemer R, Delosea N, Ballinari P, Gallati S, Crameri R. Effect of allergic bronchopulmonary aspergillosis on lung function in children with cystic fibrosis. *Am J Respir Crit Care Med* 2006;174:1211-1220.

(429) Amitani R, Taylor G, Elezis EN, Llewellyn-Jones C, Mitchell J, Kuze F, Cole PJ, Wilson R. Purification and characterization of factors produced by Aspergillus fumigatus which affect human ciliated respiratory epithelium. *Infect Immun* 1995;63:3266-3271.

(430) Holgate ST. Innate and adaptive immune responses in asthma. *Nat Med* 2012;18:673-683.

(431) Duits LA, Ravensbergen B, Rademaker M, Hiemstra PS, Nibbering PH. Expression of beta-defensin 1 and 2 mRNA by human monocytes, macrophages and dendritic cells. *Immunology* 2002;106:517-525.

(432) Brightling CE, McKenna S, Hargadon B, Birring S, Green R, Siva R, Berry M, Parker D, Monteiro W, Pavord ID, Bradding P. Sputum eosinophilia and the short term response to inhaled mometasone in chronic obstructive pulmonary disease. *Thorax* 2005;60:193-198.

(433) Sakamoto N, Mukae H, Fujii T, Ishii H, Yoshioka S, Kakugawa T, Sugiyama K, Mizuta Y, Kadota J, Nakazato M, Kohno S. Differential effects of alpha- and beta-defensin on cytokine production by cultured human bronchial epithelial cells. *Am J Physiol Lung Cell Mol Physiol* 2005;288:L508-13.

(434) Kraft M, Cassell GH, Henson JE, Watson H, Williamson J, Marmion BP, Gaydos CA, Martin RJ. Detection of Mycoplasma pneumoniae in the airways of adults with chronic asthma. *Am J Respir Crit Care Med* 1998;158:998-1001.

(435) Kanthakumar K, Taylor GW, Cundell DR, Dowling RB, Johnson M, Cole PJ, Wilson R. The effect of bacterial toxins on levels of intracellular adenosine nucleotides and human ciliary beat frequency. *Pulm Pharmacol* 1996;9:223-230.

(436) Anhalt JP, Fenselau C. Identification of Bacteria Using Mass Spectrometry. *2* 1975;47:219.

(437) Dworzanski JP, Snyder AP. Classification and identification of bacteria using mass spectrometry-based proteomics. *Expert Rev Proteomics* 2005;2:863-878.

(438) Datta B, Barton R, Hobson R, McLaughlin H. Aspergillus in Sputum Culture − Infection or Colonisation.[abstract]. *Am J Respir Crit Care Med* 2009;179:A5943.

(439) Zhang L, Bukreyev A, Thompson CI, Watson B, Peeples ME, Collins PL, Pickles RJ. Infection of ciliated cells by human parainfluenza virus type 3 in an in vitro model of human airway epithelium. *J Virol* 2005;79:1113-1124.

(440) Finkel T, Holbrook NJ. Oxidants, oxidative stress and the biology of ageing. *Nature* 2000;408:239-247.

(441) Ho JC, Chan KN, Hu WH, Lam WK, Zheng L, Tipoe GL, Sun J, Leung R, Tsang KW. The effect of aging on nasal mucociliary clearance, beat frequency, and ultrastructure of respiratory cilia. *American Journal of Respiratory and Critical Care Medicine* 2001;163:ate of Pubaton: 2001.

(442) Ito K, Herbert C, Siegle JS, Vuppusetty C, Hansbro N, Thomas PS, Foster PS, Barnes PJ, Kumar RK. Steroid-resistant neutrophilic inflammation in a mouse model of an acute exacerbation of asthma. *Am J Respir Cell Mol Biol* 2008;39:543-550.

(443) Kazachkov MY, Hu PC, Carson JL, Murphy PC, Henderson FW, Noah TL. Release of cytokines by human nasal epithelial cells and peripheral blood mononuclear cells infected with Mycoplasma pneumoniae. *Exp Biol Med (Maywood)* 2002;227:330-335.

(444) Kanazawa H, Shiraishi S, Hirata K, Yoshikawa J. Decreased peroxynitrite inhibitory activity in induced sputum in patients with bronchial asthma. *Thorax* 2002;57:509-512.

(445) Gibco I. HBSS, Calcium, Magnesium, no Phenol Red. 2012.

(446) Baker KM, Aceto JF. Angiotensin II stimulation of protein synthesis and cell growth in chick heart cells. *Am J Physiol* 1990;259:H610-8.

(447) Villanueva AG, Farber HW, Rounds S, Goldstein RH. Stimulation of fibroblast collagen and total protein formation by an endothelial cell-derived factor. *Circ Res* 1991;69:134-141.

(448) Gordillo G, Fang H, Park H, Roy S. Nox-4-dependent nuclear H2O2 drives DNA oxidation resulting in 8-OHdG as urinary biomarker and hemangioendothelioma formation. *Antioxid Redox Signal* 2010;12:933-943.

(449) Finnzymes. Principles of qPCR. Helsinki: Finnzymes Oy; 2009.

(450) Lee YJ, Lee SH. Sulforaphane induces antioxidative and antiproliferative responses by generating reactive oxygen species in human bronchial epithelial BEAS-2B cells. *J Korean Med Sci* 2011;26:1474-1482.

(451) Choi SY, Lim JW, Shimizu T, Kuwano K, Kim JM, Kim H. Reactive oxygen species mediate Jak2/Stat3 activation and IL-8 expression in pulmonary epithelial cells stimulated with lipid-associated membrane proteins from Mycoplasma pneumoniae. *Inflamm Res* 2012;61:493-501.

(452) Smith LJ, Shamsuddin M, Sporn PH, Denenberg M, Anderson J. Reduced superoxide dismutase in lung cells of patients with asthma. *Free Radic Biol Med* 1997;22:1301-1307.

(453) Forteza R, Salathe M, Miot F, Forteza R, Conner GE. Regulated hydrogen peroxide production by Duox in human airway epithelial cells. *Am J Respir Cell Mol Biol* 2005;32:462-469.

(454) Nagai K, Betsuyaku T, Suzuki M, Nasuhara Y, Kaga K, Kondo S, Nishimura M. Dual oxidase 1 and 2 expression in airway epithelium of smokers and patients with mild/moderate chronic obstructive pulmonary disease. *Antioxid Redox Signal* 2008;10:705-714.

(455) Pickles RJ, McCarty D, Matsui H, Hart PJ, Randell SH, Boucher RC. Limited entry of adenovirus vectors into well-differentiated airway epithelium is responsible for inefficient gene transfer. *J Virol* 1998;72:6014-6023.

(456) Walters RW, Grunst T, Bergelson JM, Finberg RW, Welsh MJ, Zabner J. Basolateral localization of fiber receptors limits adenovirus infection from the apical surface of airway epithelia. *J Biol Chem* 1999;274:10219-10226.

(457) Davis CW, Dickey BF. Regulated airway goblet cell mucin secretion. *Annu Rev Physiol* 2008;70:487-512.

(458) Bloodgood RA. Sensory reception is an attribute of both primary cilia and motile cilia. *J Cell Sci* 2010;123:505-509.

(459) Sanderson MJ, Chow I, Dirksen ER. Intercellular communication between ciliated cells in culture. *Am J Physiol* 1988;254:C63-74.

(460) Boucher RC. Relationship of airway epithelial ion transport to chronic bronchitis. *Proc Am Thorac Soc* 2004;1:66-70.

(461) Sancho P, Bertran E, Caja L, Carmona-Cuenca I, Murillo MM, Fabregat I. The inhibition of the epidermal growth factor (EGF) pathway enhances TGF-beta-induced apoptosis in rat hepatoma cells through inducing oxidative stress coincident with a change in the expression pattern of the NADPH oxidases (NOX) isoforms. *Biochim Biophys Acta* 2009;1793:253-263.

(462) Hastie AT, Loegering DA, Gleich GJ, Kueppers F. The effect of purified human eosinophil major basic protein on mammalian ciliary activity. *Am Rev Respir Dis* 1987;135:848-853.

(463) Carson JL, Lu TS, Brighton L, Hazucha M, Jaspers I, Zhou H. Phenotypic and physiologic variability in nasal epithelium cultured from smokers and non-smokers exposed to secondhand tobacco smoke. *In Vitro Cell Dev Biol Anim* 2010;46:606-612.

(464) Baines KJ, Simpson JL, Wood LG, Scott RJ, Gibson PG. Transcriptional phenotypes of asthma defined by gene expression profiling of induced sputum samples. *J Allergy Clin Immunol* 2011;127:153-60, 160.e1-9.

(465) Korn SH, Wouters EF, Vos N, Janssen-Heininger YM. Cytokine-induced activation of nuclear factor-kappa B is inhibited by hydrogen peroxide through oxidative inactivation of IkappaB kinase. *J Biol Chem* 2001;276:35693-35700.

(466) Woodman L, Wan W, Milone R, Grace K, Sousa A, Williamson R, Brightling C. Synthetic Response of Stimulated Respiratory Epithelium: Modulation by Prednisolone and iKK2 Inhibition. (in submission).

(467) Doan TN, Gentry DL, Taylor AA, Elliott SJ. Hydrogen peroxide activates agonist-sensitive Ca(2+)-flux pathways in canine venous endothelial cells. *Biochem J* 1994;297 (Pt 1):209-215.

(468) Rathore R, Zheng YM, Niu CF, Liu QH, Korde A, Ho YS, Wang YX. Hypoxia activates NADPH oxidase to increase [ROS]i and [Ca2+]i through the mitochondrial ROS-PKCepsilon signaling axis in pulmonary artery smooth muscle cells. *Free Radic Biol Med* 2008;45:1223-1231.

(469) Wang YX, Zheng YM. Role of ROS signaling in differential hypoxic Ca2+ and contractile responses in pulmonary and systemic vascular smooth muscle cells. *Respir Physiol Neurobiol* 2010;174:192-200.

(470) Mizgerd JP, Skerrett SJ. Animal models of human pneumonia. *Am J Physiol Lung Cell Mol Physiol* 2008;294:L387-98.

(471) Xie Y, Jiang H, Nguyen H, Jia S, Berro A, Panettieri RA,Jr, Wolff DW, Abel PW, Casale TB, Tu Y. Regulator of G protein signaling 2 is a key modulator of airway hyperresponsiveness. *J Allergy Clin Immunol* 2012.

(472) Shankar SP, Wilson MS, DiVietro JA, Mentink-Kane MM, Xie Z, Wynn TA, Druey KM. RGS16 attenuates pulmonary Th2/Th17 inflammatory responses. *J Immunol* 2012;188:6347-6356.

(473) Krysko DV, Agostinis P, Krysko O, Garg AD, Bachert C, Lambrecht BN, Vandenabeele P. Emerging role of damage-associated molecular patterns derived from mitochondria in inflammation. *Trends Immunol* 2011;32:157-164.

(474) Watanabe T, Asai K, Fujimoto H, Tanaka H, Kanazawa H, Hirata K. Increased levels of HMGB-1 and endogenous secretory RAGE in induced sputum from asthmatic patients. *Respir Med* 2011;105:519-525.

(475) Shim EJ, Chun E, Lee HS, Bang BR, Kim TW, Cho SH, Min KU, Park HW. The role of high-mobility group box-1 (HMGB1) in the pathogenesis of asthma. *Clin Exp Allergy* 2012;42:958-965.

(476) Cheng Z, Dai LL, Cao DF, Wu QG, Song YN, Kang Y, Xia J, Si JM, Chen CY. Changes of HMGB1 and RAGE in induced sputum from patients with bronchial asthma. *Zhonghua Yi Xue Za Zhi* 2011;91:1538-1542.

(477) Zhou Y, Jiang YQ, Wang WX, Zhou ZX, Wang YG, Yang L, Ji YL. HMGB1 and RAGE Levels in Induced Sputum Correlate with Asthma Severity and Neutrophil Percentage. *Hum Immunol* 2012.

(478) Pearson CG, Giddings TH,Jr, Winey M. Basal body components exhibit differential protein dynamics during nascent basal body assembly. *Mol Biol Cell* 2009;20:904-914.